Universidade de Aveiro Departamento de Química
2015

Graça Raquel Veiga Vaz

Medição Experimental e Simulação de Dinâmica Molecular de Difusividades em Misturas Supercríticas

Experimental Measurement and Molecular Dynamics Simulation of Diffusivities in Supercritical Mixtures

Universidade de Aveiro Departamento de Química
2015

Graça Raquel Veiga Vaz

Medição Experimental e Simulação de Dinâmica Molecular de Difusividades em Misturas Supercríticas

Experimental Measurement and Molecular Dynamics Simulation of Diffusivities in Supercritical Mixtures

Tese apresentada à Universidade de Aveiro para cumprimento dos requisitos necessários à obtenção do grau de Doutor em Engenharia Química, realizada sob a orientação científica do Doutor Carlos Manuel Silva, Professor Auxiliar do Departamento de Química da Universidade de Aveiro

Apoio financeiro da FCT e do FSE no âmbito do III Quadro Comunitário de Apoio

o júri

presidente

Professor António Manuel de Brito Ferrari Almeida
Professor Catedrático do Departamento de Eletrónica, Comunicações e Informática da Universidade de Aveiro

Prof. Doutor Carlos Manuel Santos da Silva
Professor Auxiliar do Departamento de Química da Universidade de Aveiro

Prof. Doutor Pedro Miguel Calado Simões
Professor Auxiliar do Departamento de Química da Faculdade de Ciências e Tecnologia da Universidade Nova de Lisboa

Prof. Doutora Rosa Maria de Oliveira Quinta-Ferreira
Professora Associada do Departamento de Engenharia Química da Faculdade de Ciências e Tecnologia da Universidade de Coimbra

Professor Adélio Miguel Magalhães Mendes
Professor Catedrático do Departamento de Engenharia Química da Faculdade de Engenharia da Universidade do Porto

Doutor José Richard Baptista Gomes
Investigador Principal do Laboratório Associado CICECO da Universidade de Aveiro

agradecimentos

Primeiramente, agradeço ao meu orientador, Doutor Carlos Manuel Silva, pela orientação e conhecimentos transmitidos, mas também amizade e preocupação, com quem cresci muito nestes últimos anos. Todo este trabalho e o resultado dele não seriam possível de outra forma.
Agradeço a colaboração do Dr. Richard Gomes que, mesmo sem o vínculo de orientador, sempre demonstrou disponibilidade, paciência, interesse e eficiência, mas sempre com a sua descontração e bom humor característicos.
Os meus agradecimentos vão também para os atuais e antigos membros do grupo EgiChem com quem tive o prazer de partilhar o dia-a-dia, pelo convívio, entreajuda e amizade. Em particular à Doutora Ana Magalhães agradeço a colaboração e trabalho conjunto. Faço ainda um agradecimento especial aos meus "camaradas" fora do ambiente de trabalho, por todos os bons momentos.
Agradeço também ao Doutor Avelino Silva, pelo seu carinho e amizade, disponibilidade e preocupação constante em ajudar.
À minha família, um grande obrigada. São eles que sempre acreditaram em mim e cujos sonhos em mim projetados me levaram sempre mais além. Ao meu marido, a quem não agradeço com palavras pois nenhumas lhe fariam jus; apenas um obrigada por tudo.
Finalmente, agradeço o apoio financeiro que me foi concedido pela FCT no âmbito do QREN (bolsa de investigação com a referência SFRH/BD/69257/2010).

palavras-chave

Coeficiente de difusão, dinâmica molecular, modelação, previsão, propriedades de transporte, método cromatográfico de abertura de pico, método de Taylor

resumo

Neste trabalho estudaram-se coeficientes de difusão devido à sua importância no projeto e simulação de processos conduzidos por cinética. Foram seguidas três abordagens: modelação fenomenológica através do desenvolvimento de modelos macroscópicos preditivos, simulações de dinâmica molecular e medição experimental pela técnica cromatográfica de abertura de pico.

Os coeficientes de autodifusão foram primeiramente focados, analisando-se leis de redução baseadas na entropia residual. As expressões de Rosenfeld, Dzugutov e Bretonnet foram testadas usando uma extensa base de dados compilada previamente, envolvendo 1727 pontos. Mostrou-se que estas equações falham em toda a gama de densidade e temperatura, e que a difusividade depende não só da entropia residual mas também do tamanho/geometria da molécula (através de um parâmetro que caracteriza o tamanho da cadeia). Por estas razões propôs-se uma correlação universal baseada em redes neuronais, que relaciona os coeficientes de autodifusão com a entropia residual e o parâmetro de tamanho da molécula. Esta é válida para fluidos modelo e reais, quer sejam moléculas esféricas ou não esféricas, polares ou apolares (AARD global = 9.13%). Para além disso, uma expressão analítica simples foi desenvolvida para sistemas esféricos, baseada apenas na entropia residual, dando origem um erro médio de 4.61%,

Três expressões hidrodinâmicas modificadas foram propostas para estimar com exatidão difusividades binárias a diluição infinita (D_{12}) em dióxido de carbono supercrítico (SC-CO_2), baseadas nas equações de Wilke-Chang, Scheibel e Lusis-Ratcliff. Estas relacionam D_{12} com a razão entre a temperatura e a viscosidade do solvente (T/η_1), e com o volume molar do soluto à temperatura normal de ebulição (V_{bp}), tal como o fazem os modelos originais. A introdução de duas constantes universais reduziu os erros médios de [11.70–23.16]% para [8.26–8.51]%, calculados para uma extensa base de dados de 150 sistemas e 4484 pontos experimentais, varrendo gamas largas de pressão e temperatura.

Com o objetivo de se utilizar propriedades de soluto mais plausíveis, foram propostos quatro modelos baseados na relação de Stokes-Einstein, modificando as equações de Wilke-Chang, Scheibel, Lusis-Ratcliff e Tyn-Calus, onde os valores de V_{bp} foram substituídos por volumes críticos. Estas fornecem resultados similares aos da abordagem anterior (AARD = 7.86-8.56%) para uma base de dados equivalente. O cálculo de outras grandezas estatísticas permitiu confirmar a solidez destes modelos para prever difusividades binárias de quaisquer solutos em SC-CO_2.

Foi proposto outro modelo preditivo para sistemas supercríticos, combinando dois termos – regular e singular – para estimar corretamente difusividades não apenas longe mas também junto ao ponto crítico, onde se sabe existir um comportamento assimptótico de D_{12}. O modelo fornece um erro médio de 6.20% para toda a base de dados, com bom desempenho para solutos polares e não polares em toda a gama pressão-temperatura, enquanto as expressões

da literatura atingem erros de 11.62-75.17%.
Foram efetuadas simulações de dinâmica molecular para estudar as difusividades de propanona, butanona, 2-pentanona e 3-pentanona em SC-CO_2. Estas foram calculadas usando a relação de Einstein, e as suas dependências com a temperatura, pressão (ou densidade) e tamanho molecular foram analisadas. Foi ainda conduzida uma análise estrutural local dos sistemas através do cálculo de funções distribuição radial e números de coordenação, para discriminar e interpretar o ambiente local do CO_2 em torno de cada grupo que compõe as moléculas de cetona.
Foi concebida, instalada e testada uma instalação experimental para medir coeficientes de difusão pelo método cromatográfico de abertura de pico. Foram determinadas difusividades de α-pineno a diluição infinita em SC-CO_2 a 313.15, 323.15 e 333.15 K, e pressões entre 175 e 275 bar. Examinou-se em pormenor a dependência de D_{12} com a temperatura, pressão e densidade do solvente, e o seu comportamento hidrodinâmico. Por fim, os valores experimentais foram modelados usando equações desenvolvidas neste trabalho e obtiveram bons resultados (AARD = 2.48 – 3.56%); foram também consideradas expressões bem conhecidas da literatura.

keywords

Chromatographyc peak broadening, diffusion coefficient, modeling, molecular dynamics, prediction, Taylor method, transport property

abstract

This work focuses diffusivities due to their importance in the design and simulation of rate-controlled processes. Three approaches are followed: phenomenological modeling through the development of predictive macroscopic models, molecular dynamics simulations, and experimental measurement by the chromatographic peak broadening technique.

Self-diffusion coefficients of model and real fluids were firstly studied using entropy based scaling laws. Rosenfeld, Dzugutov and Bretonnet expressions were tested using a large database previously compiled, involving 1727 data points. It was shown that they fail in the entire range of density and temperature, and that diffusivity depends not only on residual entropy but also on the size/geometry of the molecule (through a chain size parameter). For these reasons, a new universal correlation using artificial neural networks was proposed, which relates self-diffusivities with residual entropy and chain size parameter. It is valid for both model and real fluids, whether spherical or asymmetrical, polar or non-polar (global AARD = 9.13%). Moreover, a simple analytical expression was devised for spherical systems, and provides only 4.61% of error based uniquely on residual entropy.

Three modified hydrodynamic expressions were proposed to accurately estimate tracer diffusivities (D_{12}) in supercritical carbon dioxide (SC-CO_2), based on the Wilke-Chang, Scheibel and Lusis-Ratcliff equations. They relate D_{12} with the ratio between temperature and solvent viscosity (T/η_1), and solute molar volume at normal boiling point (V_{bp}), as in the original models. The introduction of two universal constants reduce the average errors from [11.70–23.16]% to [8.26–8.51]% for a large database of 150 systems and 4484 data points over wide ranges of temperature and pressure.

In an attempt to adopt more reliable solute properties, four improved Stokes-Einstein based models were devised by modifying Wilke-Chang, Scheibel, Lusis-Ratcliff, and Tyn-Calus equations, where V_{bp} values were substituted by critical volumes. They achieve similar results to the previous approach (AARD = 7.86-8.56%) for an equivalent database. Further statistics confirmed the good and sturdy nature of these models to accurately predict tracer diffusivities in SC-CO_2 for any kind of solute.

Another predictive model was developed for supercritical systems, combining two terms – background plus singular – to accurately estimate diffusivities not only far but also near the critical point, where asymptotic behavior is observed. The model achieves an average error of 6.20% for a large database, performing equally well for polar and non-polar solutes, and in the whole pressure-temperature plane, while expressions from literature deliver 11.62-75.17% errors.

Molecular dynamics simulations were performed to study the diffusivities of propanone, butanone, 2-pentanone and 3-pentanone in SC-CO_2. They were computed using Einstein formula, and their dependence on temperature, pressure (or density), and molecular size was analyzed. A local structural

analysis was further accomplished by calculating some radial distribution functions and coordination numbers to disclose and interpret the local environment of CO_2 around each group composing ketone molecules.
An experimental setup to measure diffusion coefficients by chromatographic peak broadening technique was designed, assembled and tested. Tracer diffusivities of *α*-pinene in SC-CO_2 were determined at 313.15, 323.15 and 333.15 K, and pressures from 175 to 275 bar. The dependency of D_{12} upon temperature, pressure, solvent density, and hydrodynamic behavior has been examined in detail. Finally, the experimental data were modeled using equations developed in this work and good results were obtained (AARD = 2.48 – 3.56%); well-known expressions from the literature were also considered.

Index

1 Motivation and structure of the thesis

The design and simulation of rate controlled separations and multiphase reactions require the knowledge of both equilibrium and kinetic data. However, while a considerable number of solubility data has been published, diffusivities are still scarcer.

The binary diffusivities at infinite dilution, D_{12}, are frequently applied in Fick's law, being fundamental to estimate axial and radial dispersion coefficients, and convective mass transfer coefficients using dimensionless correlations [1, 2], and/or catalysts efficiency factors [3]. They can be applied directly into many industrial dilute systems, or using mixing rules such as those of Darken [4] and Vignes [5] to predict the necessary coefficients for concentrated solutions. Furthermore, when dealing with multicomponent systems, more complex approaches like Maxwell-Stefan [6] equations are required, which also need D_{12} to calculate pair diffusivities for the particular mixture composition. These facts highlight the importance of the study of this transport property.

In recent years there has been an increasing interest to replace chemically synthesized compounds by their biobased alternatives under the concept of biorefinery and sustainability [7]. Intimately related is the research and development of green and innovative solvents to perform separations and reactions, where supercritical carbon dioxide (SC-CO_2) and ionic liquids emerge as promising alternatives. Conventional organic solvents are many times non-

selective and toxic, which associated to the increasing consumer awareness of the use of hazardous substances by the chemical and food industries, along with changes in environmental regulations, constitute a driving force for the research of more environmentally friendly alternatives [7]. The choice of supercritical fluids has been attracting widespread interest owing to their well-documented properties: liquid-like densities, gas-like viscosities, negligible surface tensions, and diffusivities between those of gases and liquids [8, 9]. Furthermore, the ability to tune its solvent power by changing temperature and/or pressure or by introducing small quantities of polar co-solvents [8, 9] is undoubtedly an important feature. Then, they have a remarkable ability to be applied to mass-transfer operations, phase transition processes, reactive systems, materials related processes, and nanostructured materials, either at industrial capacity application or yet under development [10]. In last years, besides largely applied to extract edible and essential oils from natural matrices and other natural compounds [9, 11-15], supercritical fluids (SCFs) are also finding interest as solvents/desorbents in preparative chromatography and Simulated Moving Bed (SMB) separations [16, 17]. It is also worth mentioning the utilization of SC-CO_2 in the preparation and processing of advanced functional materials as catalysts or precursors, using organometallic solutes [18, 19], or other areas like impregnation and cleaning, coating, hydrogenation and biomass gasification [9, 10, 20].

Taking into account the large interest and wide applications of SC-CO_2, the availability of accurate diffusion coefficients in this solvent is crucial for the simulation and design of the implied processes.

The diffusivities may be experimentally measured, calculated *via* computer simulations, or estimated using phenomenological models. The three approaches are covered in this thesis: the molecular dynamics and macroscopic modeling are focused in Part I (Chapters 2, 3 and 4), followed by the experimental work compiled in Part II (Chapters 5 and 6). A brief description of the content of each chapter is presented hereafter.

Concerning phenomenological modeling, the development of accurate expressions to estimate diffusivities is very important since it is impossible to carry out experimental measurements for all systems at all operating conditions. Other drawbacks are the time

consuming of the measurements, the hazardous nature of some solutes, and the cost of chemicals/materials that also reinforce the need of reliable predictive D_{12} equations.

Several modeling approaches for the diffusion coefficients in dense fluids may be cited: the Enskog theory [21-23] for hard spheres and its modifications for real systems [21, 23], the effective hard sphere diameter method [23-26], the free-volume theories [23, 27-29], the van der Waals [23, 30, 31] and rough hard sphere principles [23, 32-37], the hydrodynamic models based on the Stokes-Einstein equation [38, 39], the Eyring activated-state theory [40], and excess entropy scaling laws [23, 41-43]. Several book chapters and papers reviewed most of these models [23, 38, 39, 43, 44].

The basic principles of transport of the above mentioned models prevail both in pure fluids (self-diffusivities) and mixtures (diffusivities), being possible to interconvert them by changing the properties of a trace molecule and adopting simple combining rules in the former equations. Additionally, notwithstanding the ultimate interest of diffusivities relies on real systems, the diffusive phenomena can be easily interpret by studying simplified hypothetical fluids like hard spheres and Lennard-Jones. In fact, molecularly based approaches are frequently adopted to develop equations for transport properties, particularly diffusion, by choosing approximate models as a starting point. Then, by gradually introducing additional effects and interactions, the behavior of real molecules can be finally reached. Some examples of this approach may be consulted in the works of Silva et al. [32] and Magalhães et al. [45].

In accordance with this approach, the thesis begins with the study of self-diffusion coefficients, for both model and real fluids, and the results are presented in Chapter 2. It is based on an international publication (Paper I) where entropy based scaling laws connecting reduced self-diffusion coefficients with residual entropy (almost always called excess entropy in this field) were studied. Here, a universal multivariate model (artificial neural networks) was developed for hard-sphere, Lennard-Jones, hard-sphere chain, and real (polar, non-polar, symmetrical and asymmetrical) fluids, and a new simple analytical expression was proposed and validated for spherical systems (hard-sphere and Lennard-Jones).

The investigation of tracer diffusion coefficients modeling starts in Chapter 3. Most D_{12} expressions found in the literature usually fail for systems involving polar molecules and/or very

asymmetric components (in terms of mass and size), and when applied over wide ranges of temperature and pressure. These limitations were overcome more recently with the development of accurate D_{12} correlations validated with large databases: molecularly based models, equations based on free-volume and Rice and Gray approaches [45-49], and semi-empirical expressions [50]. In the whole, excellent representations of experimental data were accomplished (errors lower than 4.44 % in general), and very good extrapolation ability was confirmed (deviations between 3.46 % and 5.27 %). Nonetheless, these models are frequently lengthy for D_{12} calculations, but fortunately some of the papers provide spreadsheets in supplementary material (online) [46, 48, 49] to carry out this task immediately. However, one limitation persists: they require one or two parameters that must be previously fitted to the experimental data of the system under study. This fact highlights the need for pure predictive models in order to estimate D_{12} for the systems of interest for research and industry nowadays.

Hence, in Chapter 3, only predictive expressions are devised to eliminate the need of any prior fitting procedure. They focus solutes in SC-CO_2 due to its recognized importance as solvent. Most of the expressions proposed are very simple and may be used by any non-expert user. They are: i) three improved Stokes-Einstein relations (Paper II) grafted on the Wilke-Chang, Scheibel and Lusis-Ratcliff equations by introducing two universal constants; ii) four improved hydrodynamic models (Paper III) embodying critical volumes instead of the volumes at normal boiling point included in the Wilke-Chang, Scheibel, Lusis-Ratcliff, and Tyn-Calus equations; and iii) a new model consisting of two contributions to accurately describe the diffusive behavior near and far from the critical point (Paper IV). It comprehends a background or regular term – based on a modified hydrodynamic equation very accurate in the critical region (far from the critical point) – and a singular term (that increases importance near the critical point) in order to describe the asymptotic behavior observed in this region (critical enhancement).

With respect to computer simulations, they are gradually preferred over experiment, which is usually more expensive and time consuming, and sometimes simply impossible. It is importante to possess reliable computational methods to predict D_{12} of solutes in SC-CO_2 for

the conditions of interest (generally those of supercritical extractions and reactions), without/diminishing the need to execute expensive (equipment and chemicals cost), dangerous (toxic compounds), demanding (exigent conditions required) and time-consuming experiments. The resulting values may be used together with experimental points to devise and validate mathematical models for their estimation and prediction. Moreover, molecular simulations give us the opportunity to study microscopic properties impossible to acess by experiments, such as microstructure and their connection to macroscopic properties. They allow us to disclose the influence of *e.g*. solute chemical groups, substituents, alkyl chain size, and molecular symmetry upon D_{12} values. Consequently, Chapter 4 contains classical modeling results from molecular dynamics simulations. It is based on a submitted essay (Paper V) where ketones were simulated in supercritical CO_2. Their tracer diffusivities were obtained and validated by comparison with experimental data, and then related with local structural properties like radial distribution functions and coordination numbers. The computer simulations were preceded by a detailed analysis of the effect of chief parameters like cut-off distance, number of solute molecules, integration time step, and length of the simulation upon the final results.

Modeling techniques are still dependent on experimental values, which cannot be totally eliminated. The diffusion coefficients in SCFs can be measured by several techniques, which are generally adapted from methodologies originally developed for gases, dense gases, and liquids: photo-correlation spectroscopy, geometric method, and chromatographic technique. The latest is the most popular nowadays because of its experimental procedure simplicity. It has been highly applied in the last decades for measuring diffusivities in supercritical systems, and it was also chosen in this work.

Accordingly, in Chapter 5 the chromatographic method is described, along with the experimental setup designed, assembled and tested in this dissertation, and the procedures adopted. The experimental results are presented in Chapter 6, where α-pinene diffusivitites in supercritical CO_2 have been assessed at 313.15, 323.15 and 333.15 K, and pressures from 175 to 275 bar (25 bar increments). The trends observed with temperature, pressure, and density are examined, together with the hydrodynamic behavior of the diffusivity values. The data are also modeled using expressions from the literature and from this work.

In Chapter 7 the main conclusions of the thesis are drawn, and suggestions for future work are presented.

References

[1] E.L.G. Oliveira, A.J.D. Silvestre, C.M. Silva, Review of kinetic models for supercritical fluid extraction, Chemical Engineering Research and Design, 89 (2011) 1104-1117.

[2] P.C. Wankat, Rate-Controlled Separations, Blackie Academic and Professional, Glasgow, UK, 1994.

[3] J.J. Carberry, Chemical and Catalytic Reaction Engineering, Dover Publications, Inc., New York, 2001.

[4] L.S. Darken, Diffusion, mobility and their interrelation through free energy in binary metallic systems, Transactions of the American Institute of Mining and Metallurgical Engineers, 175 (1948) 184-201.

[5] A. Vignes, Diffusion in binary solutions - Variation of diffusion coefficient with composition, Industrial & Engineering Chemistry Fundamentals, 5 (1966) 189-199.

[6] R. Taylor, R. Krishna, Multicomponent Mass Transfer, John Wiley & Sons, Inc, New York, 1993.

[7] C.A.M. Afonso, J.G. Crespo, Green Separation Processes. Fundamentals and Applications, Wiley – VCH Verlag, 2005.

[8] E. Kiran, P.G. Debenedetti, C.J. Peters, Supercritical Fluids: Fundamentals and Applications, 1st ed., Springer, 2000.

[9] M.M.R. de Melo, R.M.A. Domingues, A.J.D. Silvestre, C.M. Silva, Extraction and purification of triterpenoids using supercritical fluids: from lab to exploitation, Mini-Reviews in Organic Chemistry, 11 (2014) 362-381.

[10] G. Brunner, Applications of Supercritical Fluids, in: J.M. Prausnitz, M.F. Doherty, M.A. Segalman (Eds.) Annual Review of Chemical and Biomolecular Engineering, Vol 1, 2010, pp. 321-342.

[11] C.P. Passos, R.M. Silva, F.A. Da Silva, M.A. Coimbra, C.M. Silva, Supercritical fluid extraction of grape seed (Vitis vinifera L.) oil. Effect of the operating conditions upon oil composition and antioxidant capacity, Chemical Engineering Journal, 160 (2010) 634-640.

[12] A. Capuzzo, M. Maffei, A. Occhipinti, Supercritical fluid extraction of plant flavors and fragrances, Molecules, 18 (2013) 7194-7238.

[13] R.M.A. Domingues, E.L.G. Oliveira, C.S.R. Freire, R.M. Couto, P.C. Simoes, C.P. Neto, A.J.D. Silvestre, C.M. Silva, Supercritical Fluid Extraction of Eucalyptus globulus Bark-A Promising Approach for Triterpenoid Production, International Journal of Molecular Sciences, 13 (2012) 7648-7662.

[14] C.P. Passos, R.M. Silva, F.A. Da Silva, M.A. Coimbra, C.M. Silva, Enhancement of the supercritical fluid extraction of grape seed oil by using enzymatically pre-treated seed, The Journal of Supercritical Fluids, 48 (2009) 225-229.

[15] T. Fornari, G. Vicente, E. Vazquez, M.R. Garcia-Risco, G. Reglero, Isolation of essential oil from different plants and herbs by supercritical fluid extraction, Journal of Chromatography A, 1250 (2012) 34-48.

[16] M. Mazzotti, G. Storti, M. Morbidelli, Supercritical fluid simulated moving bed chromatography, Journal of Chromatography A, 786 (1997) 309-320.

[17] J.P.S. Aniceto, C.M. Silva, Simulated Moving Bed strategies and designs: from established systems to the latest developments, separation and Purifiction Reviews, (submitted).

[18] Y. Zhang, C. Erkey, Preparation of supported metallic nanoparticles using supercritical fluids: A review, The Journal of Supercritical Fluids, 38 (2006) 252-267.

[19] F. Cansell, C. Aymonier, Design of functional nanostructured materials using supercritical fluids, The Journal of Supercritical Fluids, 47 (2009) 508-516.

[20] M.M.R. de Melo, A.J.D. Silvestre, C.M. Silva, Supercritical fluid extraction of vegetable matrices: applications, trends and future perspectives of a convincing green technology, The Journal of Supercritical Fluids, 92 (2014) 115-176.

[21] J. Millat, J.H. Dymond, C.A. Nieto de Castro, Transport Properties of Fluids – Their Correlation, Prediction and Estimation, Cambridge University Press, London, 1996.

[22] H.J.M. Hanley, R.D. McCarty, E.G.D. Cohen, Analysis of the transport coefficients for simple dense fluid: Application of the modified Enskog theory, Physica, 60 (1972) 322-356.

[23] C.M. Silva, H. Liu, Modelling of Transport Properties of Hard Sphere Fluids and Related Systems, and its Applications, in: Á. Mulero (Ed.) Theory and Simulation of Hard-Sphere Fluids and Related Systems, Springer Berlin Heidelberg, 2008, pp. 383-492.

[24] J.A. Barker, D. Henderson, Perturbation theory and equation of state for fluids. II. A successful theory of liquids, Journal of Chemical Physics, 47 (1967) 4714-4721.

[25] J.D. Weeks, D. Chandler, H.C. Andersen, Role of repulsive forces in determining equilibrium structure of simple liquids, Journal of Chemical Physics, 54 (1971) 5237-5247.

[26] C.M. Silva, H.Q. Liu, E.A. Macedo, Comparison between different explicit expressions of the effective hard sphere diameter of Lennard-Jones fluid: Application to self-diffusion coefficients, Industrial & Engineering Chemistry Research, 37 (1998) 221-227.

[27] M.H. Cohen, D. Turnbull, Molecular Transport in Liquids and Glasses, The Journal of Chemical Physics, 31 (1959) 1164-1169.

[28] P.B. Macedo, T.A. Litovitz, On the relative roles of free volume and activation energy in the viscosity of liquids, The Journal of Chemical Physics, 42 (1965) 245-256.

[29] H. Liu, C.M. Silva, E.A. Macedo, Generalised free-volume theory for transport properties and new trends about the relationship between free volume and equations of state, Fluid Phase Equilibria, 202 (2002) 89-107.

[30] J.H. Dymond, Corrected Enskog theory and the transport coefficients of liquids, The Journal of Chemical Physics, 60 (1974) 969-973.

[31] J.H. Dymond, The interpretation of transport coefficients on the basis of the Van der Waals model: I dense fluids, Physica, 75 (1974) 100-114.

[32] H. Liu, C.M. Silva, E.A. Macedo, Unified approach to the self-diffusion coefficients of dense fluids over wide ranges of temperature and pressure—hard-sphere, square-well, Lennard–Jones and real substances, Chemical Engineering Science, 53 (1998) 2403-2422.

[33] S.-H. Chen, A rough-hard-sphere theory for diffusion in supercritical carbon dioxide, Chemical Engineering Science, 38 (1983) 655-660.

[34] C. Erkey, H. Gadalla, A. Akgerman, Application of rough hard sphere theory to diffusion in supercritical fluidst, The Journal of Supercritical Fluids, 3 (1990) 180-185.

[35] E. Ruckenstein, H.Q. Liu, Self-diffusion in gases and liquids, Industrial & Engineering Chemistry Research, 36 (1997) 3927-3936.

[36] H. Liu, C.M. Silva, E.A. Macedo, New equations for tracer diffusion coefficients of solutes in supercritical and liquid solvents based on the Lennard-Jones fluid model, Industrial & Engineering Chemistry Research, 36 (1997) 246-252.

[37] D. Chandler, Rough hard sphere theory of the self-diffusion constant for molecular liquids, The Journal of Chemical Physics, 62 (1975) 1358-1363.

[38] R.C. Reid, J.M. Prausnitz, B.E. Poling, The Properties of Gases and Liquids, 4th ed., McGraw-Hill, New York, 1987.

[39] K.K. Liong, P.A. Wells, N.R. Foster, Diffusion in supercritical fluids, The Journal of Supercritical Fluids, 4 (1991) 91-108.

[40] S.N. Glasstone, K. Laider, H. Eyring, The theory of rate processes, McGraw-Hill, New York, 1941.

[41] M. Dzugutov, A universal law for atomic diffusion in condensed matter, Nature, 381 (1996) 137-139.

[42] Y. Rosenfeld, Relation between the transport coefficients and the internal entropy of simple systems, Physical Review A, 15 (1977) 2545-2549.

[43] R.V. Vaz, A.L. Magalhães, D.L.A. Fernandes, C.M. Silva, Universal correlation of self-diffusion coefficients of model and real fluids based on residual entropy scaling law, Chemical Engineering Science, 79 (2012) 153-162.

[44] I. Medina, Determination of diffusion coefficients for supercritical fluids, Journal of Chromatography A, 1250 (2012) 124-140.

[45] A.L. Magalhães, F.A. Da Silva, C.M. Silva, New models for tracer diffusion coefficients of hard sphere and real systems: Application to gases, liquids and supercritical fluids, The Journal of Supercritical Fluids, 55 (2011) 898-923.

[46] A.L. Magalhães, F.A. Da Silva, C.M. Silva, Free-volume model for the diffusion coefficients of solutes at infinite dilution in supercritical CO_2 and liquid H_2O, The Journal of Supercritical Fluids, 74 (2013) 89-104.

[47] A.L. Magalhães, F.A. Da Silva, C.M. Silva, New tracer diffusion correlation for real systems over wide ranges of temperature and density, Chemical Engineering Journal, 166 (2011) 49-72.

[48] A.L. Magalhães, F.A. Da Silva, C.M. Silva, Tracer diffusion coefficients of polar systems, Chemical Engineering Science, 73 (2012) 151-168.

[49] P.F. Lito, A.L. Magalhães, J.R.B. Gomes, C.M. Silva, Universal model for accurate calculation of tracer diffusion coefficients in gas, liquid and supercritical systems, Journal of Chromatography A, 1290 (2013) 1-26.

[50] A.L. Magalhães, P.F. Lito, F.A. Da Silva, C.M. Silva, Simple and accurate correlations for diffusion coefficients of solutes in liquids and supercritical fluids over wide ranges of temperature and density, The Journal of Supercritical Fluids, 76 (2013) 94-114.

2 Modeling self-diffusion coefficients of model and real fluids

The aim of this chapter is the study of self-diffusion coefficients, D_{11}, of model and real fluids due to their importance for the development of equations to estimate Fick´s binary diffusivities. When molecularly based approaches are adopted to develop equations for transport properties, particularly diffusion, it is frequent to choose simplified hypothetical fluids represented by basic models as a starting point. Then, by gradually introducing additional effects and interactions, the behavior of real molecules is finally reached. Some examples of this approach may be consulted in the works of Silva et al. [1] and Magalhães et al. [2, 3]. Moreover, the basic principles of diffusion prevail in pure fluids and mixtures, being possible to interconvert them by changing the particle parameters of a trace molecule and using simple combining rules.

For the above reasons, the modeling results of this thesis begins with the study of self-diffusion coefficients, for both model and real fluids. Among all transport theories, the entropy based scaling laws were focused given the challenge they represent, *i.e.* to relate dynamic with structural properties. More specifically, transport properties – reduced self-diffusivities – are connected with a thermodynamic property – reduced residual entropy. The known entropy based scaling laws of Rosenfeld [4], Dzugutov [5] and Bretonnet [6] were tested (Paper I) for model (hard-sphere, Lennard-Jones, and hard-sphere chain) and real fluids, over a wide range of temperature and density. For that, an extensive database with 1727 diffusivity values was

compiled for the referred fluids. It was shown that the expressions from literature fail, even for simple fluids for which they were developed, and a dependence of D_{11} on the molecular length chain and residual entropy was identified. Accordingly, a new universal correlation was proposed to accurately estimate diffusivities of all fluids studied, as function both variables. This model was based on artificial neural networks and provided a deviation of 9.13% for the entire database: model and reals fluids, spherical or asymmetrical, and polar or nonpolar. Furthermore, another simpler analytical expression was devised for hard-spheres and Lennard-Jones, which offers only 4.61% of error for 657 data points.

References

[1] H. Liu, C.M. Silva, E.A. Macedo, Unified approach to the self-diffusion coefficients of dense fluids over wide ranges of temperature and pressure—hard-sphere, square-well, Lennard–Jones and real substances, Chemical Engineering Science, 53 (1998) 2403-2422.

[2] A.L. Magalhães, F.A. Da Silva, C.M. Silva, New models for tracer diffusion coefficients of hard sphere and real systems: Application to gases, liquids and supercritical fluids, The Journal of Supercritical Fluids, 55 (2011) 898-923.

[3] A.L. Magalhães, F.A. Da Silva, C.M. Silva, New tracer diffusion correlation for real systems over wide ranges of temperature and density, Chemical Engineering Journal, 166 (2011) 49-72.

[4] Y. Rosenfeld, Relation between the transport coefficients and the internal entropy of simple systems, Physical Review A, 15 (1977) 2545-2549.

[5] M. Dzugutov, A universal scaling law for atomic diffusion in condensed matter, Nature, 381 (1996) 137-139.

[6] J.L. Bretonnet, Self-diffusion coefficient of dense fluids from the pair correlation function, Journal of Chemical Physics, 117 (2002) 9370-9373.

Paper I

Adapted from

Universal Correlation of Self-diffusion Coefficients of Model and Real Fluids Based on Residual Entropy Scaling Law

Chemical Engineering Science, 79 (2012) 153-162

Abstract

In this work, the entropy based scaling laws of Rosenfeld, Dzugutov and Bretonnet, which connect reduced self-diffusion coefficients (D^*) with residual entropy (named excess entropy in this field), were analyzed in order to test their attributed universal character. With this purpose, an extensive database with 1727 molecular dynamic and experimental values was compiled for hard-sphere (HS), Lennard-Jones (LJ), hard-sphere chain (HSC), and real (polar, non-polar, symmetrical and asymmetrical) fluids. It was shown that these equations fail when tested over the entire range of density and temperature (through residual entropy), even for atomic and simple fluids (e.g., HS and LJ) for which they have been originally proposed. Furthermore, the dependence of the self-diffusivities upon both residual entropy and a molecular chain length parameter (r) was clearly found on the basis of HSC and real data. Accordingly, a new universal correlation for the estimation of D^* as function of residual entropy and r was obtained, giving rise to an average absolute relative deviation of 9.13% for all database. It was also devised a very simple and accurate entropy based equation for spherical systems (HS and LJ) which provides only 4.61% of error. The original Rosenfeld, Dzugutov and Bretonnet's expressions attain deviations that are several orders of magnitude higher than our values.

1. Introduction

The transport properties of fluids, such as diffusivity and viscosity, are of immense importance not only for understanding their structure and thermophysical behavior, but also for practical engineering applications. These coefficients may be defined in terms of the response of a system to a perturbation; for instance, diffusion coefficient (D) relates the particle flux with a concentration gradient [1-2].

In the past years, several models and correlations have been proposed in the literature to calculate diffusion coefficients of fluids, usually by studying hypothetical model systems and extending them to represent real systems [2-8].

At low densities, diffusivities may be estimated by some theoretical methods, like those based on the kinetic theory of Enskog and its modifications [9-11]. For dense fluids, including liquids and supercritical fluids, no theory can provide reliable predictions because departures

from dilute values become significantly larger. In this case, computer simulations play an important role to estimate proper corrections [2, 11-12].

Important approaches to calculate transport properties include the effective hard-sphere diameter method which takes advantage of the fact that repulsive molecular interactions play a major role in determining dense gas and liquid properties and attractive interactions are secondary. Hence, hard-spheres (HS) are used as first approximation and an effective diameter dependent on temperature and possibly on density is then used to account for the softness of the repulsive potential [2, 4]. An alternative procedure is that of free volume, where transport coefficients depend on the relative expansion of the fluid from an intrinsic molar volume V_{i}. The chief models include a dependence just upon the molar free volume, $V_{\mathrm{f}} = V_{\mathrm{m}} - V_{\mathrm{i}}$, or combine the concepts of free volume and activation energy, E_{a}, to account for both repulsive and attractive interactions [2-3, 5]. Some equations introduce the concept of rough hard-sphere by which angular and linear momentum are exchanged during collision [2-3, 5, 13-14]. A frontal coefficient $0 < A_{\mathrm{D}} \leq 1$ is included in order to reduce the value of the diffusion coefficient due to loss of linear momentum, depending on temperature and/or density [2, 13].

A very important theory of transport is that of the entropy based scaling laws [2, 15-17], which relate dynamic and structural properties (such as entropy), being one of the most challenging tasks in the field of condensed matter. For that reason, an interesting approach to transport properties is to connect them with equilibrium thermodynamic properties, according to plots of reduced coefficients, D^*, against reduced residual (*i.e.* configurational, over the ideal-gas value) entropy, $S^{\mathrm{res}}/Nk_{\mathrm{B}}$, though it is always referred as reduced excess entropy in the literature [15-23]:

$$D^* = D^*\left(S^{\mathrm{res}}/Nk_{\mathrm{B}}\right) \tag{1}$$

Here, k_{B} is the Boltzmann's constant and N is the number of particles.

The residual entropy can be calculated using equations of state (EoS) adequate for the fluids under study by:

$$\frac{S^{\text{res}}}{Nk_{\text{B}}} = -\int_0^{\rho}\left[\, T\left(\frac{\partial Z}{\partial T}\right)_{V,N} + (Z-1)\right]\frac{d\rho}{\rho} \tag{2}$$

where $\rho \equiv N/V$ is the number density, T is the temperature, Z is the compressibility factor, and V is the volume. The first term composing the integral of Eq. (2) vanishes when the attractive contribution is not considered (purely repulsive potentials).

A first attempt connecting dynamic and structural fluid properties was made by Rosenfeld in 1977, with a relation that revealed some universal characteristics. Rosenfeld defined a reduced self-diffusion coefficient (D_{R}^{*}) scaled by macroscopic parameters, namely a mean interparticle distance, $d = \rho^{-1/3}$, and a thermal velocity, $\upsilon = \sqrt{k_{\text{B}}T/m}$, by:

$$D_{\text{R}}^{*} = D\frac{\rho^{1/3}}{\sqrt{k_{\text{B}}T/m}} \tag{3}$$

where m is the particle mass. The reduced diffusion coefficient was shown to be regressed to the residual entropy in a quasi-universal behavior [15] by:

$$D_{\text{R}}^{*} = 0.585\exp\left(0.788\frac{S^{\text{res}}}{Nk_{\text{B}}}\right) \tag{4}$$

This relation was inspected by using molecular dynamics (MD) data for hard-sphere (HS), soft sphere (SS), one-component plasma (OCP), and Lennard-Jones (LJ) systems, though it was only demonstrated with around 35 data points for SS and LJ systems. Distinct potentials can be better fitted by somewhat different exponential argument, as in the case of HS [15]:

$$D_{\text{R}}^{*} \propto \exp\left(0.65S^{\text{res}}/Nk_{\text{B}}\right) \tag{5}$$

Later, Rosenfeld [24] recognized that his original scaling law was only approximately exponential and took a power-law form for dilute fluids with inverse power potentials of the type $\phi = \varepsilon(\sigma/r)^{\nu}$:

$$D_{\text{R}}^{*} = D_0\left(-S^{\text{res}}/Nk_{\text{B}}\right)^{-2/3} \tag{6}$$

where D_0 varies between 0.409 and 0.346 in the range 4 – ∞ of ν. The unique exponential dependence of Rosenfeld's reduction was also contradicted later in the case of softer bounded potentials [20], characteristic of inherently interpenetrable particles, whose simpler example

corresponds to the Gaussian-core fluid, $\phi = \varepsilon \exp\left[-(r/\sigma)^2\right]$. In these cases, the relationship $D_R^* = D_R^*\left(S^{res}/Nk_B\right)$ at different densities do not collapse onto a single curve, despite the similar qualitative behaviors exhibited by the distinct curves.

Dzugutov [16] proposed a variant of the entropy scaling originally devised by Rosenfeld, following a microscopic reduction approach on the basis of two prepositions. First, energy and momentum transfer in liquids is mainly governed by uncorrelated binary collisions described by the Enskog theory. Hence, the diffusion coefficients were expressed in units of $\sigma^2\Gamma_E$:

$$D_D^* = \frac{D}{\sigma^2\Gamma_E} \tag{7}$$

where σ is the hard-sphere diameter that corresponds practically to the position of the first peak of the pair correlation function, $g(\sigma)$, and $\Gamma_E = 4\sigma^2 g(\sigma)\rho\sqrt{\pi k_B T/m}$ is the collision frequency of Enskog theory. Dzugutov also supposed that the frequency of local structural relaxations, which defines the rate of cage diffusion, is proportional to the number of accessible configurations. In an equilibrium system, this number is reduced by a factor $\exp\left(S^{res}\right)$ due to the constrains imposed by the structural correlations [16]. Thus, D_D^* and $\exp\left(S^{res}\right)$ should be connected at first glance by a linear relationship. For several model liquids including HS, LJ, two component LJ, liquid Pb, liquid Cu, icosahedral local order liquid, liquid with local order topologically related to the primitive hexagonal lattice with only six nearest neighbor, and Ag diffusion in AgI (just over 40 MD points in total), Dzugutov proposed the following scaling law for the diffusion coefficient:

$$D_D^* = 0.049\exp\left(\frac{S^{res}}{Nk_B}\right) \tag{8}$$

Dzugutov assumed that the residual entropy is only given in terms of the pair correlation function, independently of whether or not the potential energy is pairwise additive, so it can be restricted to the two-body approximation.

Although Dzugutov's conjecture was tested with MD simulations of several fluids, Bretonnet [17] showed, from an analysis of HS fluid properties, that Eq. (8) is only legitimate

over a restricted range of reduced densities ($\rho^* = \rho\sigma^3$) around 0.7, corresponding to S^{res}/Nk_B = -2.5.

Additionally, Goel et al. [19] shown that Dzugutov's scaling is less accurate than Rosenfeld's relationships using Lennard-Jones chains data, whose differences originate from the different reduction parameters utilized. Moreover, in the case of Lennard-Jones fluid, the pair correlation contribution to the residual entropy attains 85 – 90% of the total property [25], which means that Dzugutov's scaling law may be viewed as a special case of the Rosenfeld's one based on microscopic, rather than macroscopic, reduction parameters [19].

Bretonnet [17] presented a new semi-empirical expression for D from the analysis of the structural, thermodynamic and transport properties of the HS fluid:

$$D = \frac{\sigma}{8}\left(\frac{\pi k_B T}{m}\right)^{1/2} \frac{(1-\varphi)^4}{\varphi(2+\varphi)} \exp\left(\frac{6\varphi}{1-\varphi}\right) \exp\left(\frac{S^{res}}{Nk_B}\right) \tag{9}$$

where $\varphi = \frac{\pi}{6}\rho\sigma^3 = \frac{\pi}{6}\rho^*$ is the packing density. Accordingly, an appropriate reduced diffusion coefficient may be proposed in order to maintain the same type of exponential dependence for D_B^*:

$$D_B^* \equiv D \frac{8\varphi(2+\varphi)}{\sigma\left(\frac{\pi k_B T}{m}\right)^{1/2}(1-\varphi)^4 \exp\left(\frac{6\varphi}{1-\varphi}\right)} \tag{10}$$

Very recently, intensive research is being carried out on residual entropy scaling laws for the diffusion coefficients, mainly testing their universal character taking into account distinct model and real fluids. For instance, the diverging dynamic behavior of Gaussian-core, star-polymer, Hertzian, Lennard-Jones chains, hard fused sphere chains, and SPC/E water potentials, as well as hydrocarbon isomers (*n*-octane, 2,2-dimethylhexane, 2,5-dimethylhexane, and 3-methyl-3-ethylpentane), homologous series of alkanes (C1-C16) and other compounds [18-23] have received much attention.

Particularly interesting is the study of the well known anomalous diffusional behavior of water, since specific models like SPC/E water or the ultrasoft ones aforementioned generate cascading regions of density, self-diffusivity, and structural (measured by the two-body entropy,

S_2) anomalies. In those regions, the relationship between D_R^* and S_2 is that perfectly expected in advance but not between D_R^* and S^{res}. This breakdown is likely due to the fact that these potentials are intrinsically soft and the macroscopic reduction parameters of Rosenfeld are not appropriate since they are based on the kinetic theory concepts for atomistic fluids with strongly repulsive cores. Nonetheless, increasing pressure, liquid water corrects its deviation and recovers normal (*i.e.* simple fluid) behavior with consequent notorious approximation to the Rosenfeld's law [23], owing to the steeply repulsive interactions which dominate its physics at sufficiently high densities. It is worth noting that the Gaussian-core fluid, with soft and bounded interparticle interactions, never returns to hard-sphere-like structural and dynamic behavior at high density, thus subsisting an appreciable departure from the trivial linear trend [20, 23].

In view of the absence of a unifying quantitative description of molecular transport in fluids, the scaling laws are important for estimating unknown diffusion coefficients and for providing guidelines for theoretical analysis. So, further studies are necessary to confidently label a universal scaling law and use it accordingly.

Taking into account this introduction, the main goals of this paper are: (i) the comparison and analysis of the various scaling laws described above, to evaluate their accuracy and universal character in the whole density range of interest; (ii) the proposal of a new entropy based correlation for the accurate prediction of self-diffusion coefficients of different fluids over wide ranges of density and temperature, where a new independent variable accounting for molecules asymmetry is included; (iii) to validate our model, a large database comprehending model and real fluids (1727 data points of HS, LJ, hard-sphere chains (HSC), and real spherical and asymmetrical, non-polar and polar molecules) was compiled in order to investigate various molecular shapes, interactions and behaviors, and more universally describe diffusional transport; (iv) finally, due to the importance of the HS and LJ systems, a simple and very accurate equation is proposed specifically for them.

2. Database

With the purpose to analyze the universal character of Rosenfeld, Dzugutov and Bretonnet's equations, a large database containing 1727 self-diffusivities of model (HS, LJ, and HSC) and real fluids has been collected. For the HS fluid, diffusion coefficients from Alder et al. [26] and Erpenbeck and Wood [27] were used, ranging from reduced densities of 0.0141 to 0.9428. Data published by Smith et al. [28] for HSC were also included (reduced density range 0.1910–0.9549). For the LJ fluid, 642 points were gathered, covering reduced density and temperature ranges 0.005–1.275 and 0.687–6.02, respectively [29-37]. The reduced temperature is given by $T^* = T/\left(\varepsilon_{\mathrm{LJ}}/k_{\mathrm{B}}\right)$, where $\varepsilon_{\mathrm{LJ}}$ is the depth of the LJ potential well. A summary of the data collected for real fluids may be found in Table 1. They comprehend 21 distinct components between polar and non-polar, symmetrical and asymmetrical, in a total of 1042 points. It is worth noting that the three scaling laws will be tested here not only with conventional fluids, like HS and LJ, but also with chainlike particles, as HSC and a set of asymmetrical real molecules.

3. Results and discussion

3.1 Hard-sphere and Lennard-Jones fluids

One objective of this essay is to present another contribution for the analysis of the universality of the Rosenfeld, Dzugutov and Bretonnet's scaling laws for the different types of fluids under study, since their original validity has been accomplish with a very small number of data points and small ranges of ρ^* and T^*.

For the HS fluid, the Carnahan-Starling [65] (CS) EoS was used (Eq. (21), Table 2) for the calculation of S^{res} by Eq. (2), giving rise to:

$$\frac{S^{\mathrm{res}}}{Nk_{\mathrm{B}}} = -\varphi\frac{4-3\varphi}{\left(1-\varphi\right)^2} \tag{11}$$

Table 1. Properties and references of the self-diffusivities of the real fluids studied.

No.	molecule	M_w (g/mol)	T_c (K)	P_c (bar)	ω	NDP	Ref.
1	acetone	58.080	508.1	47.0	0.304	3	[38]
2	benzene	78.114	562.2	48.9	0.212	82	[39-41]
3	carbon dioxide	44.010	304.1	73.8	0.239	259	[42], [43-48]
4	carbon disulphide	76.131	552	79.0	0.109	29	[49]
5	carbon monoxide	28.010	132.9	35.0	0.066	9	[50]
6	chloromethane	50.448	416.25	66.79	0.153	44	[51]
7	cyclohexane	98.189	572.2	34.7	0.236	39	[52]
8	cyclopentane	70.134	511.76	45.02	0.194	21	[53]
9	*n*-decane	142.286	617.7	21.2	0.489	6	[54]
10	dichlorometane	84.932	510.00	60.8	0.192	38	[51]
11	ethane	30.070	305.4	48.8	0.099	71	[55], [54]
12	ethylene	28.054	282.4	50.4	0.089	25	[56]
13	*n*-heptane	100.205	540.3	27.4	0.349	3	[57]
14	*n*-hexadecane	226.448	722	14.1	0.742	25	[58]
15	*n*-hexane	86.178	507.5	30.1	0.299	65	[54], [59]
16	methane	16.043	190.4	46.0	0.011	56	[60], [55], [54]
17	methylcyclohexane	98.189	572.2	34.7	0.236	31	[61]
18	*n*-octane	114.232	568.8	24.9	0.398	49	[54], [62]
19	propane	44.094	369.8	42.5	0.153	84	[55]
20	toluene	92.141	591.8	41.0	0.236	54	[62]
21	trimethylamine	59.111	433.25	40.73	0.209	49	[63]

Molecular weight, M_w, critical temperature, T_c, critical pressure, P_c, and acentric factor, ω, were taken from Yaws [64] (numbers 6, 8, 10 and 21) and Reid et al. [12] (the remaining ones).

Since the HS self-diffusivities found in the literature are commonly presented as $D^{*}_{HS} \equiv D_{HS}/D_{Enskog}$, i.e. normalized with Enskog values, they were previously converted to the reduced units of Rosenfeld, Dzugutov and Bretonnet according to:

$$D_{\mathrm{R}}^{*} = \frac{3}{8\sqrt{\pi}\, g(\sigma)\left(\rho^{*}\right)^{2/3}} D_{\mathrm{HS}}^{'} \tag{12}$$

$$D_{\mathrm{D}}^{*} = \frac{3}{32\pi\, g^{2}(\sigma)\left(\rho^{*}\right)^{2}} D_{\mathrm{HS}}^{'} \tag{13}$$

$$D_{\mathrm{B}}^{*} = \frac{3\varphi(2+\varphi)}{\pi\, g(\sigma)\rho^{*}(1-\varphi)^{4}\exp\left(\frac{6\varphi}{1-\varphi}\right)} D_{\mathrm{HS}}^{'} \tag{14}$$

Concerning the LJ fluid, the EoS of Nicolas et al. [66] (Eq. (26), Table 2) was utilized since it is one of the most successful correlations to represent simulation data. It uses a modified Benedict-Webb-Rubin (MBWR) equation with 33 parameters, 32 of which are linear. Such large number of adjustable parameters provides sufficient flexibility to correlate data accurately over a wide range of state conditions. Besides the original parameters presented by Nicolas et al. [66], we also tested the parameters refitted later by Johnson et al. [67] since the computer simulation data used by the first authors are prior to 1980s, mainly for small systems and short run times, and, in addition, there were few vapor-liquid equilibrium data available, and the LJ critical point was not known so accurately at that time.

The reduced form of D usually found in literature for LJ fluids ($D_{\mathrm{LJ}}^{'} \equiv D_{\mathrm{LJ}} \Big/ \sqrt{\varepsilon\sigma^{2}/m}$) also differs from those considered by Rosenfeld, Dzugutov and Bretonnet. Hence, the transformations carried out in this work in order to get the desired dimensionless units are:

$$D_{\mathrm{R}}^{*} = \frac{\left(\rho^{*}\right)^{1/3}}{\left(T^{*}\right)^{1/2}} D_{\mathrm{LJ}}^{'} \tag{15}$$

$$D_{\mathrm{D}}^{*} = \frac{D_{\mathrm{LJ}}^{'}}{4\sqrt{\pi}\, g(\sigma)\rho^{*}\left(T^{*}\right)^{1/2}} \tag{16}$$

$$D_{\mathrm{B}}^{*} = \frac{8}{\sqrt{\pi}\left(T^{*}\right)^{1/2}} \frac{\varphi(2+\varphi)}{(1-\varphi)^{4}\exp\left(\frac{6\varphi}{1-\varphi}\right)} D_{\mathrm{LJ}}^{'} \tag{17}$$

The radial distribution function at contact, $g(\sigma)$, in Eq. (16) was calculated with Carnahan-Starling EoS after substituting σ by the effective diameter of Liu et al. [2-4]:

$$\sigma_{eff} = 2^{1/6}\sigma\left[1+\left(1.3229T^{*}\right)^{1/2}\right]^{-1/6} \tag{18}$$

In Figs. 1-3 the reduced self-diffusion coefficients of HS and LJ fluids calculated by Rosenfeld, Dzugutov and Bretonnet's approaches as function of residual entropy are shown. Also graphed for comparison are the original correlations of each author, Eqs. (4), (8) and (9), respectively. The pronounced scattering provided by Bretonnet's reduction (Fig. 3) prevents its application to LJ, though reliable linearity is observed for HS. This may be attributed to the fact that the original studies performed by Bretonnet included just HS data. For the remaining approaches similar results are observed: high diffusivities in the vicinity of ideal gas followed by a linear zone in the range $1 < -S^{res}/Nk_B < 4$. Nonetheless, HS diffusivities do not lie on the same line of the LJ results over the entire entropy region, exhibiting superior values at higher entropies due to the nonexistence of attractive forces. In fact, Figs. 1 and 2 show that for $-S^{res}/Nk_B > 2.5$, D^{*}_{HS} are higher then D^{*}_{LJ}. From our calculations it is evident not only the non-linearity of all relations, but also their non-applicability in all density range even for simple atomic fluids. However, Rosenfeld's approach provides much better results. Besides, it should be emphasized that Goel et al. [19] came to the same conclusion that Dzugutov's reduction offers worst results also for Lennard-Jones chains. For this reason, Eq. (3) has been chosen for the reduction of the diffusivities of the remaining fluids analyzed in this work, in order to seek for a universal relation between D^{*} and S^{res}.

3.2 Hard-sphere chain (HSC) fluid

With the objective to test the applicability of Eqs. (3) and (4) to molecules that clearly detach from atomic like particles, the hard-sphere chain model fluid was also included in this research. This study was fundamental to develop and propose an adequate and theoretically sound correlation for the self-diffusion coefficients of real fluids (in section 3.4) giving the variety of sizes and shapes they present.

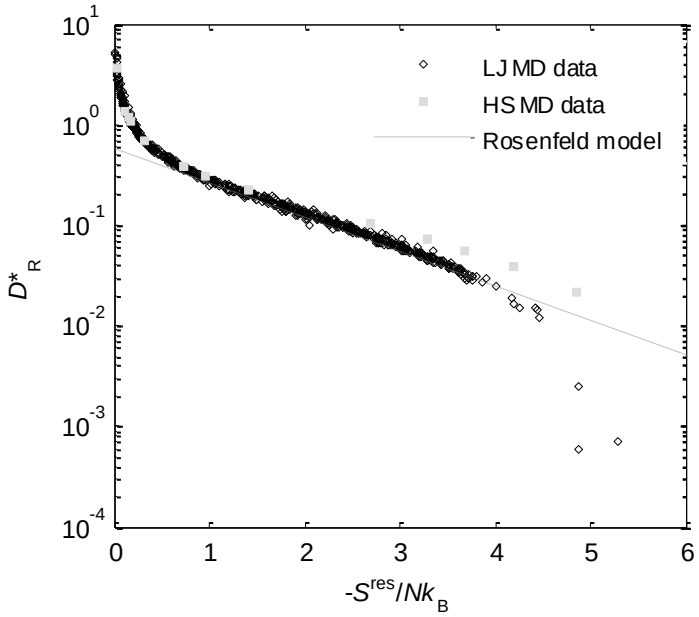

Fig. 1. Self-diffusion coefficients reduced according to Rosenfeld's approach *versus* residual entropy for LJ and HS fluids. Residual entropy of the LJ fluids was calculated with Johnson et al. EoS [67]. Data from [26-27, 29-37].

Besides its accuracy and wide application, CS equation was developed for hard-spheres, so it is not appropriate to predict properties of chainlike fluids. For that reason, an extension of the CS EoS proposed by Kim and Bae [68] (Eqs. (22)-(25), Table 2) was employed for the HSC fluid in this work. It contains one parameter, r, that represents the number of hard-sphere segments in the molecule, so it is a measure of molecular asymmetry.

Once more, it was necessary to convert the MD data of the literature to attain the pretended dimensionless units of Rosenfeld. The reduced self-diffusivities are available as $D^{'}_{\mathrm{HSC}} \equiv D_{\mathrm{HSC}} \big/ \left(k_{\mathrm{B}}T/m\sigma^2\right)^{1/2} \sigma^2$ and were converted here according to the following transformation:

$$D^*_{\mathrm{R}} = \left(\rho^*\right)^{1/3} D^{'}_{\mathrm{HSC}} \tag{19}$$

The results accomplished for the HSC fluids are plotted in Fig. 4 and demonstrate the existence of independent curves for each r. An increasing number of segments (r) in the chain leads to augmenting residual entropy (for the same D^*) due to the increasing departure to the

ideal gas behavior. These strongly divergent curves at increasing densities which depend on the chain length and converge at zero density are analogous to those obtained by Gerek and Elliott [18] for Hard Fused Sphere Chains. These findings also corroborate results achieved by Goel et al. [19] for Lennard-Jones chains, who observed distinct curves for different chain lengths in the region $S^{\mathrm{res}}/Nk_{\mathrm{B}} \in]-3;-0.75[$. Due to the small interval studied, such relations are approximately linear, which means the dependence between $\ln D_{\mathrm{R}}^{*}$ and S^{res} follows Rosenfeld's proposal but with length-specific parameters [19]. Hence, Rosenfeld's conjecture is not directly applicable to reference chain fluids, *i.e.* S^{res} is insufficient to lump all effects that ultimately affect the diffusional behavior of non-atomic fluids.

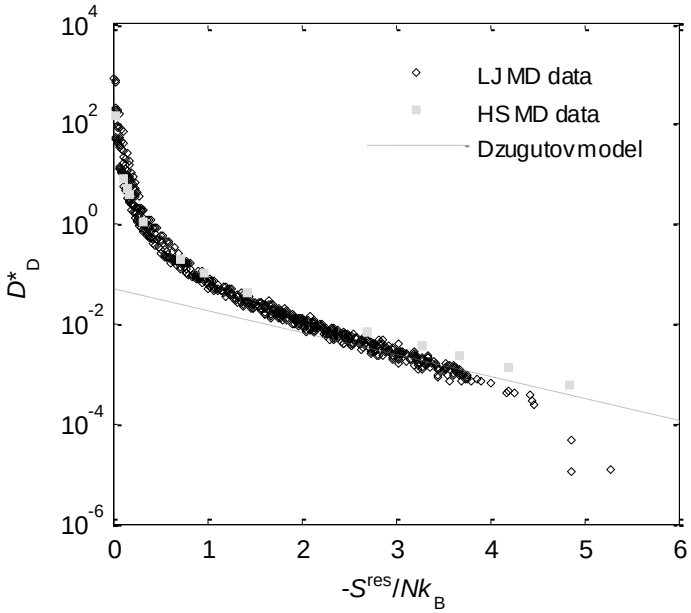

Fig. 2. Self-diffusion coefficients reduced according to Dzugutov's approach *versus* residual entropy for LJ and HS fluids. Residual entropy of the LJ fluids was calculated with Johnson et al. EoS [67]. Data from [26-27, 29-37].

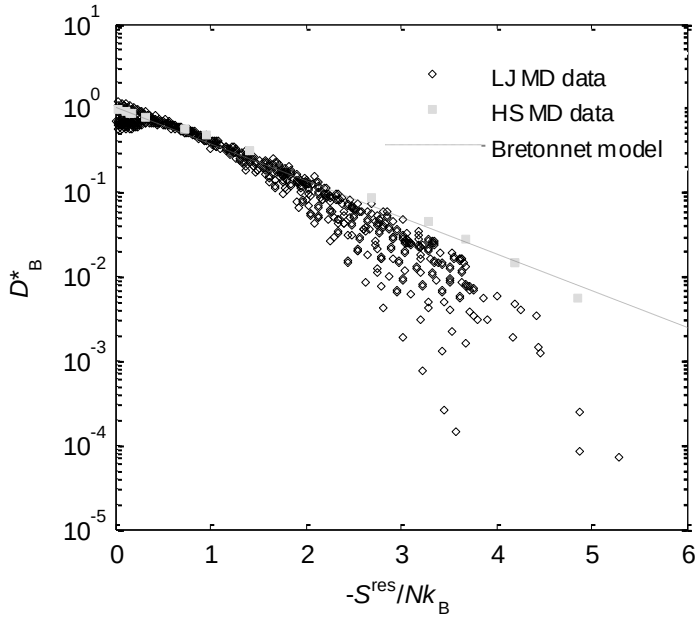

Fig. 3. Self-diffusion coefficients reduced according to Bretonnet's approach *versus* residual entropy for LJ and HS fluids. Residual entropy of the LJ fluids was calculated with Johnson et al. EoS [67]. Data from [26-27, 29-37].

3.3 Real fluids

For real fluids the well known Peng-Robinson [69] (PR) EoS was selected (Eqs. (28)-(31), Table 2) due to its simplicity allied to reliable representation of most systems. Nonetheless, the existence of highly asymmetrical molecules in our database induced us to adopt also the molecular-based EoS for chainlike molecules published later by Chiew et al. [70] (Eqs. (32)-(39), Table 2). It is a perturbed Lennard-Jones chain (PLJC) EoS which possesses physically significant parameters to capture the effects of molecular size, shape, and energy of real simple and chainlike molecules. The model is characterized by three parameters: the number of segments in a molecule, r, the segment size, σ, and the nonbonded segment energy, ε, and accounts for chain connectivity, repulsion, and attraction between chain segments.

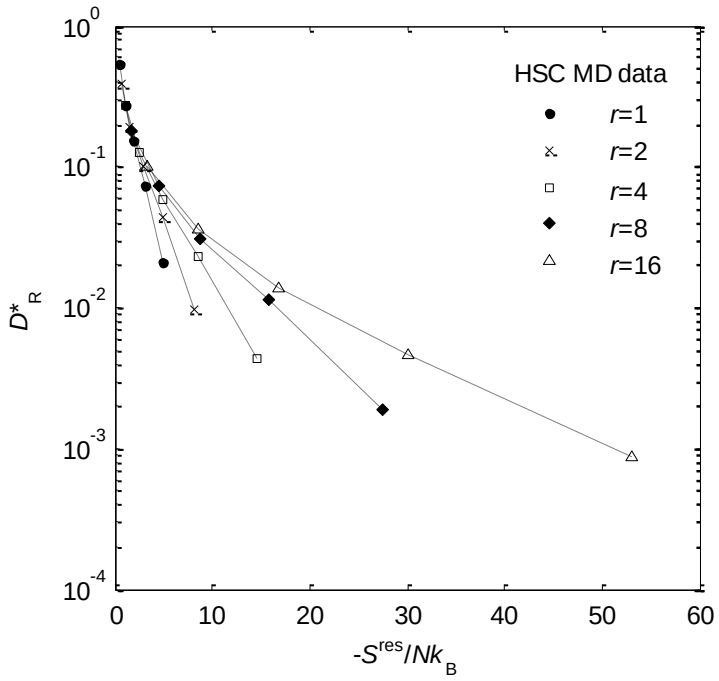

Fig. 4. Self-diffusion coefficients *versus* residual entropy for HSC fluids. Dashed lines are guidelines for the eyes. Data from [28].

In Fig. 5a the results achieved for real fluids, namely *n*-alkanes, using Chiew et al. EoS are shown, being possible to verify that their trends are qualitatively similar to those of HSC. With PR equation the calculated results are much more scattered (Fig. 5b). Chiew et al. equation not only improves the linearity of independent curves (*i.e.*, for distinct molecules) but also provides higher residual entropies for the same component. Together with Fig. 4, these observations contradict the assumption that the reduced coefficients are function of density and temperature via their lumped dependence on residual entropy alone, *i.e.* $D^*(\rho,T) = D^*\left[S^{\text{res}}(\rho,T)\right]$. Accordingly, in the following, a new universal regression is proposed for the reduced self-diffusivities of real and model fluids.

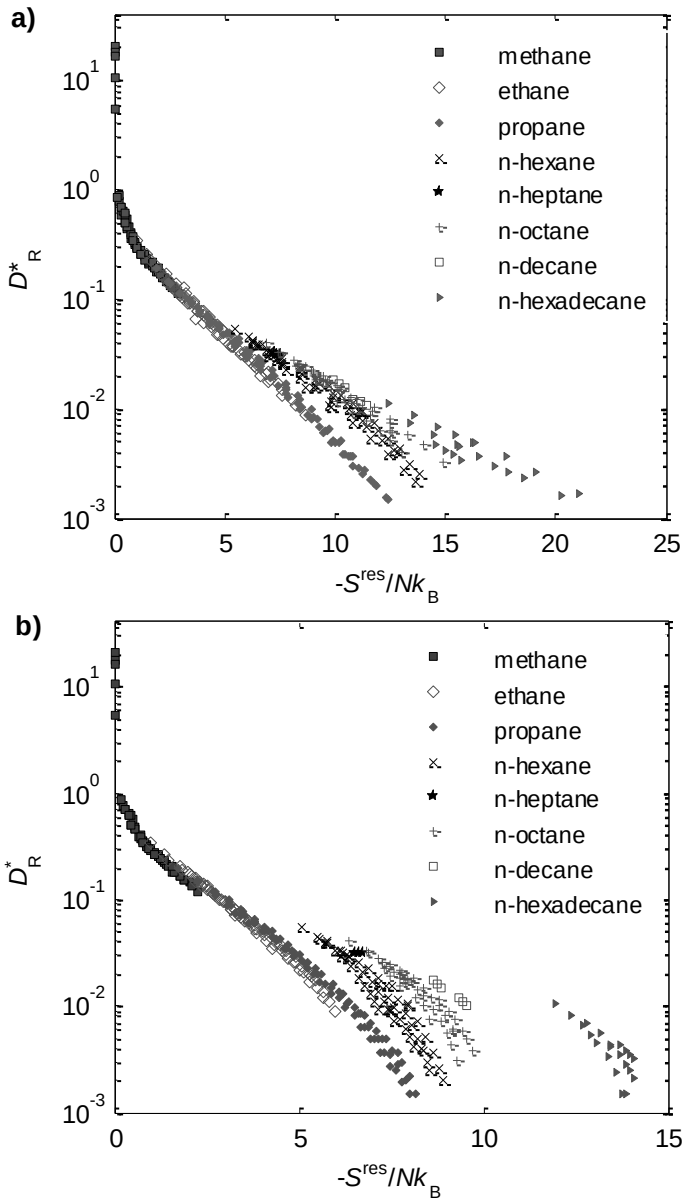

Fig. 5. Self-diffusion coefficients *versus* residual entropy for *n*-alkanes. a) Residual entropy calculated with Chiew et al. EoS [70]. b) Residual entropy calculated with Peng-Robinson EoS [69]. Data from references shown in Table 1.

3.4. New entropy-based relations

Based on the previous results and discussion, we can conclude that the diffusion coefficients are not only controlled by the residual entropy but also by the length of molecules. Hence, the

simple exponential models available in the literature involving D^* and S^{res} are not universal, being necessary to establish a new relation between D^*, S^{res} and r in order to attain that target. Hence, after exposing the weakness of the published scaling laws, new relations adequate to the fluids under study will be now proposed in this work.

3.4.1. HS and LJ systems

As spherical fluids, HS and Lennard-Jones have a diffusional behavior independent of the length parameter r, so the residual entropy should be enough to predict this dynamic property. Therefore, a simple expression was obtained in this paper to calculate the self-diffusion coefficients of these fluids:

$$\ln D^*_{\mathrm{HS,LJ}} = \frac{a + bx}{1 + cx + dx^2}, \text{ with } x \equiv \sqrt{-\frac{S^{res}}{Nk_B}} \tag{20}$$

where a = 3.7520, b = -8.6910, c = 4.5594, d = -1.6138, and $D^*_{\mathrm{HS,LJ}}$ corresponds to the dimensionless HS and LJ self-diffusivities reduced according to Rosenfeld approach since it provided the best results for these fluids (see Fig. 1 against Figs. 2 and 3). The LJ data corresponding to higher densities (or $-S^{res}$), for which diffusivities almost plummet, are not very reliable and it is not possible to devise a simple model to satisfy all points simultaneously. For that reason, the 3 LJ data points in Fig. 1 corresponding to $-S^{res}/Nk_B$ near 5 were not included. The parameters a, b, c and d in Eq. (20) were fitted to the remaining HS and LJ data (657 points), as can be seen in Fig. 6. Some scattering is observed in the region of higher residual entropies corresponding to HS diffusivities, due to the non-existence of attractive interactions, as discussed previously. However, the overall error is considerably low and the new model is able to predict HS and LJ self-diffusivities with an average absolute relative deviation (AARD) of 4.61% in the entire density range (see Table 3).

Table 2. Equations of state for the different fluids studied in this work.

Fluid	Equation of state	Eq.
Hard sphere	Carnahan-Starling [65]	
	$Z^{\mathrm{HS}} = \dfrac{1+\varphi+\varphi^2-\varphi^3}{(1-\varphi)^3}$	(21)
Hard-sphere chain	Kim- Bae [68]	
	$Z^{\mathrm{HSC}} = 1 + r\left(Z^{\mathrm{HS}} - 1\right) + Z^{\mathrm{chain}}$	(22)
	$Z^{\mathrm{HS}} = \dfrac{1+\varphi+\varphi^2-\varphi^3}{(1-\varphi)^3}$	(23)
	$Z^{\mathrm{chain}} = (1-r)\rho\partial \ln[g(\sigma)]/\partial\rho$	(24)
	$g(\sigma) = \dfrac{1-\varphi/2}{(1-\varphi)^3}$	(25)
Lennard-Jones	Nicolas et al. [66] and Johnson et al. [67]	
	$P^* = \rho^* T^* + \rho^{*2}\left(x_1 T^* + x_2 T^{*1/2} + x_3 + x_4 T^{*-1} + x_5 T^{*-2}\right)$ $+ \rho^{*3}\left(x_6 T^* + x_7 + x_8 T^{*-1} + x_9 T^{*-2}\right)$ $+ \rho^{*4}\left(x_{10} T^* + x_{11} + x_{12} T^{*-1}\right) + \rho^{*5}\left(x_{13}\right)$ $+ \rho^{*6}\left(x_{14} T^{*-1} + x_{15} T^{*-2}\right) + \rho^{*7}\left(x_{16} T^{*-1}\right)$ $+ \rho^{*8}\left(x_{17} T^{*-1} + x_{18} T^{*-2}\right) + \rho^{*9}\left(x_{19} T^{*-2}\right)$ $+ \rho^{*3}\left(x_{20} T^{*-2} + x_{21} T^{*-3}\right)\exp\left(-\gamma\rho^{*2}\right)$ $+ \rho^{*5}\left(x_{22} T^{*-2} + x_{23} T^{*-3}\right)\exp\left(-\gamma\rho^{*2}\right)$ $+ \rho^{*7}\left(x_{24} T^{*-2} + x_{25} T^{*-3}\right)\exp\left(-\gamma\rho^{*2}\right)$ $+ \rho^{*9}\left(x_{26} T^{*-2} + x_{27} T^{*-3}\right)\exp\left(-\gamma\rho^{*2}\right)$ $+ \rho^{*11}\left(x_{28} T^{*-2} + x_{29} T^{*-3}\right)\exp\left(-\gamma\rho^{*2}\right)$ $+ \rho^{*13}\left(x_{30} T^{*-2} + x_{31} T^{*-3} + x_{32} T^{*-4}\right)\exp\left(-\gamma\rho^{*2}\right)$ EoS by Nicolas et al. [66]: γ =3 and x_i = (-0.044807250, 7.27382210, -14.3433680, 3.83970960, -2.00577450, 1.90844720, -5.74417870, 25.1100730, -4532.7870, 0.00893271620, 9.81633580, -61.4345720, 14.1614540, 43.3538410, 1107.83270, -35.4295190, 10.5912980, 497.700460, -353.385420, 4503.60930, 7.78052960, 13567.1140, -8.58180230, 16646.5780, -14.0922340, 19386.9110, 38.5858680, 3380.03710, -185.677540, 8487.46930, 97.5086890, -14.4830600)	(26)

	EoS by Johnson et al. [67]: γ =3 and x_i = (0.862308510, 2.97621877, -8.40223012, 0.105413663, -0.856458383, 1.5827 947, 0.763942195, 1.75317341, 2798.29177, -0.0483942203, 0.996326520, -36.9800029, 20.8401230, 83.0540212, -957.479972, -147.774623, 63.9860785, 16.0399367, 68.0591662, -2791.29358, -6.24512830, -8116.83610, 14.8873556, -10593.4675, -113.160763, -8867.77154, -39.8698284, -4689.27030, 259.353528, -2694.52359, -721.848763, 172.180206)	(27)
Real fluids	Peng-Robinson [69]	
	$Z = \frac{1}{(1-b\rho_{\mathrm{m}})} - \frac{a}{bRT}\frac{b\rho_{\mathrm{m}}}{1+2b\rho_{\mathrm{m}}-b^2{\rho_{\mathrm{m}}}^2}$	(28)
	$a = 0.45723553\frac{R^2T_{\mathrm{c}}^2}{P_{\mathrm{c}}}\left[1+\kappa\left(1-\sqrt{T_{\mathrm{r}}}\right)\right]^2$	(29)
	$b = 0.0777960R\frac{T_{\mathrm{c}}}{P_{\mathrm{c}}}$	(30)
	$\kappa \equiv 0.37464+1.54226\omega-0.26993\omega^2$	(31)
	Chiew et al. [70]	
	$Z = Z^{\mathrm{ref}} + Z^{\mathrm{pert}}$	(32)
	$Z^{\mathrm{ref}} = r\frac{1+\varphi+\varphi^2-\varphi^3}{(1-\varphi)^3} - (r-1)\frac{1+\varphi/2}{(1-\varphi)^2}$	(33)
	$Z^{\mathrm{pert}} = \frac{12m\varphi}{T^*a^6}J_A(\varphi,r) + \frac{12m\varphi}{T^*a^6}\left(\frac{1}{a^6}-1\right)J_B(\varphi,r)$	(34)
	$J_A(\varphi,r) = \frac{(-1.0755-0.22169r)+\varphi(2.077-4.5236r)-\varphi^2(1.6623-4.41r)}{0.4571+r}$	(35)
	$J_B(\varphi,r) = \frac{(0.42130+0.03171r)+\varphi(0.1974+1.3253r)+5.3598r\varphi^2}{r}$	(36)
	$\left(\frac{2^{1/6}}{a}-1\right)^3 = \frac{0.005397r+0.006354}{9.44+r}\frac{k_{\mathrm{B}}T}{\varepsilon} + \frac{0.01222r+0.005102}{9.947+r}$	(37)
	$\varphi = \frac{\pi}{6}\rho^* a^3$	(38)
	$\rho^* = r\rho\sigma^3$	(39)

Note: ρ_{m} in Eq. (28) is molar density.

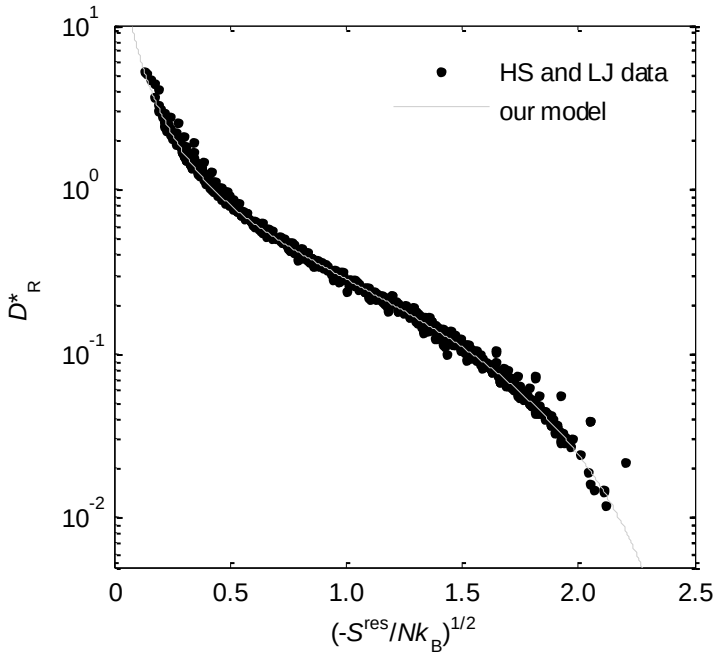

Fig. 6. Relation between reduced self-diffusion coefficients (according to Rosenfeld's approach) and residual entropy for HS and LJ fluids. Data from [26-27, 29-37].

3.4.2. HS, LJ, HSC and real systems

The equation newly proposed (Eq. (20)) is only valid for perfectly spherical fluids and is not applicable to asymmetrical molecules. As was demonstrated in the previous sections, HSC and real fluids behave more complexly and their diffusion coefficients strongly depend on their length, represented in this work by the parameter r. The importance of a third parameter associated to molecules length/shape was highlighted by Chopra and collaborators [22] who observed distinct residual entropy scaling relationships of Rosenfeld type for hydrocarbon isomers (*n*-octane, 2,2-dimethylhexane, 2,5-dimethylhexane, and 3-methyl-3-ethylpentane). Their work shows that, despite possessing the same S^{res}, such isomers present individual dynamic properties. Also, in an attempt to correct the effect of molecules length in the case of long hard sphere fused chains, Gerek and Elliott [18] divided the entropy by the van der Waals volume of the molecule, originating what they called an entropy density. Their results of D_R^* plotted against entropy density evidenced asymptotic convergence at high density, whereas the

low density behavior was clearly separated, owing in part to Rosenfeld's peculiar scaling with respect to density.

In this paper we adopt parameter r to take into account the non-sphericity of long chain fluids and real molecules in general. With this purpose, Kim and Bae [68] and Chiew et al. [70] equations were used for HSC and real fluids, respectively, and the parameter r was included together with S^{res} in an attempt to universally predict self-diffusion coefficients of fluids. (In the case of HS and LJ particles, $r = 1$.) That way, all fluids can be included and a new relation exhibiting universal behavior may be proposed. It consists of an artificial neural network (ANN) which uses r and $\sqrt{-S^{\text{res}}/Nk_{\text{B}}}$ as independent variables to calculate D_{R}^{*}. This ANN was constructed as a multilayer feed-forward network and it was trained with Levenberg-Marquardt backpropagation algorithm, with three sets of samples randomly divided into training set, validation set, and test set. The structure of the artificial neural network consists of three layers, each one having 6, 6 and 1 neurons, respectively. Hyperbolic tangent sigmoid transfer function has been applied for all neurons of all layers.

The proposed correlation was validated with model and real fluids, comprising the 1724 points of our database (HS, LJ, HSC, real systems). Although the ANN has been generated with random samples of points from the database, the resulting equation shows a good predictive ability. In fact, this model enables the calculation of self-diffusion coefficients as function of residual entropy and length r, with AARD = 9.13%, for all repulsive and attractive, polar and non-polar, spherical and highly asymmetrical molecules. As an example, Fig. 7 shows experimental data for four real fluids, namely chloromethane, cyclohexane, propane and *n*-hexane, along with the corresponding modeling results. It is perceptible the capability of the new equation to predict self-diffusion coefficients of distinct molecules, regardless of their nature. Similar results and behavior are obtained for the remaining database. In Figs. 8a and 8b, all calculated diffusivities are plotted against the experimental values. A good distribution of the points along diagonal, even in the region of lower diffusivities (see Fig. 8b), is evident, which highlights the accurate model performance. It is also important to emphasize that the validation covers the temperature range from T^{*} = 0.179 to 6.02, and the density range from low-density gaseous states up to compressed liquid close to the freezing line. On the other hand,

the equations published in literature are restricted to small well behaved regions where the calculated deviations still attain 30-40%, preventing their possible utilization. Therefore, the model devised in this work may be of great utility to estimate self-diffusion coefficients over wide ranges of physical conditions when experimental data are not available.

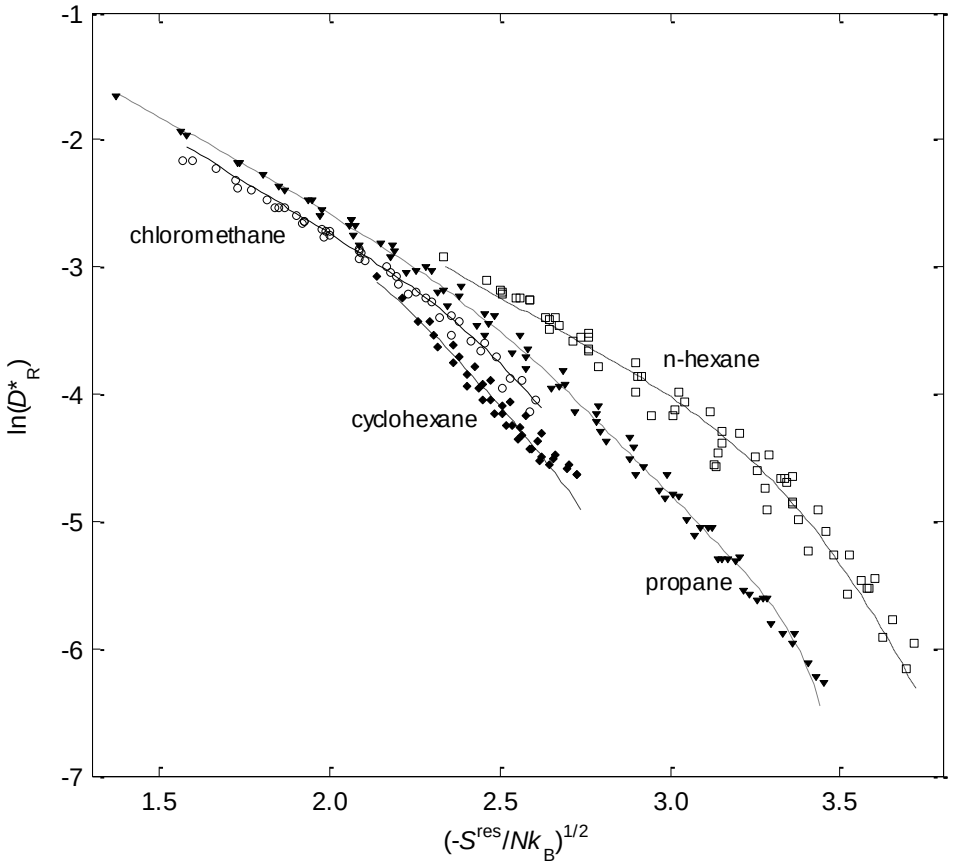

Fig. 7. Comparison between experimental data (symbols) and model results (lines) achieved in this work, for some distinct molecules.

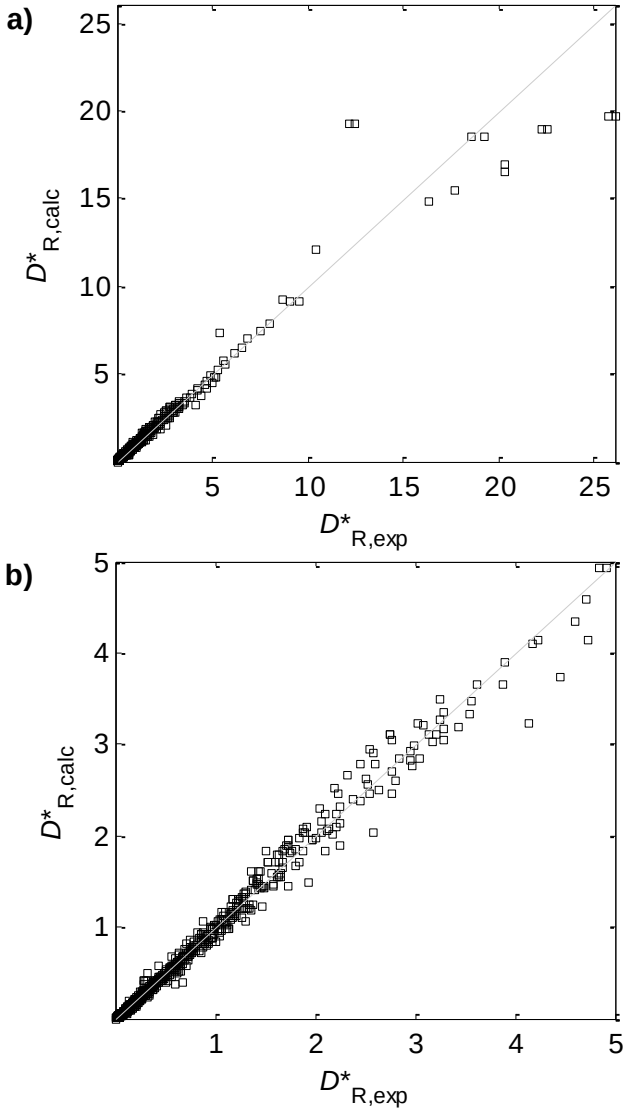

Fig. 8. Experimental *versus* calculated reduced self-diffusion coefficients for all fluids studied. a) All points of database; b) Data on the range 0-5 to point out the model behavior for low D^*.

The prediction of self-diffusion coefficients of spherical fluids (HS and LJ) can be also accomplished using this new equation with large accuracy since the mean deviation is only 5.38%, which is quite close to the 4.61% obtained with Eq. (20) (see Table 3). Even for asymmetrical systems (HSC and real fluids) it is possible to calculate the corresponding self-diffusivities with a reasonable mean error of 11.55% (see Table 3), due to the robustness of the

Table 3. Average absolute relative deviations obtained in this work for the various fluids under study.

equation	systems	NDP	AARD (%)
Eq.(19)	HS, LJ	657	4.61
ANN*	HS, LJ	659	5.38
	HSC, real fluids	1065	11.55
	all	1724	9.13

* Artificial neural network provided in Supplementary Material.

new model. Although the correlation proposed is an artificial neural network, it is of very simple and quick utilization since it is provided in supplementary material of the original paper, along with instructions to use it straightforwardly.

4. Conclusions

In this work, entropy based scaling laws which presume the existence of a universal relation between reduced self-diffusion coefficient and residual entropy were revisited and analyzed. With that purpose a large database has been compiled, embodying 1727 points of model (HS, HSC, LJ) and real fluids (between polar, non-polar, symmetrical and asymmetrical molecules). The existent scaling laws of Rosenfeld, Dzugutov and Bretonnet were tested and their universal character was refuted since they fail over the entire range of ρ and T, even for atomic and simple fluids (*e.g.*, HS and LJ) for which they have been originally proposed. Moreover, the dependence of the self-diffusivities upon molecule's chain parameter, r, and not only on density and temperature through S^{res} was found. Hence, a new model consisting of an artificial neural network was proposed, being able to accurately predict the diffusivities of all fluids studied (AARD = 9.13%) as function of the residual entropy and r. Another equation only valid for spherical particles was devised, based on the self-diffusivity data of HS and LJ fluids. It is a very simple analytical expression with four parameters, and depends just upon S^{res}; the calculated average absolute relative deviation is only 4.61% for 657 points.

Appendix A. Supplementary data

Supplementary data associated with this article can be found in the online version at http://dx.doi.org/10.1016/j.ces.2012.05.006. It contains the universal correlation proposed in this work and the corresponding calculation procedure.

Nomenclature

A_D	Frontal coefficient
d	Mean interparticle distance
D	Diffusion coefficient
E_a	Activation energy
$g(\sigma)$	Pair correlation function
k_B	Boltzmann's constant
m	Particle mass
MD	Molecular dynamics
N	Number of particles
P	Pressure
r	Number of segments in real or model molecules
S^{res}	Residual entropy
S_2	Two-body contribution to residual entropy
T	Temperature
V	Volume
V_f	Molar free volume
V_i	Intrinsic molar volume
V_m	Molar volume
Z	Compressibility factor

Greek letters

Γ_E	Collision frequency of Enskog theory

ε	Depth of the Lennard-Jones potential well; nonbonded segment energy in Chiew et al. EoS
ρ	Number density
ρ_m	Molar density
σ	Hard-sphere diameter; segment size in Chiew et al. EoS
σ_{eff}	Effective hard-sphere diameter
υ	Thermal velocity
φ	Packing density
ω	Acentric factor

Subscripts

B	Bretonnet's approach
c	Critical property
D	Dzugutov's approach
HS	Hard-sphere
HSC	Hard-sphere chain
LJ	Lennard-Jones
R	Rosenfeld's approach

Superscripts

*	Reduced property
´	Refers to MD data taken directly from literature

References

[1] R.B. Bird, W.E. Stewart, E.N. Lightfoot, Transport phenomena, second ed., J. Wiley, 2007.

[2] C.M. Silva, H.Q. Liu, Modeling of Transport Properties of Hard Sphere Fluids and its Applications, in: A. Mulero (Ed.) Theory and Simulation of Hard Sphere Fluids and Related Systems, Lecture Notes in Physics 753, Springer, 2008, pp. 383-492.

[3] H.Q. Liu, C.M. Silva, E.A. Macedo, Unified approach to the self-diffusion coefficients of dense fluids over wide ranges of temperature and pressure - Hard-sphere, square-well, Lennard-Jones and real substances, Chemical Engineering Science, 53 (1998) 2403-2422.

[4] C.M. Silva, H.Q. Liu, E.A. Macedo, Comparison between different explicit expressions of the effective hard sphere diameter of Lennard-Jones fluid: Application to self-diffusion coefficients, Industrial & Engineering Chemistry Research, 37 (1998) 221-227.

[5] C.M. Silva, H.Q. Liu, E.A. Macedo, Models for self-diffusion coefficients of dense fluids, including hydrogen-bonding substances, Chemical Engineering Science, 53 (1998) 2423-2429.

[6] A.L. Magalhaes, S.P. Cardoso, B.R. Figueiredo, F.A. Da Silva, C.M. Silva, Revisiting the Liu-Silva-Macedo Model for Tracer Diffusion Coefficients of Supercritical, Liquid, and Gaseous Systems, Industrial & Engineering Chemistry Research, 49 (2010) 7697-7700.

[7] A.L. Magalhaes, F.A. Da Silva, C.M. Silva, New models for tracer diffusion coefficients of hard sphere and real systems: Application to gases, liquids and supercritical fluids, Journal of Supercritical Fluids, 55 (2011) 898-923.

[8] A.L. Magalhaes, F.A. Da Silva, C.M. Silva, New tracer diffusion correlation for real systems over wide ranges of temperature and density, Chemical Engineering Journal, 166 (2011) 49-72.

[9] S. Chapman, T.G. Cowling, The Mathematical Theory of Non Uniform Gases, third ed., Cambridge University Press, Cambridge, 1970.

[10] J.O. Hirshfelder, C.F. Curtiss, R.B. Bird, Molecular Theory of Gases and Liquids, first ed., John Wiley & Sons, New York, 1967.

[11] J. Millat, J.H. Dymond, C.A. Nieto de Castro, Modified hard-spheres scheme, in: Transport properties of fluids: their correlation, prediction and estimation, Cambridge University Press, New York, 1996.

[12] R.C. Reid, J.M. Prausnitz, B.E. Poling, The Properties of Gases and Liquids, fourth ed., McGraw-Hill, New York, 1987.

[13] D. Chandler, Rough hard-sphere theory of self-diffusion constant for molecular liquids, Journal of Chemical Physics, 62 (1975) 1358-1363.

[14] E. Ruckenstein, H.Q. Liu, Self-diffusion in gases and liquids, Industrial & Engineering Chemistry Research, 36 (1997) 3927-3936.

[15] Y. Rosenfeld, Relation between transport-coefficients and internal entropy of simple systems, Physical Review A, 15 (1977) 2545-2549.

[16] M. Dzugutov, A universal scaling law for atomic diffusion in condensed matter, Nature, 381 (1996) 137-139.

[17] J.L. Bretonnet, Self-diffusion coefficient of dense fluids from the pair correlation function, Journal of Chemical Physics, 117 (2002) 9370-9373.

[18] Z.N. Gerek, J.R. Elliott, Self-diffusivity estimation by molecular dynamics, Industrial & Engineering Chemistry Research, 49 (2010) 3411-3423.

[19] T. Goel, C.N. Patra, T. Mukherjee, C. Chakravarty, Excess entropy scaling of transport properties of Lennard-Jones chains, The Journal of chemical physics, 129 (2008) 164904.

[20] W.P. Krekelberg, T. Kumar, J. Mittal, J.R. Errington, T.M. Truskett, Anomalous structure and dynamics of the Gaussian-core fluid, Physical Review E, 79 (2009).

[21] M.J. Pond, J.R. Errington, T.M. Truskett, Mapping between long-time molecular and Brownian dynamics, Soft Matter, 7 (2011) 9859-9862.

[22] R. Chopra, T.M. Truskett, J.R. Errington, On the use of excess entropy scaling to describe single-molecule and collective dynamic properties of hydrocarbon isomer fluids, Journal of Physical Chemistry B, 114 (2010) 16487-16493.

[23] R. Chopra, T.M. Truskett, J.R. Errington, On the use of excess entropy scaling to describe the dynamic properties of water, Journal of Physical Chemistry B, 114 (2010) 10558-10566.

[24] Y. Rosenfeld, A quasi-universal scaling law for atomic transport in simple fluids, Journal of Physics-Condensed Matter, 11 (1999) 5415-5427.

[25] A. Baranyai, D.J. Evans, Direct entropy calculation from computer-simulation of liquids, Physical Review A, 40 (1989) 3817-3822.

[26] B.J. Alder, D.M. Gass, T.E. Wainwrig, Studies in molecular dynamics. VIII. Transport coefficients for a hard-sphere fluid, Journal of Chemical Physics, 53 (1970) 3813-3826.

[27] J.J. Erpenbeck, W.W. Wood, Self-diffusion coefficient for the hard-sphere fluid, Physical Review A, 43 (1991) 4254-4261.

[28] S.W. Smith, C.K. Hall, B.D. Freeman, Molecular dynamics study of transport coefficients for hard-chain fluids, Journal of Chemical Physics, 102 (1995) 1057-1073.

[29] D.M. Heyes, J.G. Powles, J.C.G. Montero, Information theory applied to the transport coefficients of Lennard-Jones fluids. II, Molecular Physics, 78 (1993) 229-234.

[30] J. Kushick, B.J. Berne, Role of attractive forces in self-diffusion in dense Lennard-Jones fluids, Journal of Chemical Physics, 59 (1973) 3732-3736.

[31] D.M. Heyes, Self-diffusion and shear viscosity of simple fluids - a molecular-dynamics study, Journal of the Chemical Society-Faraday Transactions I, 79 (1983) 1741-1758.

[32] P. Carelli, A. Desantis, I. Modena, F.P. Ricci, Self-diffusion in simple dense fluids, Physical Review A, 13 (1976) 1131-1139.

[33] J.E. Straub, Analysis of the role of attractive forces in self-diffusion of a simple fluid, Molecular Physics, 76 (1992) 373-385.

[34] D. Levesque, L. Verlet, Computer "experiments" on classical fluids. III. Time-dependent self-correlation functions, Physical Review A-General Physics, 2 (1970) 2514-2528.

[35] K. Lucas, B. Moser, Memory function model for the velocity autocorrelation function and the self-diffusion coefficient in simple dense fluids, Molecular Physics, 37 (1979) 1849-1857.

[36] K. Meier, A. Laesecke, S. Kabelac, Transport coefficients of the Lennard-Jones model fluid. II Self-diffusion, Journal of Chemical Physics, 121 (2004) 9526-9535.

[37] R.L. Rowley, M.M. Painter, Diffusion and viscosity equations of state for a Lennard-Jones fluid obtained from molecular dynamics simulations, International Journal of Thermophysics, 18 (1997) 1109-1121.

[38] M. Holz, X.A. Mao, D. Seiferling, A. Sacco, Experimental study of dynamic isotope effects in molecular liquids: Detection of translation-rotation coupling, Journal of Chemical Physics, 104 (1996) 669-679.

[39] M.A. McCool, L.A. Woolf, Pressure and temperature dependence of self-diffusion of carbon-tetrachloride, Journal of the Chemical Society-Faraday Transactions I, 68 (1972) 1971-1981.

[40] A.F. Collings, L.A. Woolf, Self-diffusion in benzene under pressure, Journal of the Chemical Society-Faraday Transactions I, 71 (1975) 2296-2298.

[41] H.J. Parkhurst, J. Jonas, Dense liquids. I. Effect of density and temperature on self-diffusion of tetramethylsilane and benzene-d_6, Journal of Chemical Physics, 63 (1975) 2698-2704.

[42] T. Gross, J. Buchhauser, W.E. Price, I.N. Tarassov, H.D. Ludemann, The P,T-dependence of self-diffusion in fluid ammonia, Journal of Molecular Liquids, 73-4 (1997) 433-444.

[43] L.I. Stiel, G. Thodos, Self-diffusivity of dilute and dense gases, Canadian Journal of Chemical Engineering, 43 (1965) 186-190.

[44] R.C. Robinson, W.E. Stewart, Self-diffusion in liquid carbon dioxide and propane, Industrial & Engineering Chemistry Fundamentals, 7 (1968) 90-95.

[45] H.A. O'Hern, J.J. Martin, Diffusion in carbon dioxide at elevated pressures, Industrial and Engineering Chemistry, 47 (1955) 2081-2087.

[46] P. Etesse, J.A. Zega, R. Kobayashi, High-pressure nuclear-magnetic-ressonance measurement of spin-lattice relaxation and self-diffusion in carbon-dioxide, Journal of Chemical Physics, 97 (1992) 2022-2029.

[47] J. Naghizadeh, S.A. Rice, Kinetic theory of dense fluids. X. Measurement and interpretation of self-diffusion in liquid Ar, Kr, Xe, and CH_4, Journal of Chemical Physics, 36 (1962) 2710-2720.

[48] C.R. Mueller, R.W. Cahill, Mass spectrometric measurement of diffusion coefficients, Journal of Chemical Physics, 40 (1964) 651-654.

[49] L.A. Woolf, Self-diffusion in carbon-disulfide under pressure, Journal of the Chemical Society-Faraday Transactions I, 78 (1982) 583-590.

[50] I. Amdur, L.M. Shuler, Diffusion coefficients of systems CO-CO and CO-N_2, Journal of Chemical Physics, 38 (1963) 188-192.

[51] F.X. Prielmeier, H.D. Ludemann, Self-diffusion in compressed liquid chloromethane, dichloromethane and trichloromethane, Molecular Physics, 58 (1986) 593-604.

[52] J. Jonas, D. Hasha, S.G. Huang, Density effects on transport-properties in liquid cyclohexane, Journal of Physical Chemistry, 84 (1980) 109-112.

[53] A. Enninghorst, F.D. Wayne, M.D. Zeidler, Density dependence of self-diffusion in liquid pentanes and pentane mixtures, Molecular Physics, 88 (1996) 437-452.

[54] M. Helbaek, B. Hafskjold, D.K. Dysthe, G.H. Sorland, Self-diffusion coefficients of methane or ethane mixtures with hydrocarbons at high pressure by NMR, Journal of Chemical and Engineering Data, 41 (1996) 598-603.

[55] A. Greiner-Schmid, S. Wappmann, M. Has, H.D. Ludemann, Self-diffusion in the compressed fluid lower alkanes - methane, ethane, and propane, Journal of Chemical Physics, 94 (1991) 5643-5649.

[56] S. Takahashi, Diffusion-coefficient of ^{14}C-labeled ethylene in normal ethylene at high pressure, Journal of Chemical Engineering of Japan, 10 (1977) 339-342.

[57] J.W. Moore, R.M. Wellek, Diffusion-coefficients of *n*-heptane and *n*-decane in *n*-alkanes and *n*-alcohols at several temperatures, Journal of Chemical and Engineering Data, 19 (1974) 136-140.

[58] J.H. Dymond, K.R. Harris, The temperature and density dependence of the self-diffusion coefficient of normal-hexadecane, Molecular Physics, 75 (1992) 461-466.

[59] K.R. Harris, Temperature and density dependence of the self-diffusion coefficient of *n*-hexane from 223K to 333K and up to 400 MPa, Journal of the Chemical Society-Faraday Transactions I, 78 (1982) 2265-2274.

[60] E.B. Winn, The temperature dependence of the self-diffusion coefficients of argon, neon, nitrogen, oxygen, carbon dioxide, and methane, Physical Review, 80 (1950) 1024-1027.

[61] J. Jonas, D. Hasha, S.G. Huang, Self-diffusion and viscosity of methylcyclohexane in the dense liquid region, Journal of Chemical Physics, 71 (1979) 3996-4000.

[62] K.R. Harris, J.J. Alexander, T. Goscinska, R. Malhotra, L.A. Woolf, J.H. Dymond, Temperature and density dependence of the self-diffusion coefficients of liquid *n*-octane and toluene, Molecular Physics, 78 (1993) 235-248.

[63] L.P. Chen, T. Gross, H.D. Ludemann, The density dependence of self-diffusion in some simple amines, Physical Chemistry Chemical Physics, 1 (1999) 3503-3508.

[64] C.L. Yaws, Chemical Properties Handbook, 1st ed., McGraw-Hill, New York, 1999.

[65] N.F. Carnahan, K.E. Starling, Equation of state for nonattracting rigid spheres, Journal of Chemical Physics, 51 (1969) 635-636.

[66] J.J. Nicolas, K.E. Gubbins, W.B. Streett, D.J. Tildesley, Equation of state for the Lennard-Jones fluid, Molecular Physics, 37 (1979) 1429-1454.

[67] J.K. Johnson, J.A. Zollweg, K.E. Gubbins, The Lennard-Jones equation of state revisited, Molecular Physics, 78 (1993) 591-618.

[68] I.H. Kim, Y.C. Bae, Equations of state for hard spheres and hard-sphere chains, Fluid Phase Equilibria, 167 (2000) 187-206.

[69] D. Peng, D.B. Robinson, New 2-constant equation of state, Industrial & Engineering Chemistry Fundamentals, 15 (1976) 59-64.

[70] Y.C. Chiew, D. Chang, J. Lai, G.H. Wu, A molecular-based equation of state for simple and chainlike fluids, Industrial & Engineering Chemistry Research, 38 (1999) 4951-4958.

3 Modeling tracer diffusivities in supercritical carbon dioxide

The phenomenological modeling of tracer diffusion coefficients in supercritical carbon dioxide is the main focus of this chapter. Distinct methodologies were adopted in order to develop and propose simple and straightforward expressions to estimate D_{12} for all kinds of solutes in SC-CO_2: spherical and asymmetrical, light and heavy, polar and non-polar.

Until a few years ago, a gap was still evident in the literature in terms of models capable of providing satisfactory results for systems involving polar and/or very asymmetrical components, over wide ranges of temperature and pressure. Those limitations were overcame with the publication of accurate models based on distinct methodologies, and validated with the largest database compiled up until now [1-7]. However, some of these expressions are lengthy for calculations and require at least one parameter that must be previously fitted to experimental data for the system under study, which limits their application. Within this perspective, alternative approaches were focused in this thesis in order to provide simple expressions for D_{12} prediction, which may be easily computed by any non-expert user. This work was the basis of three papers.

Hydrodynamic expressions [8-12] are a good starting point due to their simplicity and predictive nature (no parameters involved), thought the existing equations using this approach frequently present significant errors, particularly when they are applied over wide ranges of temperature and pressure, or near the critical point. Hence, three simple hydrodynamic

expressions (Paper II) were proposed for the pure prediction of D_{12} values in SC-CO_2, based on the well-known Wilke–Chang [8], Scheibel [11] and Lusis–Ratcliff [12] equations. The deviations to the Stokes-Einstein (or hydrodynamic) behavior of the original models were corrected by introducing two universal constants that greatly decreased the average errors. The new modified expressions presented only [8.26-8.51]% of error for a large database involving 150 systems and 4484 data points over wide ranges of temperature and pressure, while models from literature provided deviations between 11.70% and 23.16%. The dispersion of the computed errors around the average was also much lower in the case of the new models, which highlights their reliability and accuracy.

Hydrodynamic equations were revisited (Paper III) and four new improved expressions were proposed for D_{12} prediction in supercritical CO_2. In this case, Wilke-Chang [8], Scheibel [11], Lusis-Ratcliff [12] and Tyn-Calus [9] equations were modified with new universal constants, and the dependence of the original models on the solute and solvent molar volumes at normal boiling point was replaced by analogous dependencies upon critical molar volumes. The availability and also reliable predictions of critical volumes justifies this choice, being also more realistic for the case of CO_2 and other gases. The proposed models achieved average absolute errors between 7.86% and 8.56%, and average deviations from 0.47% to 0.53% when tested with a similar database. These results evidenced their performance for any solutes in supercritical CO_2.

A common feature to all hydrodynamic expressions is that, despite their prediction ability, they only take into account the regular (or background) behavior of systems, which results from the fact that they have been essentially developed for liquids and later extended to supercritical systems. However, it is known that near the critical point a clear growing of D_{12} (critical enhancement) is observed as a result of the abrupt density variation, which can be accounted by a distinct singular term. This lead us to propose a new predictive model (Paper IV) for tracer diffusivities in SC-CO_2 embodying both contributions (regular/background and singular) for the correct description of diffusion in all supercritical region, even in the vicinity of the critical point where common models usually fail. The small errors obtained (6.20% on average), along with their unbiased distributions, showed the better performance of our model in comparison to other expressions from literature (mean deviations up to 75.17%).

References

[1] A.L. Magalhães, F.A. Da Silva, C.M. Silva, Free-volume model for the diffusion coefficients of solutes at infinite dilution in supercritical CO_2 and liquid H_2O, The Journal of Supercritical Fluids, 74 (2013) 89-104.

[2] A.L. Magalhães, F.A. Da Silva, C.M. Silva, New models for tracer diffusion coefficients of hard sphere and real systems: Application to gases, liquids and supercritical fluids, The Journal of Supercritical Fluids, 55 (2011) 898-923.

[3] A.L. Magalhães, F.A. Da Silva, C.M. Silva, New tracer diffusion correlation for real systems over wide ranges of temperature and density, Chemical Engineering Journal, 166 (2011) 49-72.

[4] A.L. Magalhães, F.A. Da Silva, C.M. Silva, Tracer diffusion coefficients of polar systems, Chemical Engineering Science, 73 (2012) 151-168.

[5] P.F. Lito, A.L. Magalhães, J.R.B. Gomes, C.M. Silva, Universal model for accurate calculation of tracer diffusion coefficients in gas, liquid and supercritical systems, Journal of Chromatography A, 1290 (2013) 1-26.

[6] H. Liu, C.M. Silva, E.A. Macedo, New equations for tracer diffusion coefficients of solutes in supercritical and liquid solvents based on the Lennard-Jones fluid model, Industrial and Engineering Chemistry Research, 36 (1997) 246-252.

[7] A.L. Magalhães, S.P. Cardoso, B.R. Figueiredo, F.A. Da Silva, C.M. Silva, Revisiting the Liu-Silva-Macedo model for tracer diffusion coefficients of supercritical, liquid, and gaseous systems, Industrial and Engineering Chemistry Research, 49 (2010) 7697-7700.

[8] C.R. Wilke, P. Chang, Correlation of diffusion coefficients in dilute solutions, AIChE Journal, 1 (1955) 264-270.

[9] M.T. Tyn, W.F. Calus, Diffusion coefficients in dilute binary liquid mixtures, Journal of Chemical & Engineering Data, 20 (1975) 106-109.

[10] K.A. Reddy, L.K. Doraiswamy, Estimating liquid diffusivity, Industrial & Engineering Chemistry Fundamentals, 6 (1967) 77-79.

[11] E.G. Scheibel, Liquid diffusivities. Viscosity of gases, Industrial & Engineering Chemistry, 46 (1954) 2007-2008.

[12] M.A. Lusis, C.A. Ratcliff, Diffusion in binary liquid mixtures at infinite dilution, The Canadian Journal of Chemical Engineering, 46 (1968) 385-387.

Paper II

Adapted from

Improved Stokes-Einstein based Models for Diffusivities in Supercritical CO_2

Journal of the Taiwan Institute of Chemical Engineers, 45 (2014) 1280–1284

Abstract

The large interest and applications of supercritical carbon dioxide (SC-CO_2) require the existence of transport properties for simulation and/or design. In this work, pure predictive models are proposed for the accurate estimation of binary diffusivities at infinite dilution in SC-CO_2. They are three simple and straightforward expressions grafted on the Wilke-Chang, Scheibel and Lusis-Ratcliff equations, whose deviations to the Stokes-Einstein behavior in the supercritical domain are corrected by introducing two universal constants. Such modifications decrease the average errors from [11.70–23.16]% to [8.26–8.51]% for a large database of 150 systems and 4484 data points over wide ranges of temperature and pressure. The dispersion of the computed errors is also significantly lower, which highlights the reliability of our improved models to accurately predict tracer diffusivities.

1. Introduction

The increasing attention to biorefinery and sustainability in general is leading green solvents and processes, like carbon dioxide and supercritical fluid extraction, to attract relevance in chemistry and chemical engineering research, food and pharmaceutical industries, and environmental engineering [1-2]. As a result of the large interest upon supercritical carbon dioxide (SC-CO_2), the existence of diffusion data for the simulation and design of the implied processes is necessary. Nonetheless, the lack of experimental tracer diffusivities (D_{12}) for most solutes in SC-CO_2 or, in the case of known systems, for distinct operating conditions (pressure and temperature) demands the existence of accurate models for their estimation. Other drawbacks like the time consuming measurements, the hazardous nature of some solutes, and the cost of chemicals/materials also reinforce the need of reliable predictive D_{12} equations.

Several approaches for the calculation of diffusivities have been proposed in the literature, namely, the Enskog theory and its modifications, the effective hard-sphere diameter method, the free-volume theories, the van der Waals and rough hard sphere principles, the hydrodynamic models, the Eyring activated-state theory, and excess entropy scaling laws [3-8]. More recent models [9-14] overcome well-known limitations of most D_{12} expressions in what concerns the polarity and/or high asymmetry (in terms of mass and size) of the molecules, mainly when

applied over wide ranges of temperature and pressure. However, they usually contain one or two parameters that must be previously fitted to data for the specific system under study, which remains a strict limitation. An attractive approach is provided by predictive hydrodynamic equations [15-20] though they offer significant errors in large intervals of temperature and density, and near the critical point [9-10, 14]. Accordingly, in this work, three hydrodynamic equations are revisited and improved in order to ensure trustworthy predictions of D_{12} in SC-CO_2, namely the Wilke-Chang (WC) [15], Scheibel (Sch) [20] and Lusis-Ratcliff (LR) [16] expressions (see Eqs. A.1-A.3 in Appendix A). These models are based on the Stokes-Einstein relation, *i.e.* $D_{12} \propto T/(r_2 \eta_1)$, which assumes that a large rigid spherical molecule of solute (component 2) is moving through a continuum of solvent (component 1) of much smaller size [3, 21]; T represents the absolute temperature, η_1 is the solvent viscosity, and r_2 is the radius of the solute molecule. These previous assumptions and the simple proportionality between D_{12} and T/η_1 are not valid for all cases, and thus empirical or semi-empirical modifications are frequently needed in the low density and/or high temperature ranges, and particularly in supercritical state.

In this essay, we propose a correction for the functional dependencies between D_{12} and T/η_1 and V_{bp} (molar volume at normal boiling point) existent in the original models of Wilke-Chang, Scheibel and Lusis-Ratcliff (see Appendix A). The modifications are introduced by inserting two universal parameters valid for systems in SC-CO_2, and by refitting the frontal coefficient of the three expressions.

2. Improved Stokes-Einstein based equations

In this section, three improved Stokes-Einstein based equations grafted on the Wilke-Chang (mWC), Scheibel (mSch) and Lusis-Ratcliff (mLR) models are proposed with the objective to provide accurate predictions of diffusion coefficients in supercritical carbon dioxide. (The prefix 'm' of the acronyms mWC, mSch and mLR stands for 'modified'). More specifically, universal constants α_i and β_i will correct the dependence of D_{12} upon T/η_1 and V_{bp}, and frontal coefficient A_i will be reoptimized. Accordingly:

$$D_{12,\mathrm{mWC}} = A_1 \left(\frac{T}{\eta_1}\right)^{\alpha_1} \frac{1}{V_{\mathrm{bp},2}^{\beta_1}} \tag{1}$$

$$D_{12,\mathrm{mSch}} = A_2 \left(\frac{T}{\eta_1}\right)^{\alpha_2} \frac{1}{V_{\mathrm{bp},2}^{\beta_2}} \left[1 + \left(\frac{3V_{\mathrm{bp},1}}{V_{\mathrm{bp},2}}\right)^{2/3}\right] \tag{2}$$

$$D_{12,\mathrm{mLR}} = A_3 \left(\frac{T}{\eta_1}\right)^{\alpha_3} \left[\beta_3 \left(\frac{V_{\mathrm{bp},1}}{V_{\mathrm{bp},2}}\right)^{1/3} + \left(\frac{V_{\mathrm{bp},1}}{V_{\mathrm{bp},2}}\right)\right] \tag{3}$$

When $A_1 = 7.4\times10^{-8}\sqrt{\phi M_1}$, $\alpha_1 = 1$ and $\beta_1 = 0.6$, the original Wilke-Chang equation (Eq. (A.1)) is recovered. Comparing Eqs. (2) and (A.2), one concludes that, if $A_2 = 8.2\times10^{-8}$, $\alpha_2 = 1$ and $\beta_2 = 1/3$, the original Scheibel equation is obtained. Finally, the classical Lusis-Ratcliff model (Eq. (A.3)) corresponds to the case where $A_3 = 8.52\times10^{-8}V_{\mathrm{bp},1}^{-1/3}$, $\alpha_3 = 1$ and $\beta_3 = 1.4$ are substituted in Eq. (3). In the next section the large database utilized for the correlation of A_i, α_i, β_i $(\mathrm{i} = 1,2,3)$ is presented.

3. Database and models validation

The database compiled in this work comprehends 150 supercritical systems and 4484 data points; data published exclusively in graphical form are discarded. It includes an extensive variety of solutes in terms of size, shape, functional groups, polarity, etc, and covers wide ranges of temperature and pressure. In Table S.1 (Supplementary data) the identification of all systems, number of data points (NDP), reduced ranges of temperature, pressure and SC-CO_2 density, and data sources are listed. In Table S.2 (Supplementary data) the name, molecular formula, CAS number, molecular weight, critical constants, normal boiling point, and molar volume at normal boiling point of all molecules involved in calculations are also listed. Whenever absent in the original papers, SC-CO_2 densities and viscosities are computed by the correlations of Pitzer and Schreiber [22] and Altunin and Sakhabetdinov [23], respectively. The unknown critical constants are estimated by the Joback [3, 24-25], Somayajulu [26], Klincewicz [3, 27], Ambrose [3, 28-29], Wen–Qiang [30], and Constantinou–Gani [31] methods. The solute molar volumes at normal boiling point (V_{bp}) are estimated by Tyn-Calus equation [3, 32] and further corrected

by an analysis similar to that devised by Sassiat et al. [33]: the experimental V_{bp} s of 97 molecules plotted against their estimated values was found to be well correlated by $V_{bp}^{exp} = 1.459\left(V_{bp}^{TC}\right)^{0.894}$, where superscrips 'exp' and 'TC' mean 'experimental' and 'computed by Tyn-Calus equation', respectively.

4. Results and discussion

The performance of the proposed equations is analyzed on the basis of the average absolute relative deviations (AARD) computed for each system and for the whole database, and also by the standard deviations of the AARDs (σ_{AARD}). The AARD is defined in percentage by:

$$\text{AARD}\,(\%) = \frac{100}{\text{NDP}} \sum_{i=1}^{\text{NDP}} \left| \frac{D_{12}^{calc} - D_{12}^{exp}}{D_{12}^{exp}} \right|_i \tag{4}$$

where the exponents 'exp' and 'calc' refer to the experimental and calculated tracer diffusivities.

Four predictive hydrodynamic models are taken from the literature for comparison: the original equations of Wilke-Chang (WC), Scheibel (Sch) and Lusis-Ratcliff (LR), and the more recent correlation of Lai-Tan (LT) [34] specifically developed for SC-CO_2 systems. All expressions are given in Appendix A.

The universal parameters A_i, α_i and β_i fitted to the entire database are shown in Table 1 for each model. From their analysis one may observe the resemblance between their α_i values (0.8556, 0.8600 and 0.8598), which denotes the similar and chief dependence of D_{12} upon T/η_1. The β_1 and β_2 constants are the exponents of $V_{bp,2}$ in the mWC and mSch models (Eqs. (1) and (2)). They achieve distinct values ($\beta_1 = 0.5304$ and $\beta_2 = 0.2774$) due to the additional correction introduced by the second term inside the square brackets of mSch expression. With respect to A_i, their values possess the same order of magnitude in the case of mSch and mLR (10^{-7}) but increase one order in the case of mWC (10^{-6}). Such difference dues to the dissimilar functional dependence of D_{12}, *i.e.* the sum inside the brackets of Eqs. (2) and (3) does not occur in Eq. (1).

The individual AARDs obtained in this essay are listed in Table S.3 (Supplementary data) for the new (mWC, mSch, mLR) and seminal (WC, Sch, LR, LT) equations. Readers may consult this table in order to select the best expression for a particular system that has been already studied in this work.

In Table 2 the global errors and standard deviations (σ_{AARD}) are presented for each model, being possible to observe the better results provided by the new ones. The modifications introduced by A_i, α_i and β_i are able to reduce the average errors from 11.70% (WC) to 8.26% (mWC), 14.88% (Sch) to 8.51% (mSch), and 23.16% (LR) to 8.45% (mLR). The Lai-Tan model is specific for SC-CO_2 systems but provides higher errors (14.68%) than the modified equations of this work. The accuracy and reliability of mWC, mSch and mLR models are reinforced by the computed standard deviations: they lie between 4.92% and 5.14%, against interval 6.36-11.60% for the equations of literature. In general, they drop approximately by half, which strengthens their robust and unbiased behavior around average. A similar conclusion may be drawn from the observation of Fig. 1, where calculated diffusivities are plotted against experimental values for the three improved and original expressions. A better distribution of data points along diagonal is achieved with our models, while literature equations deliver more scatter and biased results.

Table 1. Optimized parameters of the D_{12} equations proposed in this work, when variables are expressed in cgs system except viscosity (cP) and pressure (bar).

Model	Equation	A_i	α_i	β_i
mWC	(1)	1.0681×10^{-6}	0.8556	0.5304
mSch	(2)	1.6120×10^{-7}	0.8600	0.2774
mLR	(3)	1.1126×10^{-7}	0.8598	0.6868

mWC, modified Wilke-Chang equation; mSch, modified Scheibel equation; mLR, modified Lusis-Ratcliff equation.

Table 2. Global errors (AARD) and standard deviations (σ_{AARD}) obtained by the new models and by those adopted for comparison.

Model	mWC	mSch	mLR	WC	Sch	LR	LT

Equation	(1)	(2)	(3)	(A.1)	(A.2)	(A.3)	(A.4)
AARD (%)	8.26	8.51	8.45	11.70	14.88	23.16	14.68
σ_{AARD}	5.14	4.92	4.95	6.36	11.60	10.77	8.06

mWC, modified Wilke-Chang equation; mSch, modified Scheibel equation; mLR, modified Lusis-Ratcliff equation; WC, Wilke-Chang equation; Sch, Scheibel equation; LR, Lusis-Ratcliff equation; LT, Lai-Tan equation.

In Fig. 2, the experimental diffusion coefficients of four distinct systems (CO_2/chlorobenzene, CO_2/dibenzo-24-crown-8, CO_2/linoleic acid, CO_2/tetrahydrofuran,) are plotted in Stokes-Einstein coordinates (D_{12} against T/η_1), along with modeling results achieved by the modified and original Wilke-Chang equations. It is evident that the Stokes-Einstein dependence between D_{12} and T/η_1 needed to be corrected since both quantities are not directly proportional, which penalizes the Wilke-Chang trends, especially at higher T/η_1. On the other hand, the power relation assumed in the mWC expression (and similarly in the other two) is greatly effective to describe reliably the diffusive phenomenon, as the modeling curves follow the experimental data very well.

5. Conclusions

In this work, three Stokes-Einstein based expressions for the estimation of binary diffusivities of solutes at infinite dilution in supercritical carbon dioxide are proposed and validated. They are completely predictive and are developed embodying modifications into the hydrodynamic equations of Wilke-Chang, Scheibel and Lusis-Ratcliff. The improved models are tested with a large database containing 150 systems with 4484 data points of very distinct molecules under supercritical conditions, giving rise to global average absolute relative deviations between 8.26% and 8.51%. On the other hand, the three seminal models and the Lai-Tan equation (also adopted for comparison) provide errors between 11.70% and 23.16%. The dispersion of the computed errors around the average is also much lower in the case of the new models, for which the standard deviations are approximately one half.

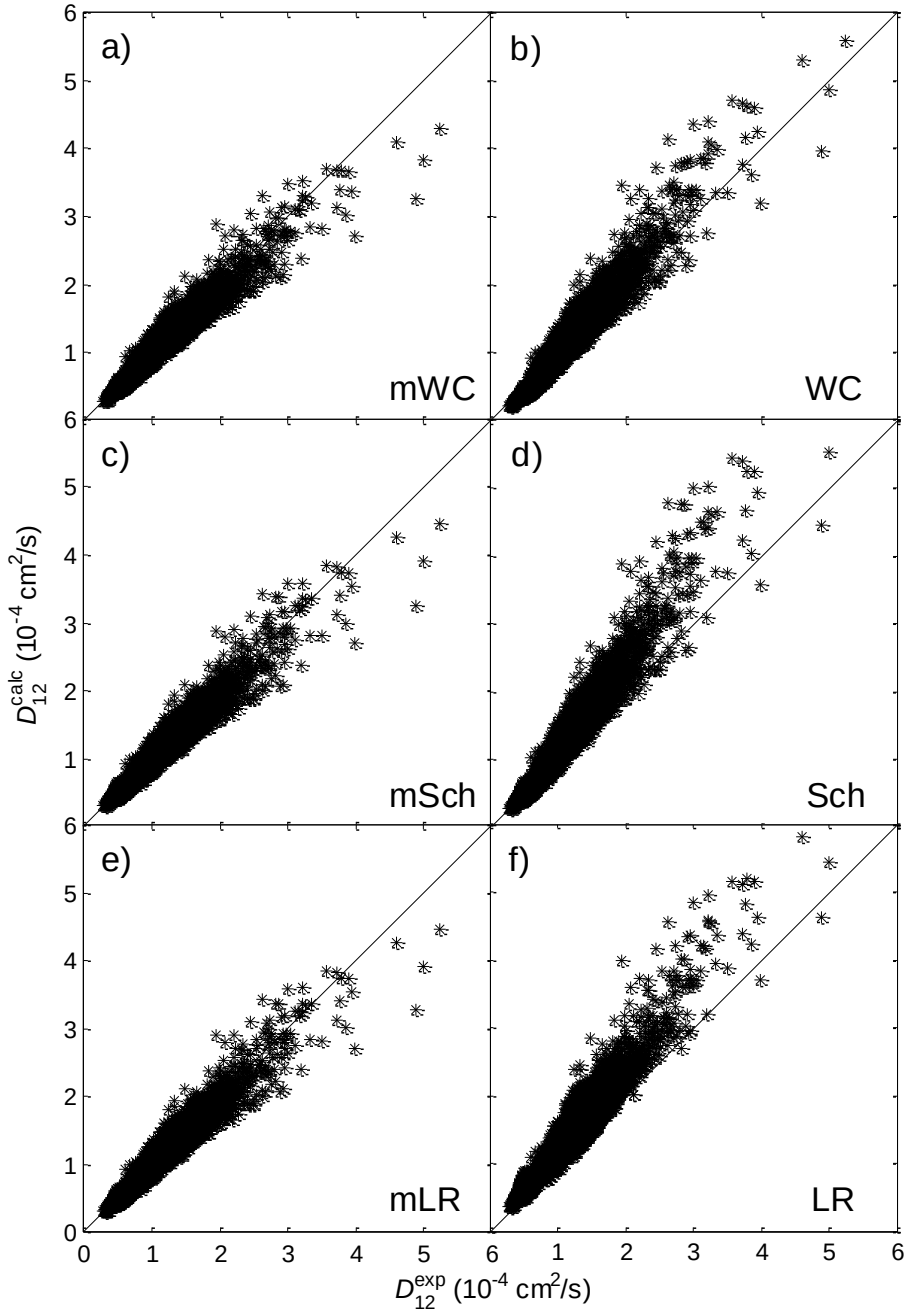

Fig. 1. Calculated *versus* experimental tracer diffusivities computed by the improved equations proposed in this work (left) and by the original models (right).

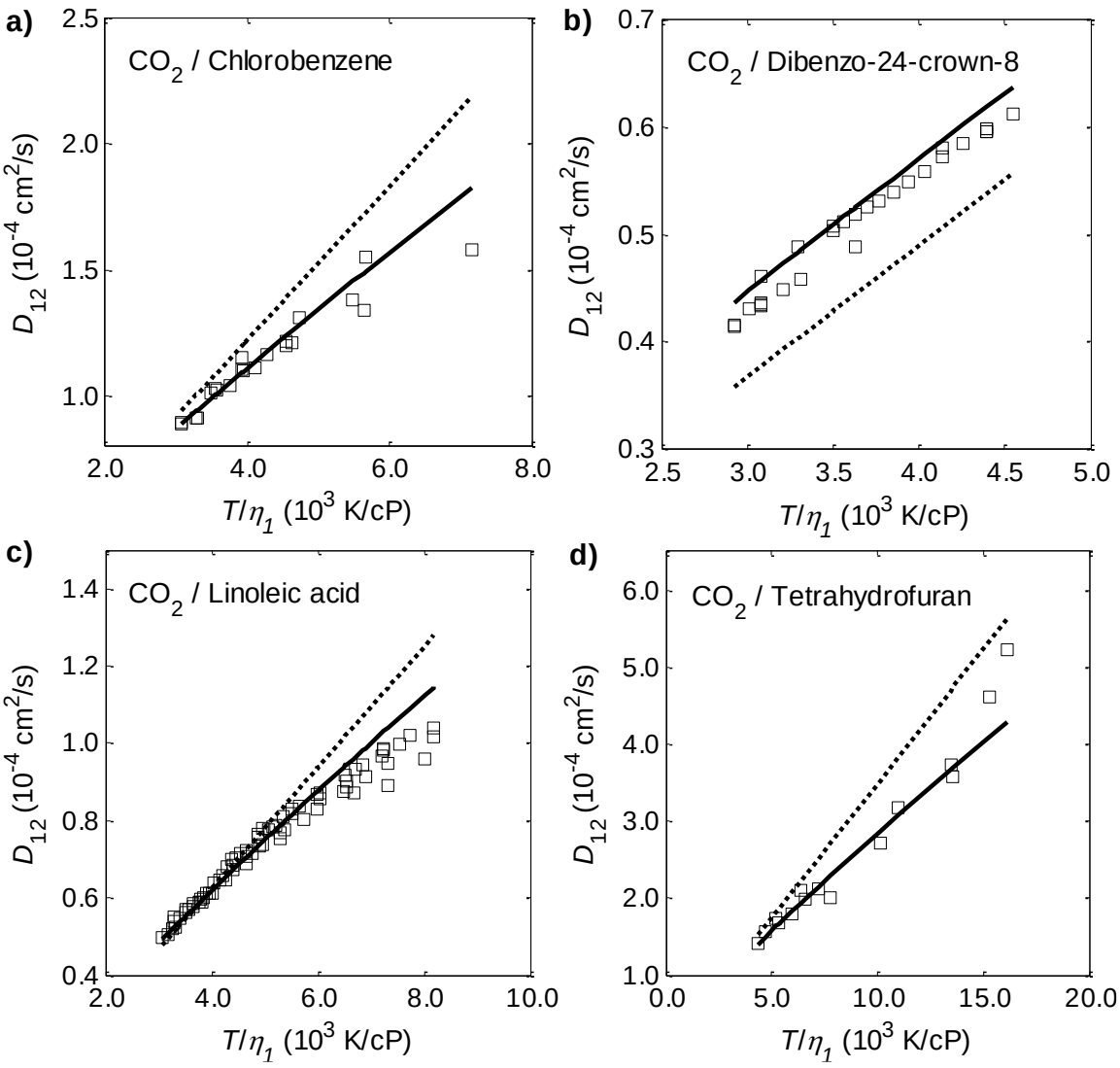

Fig. 2. Experimental and calculated tracer diffusion coefficients plotted in Stokes-Einstein coordinates: a) CO_2/linoleic acid, b) CO_2/chlorobenzene, c) CO_2/tetrahydrofuran, d) CO_2/dibenzo-24-crown-8. Data from [35-39]. Models: (—) modified Wilke-Chang, (---) Wilke-Chang.

Appendix A. Models adopted for comparison

The expressions of Wilke-Chang (WC), Scheibel (Sch), Lusis-Ratcliff (LR) and Lai-Tan (LT), which are the models adopted for comparison in this work, are presented in the following.

$$D_{12,\mathrm{WC}}\left(\mathrm{cm}^2/\mathrm{s}\right)=7.4\times10^{-8}\frac{T\sqrt{\phi M_1}}{\eta_1 V_{\mathrm{bp},2}^{0.6}} \tag{A.1}$$

$$D_{12,\mathrm{Sch}}\left(\mathrm{cm}^2/\mathrm{s}\right)=\frac{8.2\times10^{-8}T}{\eta_1 V_{\mathrm{bp},2}^{1/3}}\left[1+\left(\frac{3V_{\mathrm{bp},1}}{V_{\mathrm{bp},2}}\right)^{2/3}\right] \tag{A.2}$$

$$D_{12,\mathrm{LR}}\left(\mathrm{cm}^2/\mathrm{s}\right)=\frac{8.52\times10^{-8}T}{\eta_1 V_{\mathrm{bp},1}^{1/3}}\left[1.40\left(\frac{V_{\mathrm{bp},1}}{V_{\mathrm{bp},2}}\right)^{1/3}+\left(\frac{V_{\mathrm{bp},1}}{V_{\mathrm{bp},2}}\right)\right] \tag{A.3}$$

$$D_{12,\mathrm{LT}}\left(\mathrm{cm}^2/\mathrm{s}\right)=2.50\times10^{-7}\frac{T\sqrt{M_1}}{\left(10\times\eta_1\right)^{0.688}V_{\mathrm{c},2}{}^{1/3}} \tag{A.4}$$

In the equations, the absolute temperature is in K, and the solvent viscosity in cP; ϕ is a dimensionless association factor of the solvent, M_1 is the solvent molecular weight (g/mol), $V_{\mathrm{bp},1}$ and $V_{\mathrm{bp},2}$ are the solvent and solute molar volumes at their normal boiling points (cm^3/mol), respectively, and $V_{\mathrm{c},2}$ is the solute critical volume (cm^3/mol).

Appendix B – Supplementary data

Supplementary data associated with this article can be found, in the online version, at http://dx.doi.org/10.1016/j.jtice.2013.12.005.

Nomenclature

A_i	Universal constants in Eqs. (1)-(3) (Table 1)
AARD	Average absolute relative deviation, Eq. (4)
D_{12}	Tracer diffusion coefficient of solute 2 through solvent 1
LR	Lusis-Ratcliff equation, Eq. (A.3)

LT	Lai-Tan equation, Eq. (A.4)
M	Molecular weight
mLR	Modified Lusis-Ratcliff equation, Eq. (3)
mSch	Modified Scheibel equation, Eq. (2)
mWC	Modified Wilke-Chang equation, Eq. (1)
NDP	Number of data points
r	Molecule radius
SC-CO_2	Supercritical carbon dioxide
Sch	Scheibel equation, Eq. (A.2)
T	Absolute temperature
V_{bp}	Molar volume at normal boiling point
V_c	Critical molar volume
WC	Wilke-Chang equation, Eq. (A.1)

Greek letters

α_i	Universal constants in Eqs. (1)-(3) (Table 1)
β_i	Universal constants in Eqs. (1)-(3) (Table 1)
ϕ	Association factor in Wilke-Chang equation, Eq. (A.1)
η_1	Solvent (SC-CO_2) viscosity
σ_{AARD}	Standard deviation of the errors AARD

Subscripts

1	Solvent (SC-CO_2)
2	Solute
12	Binary
bp	Normal boiling point
c	Critical property
i	Component; equation

Superscripts

calc	Calculated value
exp	Experimental value
TC	Estimated by the group contribution method of Tyn-Calus

References

[1] C.A.M. Afonso, J.G. Crespo, Green Separation Processes. Fundamentals and Applications, Wiley - VCH Verlag, 2005.

[2] E. Kiran, P.G. Debenedetti, C.J. Peters, Supercritical Fluids: Fundamentals and Applications, 1st ed., Springer, 2000.

[3] R.C. Reid, J.M. Prausnitz, B.E. Poling, The Properties of Gases and Liquids, 4th ed., McGraw-Hill, New York, 1987.

[4] R.V. Vaz, A.L. Magalhães, D.L.A. Fernandes, C.M. Silva, Universal correlation of self-diffusion coefficients of model and real fluids based on residual entropy scaling law, Chemical Engineering Science, 79 (2012) 153-162.

[5] H.Q. Liu, C.M. Silva, E.A. Macedo, Unified approach to the self-diffusion coefficients of dense fluids over wide ranges of temperature and pressure - Hard-sphere, square-well, Lennard-Jones and real substances, Chemical Engineering Science, 53 (1998) 2403-2422.

[6] C.M. Silva, H. Liu, Modelling of Transport Properties of Hard Sphere Fluids and Related Systems, and its Applications, in: Á. Mulero (Ed.) Theory and Simulation of Hard-Sphere Fluids and Related Systems, Springer Berlin Heidelberg, 2008, pp. 383-492.

[7] I. Medina, Determination of diffusion coefficients for supercritical fluids, Journal of Chromatography A, 1250 (2012) 124-140.

[8] K.K. Liong, P.A. Wells, N.R. Foster, Diffusion in supercritical fluids, The Journal of Supercritical Fluids, 4 (1991) 91-108.

[9] A.L. Magalhães, F.A. Da Silva, C.M. Silva, Free-volume model for the diffusion coefficients of solutes at infinite dilution in supercritical CO_2 and liquid H_2O, The Journal of Supercritical Fluids, 74 (2013) 89-104.

[10] A.L. Magalhães, P.F. Lito, F.A. Da Silva, C.M. Silva, Simple and accurate correlations for diffusion coefficients of solutes in liquids and supercritical fluids over wide ranges of temperature and density, The Journal of Supercritical Fluids, 76 (2013) 94-114.

[11] A.L. Magalhães, F.A. Da Silva, C.M. Silva, New models for tracer diffusion coefficients of hard sphere and real systems: Application to gases, liquids and supercritical fluids, The Journal of Supercritical Fluids, 55 (2011) 898-923.

[12] A.L. Magalhães, F.A. Da Silva, C.M. Silva, New tracer diffusion correlation for real systems over wide ranges of temperature and density, Chemical Engineering Journal, 166 (2011) 49-72.

[13] A.L. Magalhães, F.A. Da Silva, C.M. Silva, Tracer diffusion coefficients of polar systems, Chemical Engineering Science, 73 (2012) 151-168.

[14] P.F. Lito, A.L. Magalhães, J.R.B. Gomes, C.M. Silva, Universal model for accurate calculation of tracer diffusion coefficients in gas, liquid and supercritical systems, Journal of Chromatography A, 1290 (2013) 1-26.

[15] C.R. Wilke, P. Chang, Correlation of diffusion coefficients in dilute solutions, AIChE Journal, 1 (1955) 264-270.

[16] M.A. Lusis, C.A. Ratcliff, Diffusion in binary liquid mixtures at infinite dilution, The Canadian Journal of Chemical Engineering, 46 (1968) 385-387.

[17] M.T. Tyn, W.F. Calus, Diffusion coefficients in dilute binary liquid mixtures, Journal of Chemical & Engineering Data, 20 (1975) 106-109.

[18] W. Hayduk, B.S. Minhas, Correlations for prediction of molecular diffusivities in liquids, The Canadian Journal of Chemical Engineering, 60 (1982) 295-299.

[19] K.A. Reddy, L.K. Doraiswamy, Estimating liquid diffusivity, Industrial & Engineering Chemistry Fundamentals, 6 (1967) 77-79.

[20] E.G. Scheibel, Correspondence. Liquid Diffusivities. Viscosity of Gases, Industrial & Engineering Chemistry, 46 (1954) 2007-2008.

[21] E.I. Cussler, Diffusion: Mass Transfer in Fluid Systems, Cambridge University Press, New York, 2009.

[22] K.S. Pitzer, D.R. Schreiber, Improving equation-of-state accuracy in the critical region; equations for carbon dioxide and neopentane as examples, Fluid Phase Equilibria, 41 (1988) 1-17.

[23] V.V. Altunin, M.A. Sakhabetdinov, Viscosity of liquid and gaseous carbon dioxide at temperatures 220-1300 K and pressure up to 1200 bar, Teploenergetika, 8 (1972) 85-89.

[24] K.G. Joback, A unified approach to physical property estimation using multivariate statistical techniques, in: Department of Chemical Engineering, Massachusetts Institute of Technology, Cambridge, MA, 1984.

[25] K.G. Joback, R.C. Reid, Estimation of pure-component properties from group-contributions, Chemical Engineering Communications, 57 (1987) 233 - 243.

[26] G.R. Somayajulu, Estimation procedures for critical constants, Journal of Chemical & Engineering Data, 34 (1989) 106-120.

[27] K.M. Klincewicz, R.C. Reid, Estimation of critical properties with group contribution methods, AIChE Journal, 30 (1984) 137-142.

[28] D. Ambrose, Correlation and Estimation of Vapour-liquid Critical Properties: I, Critical Temperatures of Organic Compounds, in: NPL Technical Report. Chem 92, Nat. Physical Lab., Madison, WI, 1978.

[29] D. Ambrose, Correlation and Estimation of Vapour-Liquid Critical Properties. II: Critical Pressure and Critical Volume, in: NPL Technical Report. Chem. 92, Nat. Physical Lab., Teddington, UK, 1979.

[30] X. Wen, Y. Qiang, A new group contribution method for estimating critical properties of organic compounds, Industrial & Engineering Chemistry Research, 40 (2001) 6245-6250.

[31] L. Constantinou, R. Gani, New group contribution method for estimating properties of pure compounds, AIChE Journal, 40 (1994) 1697-1710.

[32] M.T. Tyn, W.F. Calus, Estimating liquid molar volume, Processing, 21 (1975) 16-17.

[33] P.R. Sassiat, P. Mourier, M.H. Caude, R.H. Rosset, Measurement of diffusion coefficients in supercritical carbon dioxide and correlation with the equation of Wilke and Chang, Analytical Chemistry, 59 (1987) 1164-1170.

[34] C.C. Lai, C.S. Tan, Measurement of molecular diffusion coefficients in supercritical carbon dioxide using a coated capillary column, Industrial & Engineering Chemistry Research, 34 (1995) 674-680.

[35] T. Funazukuri, C.Y. Kong, T. Kikuchi, S. Kagei, Measurements of binary diffusion coefficient and partition ratio at infinite dilution for linoleic acid and arachidonic acid in supercritical carbon dioxide, Journal of Chemical & Engineering Data, 48 (2003) 684-688.

[36] L.M. González, O. Suárez-Iglesias, J.L. Bueno, C. Pizarro, I. Medina, Application of the corresponding states principle to the diffusion in CO_2, AIChE Journal, 53 (2007) 3054-3061.

[37] J.J. Suarez, I. Medina, J.L. Bueno, Diffusion coefficients in supercritical fluids: available data and graphical correlations, Fluid Phase Equilibria, 153 (1998) 167-212.

[38] C.M. Silva, E.A. Macedo, Diffusion coefficients of ethers in supercritical carbon dioxide, Industrial & Engineering Chemistry Research, 37 (1998) 1490-1498.

[39] C.Y. Kong, N. Takahashi, T. Funazukuri, S. Kagei, Measurements of binary diffusion coefficients and retention factors for dibenzo-24-crown-8 and 15-crown-5 in supercritical carbon dioxide by chromatographic impulse response technique, Fluid Phase Equilibria, 257 (2007) 223-227.

Paper III

Adapted from

Improved Hydrodynamic Equations for the Accurate Prediction of Diffusivities in Supercritical Carbon Dioxide

Fluid Phase Equilibria, 360 (2013) 401–415

Abstract

The tracer diffusion coefficients are fundamental quantities in simulation and design. Due to the increasing interest upon biorefinery and sustainability in general, green solvents and processes, like carbon dioxide and supercritical fluid extraction, are attracting relevance in both chemistry and chemical engineering research and development. In this work, tracer diffusion coefficients at infinite dilution are focused aiming to propose reliable models for their pure estimation. Four predictive hydrodynamic models were proposed on the basis of modifications introduced in the original expressions of Wilke-Chang, Scheibel, Lusis-Ratcliff, and Tyn-Calus. The modified equations provide reliable results with average absolute errors between 7.86% and 8.56%, and inferior dispersion around the averages. On the contrary, the original correlations taken from the literature achieve errors between 11.89% and 27.25%, along with higher scattering of results. Furthermore, the new expressions offer average errors between 0.47% and 0.53%, while the original ones provide systematic overestimations between 2.95% and 27.23%. In the whole, the new expressions proposed in this work are equally able to predict accurately tracer diffusion coefficients of any solutes in supercritical carbon dioxide.

1. Introduction

The design and simulation of rate controlled separations and multiphase reactions require the knowledge of both equilibrium and kinetic data. In terms of transport properties, the binary diffusivities at infinite dilution, $D_{12,}$ are fundamental to estimate axial and radial dispersion coefficients, and convective mass transfer coefficients using dimensionless correlations [1-2], and/or catalysts efficiency factors [3]. However, while a considerable number of solubility data has been published, diffusivities are still scarcer. This fact is inducing researchers to develop, test and extend models for their estimation and correlation.

In recent years there has been an increasing interest to replace chemically synthesized compounds by their biobased alternatives under the concept of biorefinery and sustainability [4]. Intimately related is the research/development of green and innovative solvents to perform separations and reactions, where supercritical carbon dioxide (SC-CO_2) and ionic liquids emerge as promising alternatives. Conventional solvents are many times non-selective and

toxic, which associated to the increasing consumer awareness of the use of hazardous substances by the chemical and food industries, along with changes in environmental regulations, constitute a driving force for the research of more environmentally friendly alternatives [4]. The choice of supercritical fluids has been attracting widespread interest owing to their well-documented properties: liquid-like densities, gas-like viscosities, negligible surface tension, and diffusivities between those of gases and liquids [5-6]. Furthermore, the ability to tune its solvent power by changing temperature and/or pressure, or by introducing small quantities of polar co-solvents [5-6] is undoubtedly an important feature.

In last years, besides largely applied to extract edible and essential oils from natural matrices and other natural compounds [5, 7-11], supercritical fluids (SCFs) are also finding interest as solvents/desorbents in preparative chromatography and Simulated Moving Bed (SMB) separations [12-13]. It is also worth mentioning the utilization of SC-CO_2 in the preparation and processing of advanced functional materials as catalysts or precursors, using organometallic solutes [14-15].

Taking into account the large interest and wide applications of SC-CO_2, the existence of diffusion coefficients in this solvent is crucial for the simulation and design of the implied processes, which requires the development of accurate models for their estimation since it is impossible to carry out experimental measurements for all systems at all operating conditions. Several modeling approaches for the diffusion coefficients in dense fluids may be cited: the Enskog theory [16-18] for hard spheres and its modifications for real systems [16, 18], the effective hard sphere diameter method [18-21], the free-volume theories [18, 22-24], the van der Waals [18, 25-26] and rough hard sphere principles [18, 27-32], the hydrodynamic models based on the Stokes-Einstein equation [33-34], the Eyring activated-state theory [35], and excess entropy scaling laws [18, 36-38]. Several papers reviewed most of these models [18, 33-34, 38-39].

Most models found in the literature usually fail in systems involving polar molecules and/or very asymmetric components (in terms of mass and size), and when applied over wide ranges of temperature and pressure. Hence, very recently, we developed accurate D_{12} correlations validated with large databases: molecularly based models, equations based on free-volume and Rice and Gray approaches [40-44], and semi-empirical expressions [45]. In the whole, excellent

representations of the experimental diffusivities were accomplished, generally with errors lower than 4.44 %, and very good extrapolation ability was confirmed with deviations between 3.46 % and 5.27 %. Since theoretical models are frequently lengthy for D_{12} calculations, spreadsheets were provided in the supplementary material (online) of the original papers [40, 43-44] to perform this task with simplicity. Nonetheless, one limitation persists: they require one or two parameters previously fitted to data for the specific system under study. An alternative are predictive hydrodynamic equations like Wilke-Chang [46], Tyn-Calus [47], Hayduk-Minhas [48], Reddy-Doraiswamy [49], Scheibel [50], and Lusis-Ratcliff [51], since they are simple and involve a small set of input data. However, significant errors are obtained, particularly when they are applied over large ranges of temperature and density, or near the critical point [40, 44-45].

Hence, in this work, four hydrodynamic equations are revisited and improved in order to provide reliable predictions of diffusivities in supercritical CO_2. The modified models are validated with the largest database compiled, and much smaller errors are achieved in comparison with the original formulae. The equations under study are Wilke-Chang, Scheibel, Lusis-Ratcliff and Tyn-Calus.

2. Modified hydrodynamic models under investigation

Mass transport may be described by the hydrodynamic approach, which establishes a proportionality between diffusion coefficients and the ratio T/η_1, embodied in the Stokes-Einstein expression:

$$D_{12} = \frac{k_B T}{6 \pi r_2 \eta_1} \tag{1}$$

where T is the absolute temperature, η_1 is the solvent viscosity, k_B is the Boltzmann's constant, and r_2 is the radius of the solute molecule. This model assumes that a large rigid spherical molecule of solute is moving through a continuum of solvent ($r_1 << r_2$) under infinitely dilute conditions [33, 52].

A large group of hydrodynamic equations was originally developed for liquids and then extended to SCFs [34, 53], which gives rise to significant overestimations of D_{12}, most likely due to their inability to describe the role of viscosity in the diffusion process [34, 54-55]. Since the Stokes-Einstein assumptions do not hold for all conditions, namely for supercritical systems, some modifications have been suggested, comprising dependencies with the solute properties to take into account the effect of its size or the fluid surface tensions [16, 34, 48, 55-56]. Alternatively, some authors adopted power law relationships between D_{12} and the variables involved.

In this work the hydrodynamic equations of Wilke-Chang (WC), Scheibel (Sch), Lusis-Ratcliff (LR) and Tyn-Calus (TC), whose expressions are compiled in Appendix A (Eqs. (A.1)-(A.4)), were modified in order to improve their behavior and predictive ability in the supercritical domain. The modified models are denoted by mWC, mSch, mLR and mTC, where the prefix 'm' stands for 'modified'. The dependence of the original WC, Sch, LR and TC models on the molar volumes at normal boiling point of both solute and solvent, $V_{\mathrm{bp,i}}$, was replaced by analogous dependencies upon critical molar volumes, $V_{\mathrm{c,i}}$. This choice is justified by the availability and also reliable predicted values of the critical volumes. Moreover, it is more realistic for the particular case of CO_2. The modified models contain only three or four universal constants to be fitted to experimental data: A_{i}, α_{i} and β_{i} (for mWC, mSch, mLR) or A_{i}, α_{i}, β_{i} and γ (for mTC). Since the SC-CO_2 is explicitly focused, the specific constants of carbon dioxide are embodied in the fitting parameters to simplify the final equations. The mathematical expressions are presented in the following and the units are the same in all cases.

2.1. Modified Wilke-Chang equation (mWC). The proposed modification establishes a new dependence of D_{12} on T/η_1 and, as explained before, on the critical molar volume, $V_{\mathrm{c,2}}$:

$$D_{12}\left(\mathrm{cm^2/s}\right) = A_1\left(\frac{T}{\eta_1}\right)^{\alpha_1}\frac{1}{V_{\mathrm{c,2}}^{\beta_1}} \tag{2}$$

Here, the absolute temperature is in K, the solvent viscosity in cP, and $V_{\mathrm{c,2}}$ in $\mathrm{cm^3/mol}$.

2.2. Modified Scheibel equation (mSch). Similarly to the mWC model, a new dependence upon T/η_1 and $V_{c,2}$ is considered:

$$D_{12}\left(\mathrm{cm^2/s}\right)= A_2\left(\frac{T}{\eta_1}\right)^{\alpha_2}\frac{1}{V_{c,2}^{\beta_2}}\left[1+\left(\frac{3V_{c,1}}{V_{c,2}}\right)^{2/3}\right] \tag{3}$$

where $V_{c,1}$ is the critical volume of the solvent (cm^3/mol).

2.3. Modified Lusis-Ratcliff equation (mLR). Once again, the dependence upon temperature and solvent viscosity were changed along with the introduction of critical volumes:

$$D_{12}\left(\mathrm{cm^2/s}\right)= A_3\left(\frac{T}{\eta_1}\right)^{\alpha_3}\left[\beta_3\left(\frac{V_{c,1}}{V_{c,2}}\right)^{1/3}+\left(\frac{V_{c,1}}{V_{c,2}}\right)\right] \tag{4}$$

The terms inside the square parenthesis remain the same functional dependence.

2.4. Modified Tyn-Calus equation (mTC). The modification introduced in this case is patent in Eqs. (5)-(7), where $\mathbf{P}_{bp,2}$ ($cm^3\,g^{1/4}$/(mol $s^{1/2}$)) identifies the parachor of the solute at normal boiling point, which is related with its surface tension at the same conditions ($\sigma_{bp,2}$, g/s^2) and may be estimated by additive group contributions. The relation between both variables is $\mathbf{P}_{bp,2}=V_{bp,2}\,\sigma_{bp,2}^{1/4}$ [33]. For simplicity, $\sigma_{bp,2}$ is estimated in this work by the corresponding states method of Brock and Bird [33, 57] combined with Miller's equation [33, 58].

$$D_{12}\left(\mathrm{cm^2/s}\right)= A_4\left(\frac{T}{\eta_1}\right)^{\alpha_4}\frac{\mathbf{P}_{bp,2}^{\beta_4}}{V_{c,2}^{\gamma}} \tag{5}$$

$$\sigma_{bp,2}\left(\mathrm{g/s^2}\right)= P_{c,2}^{2/3}\,T_{c,2}^{1/3}\left(0.132\alpha_{c,2}-0.279\right)\left(1-T_{bp,2,r}\right)^{11/9} \tag{6}$$

$$\alpha_{c,2}=0.9076\left[1+\frac{T_{bp,2,r}\,\ln\left(P_{c,2}/1.013\right)}{1-T_{bp,2,r}}\right] \tag{7}$$

where $P_{c,2}$ (bar), $T_{c,2}$ (K) and $T_{bp,2,r} = T_{bp,2}/T_{c,2}$ are the critical pressure, the critical temperature, and the reduced normal boiling point of solute, respectively. It is important to refer that experimental solute molar volumes at normal boiling point, $V_{bp,2}$, are frequently unavailable, which makes its estimation mandatory for use in the parachor. However, the deviations found between both values can be significant and this requires a previous correction [53]. The well known method of Tyn-Calus [33, 59] has been selected in this essay with advantage due to its simplicity. Accordingly, the following explicit regression obtained after plotting data available for 97 molecules is used:

$$V_{bp}^{exp} = 1.459\left(V_{bp}^{TC}\right)^{0.894} \quad (8)$$

where superscripts 'exp' and 'TC' stand for 'experimental' and 'estimated by Tyn-Calus method' respectively. Fig. S.1 (see Supplementary data) confirms that the direct substitution of the experimental molar volume at normal boiling point by its estimated value would originate large discrepancies since data points do not distribute unbiasedly along diagonal. For this reason, Eq. (8) will be always employed in Eq. (5) *via* the parachor.

3. Database and data for the calculations

Table 1 compiles the name, molecular formula, CAS number, critical constants, normal boiling point, and molar volume at normal boiling point of all molecules involved in calculations. When densities of SC-CO_2 were not provided by the authors, the correlation of Pitzer and Schreiber [60] was employed. The correlation of Altunin and Sakhabetdinov [61] was used to estimate absent SC-CO_2 viscosities. Finally, the solute molar volumes at normal boiling point were computed by Tyn-Calus equation [33], and the non-existent critical constants were estimated by Joback [33, 62-63], Somayajulu [64], Klincewicz [33, 65], Ambrose [33, 66-67], Wen–Qiang [68], and Constantinou–Gani [69] methods.

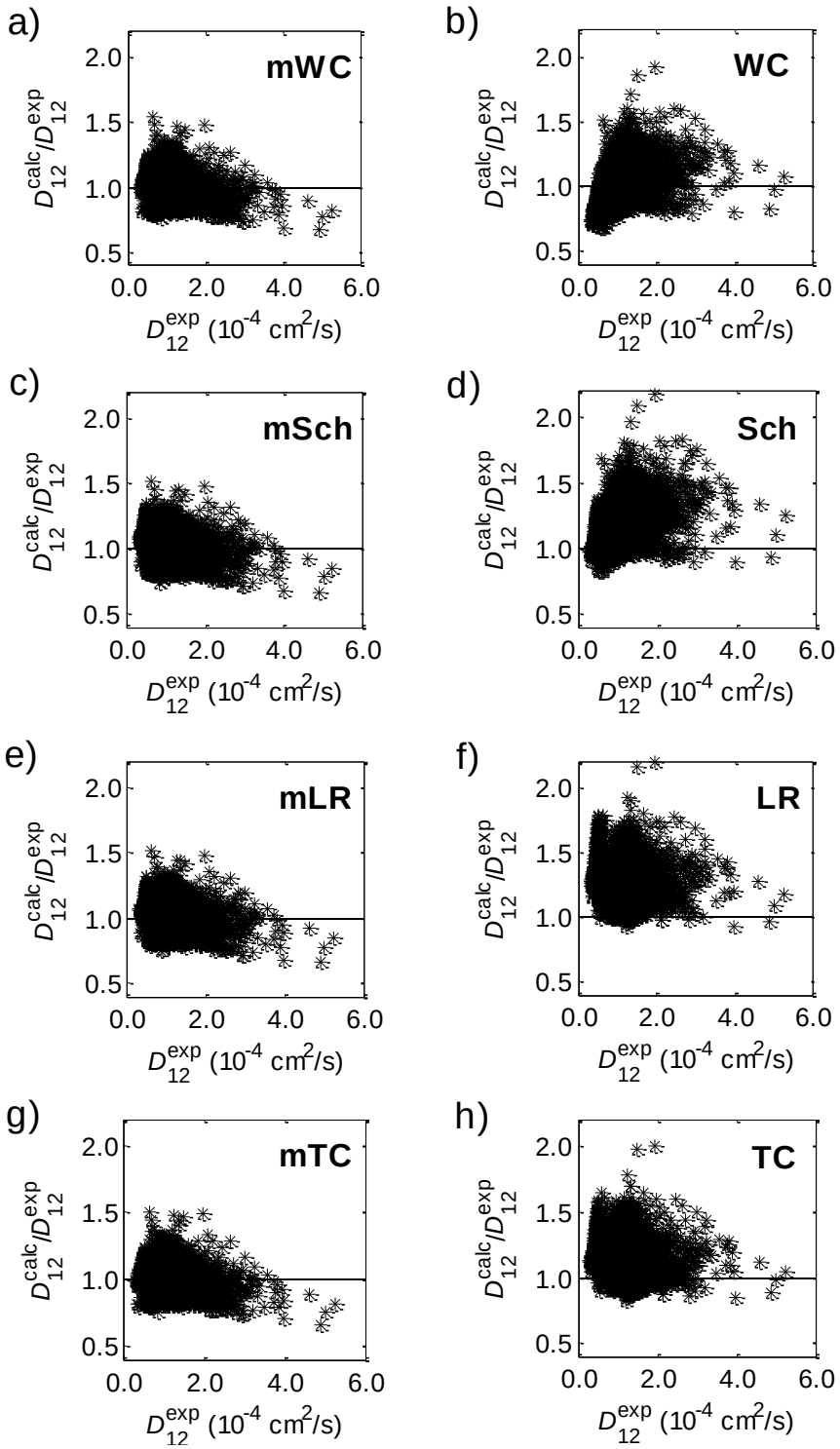

Fig. 1. Ratio of calculated and measured diffusivities *versus* experimental data computed by the equations proposed in this work (left) and the equations adopted for comparison (right).

The new models were validated with the largest database of experimental tracer diffusivities in SC-CO_2 ever compiled: 4529 data points of 159 systems. It is described in detail in Table 2, where system identification, number of points, reduced ranges of temperature, pressure and solvent density, and data sources are listed. Data available exclusively in graphical form were not included in the calculations. Furthermore, *n*-alkanes were not considered for the overall correlation because their calculated diffusivities are systematically lower. It is worth noting that most equations generally fail to describe this group of molecules in SC-CO_2 [33, 45, 70-71], which frequently induces authors to optimize specific constants for them.

4. Results and discussion

In this section, the predictions accomplished with the new modified hydrodynamic equations (mWC, mSch, mLR, mTC) are presented and analyzed, along with the estimations obtained with the equations adopted for comparison (WC, Sch, LR, TC). The errors achieved in all cases are expressed in terms of the average absolute relative deviation (AARD) and average relative deviations (ARD) computed by, respectively:

$$\mathrm{AARD}\,(\%) = \frac{100}{\mathrm{NDP}} \sum_{i=1}^{\mathrm{NDP}} \left| \frac{D_{12}^{\mathrm{calc}} - D_{12}^{\mathrm{exp}}}{D_{12}^{\mathrm{exp}}} \right|_i \tag{9}$$

$$\mathrm{ARD}\,(\%) = \frac{100}{\mathrm{NDP}} \sum_{i=1}^{\mathrm{NDP}} \left(\frac{D_{12}^{\mathrm{calc}} - D_{12}^{\mathrm{exp}}}{D_{12}^{\mathrm{exp}}} \right)_i \tag{10}$$

In Table 2, the detailed results achieved by both new and original equations are listed, giving readers the opportunity to select the best expressions for a particular system already studied in this work. From a general comparison it is evident the great improvement skilled by our modifications into the original models, mainly Scheibel, Lusis-Ratcliff and Tyn-Calus.

Table 1. Data and properties of pure substances.

Substance	Formula	CAS Number	T_c (K)	P_c (bar)	V_c (cm^3/mol)	T_{bp} (K)	V_{bp} (cm^3/mol) [q]
Acetone[a]	C_3H_6O	67-64-1	508.10	47.00	209.00	329.20	76.98
Acridine[b]	$C_{13}H_9N$	260-94-6	905.00	36.40	543.00	619.15	209.37
Allylbenzene[c]	C_9H_{10}	300-57-2	639.86	33.50	419.80	429.16[d]	159.88
Aniline[a]	C_6H_7N	62-53-3	699.00	53.10	274.00	457.60	102.24
Anisole[e]	C_7H_8O	100-66-3	641.65	41.75	337.00	426.73	127.00
Anthracene[e]	$C_{14}H_{10}$	120-12-7	873.00	29.00	554.00	615.18	213.82
Arachidonic acid (AA)[f]	$C_{20}H_{32}O_2$	506-32-1	1013.42	12.74	1093.20	819.15[d]	435.92
AA ethyl ester[g]	$C_{22}H_{36}O_2$	1808-26-0	960.63	11.31	1195.26	777.62[d]	478.66
Behenic acid ethyl ester[g]	$C_{24}H_{48}O_2$	5908-87-2	984.94	9.15	1394.66	806.74[d]	562.66
Benzene[a]	C_6H_6	71-43-2	562.20	48.90	259.00	353.20	96.38
Benzoic acid[a]	$C_7H_6O_2$	65-85-0	752.00	45.60	341.00	523.00	128.58
Benzyl acetate[e]	$C_9H_{10}O_2$	140-11-4	699.00	31.80	449.00	486.65	171.55
Benzylacetone[c]	$C_{10}H_{12}O$	2550-26-7	722.51	31.20	500.50	506.66[d]	192.23
Biphenyl[a]	$C_{12}H_{10}$	92-52-4	789.00	38.50	502.00	529.30	192.83
2-Bromoanisole[c]	C_7H_7BrO	578-57-4	737.58	40.04	378.05	489.16[d]	143.26
Bromobenzene[a]	C_6H_5Br	108-86-1	670.00	45.20	324.00	429.20	121.87
2-Butanone[a]	C_4H_8O	78-93-3	536.80	42.10	267.00	352.70	99.50
n-Butylbenzene[a]	$C_{10}H_{14}$	104-51-8	660.50	28.90	497.00	456.50	190.82
sec-Butylbenzene[e]	$C_{10}H_{14}$	135-98-8	664.54	29.51	497.00	446.48	190.82
tert-Butylbenzene[a]	$C_{10}H_{14}$	98-06-6	660.00	29.60	492.00[b]	442.30	188.81
Butyric acid ethyl ester[h]	$C_6H_{12}O_2$	105-54-4	579.00	31.40	400.00	393.15[i]	151.99
Caffeine[h]	$C_8H_{10}N_4O_2$	58-08-2	855.60	41.50	488.00	451.15[i]	187.20
Capric acid ethyl ester[h]	$C_{12}H_{24}O_2$	110-38-3	699.30	17.88	733.50	514.65[b]	286.94

Table 1. (continued)

Substance	Formula	CAS Number	T_c (K)	P_c (bar)	V_c (cm^3/mol)	T_{bp} (K)	V_{bp} (cm^3/mol) [q]
Caprylic acid ethyl ester[h]	$C_{10}H_{20}O_2$	106-32-1	655.70	21.18	621.50	480.15[i]	241.20
Carbon dioxide[a]	CO_2	124-38-9	304.10	73.80	93.90	194.70[e]	33.28
β-Carotene[f]	$C_{40}H_{56}$	7235-40-7	1450.76	6.90	1934.95	1209.38[d]	793.00
L-Carvone[j]	$C_{10}H_{14}O$	6485-40-1	709.40	26.30	504.65	507.92	193.90
Chlorobenzene[a]	C_6H_5Cl	108-90-7	632.40	45.20	308.00	404.90	115.57
Chrysene[e]	$C_{18}H_{12}$	218-01-9	979.00	23.90	690.00	714.15	269.13
Citral[f]	$C_{10}H_{16}O$	5392-40-5	692.70	23.15	591.00	502.20[k]	228.81
Cobalt(III) acetylacetonate[l]	$C_{15}H_{21}CoO_6$	21679-46-9	573.48	2.52	640.95	423.15[m]	249.11
Copper(II) trifluoroacetylacetonate[l]	$C_{10}H_8CuF_6O_4$	14324-82-4	412.85	20.63	441.13	299.15[i]	168.40
Dibenzo-24-crown-8[f]	$C_{24}H_{32}O_8$	14174-09-5	1396.77	15.80	1174.35	1111.44[d]	469.89
15-Crown-5[f]	$C_{10}H_{20}O_5$	33100-27-5	876.80	28.72	548.75	625.60[d]	211.69
Cycloheptanone[l]	$C_7H_{12}O$	502-42-1	671.19	36.86	297.87	453.15[i]	111.59
Cyclononanone[l]	$C_9H_{16}O$	3350-30-9	702.10	31.47	380.74	478.25[i]	144.33
Cyclopentanone[e]	C_5H_8O	120-92-3	626.00	58.50	258.00	403.80	95.99
n-Decane[a]	$C_{10}H_{22}$	124-18-5	617.70	21.20	603.00	447.30	233.68
Dibenzyl ether[e]	$C_{14}H_{14}O$	103-50-4	777.00	25.60	608.00	561.45	235.71
1,2-Dichlorobenzene[a]	$C_6H_4Cl_2$	95-50-1	729.00	41.00	360.00	452.00	136.10
1,3-Dichlorobenzene[e]	$C_6H_4Cl_2$	541-73-1	683.95	40.70	351.00	446.23	132.53
p-Dichlorobenzene[e]	$C_6H_4Cl_2$	106-46-7	684.75	40.70	351.00	447.21	132.53
Diethyl ether[a]	$C_4H_{10}O$	60-29-7	466.70	36.40	280.00	307.60	104.58
1,2-Diethylbenzene[e]	$C_{10}H_{14}$	135-01-3	668.00	28.80	502.00	456.61	192.83
1,4-Diethylbenzene[e]	$C_{10}H_{14}$	105-05-5	657.96	28.03	497.00	456.94	190.82
Diisopropyl ether[a]	$C_6H_{14}O$	108-20-3	500.30	28.80	386.00	341.70	146.42
2,3-Dimethylaniline[c]	$C_8H_{11}N$	87-59-2	717.00	36.30	400.38	494.66[d]	152.14

Table 1. (continued)

Substance	Formula	CAS Number	T_c (K)	P_c (bar)	V_c (cm^3/mol)	T_{bp} (K)	V_{bp} (cm^3/mol) [q]
2,6-Dimethylaniline[n]	$C_8H_{11}N$	87-62-7	722.00	42.00	400.38[c]	491.05	152.14
1,1'-Dimethylferrocene[l]	$C_{12}H_{14}Fe$	1291-47-0	514.45	27.41	400.64	353.55[i]	152.24
2,6-Dimethylnaphthalene[e]	$C_{12}H_{12}$	581-42-0	777.00	31.70	520.00	535.15	200.09
2,7-Dimethylnaphthalene[e]	$C_{12}H_{12}$	582-16-1	778.00	31.70	520.00	536.15	200.09
2,4-Dimethylphenol[a]	$C_8H_{10}O$	105-67-9	707.60	44.00[e]	390.00[e]	484.10	148.01
Diolein[b]	$C_{39}H_{72}O_5$	2465-32-9	1025.00	7.92	2150.00	920.00	885.61
1,3-Divinylbenzene[e]	$C_{10}H_{10}$	108-57-6	692.00	31.20	440.00	472.65	167.95
Docosahexaenoic acid (DHA)[g]	$C_{22}H_{32}O_2$	6217-54-5	1075.45	12.41	1148.05	873.23[d]	458.86
DHA ethyl ester[g]	$C_{24}H_{36}O_2$	84494-72-4	1023.28	10.84	1262.06	831.70[d]	506.73
DHA methyl ester[g]	$C_{23}H_{34}O_2$	28061-46-3	999.34	11.41	1206.56	808.82[d]	483.40
n-Dodecane[a]	$C_{12}H_{26}$	112-40-3	658.20	18.20	713.00	489.50	278.54
Eicosapentaenoic acid (EPA)[g]	$C_{20}H_{30}O_2$	10417-94-4	1020.90	13.47	1059.15	823.31[d]	421.70
EPA ethyl ester[g]	$C_{22}H_{34}O_2$	84494-70-2	968.16	11.67	1173.16	781.78[d]	469.39
EPA methyl ester[g]	$C_{21}H_{32}O_2$	2734-47-6	890.55	11.90	1187.03	758.90[d]	475.20
Ethanol[a]	C_2H_6O	64-17-5	513.90	61.40	167.10	351.40	60.89
Ethyl acetate[a]	$C_4H_8O_2$	141-78-6	523.20	38.30	286.00	350.30	106.93
Ethylbenzene[a]	C_8H_{10}	100-41-4	617.20	36.00	374.00	409.30	141.65
Ethyl benzoate[a]	$C_9H_{10}O_2$	93-89-0	668.70	23.20	489.00[c]	485.90[e]	187.60
2-Ethyltoluene[a]	C_9H_{12}	611-14-3	651.00	30.40	460.00	438.30	175.96
3-Ethyltoluene[a]	C_9H_{12}	620-14-4	637.00	28.40	490.00	434.50	188.01
4-Ethyltoluene[a]	C_9H_{12}	622-96-8	640.00	29.40	470.00	435.20	179.97
Eugenol[c]	$C_{10}H_{12}O_2$	97-53-0	735.31	33.52	447.23	526.36[d]	170.84
Ferrocene[l]	$C_{10}H_{10}Fe$	102-54-5	786.27	32.07	317.77	522.15[m]	119.42
2-Fluoroanisole[c]	C_7H_7FO	321-28-8	644.81	38.11	328.87	427.66[d]	123.79

Table 1. (continued)

Substance	Formula	CAS Number	T_c (K)	P_c (bar)	V_c (cm^3/mol)	T_{bp} (K)	V_{bp} (cm^3/mol) [q]
Fluorobenzene[a]	C_6H_5F	462-06-6	560.10	45.50	269.00	357.90	100.28
3-Fluorophenol[f]	C_6H_5FO	372-20-3	665.54	54.83	339.60	443.25[d]	128.03
Geraniol[f]	$C_{10}H_{18}O$	106-24-1	688.44	25.78	571.30	528.46[d]	220.82
n-Heptane[a]	C_7H_{16}	142-82-5	540.30	27.40	432.00	371.60	164.75
Hexachlorobenzene[e]	C_6Cl_6	118-74-1	825.00	28.50	526.00	582.55	202.51
1-Hexadecene[o]	$C_{16}H_{32}$	629-73-2	722.00	14.80	933.00	558.02	369.22
1,1,1,5,5,5-Hexafluoroacetylacetone[g]	$C_5H_2F_6O_2$	1552-22-1	569.07	27.17	406.05	410.70[d]	154.40
n-Hexane[a]	C_6H_{14}	110-54-3	507.50	30.10	370.00	341.90	140.06
Iodobenzene[a]	C_6H_5I	591-50-4	721.00	45.20	351.00	461.60	132.53
Isobutylbenzene[o]	$C_{10}H_{14}$	538-93-2	650.00	30.50	478.00	445.94	183.18
D-Limonene[e]	$C_{10}H_{16}$	138-86-3	660.00	27.50	524.00	449.65	201.70
Linalool[f]	$C_{10}H_{18}O$	78-70-6	645.80	25.95	558.00	472.00[k]	215.44
Linoleic acid[b]	$C_{18}H_{32}O_2$	60-33-3	775.00	14.10	990.00	628.00	392.89
Linoleic acid methyl ester[g]	$C_{19}H_{34}O_2$	112-63-0	870.78	12.54	1070.95	700.66[d]	426.62
α-Linolenic acid[b]	$C_{18}H_{30}O_2$	463-40-1	780.00	14.40	1070.00	632.00	426.23
γ-Linolenic acid[g]	$C_{18}H_{30}O_2$	506-26-3	958.98	14.17	992.35	769.23[d]	393.87
γ-Linolenic acid ethyl ester[l]	$C_{20}H_{34}O_2$	1191-41-9	937.02	17.56	797.37	663.73[i]	313.17
γ-Linolenic acid methyl ester[g]	$C_{19}H_{32}O_2$	16326-32-2	882.79	12.92	1050.86	704.82[d]	418.24
L-Menthone[j]	$C_{10}H_{18}O$	14073-97-3	699.44	25.30	525.24	499.40	202.20
Methanol[a]	CH_4O	67-56-1	512.60	80.90	118.00	337.70	42.28
2-Methylanisole[c]	$C_8H_{10}O$	578-58-5	648.79	35.60	371.70	444.16[d]	140.74
4-Methylanisole[c]	$C_8H_{10}O$	104-93-8	655.36	35.60	371.70	448.66[d]	140.74
3-Methylbutylbenzene[b]	$C_{11}H_{16}$	2049-94-7	676.37	26.71	537.50	472.05	207.15
1-Methylnaphthalene[o]	$C_{11}H_{10}$	90-12-0	772.00	36.00	465.00	517.83	117.97
Monoolein[b]	$C_{21}H_{40}O_4$	111-03-5	885.00	12.40	1210.00	714.00	484.85

Table 1. (continued)

Substance	Formula	CAS Number	T_c (K)	P_c (bar)	V_c (cm^3/mol)	T_{bp} (K)	V_{bp} (cm^3/mol) [q]
Myristic acid ethyl ester[g]	$C_{16}H_{32}O_2$	124-06-1	789.35	13.89	950.66	623.70[d]	376.54
Myristoleic acid[f]	$C_{14}H_{26}O_2$	544-64-9	854.23	16.97	819.90	669.39[d]	322.45
Myristoleic acid methyl ester[f]	$C_{15}H_{28}O_2$	56219-06-8	777.79	15.26	876.45	604.98[d]	345.80
Naphthalene[a]	$C_{10}H_8$	91-20-3	748.40	40.50	413.00	491.10	157.17
1-Naphthol[e]	$C_{10}H_8O$	90-15-3	802.00	47.37	375.50	561.15	142.24
2-Naphthol[h]	$C_{10}H_8O$	135-19-3	811.40	47.40	375.50	558.65[i]	142.24
2-Nitroanisole[e]	$C_7H_7NO_3$	91-23-6	782.00	37.60	422.00	546.15	160.76
Nitrobenzene[e]	$C_6H_5NO_2$	98-95-3	719.00	44.00	349.00	483.95	131.74
3-Nitrotoluene[e]	$C_7H_7NO_2$	99-08-1	734.00	38.00	441.00	505.00	168.35
n-Nonane[a]	C_9H_{20}	111-84-2	594.60	22.90	548.00	424.00	211.39
n-Octane[a]	C_8H_{18}	111-65-9	568.80	24.90	492.00	398.80	188.81
Oleic acid[b]	$C_{18}H_{34}O_2$	112-80-1	781.00	13.90	1000.00	633.00	397.05
Oleic acid ethyl ester[f]	$C_{20}H_{38}O_2$	111-62-6	891.97	11.38	1154.20	719.38[d]	461.44
Oleic acid methyl ester[f]	$C_{19}H_{36}O_2$	112-62-9	868.65	12.01	1098.65	696.50[d]	438.19
Palladium(II) acetylacetonate[l]	$C_{10}H_{14}O_4Pd$	14024-61-4	651.12	4.13	435.41	573.15[m]	166.11
Palmitic acid ethyl ester[g]	$C_{18}H_{36}O_2$	628-97-7	835.62	12.36	1061.66	669.46[d]	422.74
n-Pentane[a]	C_5H_{12}	109-66-0	469.70	33.70	304.00	309.20	114.00
2-Pentanone[a]	$C_5H_{10}O$	107-87-9	561.10	36.90	301.00	375.40	112.82
3-Pentanone[a]	$C_5H_{10}O$	96-22-0	561.00	37.30	336.00	375.10	126.60
n-Pentylbenzene[e]	$C_{11}H_{16}$	538-68-1	679.90	26.04	550.00	478.61	212.20
Phenanthrene[a]	$C_{14}H_{10}$	85-01-8	873.00	29.00[e]	554.00	613.00	213.82
Phenol[a]	C_6H_6O	108-95-2	694.20	61.30	229.00	455.00	84.71
Phenylacetic acid[f]	$C_8H_8O_2$	103-82-2	783.55	38.50	422.60	554.63[d]	161.00
Phenylacetylene[e]	C_8H_6	536-74-3	655.43	44.03	337.50	418.36	127.20

Table 1. (continued)

Substance	Formula	CAS Number	T_c (K)	P_c (bar)	V_c (cm^3/mol)	T_{bp} (K)	V_{bp} (cm^3/mol) [q]
Phenylbutazone[f]	$C_{19}H_{20}N_2O_2$	50-33-9	861.18	18.38	933.55	674.85[m]	369.44
1-Phenyldodecane[e]	$C_{18}H_{30}$	123-01-3	774.26	15.79	1000.00	600.76	397.05
1-Phenylethanol[c]	$C_8H_{10}O$	98-85-1	675.30	40.60	392.15	478.16[d]	148.86
2-Phenylethanol[e]	$C_8H_{10}O$	60-12-8	684.00	39.20	387.00	492.05	146.81
2-Phenylethyl acetate[c]	$C_{10}H_{12}O_2$	103-45-7	712.23	30.12	524.15	505.16[d]	201.76
1-Phenylhexane[e]	$C_{12}H_{18}$	1077-16-3	698.00	23.80	618.00	499.26	239.77
Phenylmethanol[a]	C_7H_8O	100-51-6	720.20	44.00	335.00[e]	478.60	126.21
1-Phenyloctane[e]	$C_{14}H_{22}$	2189-60-8	729.00	20.20	703.00	537.55	274.44
3-Phenylpropyl acetate[c]	$C_{11}H_{14}O_2$	122-72-5	718.70	27.23	580.37	518.16[d]	224.50
α-Pinene[e]	$C_{10}H_{16}$	80-56-8	632.00	27.60	504.00	429.29	193.64
β-Pinene[e]	$C_{10}H_{16}$	127-91-3	643.00	27.60	506.00	439.19	194.44
2-Phenyl-1-propanol[c]	$C_9H_{12}O$	1123-85-9	662.02	36.90	443.23	476.16[d]	169.24
3-Phenyl-1-propanol[c]	$C_9H_{12}O$	122-97-4	702.30	36.40	455.45	508.16[d]	174.14
1-Propanol[a]	C_3H_8O	71-23-8	536.80	51.70	219.00	370.30	80.84
2-Propanol[a]	C_3H_8O	67-63-0	508.30	47.60	220.00	355.40	81.23
i-Propylbenzene[a]	C_9H_{12}	98-82-8	631.10	32.10	427.70[e]	425.60	163.03
n-Propylbenzene[a]	C_9H_{12}	103-65-1	638.20	32.00	440.00	432.40	167.95
Pyrene[e]	$C_{16}H_{10}$	129-00-0	936.00	26.10	630.00	667.95	244.65
Squalene[l]	$C_{30}H_{50}$	111-02-4	974.94	13.23	1128.14	702.45[i]	450.53
Stearic acid ethyl ester[o]	$C_{20}H_{40}O_2$	111-61-5	777.90	10.19	1380.00	629.30	556.47
Styrene[a]	C_8H_8	100-42-5	647.00	39.90	352.00[e]	418.30	132.93
n-Tetradecane[a]	$C_{14}H_{30}$	629-59-4	693.00	14.40	830.00	526.70	326.62
Tetrahydrofuran[a]	C_4H_8O	109-99-9	540.10	51.90	224.00	338.00	82.78
Thenoyltrifluoroacetone[l]	$C_8H_5F_3O_2S$	326-91-0	838.69	26.32	428.15	584.42[i]	163.21
α-Tocopherol[p]	$C_{29}H_{50}O_2$	59-02-9	964.30	10.80	1720.00	787.80	700.94

Table 1. (continued)

Substance	Formula	CAS Number	T_c (K)	P_c (bar)	V_c (cm^3/mol)	T_{bp} (K)	V_{bp} (cm^3/mol) [q]
Toluene[a]	C_7H_8	108-88-3	591.80	41.00	316.00	383.80	118.72
Triarachidonin[l]	$C_{63}H_{98}O_6$	23314-57-0	1499.66	6.51	2341.53	1135.95[i]	968.46
Trierucin[l]	$C_{69}H_{128}O_6$	2752-99-0	1549.28	5.62	2832.93	1182.75[i]	1182.46
Trifluoroacetylacetone[g]	$C_5H_5F_3O_2$	367-57-7	594.02	32.89	365.58	416.12[d]	138.31
1,3,5-Trimethylbenzene[a]	C_9H_{12}	108-67-8	637.30	31.30	433.00[e]	437.90	165.15
Trinervonin[l]	$C_{75}H_{140}O_6$	81913-24-8	1601.10	5.20	3081.54	1229.05[i]	129.44
Triolein[b]	$C_{57}H_{104}O_6$	122-32-7	1640.00	4.70	3090.00	1200.00	1295.15
Ubiquinone CoQ10[l]	$C_{59}H_{90}O_4$	303-98-0	1522.50	7.09	2146.17	1142.15[i]	883.95
n-Undecane[a]	$C_{11}H_{24}$	1120-21-4	638.80	19.70	660.00	469.10	256.88
Vanillin[e]	$C_8H_8O_3$	121-33-5	777.00	40.10	415.00	558.00	157.96
Vitamin K_1[f]	$C_{31}H_{46}O_2$	84-80-0	1329.54	8.58	1620.20	1099.02[d]	658.37
Vitamin K_3[f]	$C_{11}H_8O_2$	58-27-5	893.85	31.96	537.20	638.20[d]	207.03
m-Xylene[a]	C_8H_{10}	108-38-3	617.10	35.40	376.00	412.30	142.44
5-*tert*-Butyl-*m*-xylene[c]	$C_{12}H_{18}$	98-19-1	684.85	23.90	591.75	480.16[d]	229.11
p-Xylene[a]	C_8H_{10}	106-42-3	616.20	35.10	379.00	411.50	143.63

[a]Taken from Reid et al. [33]; [b]Taken from Yaws, 2008 [70]; [c]Average of the values by the Joback [33, 62-63] and Wen-Qiang [68] methods; [d]Estimated by the Joback [33, 62-63] method; [e]Taken from Yaws, 1998 [71]; [f]Average of the values by the Joback [33, 62-63] and Ambrose [33, 66-67] methods; [g]Average of the values by the Joback [33, 62-63] and Somayajulu [64] methods; [h]Taken from Table 4 of Liu and Ruckenstein [72]; [i]Taken from ChemSpider [73] database; [j]Average of the values by the Joback [33, 62-63] and Constantinou-Gani [69] methods; [k]Taken from Perry and Green [74]; [l]Estimated by the Klincewicz [33, 65] method; [m]Taken from LookChem [75]; [n]Taken from Korea Thermophysical Properties Data Bank (KDB) [76]; [o]Taken from DIPPR database [77]; [p]Taken from ASPEN database [78]; [q]Estimated by Tyn-Calus expression [33].

Table 2. Database and calculated results: experimental ranges of reduced temperature, pressure and density, number of data points (NDP) and references of the database; average absolute relative deviations (AARD, Eq. (9)) calculated for the new and original models

ID	Solute	Data Sources	NDP	$T_{r,1}$	$P_{r,1}$	$\rho_{r,1}$	mWC Eq. (2)	WC Eq. (A.1)	mSch Eq. (3)	Sch Eq. (A.2)	mLR Eq. (4)	LR Eq. (A.3)	mTC Eq. (5)+ [(6)-(8)]	TC Eq. (A.4)
1	Acetone	[53, 79-82]	214	0.9969 – 1.0955	1.0759 – 5.4350	0.77207 – 2.07624	7.33	7.01	4.16	24.16	4.39	15.39	8.18	5.07
2	Acridine	[83]	6	1.0133 – 1.0791	2.3374 – 3.7344	1.51487 – 1.95636	4.39	4.93	3.29	10.72	3.46	20.98	7.10	12.06
3	Allylbenzene	[84]	15	1.0298 – 1.0956	2.0325 – 4.7425	1.29531 – 1.99727	3.23	5.36	3.70	11.96	3.59	17.71	3.13	8.42
4	Aniline	[85]	15	1.0298 – 1.0956	2.0325 – 4.7425	1.29589 – 1.91043	26.54	42.39	28.49	63.36	28.37	57.38	28.69	40.42
5	Anisole	[86]	15	1.0293 – 1.0950	2.0325 – 4.7425	1.29553 – 1.99715	5.00	17.53	4.77	33.27	4.92	32.11	6.10	19.34
6	Anthracene	[87]	22	1.0293 – 1.0950	14.4986 – 47.4255	0.76810 – 1.99492	8.32	1.86	10.50	9.95	10.08	17.80	6.44	9.02
7	Arachidonic acid (AA)	[88]	75	1.0133 – 1.1284	1.2873 – 4.1314	1.18797 – 1.98904	3.02	9.70	2.91	7.12	2.89	25.84	3.25	16.13
8	AA ethyl ester	[89]	48	1.0133 – 1.1120	1.1409 – 4.0583	1.06846 – 1.81567	5.79	15.16	6.53	0.94	6.46	19.76	5.69	10.26
9	Behenic acid ethyl ester	[90]	17	1.0128 – 1.0457	1.3103 – 2.8523	1.28016 – 1.81357	9.21	21.34	9.09	6.43	9.23	14.66	9.81	5.03
10	Benzene	[53, 91-98]	249	0.9969 – 1.0955	1.0840 – 4.7425	0.59522 – 1.99602	10.35	8.70	9.27	18.73	9.35	14.22	10.28	8.54
11	Benzoic acid	[83, 99-101]	35	0.9640 – 1.0791	0.9621 – 4.0650	1.14645 – 1.95636	7.50	10.18	7.29	22.93	7.40	25.05	9.39	14.17
12	Benzyl acetate	[102]	15	1.0298 – 1.0956	2.0325 – 4.7425	1.29531 – 1.99727	9.04	19.98	7.05	34.52	7.46	39.09	10.26	27.43
13	Benzylacetone	[103]	15	1.0298 – 1.0956	2.0325 – 4.7425	1.29531 – 1.99727	8.60	6.19	6.21	18.07	6.68	27.48	10.35	17.90
14	Biphenyl	[101, 104]	83	0.9640-1.0871	0.9623-2.7209	1.04739-1.92670	6.92	7.90	8.64	7.23	8.29	13.91	4.91	7.19
15	2-Bromoanisole	[84]	15	1.0298 – 1.0956	2.0325 – 4.7425	1.29531 – 1.99727	15.46	16.52	14.34	30.64	14.63	35.12	17.29	23.81
16	Bromobenzene	[105-106]	21	1.0293 – 1.0950	2.0325 – 4.7425	1.29553 – 1.99715	4.41	13.90	4.44	29.41	4.47	27.59	4.74	15.01
17	2-Butanone	[79, 106-107]	40	1.0133 – 1.0791	1.1287 – 4.6789	1.24269 – 2.02871	8.74	4.23	7.20	18.04	7.31	13.42	9.11	3.92
18	*n*-Butylbenzene	[108]	15	1.0293 – 1.0950	2.0325 – 4.7425	1.29531 – 1.99727	3.11	6.41	4.99	19.07	4.59	24.81	2.47	14.76
19	*sec*-Butylbenzene	[109]	15	1.0293 – 1.0950	2.0325 – 4.7425	1.29531 – 1.99727	2.32	8.41	3.90	21.31	3.59	27.14	1.96	16.90
20	*tert*-Butylbenzene	[110]	15	1.0293 – 1.0950	2.0325 – 4.7425	1.29553 – 1.99715	5.59	3.81	7.21	15.73	6.86	21.20	5.16	11.41
21	Butyric acid ethyl ester	[111-112]	16	1.0128 – 1.0457	1.3103 – 2.8523	1.28016 – 1.81357	6.05	3.79	7.21	16.54	6.94	19.16	6.12	8.82
22	Caffeine	[113-115]	25	1.0128 – 1.0955	1.0881 – 2.2846	0.91997 – 1.72280	16.08	19.34	13.97	32.43	14.40	42.21	17.28	31.71
23	Capric acid ethyl ester	[111-112]	16	1.0128 – 1.0457	1.3103 – 2.8523	1.28016 – 1.81357	7.95	2.21	10.24	9.90	9.82	21.83	8.07	13.00

Table 2. (continued)

ID	Solute	Data Sources	NDP	$T_{r,1}$	$P_{r,1}$	$\rho_{r,1}$	mWC Eq. (2)	WC Eq. (A.1)	mSch Eq. (3)	Sch Eq. (A.2)	mLR Eq. (4)	LR Eq. (A.3)	mTC Eq. (5)+ [(6)-(8)]	TC Eq. (A.4)
24	Caprylic acid ethyl ester	[111-112]	16	1.0128 – 1.0457	1.3103 – 2.8523	1.28016 – 1.81357	6.60	1.67	8.96	12.42	8.51	22.03	6.49	12.94
25	β-Carotene	[116-118]	90	1.0133 – 1.0955	1.2358 – 4.1111	1.33461 – 1.98745	4.65	14.88	7.49	5.82	6.61	33.25	4.19	20.36
26	L-Carvone	[119-120]	27	1.0133 – 1.1120	2.0325 – 4.0650	1.38940 – 1.98382	3.71	3.66	2.79	12.01	2.90	21.08	4.19	12.00
27	Chlorobenzene	[105-106]	21	1.0293 – 1.0950	2.0325 – 4.7425	1.29553 – 1.99715	3.40	12.70	3.51	28.30	3.52	25.85	3.61	13.20
28	Chrysene	[53]	4	0.9969 – 1.0955	2.1680 – 3.5908	1.70688 – 1.87757	8.84	16.16	11.24	5.59	10.79	6.63	6.80	2.80
29	Citral	[121]	15	1.0298 – 1.0955	1.6260 – 2.7100	0.95300 – 1.79863	7.30	8.63	9.54	3.45	9.11	13.20	6.79	5.29
30	Cobalt(III) acetylacetonate	[122]	38	1.0298 – 1.0955	1.3144 – 5.4201	1.28832 – 2.04129	17.52	11.53	14.50	25.24	15.08	40.06	4.10	29.97
31	Copper(II) trifluoroacetylacetonate	[123]	12	1.0133 – 1.0462	1.4661 – 2.2425	1.28443 – 1.75894	35.54	37.09	33.26	53.26	33.74	62.37	31.99	49.65
32	Dibenzo-24-crown-8	[124]	28	1.0134 – 1.0299	2.0339 – 4.7425	1.66636 – 2.02373	3.27	12.73	2.36	2.71	2.46	22.77	6.33	13.08
33	15-Crown-5	[124]	29	1.0134 – 1.0299	1.1883 – 4.0705	0.89973 – 1.94298	4.43	7.85	5.64	11.20	5.39	21.59	3.83	12.64
34	Cycloheptanone	[125]	8	1.0330 – 1.0330	1.3550 – 2.4390	1.29705 – 1.73773	15.50	24.01	16.50	40.45	16.49	39.72	15.40	26.38
35	Cyclononanone	[125]	8	1.0330 – 1.0330	1.3550 – 2.4390	1.29705 – 1.73773	13.16	17.62	12.13	31.85	12.40	36.52	13.34	25.13
36	Cyclopentanone	[125]	8	1.0330 – 1.0330	1.3550 – 2.4390	1.29705 – 1.73773	9.90	25.81	12.37	44.65	12.16	38.71	11.76	23.48
37	*n*-Decane	[126]	5	0.9837 – 1.0133	1.2195 – 1.4228	1.55921 – 1.74504	*	38.51	*	31.07	*	23.56	*	19.51
38	Dibenzyl ether	[102]	15	1.0298 – 1.0956	2.0325 – 4.7425	1.29531 – 1.99727	10.30	18.77	7.48	32.74	8.02	43.15	12.02	32.36
39	1,2-Dichlorobenzene	[110]	15	1.0293 – 1.0950	2.0325 – 4.7425	1.29553 – 1.99715	4.73	18.56	4.13	34.19	4.31	33.75	5.60	21.07
40	1,3-Dichlorobenzene	[120]	4	1.0298 – 1.0298	2.0325 – 3.2520	1.66680 – 1.86317	10.78	21.73	10.18	37.67	10.39	37.52	11.94	24.59
41	*p*-Dichlorobenzene	[101]	13	0.9804 – 1.0462	1.2519 – 2.3169	1.14788 – 1.86691	7.63	10.61	7.14	24.31	7.31	27.05	8.78	16.00
42	Diethyl ether	[106-107, 127]	17	1.0298 – 1.0955	1.0984 – 2.1967	0.41819 – 1.70411	6.82	10.51	6.26	23.20	6.29	21.31	7.51	10.94
43	1,2-Diethylbenzene	[128]	15	1.0298 – 1.0956	2.0325 – 4.7425	1.29531 – 1.99727	2.90	8.78	4.78	21.78	4.41	27.24	2.34	16.90
44	1,4-Diethylbenzene	[128]	15	1.0298 – 1.0956	2.0325 – 4.7425	1.29531 – 1.99727	2.48	7.81	4.28	20.64	3.91	26.44	2.29	16.25
45	Diisopropyl ether	[127]	15	1.0298 – 1.0955	1.0984 – 2.1967	0.41819 – 1.70411	12.51	6.63	13.21	11.10	13.03	14.04	13.41	7.07
46	2,3-Dimethylaniline	[129]	15	1.0293 – 1.0950	2.0325 – 4.7425	1.29553 – 1.99715	16.12	16.04	14.61	29.92	14.96	35.59	17.80	24.54
47	2,6-Dimethylaniline	[129]	15	1.0293 – 1.0950	2.0325 – 4.7425	1.29553 – 1.99715	11.51	11.47	10.06	24.80	10.39	30.25	14.08	19.64
48	1,1′-Dimethylferrocene	[130]	68	1.0133 – 1.0626	1.1138 – 5.4363	0.82775 – 2.07666	8.34	12.16	7.05	25.53	7.35	31.02	7.14	20.35
49	2,6-Dimethylnaphthalene	[131-132]	6	1.0135 – 1.0135	1.2331 – 2.6423	1.42716 – 1.83924	4.35	7.15	5.09	8.88	4.79	17.98	4.44	9.26

Table 2. (continued)

ID	Solute	Data Sources	NDP	$T_{r,1}$	$P_{r,1}$	$\rho_{r,1}$	mWC Eq. (2)	WC Eq. (A.1)	mSch Eq. (3)	Sch Eq. (A.2)	mLR Eq. (4)	LR Eq. (A.3)	mTC Eq. (5)+ [(6)-(8)]	TC Eq. (A.4)
50	2,7-Dimethylnaphthalene	[131-132]	6	1.0135 – 1.0135	1.4499 – 2.7100	1.57070 – 1.84816	4.45	6.91	5.54	5.64	5.15	13.01	4.43	6.00
51	2,4-Dimethylphenol	[86]	15	1.0293 – 1.0950	2.0325 – 4.7425	1.29553 – 1.99715	9.07	23.84	7.81	39.73	8.11	40.68	11.78	27.82
52	Diolein	[133]	9	1.0300 – 1.0300	1.3550 – 3.3889	1.34136 – 1.87770	6.58	10.37	3.16	8.90	3.98	35.72	6.10	23.45
53	1,3-Divinylbenzene	[84]	15	1.0298 – 1.0956	2.0325 – 4.7425	1.29531 – 1.99727	1.67	9.61	2.58	22.96	2.36	26.82	1.54	16.12
54	Docosahexaenoic acid (DHA)	[134]	63	1.0133 – 1.1284	1.2561 – 4.0827	1.21898 – 1.98489	5.19	7.28	4.05	8.29	4.19	30.05	6.08	19.86
55	DHA ethyl ester	[89-90]	65	1.0128 – 1.1120	1.1409 – 4.0583	1.06851 – 1.81570	6.43	16.73	6.88	2.00	6.89	18.88	6.25	9.27
56	DHA methyl ester	[90]	17	1.0128 – 1.0457	1.3103 – 2.8523	1.28016 – 1.81357	5.75	16.76	6.50	2.47	6.44	17.74	5.48	8.37
57	*n*-Dodecane	[126]	5	0.9837 – 1.0133	1.2195 – 1.4228	1.55921 – 1.74504	*	40.87	*	33.32	*	24.36	*	18.94
58	Eicosapentaenoic acid (EPA)	[134]	55	1.0133 – 1.1284	1.1762 – 4.0854	1.15708 – 1.95136	2.93	7.79	1.84	7.30	1.96	27.28	3.83	17.55
59	EPA ethyl ester	[89]	48	1.0133 – 1.1120	1.1409 – 4.0583	1.06846 – 1.81567	5.80	14.98	6.64	1.02	6.55	19.58	5.56	10.14
60	EPA methyl ester	[90]	17	1.0128 – 1.0457	1.3103 – 2.8523	1.28016 – 1.81357	6.62	17.37	7.45	3.34	7.37	16.49	6.17	7.27
61	Ethanol	[99]	24	1.0300 – 1.0300	1.2873 – 3.3875	1.23600 – 1.87755	4.61	13.85	5.43	36.63	4.82	22.04	4.60	5.82
62	Ethyl acetate	[107, 113]	16	1.0128 – 1.0786	1.0244 – 2.1680	0.45553 – 1.72309	8.91	21.86	9.29	38.05	9.26	34.61	8.79	21.70
63	Ethylbenzene	[93]	15	1.0298 – 1.0955	2.0325 – 4.7425	1.29531 – 1.99727	7.50	3.06	8.35	14.43	8.12	15.59	7.08	5.26
64	Ethyl benzoate	[103]	15	1.0298 – 1.0956	2.0325 – 4.7425	1.29531 – 1.99727	6.69	18.87	5.76	33.25	5.95	37.94	6.53	26.42
65	2-Ethyltoluene	[135]	15	1.0293 – 1.0950	2.0325 – 4.7425	1.29589 – 1.91043	6.68	7.18	8.24	20.18	7.92	23.45	6.26	12.90
66	3-Ethyltoluene	[135]	15	1.0293 – 1.0950	2.0325 – 4.7425	1.29589 – 1.91043	8.84	6.47	10.74	19.26	10.36	22.88	8.52	12.47
67	4-Ethyltoluene	[135]	15	1.0293 – 1.0950	2.0325 – 4.7425	1.29589 – 1.91043	4.94	8.22	6.84	21.41	6.46	25.17	4.58	14.59
68	Eugenol	[103]	15	1.0298 – 1.0956	2.0325 – 4.7425	1.29531 – 1.99727	18.94	17.29	16.79	31.11	17.23	39.19	21.03	28.35
69	Ferrocene	[130, 136]	107	1.0133 – 1.0955	1.0867 – 5.4661	0.60020 – 2.07714	11.03	17.43	11.36	32.55	11.44	33.28	10.50	21.04
70	2-Fluoroanisole	[84]	15	1.0298 – 1.0956	2.0325 – 4.7425	1.29531 – 1.99727	15.27	18.48	15.23	33.51	15.36	35.01	15.66	22.85
71	Fluorobenzene	[105]	15	1.0293 – 1.0950	2.0325 – 4.7425	1.29589 – 1.91043	5.70	15.22	7.29	31.91	7.19	27.68	5.68	14.17
72	3-Fluorophenol	[120]	4	1.0298 – 1.0298	2.0325 – 3.2520	1.66680 – 1.86317	11.91	13.15	11.56	27.33	11.74	29.44	15.17	17.99
73	Geraniol	[120]	4	1.0298 – 1.0298	2.0325 – 3.2520	1.66680 – 1.86317	9.47	3.34	6.70	15.70	7.23	27.33	11.05	18.03
74	*n*-Heptane	[126]	5	0.9837 – 1.0133	1.2195 – 1.4228	1.55921 – 1.74504	*	28.91	*	20.51	*	16.05	*	14.34
75	Hexachlorobenzene	[137]	14	1.0128 – 1.0786	1.3103 – 3.3523	0.86978 – 1.92233	6.98	10.99	7.62	12.63	7.47	20.34	6.66	13.01
76	1-Hexadecene	[138]	11	1.0298 – 1.2271	1.3550 – 4.0650	0.91313 – 1.94292	11.55	10.30	12.57	16.19	12.39	29.84	11.53	21.80

Table 2. (continued)

ID	Solute	Data Sources	NDP	$T_{r,1}$	$P_{r,1}$	$\rho_{r,1}$	mWC Eq. (2)	WC Eq. (A.1)	mSch Eq. (3)	Sch Eq. (A.2)	mLR Eq. (4)	LR Eq. (A.3)	mTC Eq. (5)+ [(6)-(8)]	TC Eq. (A.4)
77	1,1,1,5,5,5-Hexafluoroacetylacetone	[123]	15	1.0133 – 1.0462	1.4106 – 3.0081	1.21018 – 1.86989	17.68	18.95	16.12	33.14	16.47	39.26	17.05	27.98
78	*n*-Hexane	[126]	5	0.9837 – 1.0133	1.2195 – 1.4228	1.55921 – 1.74504	*	22.91	*	13.51	*	10.86	*	10.27
79	Iodobenzene	[105-106]	20	1.0293 – 1.0950	2.0325 – 4.7425	1.29553 – 1.99715	7.78	20.62	7.22	36.58	7.42	35.94	9.60	22.99
80	Isobutylbenzene	[109]	15	1.0293 – 1.0950	2.0325 – 4.7425	1.29531 – 1.99727	1.85	5.61	3.46	17.94	3.11	23.80	1.51	13.87
81	D-Limonene	[121]	15	1.0298 – 1.0955	1.6260 – 2.7100	0.95300 – 1.79863	9.24	9.32	11.24	4.20	10.85	10.54	8.72	4.27
82	Linalool	[92]	15	1.0298 – 1.0955	1.6260 – 2.7100	0.95300 – 1.79863	6.97	7.24	8.81	4.13	8.46	13.86	6.21	5.63
83	Linoleic acid	[88]	71	1.0133 – 1.1284	1.1518 – 4.1057	1.18797 – 1.98703	3.42	7.18	3.74	20.02	3.65	38.05	3.48	28.07
84	Linoleic acid methyl ester	[139-140]	21	1.0135 – 1.0793	1.8970 – 4.5528	1.57673 – 1.98212	3.36	15.74	4.78	3.30	4.56	16.35	3.30	7.44
85	α-Linolenic acid	[134]	56	1.0133 – 1.1284	1.1518 – 4.0840	1.16293 – 1.98446	4.43	5.85	5.71	18.69	5.51	36.15	3.71	26.33
86	γ-Linolenic acid	[141]	142	1.0133 – 1.1284	1.1762 – 4.1328	0.97583 – 1.94819	3.22	7.79	2.99	8.37	3.01	26.40	3.55	16.90
87	γ-Linolenic acid ethyl ester	[141]	41	1.0300 – 1.1284	1.1382 – 2.1694	0.71647 – 1.69741	7.44	6.31	6.41	13.68	6.56	32.31	7.69	22.63
88	γ-Linolenic acid methyl ester	[139, 141]	52	1.0298 – 1.1284	1.0989 – 4.5528	0.62225 – 1.98207	8.39	13.41	9.57	4.68	9.39	19.17	8.19	10.20
89	L-Menthone	[119]	23	1.0133 – 1.1120	2.0325 – 4.0650	1.38940 – 1.98382	3.61	5.18	4.69	6.71	4.42	15.93	3.51	7.36
90	Methanol	[99]	10	1.0300 – 1.0300	1.2873 – 2.8455	1.23600 – 1.81208	5.79	19.71	10.57	51.52	9.24	26.96	5.84	6.87
91	2-Methylanisole	[129]	15	1.0293 – 1.0950	2.0325 – 4.7425	1.29553 – 1.99715	8.67	9.67	7.72	23.02	7.98	26.90	9.45	16.19
92	4-Methylanisole	[129]	15	1.0293 – 1.0950	2.0325 – 4.7425	1.29553 – 1.99715	16.51	17.52	15.49	31.83	15.76	35.98	17.36	24.50
93	3-Methylbutylbenzene	[109]	15	1.0293 – 1.0950	2.0325 – 4.7425	1.29531 – 1.99727	2.05	5.74	3.44	6.66	3.06	16.36	1.94	7.77
94	1-Methylnaphthalene	[138]	11	1.0298 – 1.2271	1.3550 – 4.0650	0.91313 – 1.94292	15.44	37.22	13.75	53.95	14.09	58.66	17.44	45.23
95	Monoolein	[133]	11	1.0300 – 1.0300	1.3564 – 3.3875	1.34299 – 1.87755	2.91	6.55	2.48	21.50	2.49	42.93	3.51	32.29
96	Myristic acid ethyl ester	[111-112]	16	1.0128 – 1.0457	1.3103 – 2.8523	1.28016 – 1.81357	7.52	3.62	9.28	9.08	8.98	24.84	7.53	15.85
97	Myristoleic acid	[142]	42	1.0300 – 1.1284	1.2466 – 4.0650	0.97697 – 1.87755	5.14	5.68	3.57	14.76	3.79	32.51	5.89	22.90
98	Myristoleic acid methyl ester	[142-143]	81	1.0298 – 1.1284	1.0840 – 3.3875	0.48065 – 1.87812	11.00	10.43	11.50	12.73	11.40	28.83	10.94	19.53
99	Naphthalene	[53, 115, 131, 136, 144]	114	0.9479 – 1.0955	0.9106 – 13.5501	0.46956 – 2.37385	10.07	10.71	10.70	19.28	10.55	21.47	9.29	13.04
100	1-Naphthol	[87]	11	1.0128 – 1.0457	1.4363 – 2.1951	1.13081 – 1.74529	9.07	5.77	9.84	5.67	9.63	9.17	6.13	0.39
101	2-Naphthol	[87]	16	1.0128 – 1.0786	1.3415 – 2.0596	0.70196 – 1.71755	13.85	7.84	14.49	5.02	14.31	7.67	11.13	2.46

Table 2. (continued)

ID	Solute	Data Sources	NDP	$T_{r,1}$	$P_{r,1}$	$\rho_{r,1}$	mWC Eq. (2)	WC Eq. (A.1)	mSch Eq. (3)	Sch Eq. (A.2)	mLR Eq. (4)	LR Eq. (A.3)	mTC Eq. (5)+ [(6)-(8)]	TC Eq. (A.4)
102	2-Nitroanisole	[110]	15	1.0293 – 1.0950	2.0325 – 4.7425	1.29553 – 1.99715	12.36	30.85	10.60	47.49	10.98	49.02	14.83	35.55
103	Nitrobenzene	[86, 106]	23	1.0293 – 1.0950	2.0325 – 4.7425	1.29553 – 1.99715	6.52	25.45	6.07	42.77	6.24	40.14	8.47	26.09
104	3-Nitrotoluene	[129]	15	1.0293 – 1.0950	2.0325 – 4.7425	1.29553 – 1.99715	2.12	22.65	2.73	38.46	2.56	39.13	3.18	26.33
105	*n*-Nonane	[126]	5	0.9837 – 1.0133	1.2195 – 1.4228	1.55921 – 1.74504	*	36.45	*	28.90	*	22.22	*	18.81
106	*n*-Octane	[126]	5	0.9837 – 1.0133	1.2195 – 1.4228	1.55921 – 1.74504	*	33.41	*	25.59	*	19.86	*	17.19
107	Oleic acid	[133]	19	1.0300 – 1.0300	1.2818 – 4.0786	1.22463 – 1.94359	3.52	7.41	3.62	19.71	3.53	38.09	3.66	28.09
108	Oleic acid ethyl ester	[133]	5	1.0300 – 1.0300	1.1653 – 1.4905	0.80523 – 1.45943	5.78	16.55	5.36	31.64	5.39	53.87	5.69	42.53
109	Oleic acid methyl ester	[133, 139, 145]	21	1.0293 – 1.0300	1.0840 – 2.1680	0.59385 – 1.70011	4.89	17.48	4.49	33.52	4.53	55.19	4.86	43.85
110	Palladium(II) acetylacetonate	[122]	125	1.0133 – 1.1284	1.1518 – 5.4201	1.20158 – 2.07571	20.84	21.93	18.86	36.33	19.28	44.15	6.06	32.80
111	Palmitic acid ethyl ester	[54]	17	1.0128 – 1.0457	1.3103 – 2.8523	1.28016 – 1.81357	5.53	1.90	6.89	11.63	6.68	29.35	5.66	19.94
112	*n*-Pentane	[126]	5	0.9837 – 1.0133	1.2195 – 1.4228	1.55921 – 1.74504	*	13.23	*	2.49	*	2.52	*	3.30
113	2-Pentanone	[79]	23	1.0133 – 1.0342	1.2033 – 3.9634	1.18413 – 1.93408	5.78	4.45	5.24	16.85	5.23	15.50	6.15	4.95
114	3-Pentanone	[79, 125]	46	1.0133 – 1.0791	1.1721 – 4.6843	1.26087 – 2.02871	11.10	4.65	11.25	15.85	11.13	14.37	11.04	4.90
115	*n*-Pentylbenzene	[108]	31	1.0128 – 1.3088	2.0325 – 4.7425	1.29553 – 2.03431	5.46	4.80	7.57	16.85	7.16	24.33	4.80	14.69
116	Phenanthrene	[53, 83, 137]	25	0.9969 – 1.0955	1.3076 – 3.7344	1.08209 – 1.95636	12.99	7.59	15.08	10.53	14.68	16.03	11.24	8.72
117	Phenol	[81, 99, 113, 117-118]	109	1.0128 – 1.0791	1.0894 – 4.1030	0.75743 – 1.98681	10.98	21.20	14.89	39.93	14.51	33.07	12.96	17.97
118	Phenylacetic acid	[56]	16	1.0133 – 1.0462	1.3103 – 2.8523	1.28016 – 1.81357	3.34	4.25	2.33	16.60	2.49	22.72	5.57	12.95
119	Phenylacetylene	[128]	15	1.0298 – 1.0956	2.0325 – 4.7425	1.29531 – 1.99727	5.00	16.98	4.76	32.55	4.91	31.66	6.16	19.02
120	Phenylbutazone	[146]	78	1.0133 – 1.1284	1.1518 – 5.4201	0.95063 – 2.07442	4.64	8.18	4.71	7.66	4.68	25.06	4.92	15.80
121	1-Phenyldodecane	[108]	15	1.0293 – 1.0950	2.0325 – 4.7425	1.29531 – 1.99727	5.65	13.38	3.85	28.08	4.12	45.96	6.67	35.46
122	1-Phenylethanol	[147]	15	1.0298 – 1.0956	2.0325 – 4.7425	1.29553 – 1.99787	9.85	24.92	8.56	40.91	8.86	41.99	12.20	29.04
123	2-Phenylethanol	[147]	15	1.0298 – 1.0956	2.0325 – 4.7425	1.29553 – 1.99787	11.44	26.44	10.21	42.67	10.51	43.59	13.65	30.45
124	2-Phenylethyl acetate	[102]	15	1.0298 – 1.0956	2.0325 – 4.7425	1.29531 – 1.99727	12.38	8.63	9.77	21.45	10.28	32.02	14.23	22.22
125	1-Phenylhexane	[108]	15	1.0293 – 1.0950	2.0325 – 4.7425	1.29531 – 1.99727	2.37	7.16	4.20	19.67	3.78	28.99	2.00	19.26
126	Phenylmethanol	[147]	15	1.0298 – 1.0956	2.0325 – 4.7425	1.29553 – 1.99787	11.13	28.01	10.94	45.59	11.09	43.17	12.91	28.91
127	1-Phenyloctane	[108]	15	1.0293 – 1.0950	2.0325 – 4.7425	1.29531 – 1.99727	2.49	4.12	4.05	16.12	3.69	27.98	2.30	18.65

Table 2. (continued)

ID	Solute	Data Sources	NDP	$T_{r,1}$	$P_{r,1}$	$\rho_{r,1}$	mWC Eq. (2)	WC Eq. (A.1)	mSch Eq. (3)	Sch Eq. (A.2)	mLR Eq. (4)	LR Eq. (A.3)	mTC Eq. (5)+ [(6)-(8)]	TC Eq. (A.4)
128	3-Phenylpropyl acetate	[102]	15	1.0298 – 1.0956	2.0325 – 4.7425	1.29531 – 1.99727	11.34	7.12	8.54	18.93	9.08	31.18	13.09	21.63
129	α-Pinene	[148]	15	1.0298 – 1.0955	1.6260 – 2.7100	0.95300 – 1.79863	7.78	5.22	9.43	17.32	9.10	23.25	7.57	13.38
130	β-Pinene	[148]	15	1.0298 – 1.0955	1.6260 – 2.7100	0.95300 – 1.79863	12.31	3.61	14.17	12.20	13.80	17.68	11.95	8.63
131	2-Phenyl-1-propanol	[147]	15	1.0298 – 1.0956	2.0325 – 4.7425	1.29553 – 1.99787	11.05	25.01	9.08	40.36	9.49	44.06	13.43	31.71
132	3-Phenyl-1-propanol	[147]	15	1.0298 – 1.0956	2.0325 – 4.7425	1.29553 – 1.99787	7.90	22.62	5.87	37.66	6.29	41.40	10.44	29.31
133	1-Propanol	[99]	17	1.0300 – 1.0300	1.2873 – 2.1680	1.23600 – 1.69712	5.11	20.58	6.58	40.74	6.37	31.17	5.20	15.04
134	2-Propanol	[99]	18	1.0300 – 1.0300	1.2873 – 2.3035	1.23600 – 1.72474	4.76	13.26	3.96	31.92	3.93	23.41	4.82	8.46
135	*i*-Propylbenzene	[53, 93, 107, 149]	36	1.0298 – 1.0955	1.7615 – 4.7425	1.08209 – 1.99602	7.80	3.75	9.29	12.80	8.97	16.24	7.34	6.55
136	*n*-Propylbenzene	[91, 93, 107]	60	1.0133 – 1.0955	1.1518 – 4.7425	0.76383 – 1.99727	8.25	13.29	9.12	23.56	8.93	27.35	8.05	17.28
137	Pyrene	[53, 87]	21	0.9969 – 1.0955	1.5583 – 47.4255	0.83211 – 1.98852	5.47	9.75	7.51	3.86	7.10	13.38	4.45	6.51
138	Squalene	[150]	5	1.0340 – 1.0340	1.7615 – 2.4390	1.56207 – 1.73393	4.86	13.56	5.02	3.78	5.00	20.60	4.83	11.21
139	Stearic acid ethyl ester	[90]	17	1.0128 – 1.0457	1.3103 – 2.8523	1.28016 – 1.81357	12.87	2.89	12.82	11.22	12.94	30.36	13.29	20.71
140	Styrene	[85]	15	1.0298 – 1.0956	2.0325 – 4.7425	1.29589 – 1.91043	3.58	13.86	3.34	28.71	3.41	28.77	4.03	16.73
141	*n*-Tetradecane	[126]	5	0.9837 – 1.0133	1.2195 – 1.4228	1.55921 – 1.74504	*	38.78	*	30.40	*	19.50	*	10.99
142	Tetrahydrofuran	[127]	15	1.0298 – 1.0955	1.0984 – 2.1967	0.41819 – 1.70411	5.55	16.67	6.07	35.09	5.91	27.75	5.58	12.92
143	Thenoyltrifluoroacetone	[123]	15	1.0133 – 1.0462	1.4295 – 3.0366	1.21018 – 1.88696	29.80	30.20	27.74	45.60	28.18	53.55	29.87	41.38
144	α-Tocopherol	[116-118]	82	1.0133 – 1.0955	1.1531 – 4.1070	1.31130 – 1.98713	17.60	11.99	16.15	4.00	16.62	23.35	16.40	13.67
145	Toluene	[93, 97, 113]	35	1.0066 – 1.0955	1.0894 – 4.7425	0.96866 – 1.99727	6.47	6.09	6.24	19.41	6.19	17.92	6.26	6.86
146	Triarachidonin	[151]	27	1.0300 – 1.0300	1.3482 – 4.0976	1.33304 – 1.94521	5.23	17.49	8.58	8.39	7.27	34.89	5.02	20.63
147	Trierucin	[151]	101	1.0133 – 1.0626	1.1192 – 4.0732	1.20406 – 1.98404	9.43	13.57	17.19	14.68	14.94	48.33	8.54	31.19
148	Trifluoroacetylacetone	[123]	15	1.0133 – 1.0462	1.4485 – 2.9241	1.23749 – 1.87309	2.00	3.74	1.85	15.88	1.86	19.21	2.04	9.06
149	1,3,5-Trimethylbenzene	[53, 85, 91, 106]	34	0.9969 – 1.0956	1.2873 – 4.7425	1.23991 – 1.99595	4.48	10.63	4.66	24.00	4.57	27.73	4.61	16.91
150	Trinervonin	[151]	38	1.0133 – 1.0626	1.2195 – 4.0718	1.26796 – 1.98414	7.41	16.62	15.84	12.12	13.29	45.38	6.50	27.91
151	Triolein	[100, 151]	14	0.9803 – 1.0300	1.2371 – 3.4011	1.10114 – 2.01472	9.83	16.34	4.79	10.40	5.83	36.93	12.35	22.42
152	Ubiquinone CoQ10	[118, 152]	80	1.0133 – 1.0955	1.1531 – 4.0949	1.31130 – 1.98436	6.80	13.90	10.61	8.60	9.48	37.98	6.35	23.98

Table 2 (continued)

ID	Solute	Data Sources	NDP	$T_{r,1}$	$P_{r,1}$	$\rho_{r,1}$	mWC Eq. (2)	WC Eq. (A.1)	mSch Eq. (3)	Sch Eq. (A.2)	mLR Eq. (4)	LR Eq. (A.3)	mTC Eq. (5)+ [(6)-(8)]	TC Eq. (A.4)
153	*n*-Undecane	[126]	5	0.9837 – 1.0133	1.2195 – 1.4228	1.55921 – 1.74504	*	40.94	*	33.60	*	25.46	*	20.86
154	Vanillin	[56]	15	1.0133 – 1.0462	1.3957 – 2.8523	1.28016 – 1.81357	11.14	12.64	9.56	26.02	9.91	32.26	14.17	21.65
155	Vitamin K_1	[124, 143]	17	1.0299 – 1.0299	1.3550 – 4.0650	1.34181 – 1.94251	13.35	27.24	12.27	11.90	12.65	9.52	13.19	4.02
156	Vitamin K_3	[118, 140, 143]	22	1.0298 – 1.0298	1.2141 – 4.0678	1.01768 – 1.94316	5.76	9.59	7.82	6.78	7.39	12.86	3.95	7.18
157	*m*-Xylene	[138]	12	1.0298 – 1.2271	1.3550 – 4.0650	0.40289 – 1.94292	10.08	27.07	9.62	43.21	9.75	44.75	10.35	31.70
158	5-*tert*-Butyl-*m*-xylene	[128]	31	1.0134 – 1.3093	2.0325 – 4.7425	1.29210 – 2.03313	4.76	8.49	6.99	3.60	6.56	14.06	4.33	5.79
159	*p*-Xylene	[106-107]	7	1.0298 – 1.0626	2.0325 – 3.3875	1.49577 – 1.87812	7.39	4.28	8.30	15.06	8.06	16.37	7.01	6.13

mWC, modified Wilke-Chang equation; WC, Wilke-Chang; mSch, modified Scheibel equation; Sch, Scheibel; mLR, modified Lusis-Ratcliff equation; LR, Lusis-Ratcliff; mTC, modified Tyn-Calus equation; TC, Tyn-Calus.

* *n*-Alkanes were not considered for the overall correlations; if included the errors lie between 15% and 30%.

The parameters of the new models that were fitted to the database – A_i, α_i, β_i (for mWC, mSch, mLR) and A_i, α_i, β_i, γ (for mTC) – are compiled in Table 3, being interesting to observe the differences between the equations. The dependence upon T/η_1 is the same for all of them as the similar exponents α_i found (0.8556, 0.8604, 0.8595 and 0.8562) evidence, though the remaining parameters are not comparable because they refer to distinct variables in distinct D_{12} relationships.

The global results (ARDs and AARDs) provided by each equation are shown in Table 4, together with the minimum and maximum AARDs, and the standard deviations of the errors (σ_{ARD}).

The grand AARDs of the proposed equations are much smaller than those achieved by the equations taken from literature: 8.26% (mWC) *versus* 11.89% (WC), 8.56% (mSch) *versus* 18.86% (Sch), 8.45% (mLR) *versus* 27.25% (LR), 7.86% (mTC) *versus* 16.81% (TC). The minimum and maximum AARDs patent in Table 4 reinforce also the reliable behavior of the new models, as the differences between both statistics ($AARD_{max}$ - $AARD_{min}$) are: 33.87% (mWC) *versus* 40.72% (WC), 31.42% (mSch) *versus* 62.42% (Sch), 31.88% (mLR) *versus* 55.74% (LR), and 30.48% (mTC) *versus* 49.26% (TC).

Table 3. Optimized parameters of the new D_{12} equations proposed in this work. Variables are expressed in cgs system except viscosity (cP) and pressure (bar).

Model	Equation	A_i	α_i	β_i	γ
mWC	(2)	1.5853×10^{-6}	0.8556	0.4970	—
mSch	(3)	1.9813×10^{-7}	0.8604	0.2561	—
mLR	(4)	1.0338×10^{-7}	0.8595	0.8321	—
mTC	(5) + [(6)-(8)]	1.2276×10^{-6}	0.8562	0.2553	0.6914

mWC = modified Wilke-Chang equation; mTC = modified Tyn-Calus equation; mSch = modified Scheibel equation; mLR = modified Lusis-Ratcliff equation.

Table 4. Global (ARD) and standard deviations of the errors (σ_{ARD}), together with global, maximum and minimum absolute errors (AARDs) obtained by the new models and by those adopted for comparison.

Model	Equation	ARD	σ_{ARD}	$AARD_{global}$	$AARD_{min}$	$AARD_{max}$
mWC	(2)	0.50	10.35	8.26	1.67	35.54
WC	(A.1)	2.95	14.71	11.89	1.67	42.39
mSch	(3)	0.52	10.62	8.56	1.84	33.26
Sch	(A.2)	18.14	15.51	18.86	0.94	63.36
mLR	(4)	0.53	10.49	8.45	1.86	33.74
LR	(A.3)	27.23	14.06	27.25	6.63	62.37
mTC	(5) + [(6)-(8)]	0.47	9.82	7.86	1.51	31.99
TC	(A.4)	15.93	13.04	16.81	0.39	49.65

mWC = modified Wilke-Chang equation; WC = Wilke-Chang; mSch = modified Scheibel equation; Sch = Scheibel; mLR = modified Lusis-Ratcliff equation; LR = Lusis-Ratcliff; mTC = modified Tyn-Calus equation; TC = Tyn-Calus.

Other significant statistics are the average and standard deviations of the errors, since they disclose the unbiased predictions of the models. The ARDs values found range between 0.47% and 0.53% for the modified models, and between 2.95% and 27.23% for the classic ones. It is worth noting the ARDs should be theoretically zero which emphasizes the much better performance provided by the new equations. The standard deviations dropped also very significantly from 14.71% (WC) to 10.35% (mWC), 15.51% (Sch) to 10.62% (mSch), 14.06% (LR) to 10.49% (mLR), 13.04% (TC) to 9.82% (mTC).

Summarily, not only the grand averages but also the calculated dispersions are significantly smaller. This points out the reliability and trustworthiness of our models to predict tracer diffusion coefficients of solutes in supercritical CO_2 in comparison to existent hydrodynamic equations, by just introducing simple modifications into them.

The accuracy of the simple modified hydrodynamic equations of this essay can be analyzed graphically in Figs. 1 and S.2. The calculated *versus* experimental diffusivities are plotted in Fig. S.2 for mWC, mSch, mLR and mTC, side by side with original WC, Sch, LR, and TC. From these charts one may confirm the good distribution of points along diagonal for the four new equations, in contrast to the biased behavior offered by the literature models. In Fig. 1 the ratio of calculated and measured diffusivities ($D_{12}^{calc} / D_{12}^{exp}$) are plotted against the experimental

data for the various expressions, being possible to observe the clear improvement achieved by mWC, mSch, mLR and mTC in comparison to the systematic overpredictions accomplished by WC, Sch, LR, and TC.

The particular case of *n*-alkanes is graphed in Fig. 2 to evidence that equations fail their estimations by large amount. As has been mentioned above, such results are persistently reported in the literature, which suggests the experimental data may be not accurate. It is important to detach that almost all systems are well predicted (see Table 2), even large solutes like long chain fatty acid esters, but *n*-alkanes are not.

In Fig. 3, the experimental diffusion coefficients of four distinct systems (CO_2/acetone, CO_2/benzene, CO_2/naphtalene, CO_2/linoleic acid) are plotted in Stokes-Einstein coordinates (D_{12} against T/η_1), along with modeling results achieved by the modified and original Wilke-Chang equations. The predictions are very reliable particularly if one takes into account the large number of data points (NDP = 214, 249, 114 and 71), multiple sources of data (20 papers) and wide ranges of T/η_1 values.

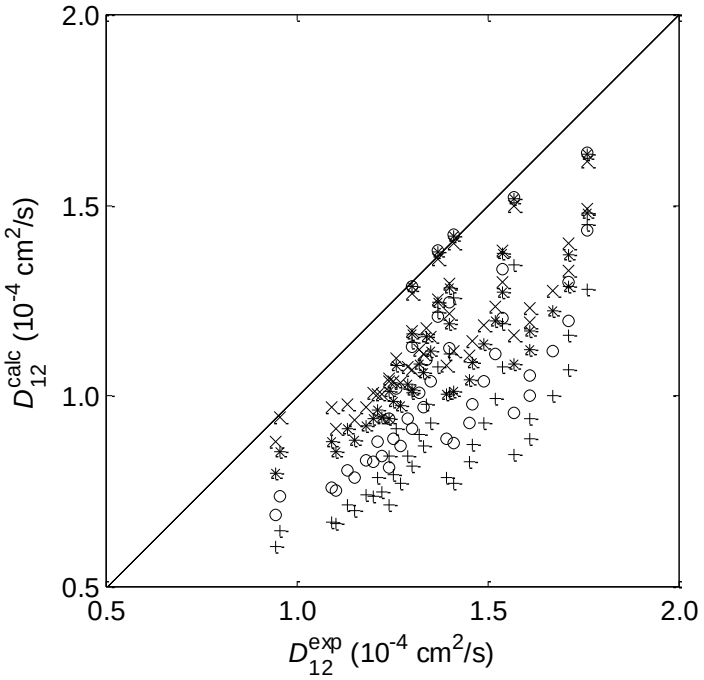

Fig. 2. Calculated *versus* experimental tracer diffusivities of *n*-alkanes computed by the (+) Wilke-Chang, (o) Scheibel, (∗) Lusis-Ratcliff, and (x) Tyn-Calus equations.

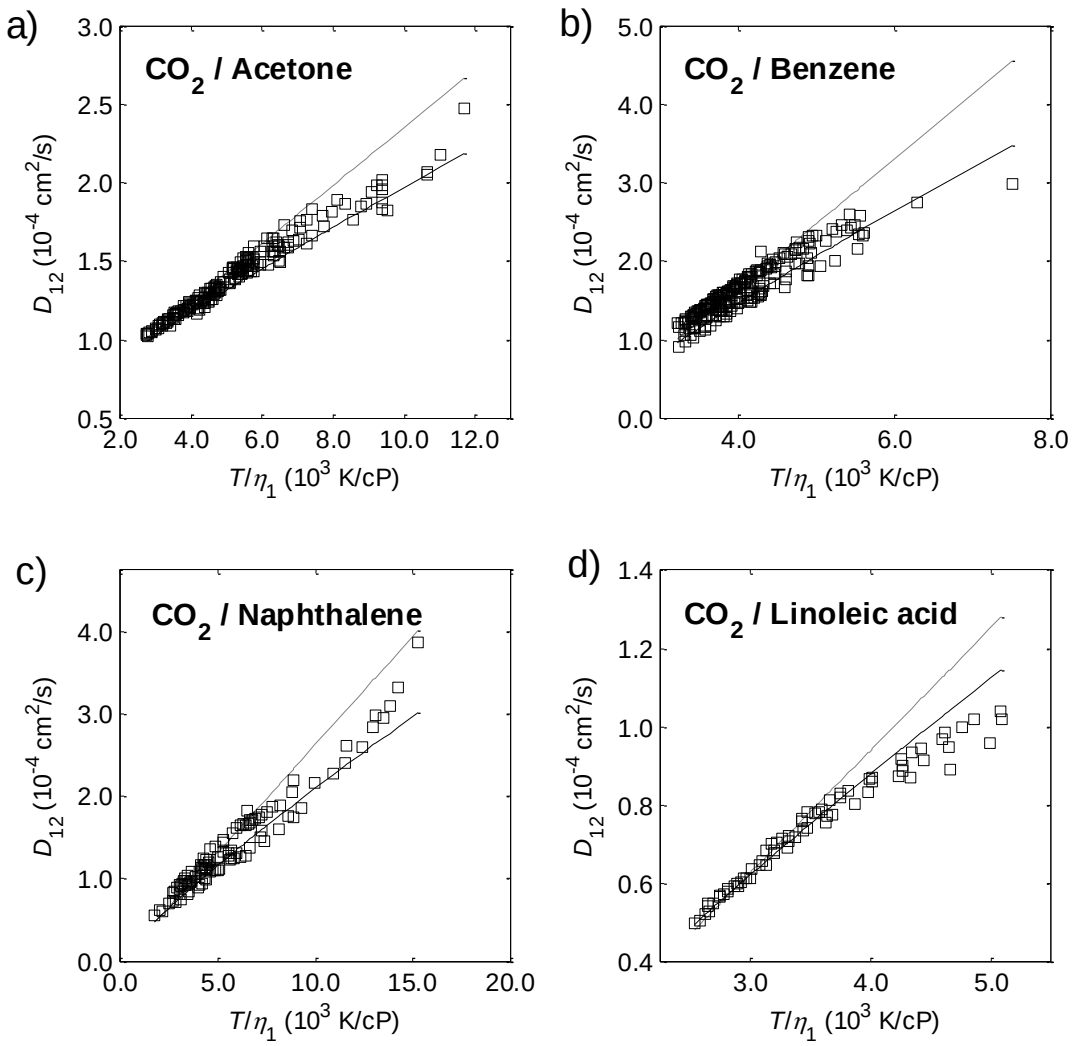

Fig. 3. Experimental and calculated tracer diffusion coefficients plotted in Stokes-Einstein coordinates: a) CO_2/acetone, b) CO_2/benzene, c) CO_2/naphtalene, d) CO_2/linoleic acid. Models: (—) modified Wilke-Chang, (---) Wilke-Chang. See data sources in Table 2.

To illustrate the behavior of our models, several tracer diffusivity isotherms of eicosapentaenoic acid, trifluoroacetylacetone and allylbenzene in carbon dioxide are graphed in Figs. 4.a to 4.c, respectively. It is difficult to distinguish the curves of the individual models as they provide very alike and accurate results, which is in conformity with the similar global deviations found above in Table 4 (7.86 – 8.56%). It may be detached that, in the whole, this trend is common to the remaining systems. Before finishing, it is worth noting the excellent

behavior guaranteed by the new models near the critical point of carbon dioxide, region where almost all equations fail their description [40, 44-45]. It is the case of eicosapentaenoic acid, and trifluoroacetylacetone in CO_2 represented in Figs. 4.b and 4.c, respectively, around 100 bar and 308-313 K. This is another important advantage of the new models proposed in this work.

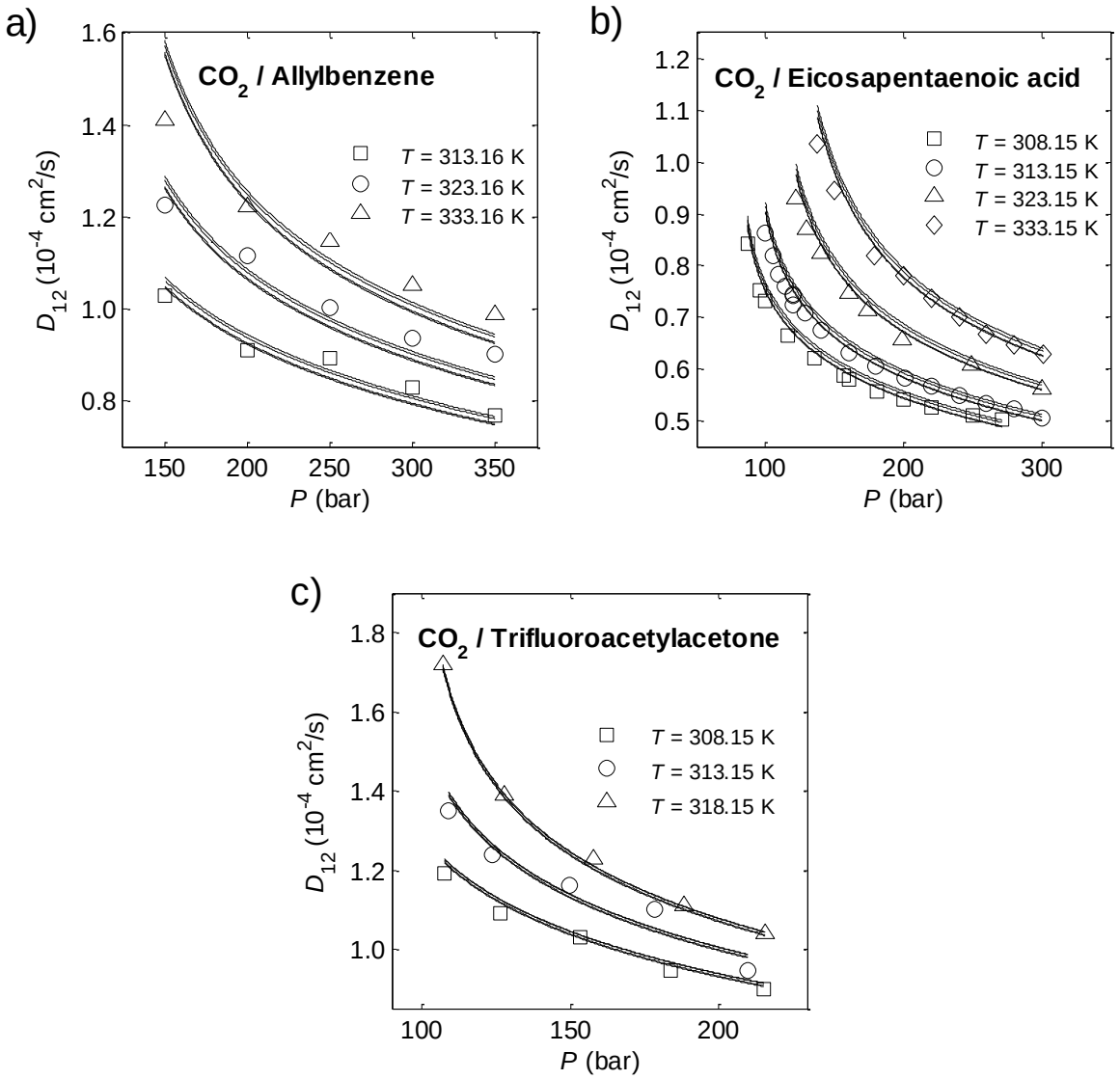

Fig. 4. Experimental and modeled tracer diffusion coefficients as function of pressure at constant temperature: a) CO_2/allylbenzene, b) CO_2/eicosapentaenoic acid, c) CO_2/trifluoroacetylacetonate. Data from [84, 123, 134]. Models (–): modified Wilke-Chang, modified Scheibel, modified Lusis-Ratcliff, modified Tyn-Calus.

5. Conclusions

The diffusion coefficients of solutes at infinite dilution in supercritical carbon dioxide were studied in this work with the main objective to develop accurate and simple equations for their pure estimation. Four predictive hydrodynamic models were proposed, on the basis of theoretically sound modifications introduced in the original expressions of Wilke-Chang, Scheibel, Lusis-Ratcliff, and Tyn-Calus. The modified models were tested and validated with the largest database compiled up till now, achieving reliable results in terms of average absolute errors (7.86 – 8.56%) and dispersion around the average. In fact, the differences between the maximum and minimum deviations were 50% to 80% lower than those obtained for the models adopted for comparison. Furthermore, the new expressions achieved average errors between 0.47% and 0.53%, while the original models provided systematic overestimations between 2.95% and 27.23%.

Appendix A. Models adopted for comparison

The expressions corresponding to the hydrodynamic equations revisited in this work are presented in the following:

Wilke-Chang equation (WC)

$$D_{12,\mathrm{WC}}\left(\mathrm{cm}^2/\mathrm{s}\right)=7.4\times10^{-8}\frac{T\sqrt{\phi M_1}}{\eta_1 V_{\mathrm{bp},2}^{0.6}} \tag{A.1}$$

Scheibel equation (Sch)

$$D_{12,\mathrm{Sch}}\left(\mathrm{cm}^2/\mathrm{s}\right)=\frac{8.2\times10^{-8}T}{\eta_1 V_{\mathrm{bp},2}^{1/3}}\left[1+\left(\frac{3V_{\mathrm{bp},1}}{V_{\mathrm{bp},2}}\right)^{2/3}\right] \tag{A.2}$$

Lusis-Ratcliff equation (LR)

$$D_{12,\mathrm{LR}}\left(\mathrm{cm}^2/\mathrm{s}\right)=\frac{8.52\times10^{-8}T}{\eta_1 V_{\mathrm{bp},1}^{1/3}}\left[1.40\left(\frac{V_{\mathrm{bp},1}}{V_{\mathrm{bp},2}}\right)^{1/3}+\left(\frac{V_{\mathrm{bp},1}}{V_{\mathrm{bp},2}}\right)\right] \tag{A.3}$$

Tyn-Calus equation (TC)

$$D_{12,\mathrm{TC}}\left(\mathrm{cm}^2/\mathrm{s}\right)=8.93\times10^{-8}\left(\frac{V_{\mathrm{bp},2}}{V_{\mathrm{bp},1}^2}\right)^{1/6}\left(\frac{\mathbf{P_1}}{\mathbf{P_2}}\right)^{0.6}\frac{T}{\eta_1}$$

$$D_{12,\mathrm{TC}}\left(\mathrm{cm}^2/\mathrm{s}\right)=8.93\times10^{-8}\frac{V_{\mathrm{bp},1}^{0.267}}{V_{\mathrm{bp},2}^{0.433}}\frac{T}{\eta_1} \qquad \text{(A.4)}$$

Appendix B. Supplementary data

Supplementary data associated with this article can be found, in the online version, at http://dx.doi.org/10.1016/j.fluid.2013.09.052.

Nomenclature

A_{i}	Universal constants in Eqs. (2)-(5) (Table 3)
AARD	Average absolute relative deviation, Eq. (9)
ARD	Average relative deviation, Eq. (10)
D_{12}	Tracer diffusion coefficient of solute 2 through solvent 1
k_{B}	Boltzmann constant
LR	Lusis-Ratcliff equation, Eq. (A.3)
M	Molecular weight
mLR	Modified Lusis-Ratcliff equation, Eq. (4)
mSch	Modified Scheibel equation, Eq. (3)
mTC	Modified Tyn-Calus equation, Eq. (5)
mWC	Modified Wilke-Chang equation, Eq. (2)
NDP	Number of data points
P	Pressure
$\mathbf{P}_i$	Parachor of component i
r	Molecule radius

SC-CO_2	Supercritical carbon dioxide
SCF	Supercritical fluid
Sch	Scheibel equation, Eq. (A.2)
SMB	Simulated Moving Bed
T	Absolute temperature
TC	Tyn-Calus equation, Eq. (A.4)
V_{bp}	Molar volume at normal boiling point
V_c	Critical molar volume
WC	Wilke-Chang equation, Eq. (A.1)

Greek letters

α_i	Universal constants in Eqs. (2)-(5) (Table 3)
β_i	Universal constants in Eqs. (2)-(5) (Table 3)
ϕ	Association factor in Wilke-Chang equation, Eq. (A.1)
γ	Universal constant in Eq. (5) (Table 3)
η_1	Solvent (SC-CO_2) viscosity
σ	Surface tension
σ_{ARD}	Standard deviation of the relative errors ARD_i

Subscripts

1	Solvent (SC-CO_2)
2	Solute
12	Binary
bp	Normal boiling point
c	Critical property
i	Component; equation
r	Reduced property

Superscripts

calc	Calculated value
exp	Experimental value
TC	Estimated by the group contribution method of Tyn-Calus

References

[1] E.L.G. Oliveira, A.J.D. Silvestre, C.M. Silva, Review of kinetic models for supercritical fluid extraction, Chemical Engineering Research & Design, 89 (2011) 1104-1117.

[2] P.C. Wankat, Rate-Controlled Separations, Blackie Academic and Professional, Great Britain, 1994.

[3] J.J. Carberry, Chemical and Catalytic Reaction Engineering, Dover Publications, Inc., New York, 2001.

[4] C.A.M. Afonso, J.G. Crespo, Green Separation Processes. Fundamentals and Applications, Wiley - VCH Verlag, 2005.

[5] M.M.R. de Melo, R.M.A. Domingues, A.J.D. Silvestre, C.M. Silva, Extraction and purification of triterpenoids using supercritical fluids: from lab to exploitation, Mini-Reviews in Organic Chemistry, 11 (2014) 362-381.

[6] E. Kiran, P.G. Debenedetti, C.J. Peters, Supercritical Fluids: Fundamentals and Applications, 1st ed., Springer, 2000.

[7] C.P. Passos, R.M. Silva, F.A. Da Silva, M.A. Coimbra, C.M. Silva, Supercritical fluid extraction of grape seed (*Vitis vinifera* L.) oil. Effect of the operating conditions upon oil composition and antioxidant capacity, Chemical Engineering Journal, 160 (2010) 634-640.

[8] A. Capuzzo, M. Maffei, A. Occhipinti, Supercritical fluid extraction of plant flavors and fragrances, Molecules, 18 (2013) 7194-7238.

[9] R.M.A. Domingues, E.L.G. Oliveira, C.S.R. Freire, R.M. Couto, P.C. Simoes, C.P. Neto, A.J.D. Silvestre, C.M. Silva, Supercritical Fluid Extraction of Eucalyptus globulus Bark-A Promising Approach for Triterpenoid Production, International Journal of Molecular Sciences, 13 (2012) 7648-7662.

[10] C.P. Passos, R.M. Silva, F.A. Da Silva, M.A. Coimbra, C.M. Silva, Enhancement of the supercritical fluid extraction of grape seed oil by using enzymatically pre-treated seed, The Journal of Supercritical Fluids, 48 (2009) 225-229.

[11] T. Fornari, G. Vicente, E. Vazquez, M.R. Garcia-Risco, G. Reglero, Isolation of essential oil from different plants and herbs by supercritical fluid extraction, Journal of Chromatography A, 1250 (2012) 34-48.

[12] M. Mazzotti, G. Storti, M. Morbidelli, Supercritical fluid simulated moving bed chromatography, Journal of Chromatography A, 786 (1997) 309-320.

[13] J.P.S. Aniceto, C.M. Silva, Simulated Moving Bed strategies and designs: from established systems to the latest developments, Separation and Purifiction Reviews, 44 (2015) 41-73.

[14] Y. Zhang, C. Erkey, Preparation of supported metallic nanoparticles using supercritical fluids: A review, The Journal of Supercritical Fluids, 38 (2006) 252-267.

[15] F. Cansell, C. Aymonier, Design of functional nanostructured materials using supercritical fluids, The Journal of Supercritical Fluids, 47 (2009) 508-516.

[16] J. Millat, J.H. Dymond, C.A. Nieto de Castro, Transport Properties of Fluids – Their Correlation, Prediction and Estimation, Cambridge University Press, London, 1996.

[17] H.J.M. Hanley, R.D. McCarty, E.G.D. Cohen, Analysis of the transport coefficients for simple dense fluid: Application of the modified Enskog theory, Physica, 60 (1972) 322-356.

[18] C.M. Silva, H. Liu, Modelling of Transport Properties of Hard Sphere Fluids and Related Systems, and its Applications, in: Á. Mulero (Ed.) Theory and Simulation of Hard-Sphere Fluids and Related Systems, Springer Berlin Heidelberg, 2008, pp. 383-492.

[19] J.A. Barker, D. Henderson, Perturbation theory and equation of state for fluids. II. A successful theory of liquids, Journal of Chemical Physics, 47 (1967) 4714-4721.

[20] J.D. Weeks, D. Chandler, H.C. Andersen, Role of repulsive forces in determining equilibrium structure of simple liquids, Journal of Chemical Physics, 54 (1971) 5237-5247.

[21] C.M. Silva, H.Q. Liu, E.A. Macedo, Comparison between different explicit expressions of the effective hard sphere diameter of Lennard-Jones fluid: Application to self-diffusion coefficients, Industrial & Engineering Chemistry Research, 37 (1998) 221-227.

[22] M.H. Cohen, D. Turnbull, Molecular Transport in Liquids and Glasses, The Journal of Chemical Physics, 31 (1959) 1164-1169.

[23] P.B. Macedo, T.A. Litovitz, On the relative roles of free volume and activation energy in the viscosity of liquids, The Journal of Chemical Physics, 42 (1965) 245-256.

[24] H. Liu, C.M. Silva, E.A. Macedo, Generalised free-volume theory for transport properties and new trends about the relationship between free volume and equations of state, Fluid Phase Equilibria, 202 (2002) 89-107.

[25] J.H. Dymond, Corrected Enskog theory and the transport coefficients of liquids, The Journal of Chemical Physics, 60 (1974) 969-973.

[26] J.H. Dymond, The interpretation of transport coefficients on the basis of the Van der Waals model: I dense fluids, Physica, 75 (1974) 100-114.

[27] H. Liu, C.M. Silva, E.A. Macedo, Unified approach to the self-diffusion coefficients of dense fluids over wide ranges of temperature and pressure—hard-sphere, square-well, Lennard–Jones and real substances, Chemical Engineering Science, 53 (1998) 2403-2422.

[28] S.-H. Chen, A rough-hard-sphere theory for diffusion in supercritical carbon dioxide, Chemical Engineering Science, 38 (1983) 655-660.

[29] C. Erkey, H. Gadalla, A. Akgerman, Application of rough hard sphere theory to diffusion in supercritical fluidst, The Journal of Supercritical Fluids, 3 (1990) 180-185.

[30] E. Ruckenstein, H.Q. Liu, Self-diffusion in gases and liquids, Industrial & Engineering Chemistry Research, 36 (1997) 3927-3936.

[31] H. Liu, C.M. Silva, E.A. Macedo, New equations for tracer diffusion coefficients of solutes in supercritical and liquid solvents based on the Lennard-Jones fluid model, Industrial & Engineering Chemistry Research, 36 (1997) 246-252.

[32] D. Chandler, Rough hard sphere theory of the self-diffusion constant for molecular liquids, The Journal of Chemical Physics, 62 (1975) 1358-1363.

[33] R.C. Reid, J.M. Prausnitz, B.E. Poling, The Properties of Gases and Liquids, 4th ed., McGraw-Hill, New York, 1987.

[34] K.K. Liong, P.A. Wells, N.R. Foster, Diffusion in supercritical fluids, The Journal of Supercritical Fluids, 4 (1991) 91-108.

[35] S.N. Glasstone, K. Laider, H. Eyring, The Theory of Rate Processes, McGraw-Hill, New York, 1941.

[36] M. Dzugutov, A universal law for atomic diffusion in condensed matter, Nature, 381 (1996) 137-139.

[37] Y. Rosenfeld, Relation between the transport coefficients and the internal entropy of simple systems, Physical Review A, 15 (1977) 2545-2549.

[38] R.V. Vaz, A.L. Magalhães, D.L.A. Fernandes, C.M. Silva, Universal correlation of self-diffusion coefficients of model and real fluids based on residual entropy scaling law, Chemical Engineering Science, 79 (2012) 153-162.

[39] I. Medina, Determination of diffusion coefficients for supercritical fluids, Journal of Chromatography A, (2012).

[40] A.L. Magalhães, F.A. Da Silva, C.M. Silva, Free-volume model for the diffusion coefficients of solutes at infinite dilution in supercritical CO2 and liquid H2O, The Journal of Supercritical Fluids, 74 (2013) 89-104.

[41] A.L. Magalhães, F.A. Da Silva, C.M. Silva, New models for tracer diffusion coefficients of hard sphere and real systems: Application to gases, liquids and supercritical fluids, The Journal of Supercritical Fluids, 55 (2011) 898-923.

[42] A.L. Magalhães, F.A. Da Silva, C.M. Silva, New tracer diffusion correlation for real systems over wide ranges of temperature and density, Chemical Engineering Journal, 166 (2011) 49-72.

[43] A.L. Magalhães, F.A. Da Silva, C.M. Silva, Tracer diffusion coefficients of polar systems, Chemical Engineering Science, 73 (2012) 151-168.

[44] P.F. Lito, A.L. Magalhães, J.R.B. Gomes, C.M. Silva, Universal model for accurate calculation of tracer diffusion coefficients in gas, liquid and supercritical systems, Journal of Chromatography A, 1290 (2013) 1-26.

[45] A.L. Magalhães, P.F. Lito, F.A. Da Silva, C.M. Silva, Simple and accurate correlations for diffusion coefficients of solutes in liquids and supercritical fluids over wide ranges of temperature and density, The Journal of Supercritical Fluids, 76 (2013) 94-114.

[46] C.R. Wilke, P. Chang, Correlation of diffusion coefficients in dilute solutions, AIChE Journal, 1 (1955) 264-270.

[47] M.T. Tyn, W.F. Calus, Diffusion coefficients in dilute binary liquid mixtures, Journal of Chemical & Engineering Data, 20 (1975) 106-109.

[48] W. Hayduk, B.S. Minhas, Correlations for prediction of molecular diffusivities in liquids, The Canadian Journal of Chemical Engineering, 60 (1982) 295-299.

[49] K.A. Reddy, L.K. Doraiswamy, Estimating liquid diffusivity, Industrial & Engineering Chemistry Fundamentals, 6 (1967) 77-79.

[50] E.G. Scheibel, Correspondence. Liquid Diffusivities. Viscosity of Gases, Industrial & Engineering Chemistry, 46 (1954) 2007-2008.

[51] M.A. Lusis, C.A. Ratcliff, Diffusion in binary liquid mixtures at infinite dilution, The Canadian Journal of Chemical Engineering, 46 (1968) 385-387.

[52] E.I. Cussler, Diffusion: Mass Transfer in Fluid Systems, Cambridge University Press, New York, 2009.

[53] P.R. Sassiat, P. Mourier, M.H. Caude, R.H. Rosset, Measurement of diffusion coefficients in supercritical carbon dioxide and correlation with the equation of Wilke and Chang, Analytical Chemistry, 59 (1987) 1164-1170.

[54] P.G. Debenedetti, R.C. Reid, Diffusion and mass transfer in supercritical fluids, AIChE Journal, 32 (1986) 2034-2046.

[55] R. Feist, G.M. Schneider, Determination of Binary Diffusion Coefficients of Benzene, Phenol, Naphthalene and Caffeine in Supercritical CO2 between 308 and 933 K in the Pressure Range 90 to 160 gar with Supercritical Fluid Chromatography (SFC), Separation Science and Technology, 17 (1982) 261-270.

[56] T. Wells, N.R. Foster, R.P. Chaplin, Diffusion of phenylacetic acid and vanillin in supercritical carbon dioxide, Industrial & Engineering Chemistry Research, 31 (1992) 927-934.

[57] J.R. Brock, R.B. Bird, Surface tension and the principle of corresponding states, AIChE Journal, 1 (1955) 174-177.

[58] D.G. Miller, G. Thodos, Correspondence. Reduced Frost-Kalkwarf vapor pressure equation, Industrial & Engineering Chemistry Fundamentals, 2 (1963) 78-80.

[59] A.L. Magalhães, R.V. Vaz, R.M.G. Gonçalves, F.A. Da Silva, C.M. Silva, Accurate hydrodynamic models for the prediction of tracer diffusivities in supercritical carbon dioxide, The Journal of Supercritical Fluids, 83 (2013) 15-27.

[60] K.S. Pitzer, D.R. Schreiber, Improving equation-of-state accuracy in the critical region; equations for carbon dioxide and neopentane as examples, Fluid Phase Equilibria, 41 (1988) 1-17.

[61] V.V. Altunin, M.A. Sakhabetdinov, Viscosity of liquid and gaseous carbon dioxide at temperatures 220-1300 K and pressure up to 1200 bar, Teploenergetika, 8 (1972) 85-89.

[62] K.G. Joback, A unified approach to physical property estimation using multivariate statistical techniques, in: Department of Chemical Engineering, Massachusetts Institute of Technology, Cambridge, MA, 1984.

[63] K.G. Joback, R.C. Reid, Estimation of pure-component properties from group-contributions, Chemical Engineering Communications, 57 (1987) 233 - 243.

[64] G.R. Somayajulu, Estimation procedures for critical constants, Journal of Chemical & Engineering Data, 34 (1989) 106-120.

[65] K.M. Klincewicz, R.C. Reid, Estimation of critical properties with group contribution methods, AIChE Journal, 30 (1984) 137-142.

[66] D. Ambrose, Correlation and Estimation of Vapour-liquid Critical Properties: I, Critical Temperatures of Organic Compounds, in: NPL Technical Report. Chem. 92, National Physical Laboratory, Madison, WI, 1978.

[67] D. Ambrose, Correlation and Estimation of Vapour-Liquid Critical Properties. II: Critical Pressure and Critical Volume, in: NPL Technical Report. Chem. 92, National Physical Laboratory, Teddington, UK, 1979.

[68] X. Wen, Y. Qiang, A new group contribution method for estimating critical properties of organic compounds, Industrial & Engineering Chemistry Research, 40 (2001) 6245-6250.

[69] L. Constantinou, R. Gani, New group contribution method for estimating properties of pure compounds, AIChE Journal, 40 (1994) 1697-1710.

[70] C.L. Yaws, Thermophysical Properties of Chemicals and Hydrocarbons, William Andrew Inc., New York, 2008.

[71] C.L. Yaws, Chemical Properties Handbook : Physical, Thermodynamic, Environmental, Transport, Safety, and Health Related Properties for Organic and Inorganic Chemicals McGraw-Hill Professional, New York, 1998.

[72] H. Liu, E. Ruckenstein, A predictive equation for the tracer diffusion of various solutes in gases, supercritical fluids, and liquids, Industrial & Engineering Chemistry Research, 36 (1997) 5488-5500.

[73] I. ChemZoo, ChemSpider - Building community for chemists, in, 2007.

[74] R.H. Perry, D.W. Green, Perry's Chemical Engineers' Handbook, 8th ed., McGraw-Hill Professional, New York, 2008.

[75] L. Hangzhou Weeqoo Technology Co., LookChem.com - Look for Chemicals, in, Hangzhou 2008.

[76] Molecular Design LAB. (Dept. of Chemical Engineering), Korea Thermophysical Properties Data Bank (KDB) in, Korea Univerity, 1995.

[77] AIChE, Design Institute for Physical Properties (DIPPR), in, 2006.

[78] AspenTech., Aspen Physical Property System - Physical Property Methods, in, Aspen Technology, Inc., Cambridge, MA, 2007.

[79] T. Funazukuri, C.Y. Kong, S. Kagei, Infinite-dilution binary diffusion coefficients of 2-propanone, 2-butanone, 2-pentanone, and 3-pentanone in CO_2 by the Taylor dispersion technique from 308.15 to 328.15 K in the pressure range from 8 to 35 MPa, International Journal of Thermophysics, 21 (2000) 1279-1290.

[80] T. Funazukuri, C.Y. Kong, S. Kagei, Binary diffusion coefficients of acetone in carbon dioxide at 308.2 and 313.2 K in the pressure range from 7.9 to 40 MPa, International Journal of Thermophysics, 21 (2000) 651-669.

[81] C.Y. Kong, T. Funazukuri, S. Kagei, Chromatographic impulse response technique with curve fitting to measure binary diffusion coefficients and retention factors using polymer-coated capillary columns, Journal of Chromatography A, 1035 (2004) 177-193.

[82] H. Nishiumi, M. Fujita, K. Agou, Diffusion of acetone in supercritical carbon dioxide, Fluid Phase Equilibria, 117 (1996) 356-363.

[83] V.M. Shenai, B.L. Hamilton, M.A. Matthews, Diffusion in Liquid and Supercritical Fluid Mixtures, in: Supercritical Fluid Engineering Science, 1993, pp. 92-103.

[84] O. Suárez-Iglesias, I. Medina, C. Pizarro, J.L. Bueno, Diffusion coefficients of 2-fluoroanisole, 2-bromoanisole, allylbenzene and 1,3-divinylbenzene at infinite dilution in supercritical carbon dioxide, Fluid Phase Equilibria, 260 (2007) 279-286.

[85] L.M. González, O. Suárez-Iglesias, J.L. Bueno, C. Pizarro, I. Medina, Limiting binary diffusivities of aniline, styrene, and mesitylene in supercritical carbon dioxide, Journal of Chemical & Engineering Data, 52 (2007) 1286-1290.

[86] L.M. González, J.L. Bueno, I. Medina, Determination of binary diffusion coefficients of anisole, 2,4-dimethylphenol, and nitrobenzene in supercritical carbon dioxide, Industrial & Engineering Chemistry Research, 40 (2001) 3711-3716.

[87] K. Abaroudi, Limpieza de Matrices Sólidas Porosas de Interés Medioambiental con Fluidos Supercríticos, in: Departamento de Ingeniería Química, Universidad Politécnica de Catalunã, 2001.

[88] T. Funazukuri, C.Y. Kong, T. Kikuchi, S. Kagei, Measurements of binary diffusion coefficient and partition ratio at infinite dilution for linoleic acid and arachidonic acid in supercritical carbon dioxide, Journal of Chemical & Engineering Data, 48 (2003) 684-688.

[89] Y.S. Han, Y.W. Yang, P.D. Wu, Binary diffusion coefficients of arachidonic acid ethyl ester, *cis*-5,8,11,14,17-eicosapentaenoic acid ethyl ester, and *cis*-4,7,10,13,16,19-docosahexanenoic acid ethyl ester in supercritical carbon dioxide, Journal of Chemical & Engineering Data, 52 (2007) 555-559.

[90] K.K. Liong, P.A. Wells, N.R. Foster, Diffusion coefficients of long-chain esters in supercritical carbon dioxide, Industrial & Engineering Chemistry Research, 30 (1991) 1329-1335.

[91] I. Swaid, G.M. Schneider, Determination of binary diffusion coefficients of benzene and some alkylbenzenes in supercritical CO_2 between 308 and 328 K in the pressure range 80 to 160 bar with supercritical fluid chromatography (SFC), Berichte Der Bunsen-Gesellschaft-Physical Chemistry Chemical Physics, 83 (1979) 969-974.

[92] C.A. Filho, C.M. Silva, M.B. Quadri, E.A. Macedo, Infinite dilution diffusion coefficients of linalool and benzene in supercritical carbon dioxide, Journal of Chemical & Engineering Data, 47 (2002) 1351-1354.

[93] J.J. Suárez, J.L. Bueno, I. Medina, Determination of binary diffusion coefficients of benzene and derivatives in supercritical carbon dioxide, Chemical Engineering Science, 48 (1993) 2419-2427.

[94] J.L. Bueno, J.J. Suárez, J. Dizy, I. Medina, Infinite dilution diffusion coefficients: benzene derivatives as solutes in supercritical carbon dioxide, Journal of Chemical & Engineering Data, 38 (1993) 344-349.

[95] T. Funazukuri, N. Nishimoto, Tracer diffusion coefficients of benzene in dense CO_2 at 313.2 K and 8.5-30 MPa, Fluid Phase Equilibria, 125 (1996) 235-243.

[96] T. Funazukuri, C.Y. Kong, S. Kagei, Infinite dilution binary diffusion coefficients of benzene in carbon dioxide by the Taylor dispersion technique at temperatures from 308.15 to 328.15 K and pressures from 6 to 30 MPa, International Journal of Thermophysics, 22 (2001) 1643-1660.

[97] J.M.H.L. Sengers, U.K. Deiters, U. Klask, P. Swidersky, G.M. Schneider, Application of the Taylor dispersion method in supercritical fluids, International Journal of Thermophysics, 14 (1993) 893-922.

[98] K. Ago, H. Nishiumi, Mutual diffusion coefficients of benzene in supercritical carbon dioxide, Journal of Chemical Engineering of Japan, 32 (1999) 563-568.

[99] C.Y. Kong, T. Funazukuri, S. Kagei, Binary diffusion coefficients and retention factors for polar compounds in supercritical carbon dioxide by chromatographic impulse response method, Journal of Supercritical Fluids, 37 (2006) 359-366.

[100] O.J. Catchpole, M.B. King, Measurement and correlation of binary diffusion coefficients in near critical fluids, Industrial & Engineering Chemistry Research, 33 (1994) 1828-1837.

[101] H. Fu, L.A.F. Coelho, M.A. Matthews, Diffusion coefficients of model contaminants in dense CO_2, Journal of Supercritical Fluids, 18 (2000) 141-155.

[102] O. Suárez-Iglesias, I. Medina, C. Pizarro, J.L. Bueno, Diffusion of benzyl acetate, 2-phenylethyl acetate, 3-phenylpropyl acetate, and dibenzyl ether in mixtures of carbon dioxide and ethanol, Industrial & Engineering Chemistry Research, 46 (2007) 3810-3819.

[103] O. Suárez-Iglesias, I. Medina, C. Pizarro, J.L. Bueno, Limiting diffusion coefficients of ethyl benzoate, benzylacetone, and eugenol in carbon dioxide at supercritical conditions, Journal of Chemical & Engineering Data, 53 (2008) 779-784.

[104] H. Weingärtner, U. Klask, G.M. Schneider, Solute diffusion in supercritical solvents - diffusion coefficients D_{12}^{∞} and diffusion-viscosity relationship for the aromatic model solute biphenyl in carbon dioxide, Zeitschrift Fur Physikalische Chemie-International Journal of Research in Physical Chemistry & Chemical Physics, 219 (2005) 1261-1271.

[105] L.M. González, O. Suárez-Iglesias, J.L. Bueno, C. Pizarro, I. Medina, Application of the corresponding states principle to the diffusion in CO_2, AIChE Journal, 53 (2007) 3054-3061.

[106] J.J. Suárez, I. Medina, J.L. Bueno, Diffusion coefficients in supercritical fluids: available data and graphical correlations, Fluid Phase Equilibria, 153 (1998) 167-212.

[107] T. Funazukuri, Measurements of binary diffusion coefficients of 20 organic compounds in CO_2 at 313.2 K and 16.0 MPa, Journal of Chemical Engineering of Japan, 29 (1996) 191-192.

[108] C. Pizarro, O. Suárez-Iglesias, I. Medina, J.L. Bueno, Diffusion coefficients of *n*-butylbenzene, *n*-pentylbenzene, 1-phenylhexane, 1-phenyloctane, and 1-phenyldodecane in supercritical carbon dioxide, Industrial & Engineering Chemistry Research, 47 (2008) 6783-6789.

[109] C. Pizarro, O. Suárez-Iglesias, I. Medina, J.L. Bueno, Diffusion coefficients of isobutylbenzene, *sec*-butylbenzene, and 3-methylbutylbenzene in supercritical carbon dioxide, Journal of Chemical & Engineering Data, 58 (2013) 2001-2007.

[110] K.M. González, J.L. Bueno, I. Medina, Measurement of diffusion coefficients for 2-nitroanisole, 1,2-dichlorobenzene and *tert*-butylbenzene in carbon dioxide containing modifiers, Journal of Supercritical Fluids, 24 (2002) 219-229.

[111] P.A. Wells, Diffusion in Supercritical Fluids, in, The University of New South Wales, Kensington, Australia, 1991.

[112] K.K. Liong, P.A. Wells, N.R. Foster, Diffusion of fatty acid esters in supercritical carbon dioxide, Industrial & Engineering Chemistry Research, 31 (1992) 390-399.

[113] C.C. Lai, C.S. Tan, Measurement of molecular diffusion coefficients in supercritical carbon dioxide using a coated capillary column, Industrial & Engineering Chemistry Research, 34 (1995) 674-680.

[114] G. Knaff, E.U. Schlünder, Diffusion coefficients of naphthalene and caffeine in supercritical carbon dioxide, Chemical Engineering and Processing, 21 (1987) 101-105.

[115] H.H. Lauer, D. Mcmanigill, R.D. Board, Mobile-phase transport-properties of liquefied gases in near-critical and supercritical fluid chromatography, Analytical Chemistry, 55 (1983) 1370-1375.

[116] T. Funazukuri, C.Y. Kong, S. Kagei, Binary diffusion coefficients, partition ratios and partial molar volumes at infinite dilution for β-carotene and α-tocopherol in supercritical carbon dioxide, Journal of Supercritical Fluids, 27 (2003) 85-96.

[117] T. Funazukuri, C.Y. Kong, N. Murooka, S. Kagei, Measurements of binary diffusion coefficients and partition ratios for acetone, phenol, α-tocopherol, and β-carotene in supercritical carbon dioxide with a poly(ethylene glycol)-coated capillary column, Industrial & Engineering Chemistry Research, 39 (2000) 4462-4469.

[118] T. Funazukuri, C.Y. Kong, S. Kagei, Measurements of binary diffusion coefficients for some low volatile compounds in supercritical carbon dioxide by input-output response technique with two diffusion columns connected in series, Fluid Phase Equilibria, 194 (2002) 1169-1178.

[119] X.Y. Dong, B.G. Su, H.B. Xing, Y.W. Yang, Q.L. Ren, Diffusion coefficients of L-menthone and L-carvone in mixtures of carbon dioxide and ethanol, Journal of Supercritical Fluids, 55 (2010) 86-95.

[120] X.Y. Dong, B.G. Su, H.B. Xing, Z.B. Bao, Y.W. Yang, Q.L. Ren, Cosolvent effects on the diffusions of 1,3-dichlorobenzene, L-carvone, geraniol and 3-fluorophenol in supercritical carbon dioxide, Journal of Supercritical Fluids, 58 (2011) 216-225.

[121] C.A. Filho, C.M. Silva, M.B. Quadri, E.A. Macedo, Tracer diffusion coefficients of citral and D-limonene in supercritical carbon dioxide, Fluid Phase Equilibria, 204 (2003) 65-73.

[122] C.Y. Kong, Y.Y. Gu, M. Nakamura, T. Funazukuri, S. Kagei, Diffusion coefficients of metal acetylacetonates in supercritical carbon dioxide, Fluid Phase Equilibria, 297 (2010) 162-167.

[123] Y.N. Yang, M.A. Matthews, Diffusion of chelating agents in supercritical CO_2 and a predictive approach for diffusion coefficients, Journal of Chemical & Engineering Data, 46 (2001) 588-595.

[124] C.Y. Kong, N. Takahashi, T. Funazukuri, S. Kagei, Measurements of binary diffusion coefficients and retention factors for dibenzo-24-crown-8 and 15-crown-5 in supercritical carbon dioxide by chromatographic impulse response technique, Fluid Phase Equilibria, 257 (2007) 223-227.

[125] N. Dahmen, A. Dulberg, G.M. Schneider, Determination of binary diffusion coefficients in supercritical carbon dioxide with supercritical fluid chromatography (SFC), Berichte Der Bunsen-Gesellschaft-Physical Chemistry Chemical Physics, 94 (1990) 384-386.

[126] S. Umezawa, A. Nagashima, Measurement of the diffusion coefficients of acetone, benzene, and alkane in supercritical CO_2 by the Taylor dispersion method, Journal of Supercritical Fluids, 5 (1992) 242-250.

[127] C.M. Silva, E.A. Macedo, Diffusion coefficients of ethers in supercritical carbon dioxide, Industrial & Engineering Chemistry Research, 37 (1998) 1490-1498.

[128] C. Pizarro, O. Suárez-Iglesias, I. Medina, J.L. Bueno, Using supercritical fluid chromatography to determine diffusion coefficients of 1,2-diethylbenzene, 1,4-diethylbenzene, 5-*tert*-butyl-*m*-xylene and phenylacetylene in supercritical carbon dioxide, Journal of Chromatography A, 1167 (2007) 202-209.

[129] C. Pizarro, O. Suarez-Iglesias, I. Medina, J.L. Bueno, Binary diffusion coefficients for 2,3-dimethylaniline, 2,6-dimethylaniline, 2-methylanisole, 4-methylanisole and 3-nitrotoluene in supercritical carbon dioxide, Journal of Supercritical Fluids, 48 (2009) 1-8.

[130] C.Y. Kong, M. Nakamura, K. Sone, T. Funazukuri, S. Kagei, Measurements of binary diffusion coefficients for ferrocene and 1,1'-dimethylferrocene in supercritical carbon dioxide, Journal of Chemical & Engineering Data, 55 (2010) 3095-3100.

[131] H. Higashi, Y. Iwai, Y. Nakamura, S. Yamamoto, Y. Arai, Correlation of diffusion coefficients for naphthalene and dimethylnaphthalene isomers in supercritical carbon dioxide, Fluid Phase Equilibria, 166 (1999) 101-110.

[132] H. Higashi, Y. Iwai, Y. Takahashi, H. Uchida, Y. Arai, Diffusion coefficients of naphthalene and dimethylnaphthalene in supercritical carbon dioxide, Fluid Phase Equilibria, 144 (1998) 269-278.

[133] T. Funazukuri, C.Y. Kong, S. Kagei, Effects of molecular weight and degree of unsaturation on binary diffusion coefficients for lipids in supercritical carbon dioxide, Fluid Phase Equilibria, 219 (2004) 67-73.

[134] T. Funazukuri, C.Y. Kong, S. Kagei, Binary diffusion coefficient, partition ratio, and partial molar volume for docosahexaenoic acid, eicosapentaenoic acid and α-linolenic acid at infinite dilution in supercritical carbon dioxide, Fluid Phase Equilibria, 206 (2003) 163-178.

[135] C. Pizarro, O. Suárez-Iglesias, I. Medina, J.L. Bueno, Binary diffusion coefficients of 2-ethyltoluene, 3-ethyltoluene, and 4-ethyltoluene in supercritical carbon dioxide, Journal of Chemical & Engineering Data, 54 (2009) 1467-1471.

[136] C.Y. Kong, K. Sone, T. Sako, T. Funazukuri, S. Kagei, Solubility determination of organometallic complexes in supercritical carbon dioxide by chromatographic impulse response method, Fluid Phase Equilibria, 302 (2011) 347-353.

[137] A. Akgerman, C. Erkey, M. Orejuela, Limiting diffusion coefficients of heavy molecular weight organic contaminants in supercritical carbon dioxide, Industrial & Engineering Chemistry Research, 35 (1996) 911-917.

[138] R.H. Lin, L.L. Tavlarides, Diffusion coefficients of diesel fuel and surrogate compounds in supercritical carbon dioxide, Journal of Supercritical Fluids, 52 (2010) 47-55.

[139] T. Funazukuri, S. Hachisu, N. Wakao, Measurements of binary diffusion coefficients of C_{16}-C_{24} unsaturated fatty acid methyl esters in supercritical carbon dioxide, Industrial & Engineering Chemistry Research, 30 (1991) 1323-1329.

[140] T. Funazukuri, Y. Ishiwata, Diffusion coefficients of linoleic acid methyl ester, vitamin K_3 and indole in mixtures of carbon dioxide and *n*-hexane at 313.2 K, and 16.0 MPa and 25.0 MPa, Fluid Phase Equilibria, 164 (1999) 117-129.

[141] C.Y. Kong, N.R.W. Withanage, T. Funazukuri, S. Kagei, Binary diffusion coefficients and retention factors for γ-linolenic acid and its methyl and ethyl esters in supercritical carbon dioxide, Journal of Supercritical Fluids, 37 (2006) 63-71.

[142] C.Y. Kong, M. Mori, T. Funazukuri, S. Kagei, Measurements of binary diffusion coefficients, retention factors and partial molar volumes for myristoleic acid and its methyl ester in supercritical carbon dioxide, Analytical Sciences, 22 (2006) 1431-1436.

[143] T. Funazukuri, Y. Ishiwata, N. Wakao, Predictive correlation for binary diffusion coefficients in dense carbon dioxide, AIChE Journal, 38 (1992) 1761-1768.

[144] D.M. Lamb, S.T. Adamy, K.W. Woo, J. Jonas, Transport and relaxation of naphthalene in supercritical fluids, Journal of Physical Chemistry, 93 (1989) 5002-5005.

[145] T. Funazukuri, S. Hachisu, N. Wakao, Measurement of diffusion coefficients of C_{18} unsaturated fatty acid methyl esters, naphthalene, and benzene in supercritical carbon dioxide by a tracer response technique, Analytical Chemistry, 61 (1989) 118-122.

[146] C.Y. Kong, K. Watanabe, T. Funazukuri, Diffusion coefficients of phenylbutazone in supercritical CO2 and in ethanol, Journal of Chromatography A, 1279 (2013) 92-97.

[147] C. Pizarro, O. Suárez-Iglesias, I. Medina, J.L. Bueno, Molecular diffusion coefficients of phenylmethanol, 1-phenylethanol, 2-phenylethanol, 2-phenyl-1-propanol, and 3-phenyl-1-propanol in supercritical carbon dioxide, Journal of Supercritical Fluids, 43 (2008) 469-476.

[148] C.M. Silva, C.A. Filho, M.B. Quadri, E.A. Macedo, Binary diffusion coefficients of α-pinene and β-pinene in supercritical carbon dioxide, The Journal of Supercritical Fluids, 32 (2004) 167-175.

[149] J.J. Suárez, J.L. Bueno, I. Medina, J. Dizy, Applications of supercritical chromatography - Determination of molecular diffusivity, Afinidad, 49 (1992) 101-113.

[150] N. Dahmen, A. Kordikowski, G.M. Schneider, Determination of binary diffusion coefficients of organic compounds in supercritical carbon dioxide by supercritical fluid chromatography, Journal of Chromatography A, 505 (1990) 169-178.

[151] C.Y. Kong, N.R.W. Withanage, T. Funazukuri, S. Kagei, Binary diffusion coefficients and retention factors for long-chain triglycerides in supercritical carbon dioxide by the chromatographic impulse response method, Journal of Chemical & Engineering Data, 50 (2005) 1635-1640.

[152] T. Funazukuri, C.Y. Kong, S. Kagei, Infinite-dilution binary diffusion coefficient, partition ratio, and partial molar volume for ubiquinone CoQ10 in supercritical carbon dioxide, Industrial & Engineering Chemistry Research, 41 (2002) 2812-2818.

Paper IV

Adapted from

Prediction of binary diffusion coefficients in supercritical CO_2 with improved behavior near the critical point

Journal of Supercritical Fluids, 91 (2014) 24–36

Abstract

In this work, a predictive model for binary diffusivities at infinite dilution (D_{12}) in SC-CO_2 is proposed. It combines two terms – background and singular – with the objective to represent D_{12} accurately not only far but also near the critical point, where critical enhancement is always observed. The model provides an average error of 6.20% for a large database including 149 systems and 4469 data points over wide ranges of temperature and pressure. The models selected for comparison (Wilke-Chang, Scheibel, Lusis-Ratcliff, Lai-Tan, Tyn-Calus and Reddy-Doraiswamy) achieve scattered and biased results, with average errors from 11.62% to 75.17%. In the whole, the new model exhibits an excellent performance for any kind of molecules in terms of size, molecular weight, polarity and sphericity, in all critical region. In order to help interested readers, a spreadsheet for the calculation of D_{12} is given in Supplementary data. The input data is: temperature, pressure, CO_2 viscosity, and solute properties (acentric factor, critical constants, molar volume at normal boiling point, and molecular weight – given in this paper for the systems studied).

1. Introduction

Transport coefficients are fundamental properties for simulation, design and scale-up of rate-controlled processes. Here, supercritical fluids (SCFs) get special attention due to their remarkable ability to be applied to mass-transfer operations, phase transition processes, reactive systems, materials related processes, and nanostructured materials, either at industrial capacity application or yet under development [1]. The application areas include extraction, but also impregnation and cleaning, multistage countercurrent separation, particle formation, coating, and reactive systems such as hydrogenation and biomass gasification [1-3]. The successful study of these applications lies on the accurate knowledge of the properties and behavior of the supercritical fluids and the materials involved. In particular, the infinitely dilute diffusion coefficient of a solute (2) in a solvent (1), D_{12}, frequently called tracer diffusion coefficient, is one of the most significant transport properties in rate-controlled processes [4-6]. While in

several industrial applications the systems are dilute, which allows D_{12} to be directly utilized in the calculations, for most concentrated liquid mixtures the diffusivities should be estimated based on their individual tracer coefficients using, for example, the Darken and the Vignes mixing rules [6-8].

Because of their chief relevance, distinct D_{12} expressions applicable to compressed gases, liquids and SCFs, especially supercritical CO_2 (SC-CO_2), have been developed and reported in the literature. They may be divided into several groups like molecularly based models (e.g., hard sphere, rough hard sphere, Lennard-Jones) [9-13], free-volume theories [9, 13-15], Rice and Gray approach [16-18], empirical or semi-empirical expressions [19-20], and hydrodynamic equations [21-26]. Some of these equations provide good results [13, 15, 17, 19, 27-28] but usually require system-specific parameters. Therefore, pure predictive models are highly desirable, particularly under the context of biorefinery where a large number of natural compounds and unknown systems are increasingly being identified/studied.

The information compiled and analyzed in this paper emphasizes the importance and the need of accurate equations to predict tracer diffusivities not only far but also near the critical point, where a clear growing of D_{12} (critical enhancement) is observed as a result of the abrupt density variation. (However, it is worth noting that D_{12} vanishes at the critical point because of sharp clustering phenomenon [22]).

In this work, a new predictive model for tracer diffusivities in SC-CO_2 is proposed. It embodies two contributions – regular/background and singular – for the correct description of diffusion in the critical region, even in the vicinity of the critical point where common models usually fail. The model is validated with a large database of solutes in SC-CO_2, for which various error statistics are computed. The results achieved are much better than those provided by other predictive models from literature, namely, Wilke-Chang, Scheibel, Lusis-Ratcliff, Lai-Tan, Tyn-Calus and Reddy-Doraiswamy. These are hydrodynamic equations that embody only universal parameters, being thus applicable to all database. They have been extended in last decades from liquids to SCFs, especially Wilke-Chang, although Lai-Tan was specifically developed for SC-CO_2. A common feature to all them is that they only take into account the regular or background behavior of systems.

2. Model development

The isothermal and isobaric diffusional flux in a binary mixture (J_d) is proportional to the chemical potential gradient, $J_d \propto \nabla\mu$, being the proportionality constant the Onsager kinetic coefficient $\tilde{\alpha}$, which is associated with the diffusion coefficient by [29-30]:

$$D_{12} = (\tilde{\alpha}/\rho)(\partial\mu/\partial x_2)_{P,T} \quad (1)$$

where ρ is the number density, P is pressure, and x_2 is solute molar fraction. Near the critical point of the mixture, $\tilde{\alpha}$ is the sum of two contributions, background and singular, respectively:

$$\tilde{\alpha} = \tilde{\alpha}^{b} + \tilde{\alpha}^{s} \quad (2)$$

which means that D_{12} can be expressed by two distinct terms that take into account the various phenomena experienced by supercritical fluids:

$$D_{12} = D_{12}^{b} + D_{12}^{s} \quad (3)$$

Here, D_{12}^{b} represents the regular behavior observed far from the critical point, and any good conventional equation can be proposed for its quantification. In this work, a Stokes-Einstein based model is adopted for this purpose. D_{12}^{s} is the singular term whose importance raises in the vicinity of the critical point; this contributions is necessary to correctly represent the anomalous asymptotic behavior of the diffusion coefficient in this region. Accordingly, D_{12}^{s} gradually vanishes as the critical point becomes more distant, and the classical or background diffusivity prevails.

2.1 Background diffusivity (D_{12}^{b})

At temperatures and pressures far away from the critical point, diffusion coefficients are generally well behaved and can be estimated as function of the density, temperature, and properties of the binary system. On the basis of the hydrodynamic theory, a relationship between D_{12}, temperature (T) and solvent viscosity (η_1) can be assumed [22, 31]:

$$D_{12} \propto \frac{T}{\eta_1} \tag{4}$$

Deviations to the Stokes-Einstein behavior are frequently observed [19, 24-25] and can be easily detected by plotting D_{12} *versus* T/η_1. The experimental diffusivities generally obey Eq. (4) in part of the T/η_1 domain as Fig. 1 illustrates, without loss of generality, for the CO_2/linoleic acid pair. Accordingly, all systems of our database should be previously scanned and graphed in T/η_1 – D_{12} coordinates, in order to identify the experimental points that follow the hydrodynamic behavior. This task allows us to split the database into two distinct sets of D_{12} values.

The expression proposed in this work for the background contribution of the diffusion model is the following:

$$D_{12}^{b} = A\left(\frac{T}{\eta_1}\right)^{\alpha} \frac{1}{\left(M_2 V_{\mathrm{bp},2}\right)^{\beta}} \tag{5}$$

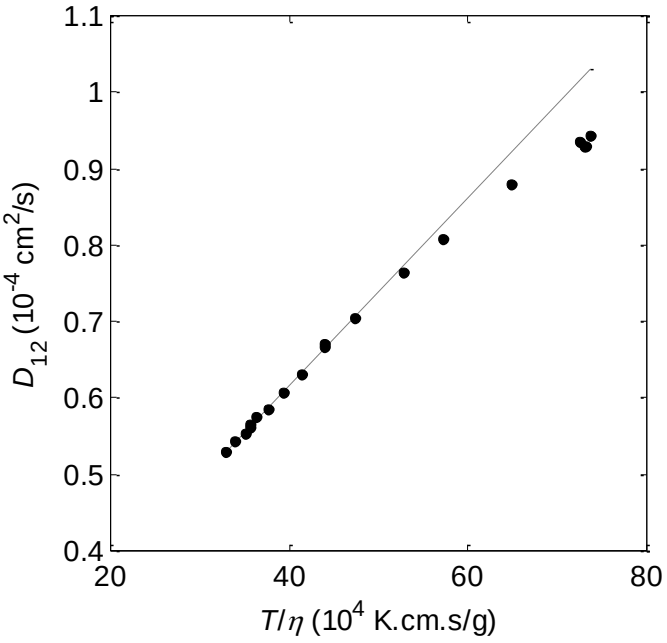

Fig. 1. Diffusion coefficient of linoleic acid in carbon dioxide plotted in Stokes-Einstein coordinates. Data from [32].

where M_2 is the solute molecular weight, $V_{bp,2}$ is the solute molar volume at normal boiling point, and A, α and β are universal constants to be fitted to the group of data that follows hydrodynamic behavior. (As it is shown in section 2.3, only α and β are necessary in the final model).

2.2 Singular diffusivity (D_{12}^s)

The singular component is required to enhance D_{12} accuracy near the critical point. This contribution may be obtained from a modification to the Stokes-Einstein equation [29], starting from the expression of Ferrell [33] for the binary diffusion coefficient:

$$D^s = \frac{\langle G(r)F(r)\rangle}{3\langle G(r)\rangle} \tag{6}$$

where $F(r) = k_B T/(2\pi\eta r)$ is the integrated velocity correlation function, and $G(r) = (b/r)\exp(-r/\xi)$ is the number density correlation function, both written for spherical particles. Here, $k_B = 1.38065\times10^{-16}\,\mathrm{erg\,K^{-1}}$ is the Boltzmann's constant, η is the mixture viscosity, $r = \left|\bar{r}_2 - \bar{r}_1\right|$ is the average interparticle distance, b is a quantity with dimension length^{-5}, and ξ is the correlation length. The integration of Eq. (6) is accomplished from the binary diameter, σ_{12}, to infinity to yield:

$$D^s = \frac{k_B T}{6\pi\eta\sigma_{12}(1+\xi/\sigma_{12})} \tag{7}$$

(Readers may consult this derivation in Supplementary data). The binary diameter is computed in terms of the individual diameters, σ_i, by the well-known combining rule of Lorentz-Berthelot. In this work, σ_i is estimated as function of the critical volume of component i, , by a relation obtained from experimental viscosity data for the Lennard-Jones fluid [31].

Hence:

$$\sigma_{12} = \frac{\sigma_1 + \sigma_2}{2} \tag{8}$$

$$\sigma_{\mathrm{LJ,i}}(\mathrm{cm}) = 0.7889\times10^{-8}\left[V_{\mathrm{c,i}}\left(\mathrm{cm}^3/\mathrm{mol}\right)\right]^{1/3} \tag{9}$$

The infinite dilution coefficient, D_{12}^{s}, corresponds to limit of Eq. (7) when $x_2 \to 0$. In this case, the solution viscosity, η, equals that of the pure solvent, η_1.

$$D_{12}^{s} = \frac{k_{\mathrm{B}}T}{6\pi\eta_1\sigma_{12}\left(1+\sigma_{12}^{-1}\lim\limits_{x_2\to0}\xi\right)} \tag{10}$$

To develop the correlation length ξ, one may use the total correlation function integral (H_{ij}) expressed as function of the number density correlation function (G_{ij}) [29, 34]:

$$H_{\mathrm{ij}} = \rho_{\mathrm{i}}^{-1}\left[\rho_{\mathrm{j}}^{-1}\int G_{\mathrm{ij}}(r)4\pi r^2 dr - \delta_{\mathrm{ij}}\right] = \rho_{\mathrm{i}}^{-1}\left[\rho_{\mathrm{j}}^{-1}4\pi b_{\mathrm{ij}}\xi_{\mathrm{ij}}^2 - \delta_{\mathrm{ij}}\right] \tag{11}$$

where δ_{ij} is the Kronecker delta. The quantity $\Delta H \equiv \left(H_{11} + H_{22} - 2H_{12}\right)$ should be now introduced:

$$\Delta H = \rho_1^{-2}4\pi b_{11}\xi_{11}^2 - \rho_1^{-1} + \rho_2^{-2}4\pi b_{22}\xi_{22}^2 - \rho_2^{-1} - \rho_1^{-1}\rho_2^{-1}8\pi b_{12}\xi_{12}^2 \tag{12}$$

Similarly to Cussler [35] and Liu and Ruckenstein [29], one writes:

$$\begin{aligned} 4\pi\rho^{-2}b\xi^2 - \rho^{-1} = \frac{1}{2}\big(&4\pi\rho_1^{-2}b_{11}\xi_{11}^2 - \rho_1^{-1} + 4\pi\rho_2^{-2}b_{22}\xi_{22}^2 - \rho_2^{-1} \\ &- 8\pi\rho_1^{-1}\rho_2^{-1}b_{12}\xi_{12}^2\big) \end{aligned} \tag{13}$$

which simplifies Eq. (12) to:

$$\frac{1}{2}\Delta H = 4\pi\rho^{-2}b\xi^2 - \rho^{-1} \Leftrightarrow \xi = \left[\frac{\rho}{4\pi b}\left(1+\frac{1}{2}\rho\Delta H\right)\right]^{1/2} \tag{14}$$

On the other hand, ΔH is related to the solute fugacity coefficient (ϕ_2) by [34]:

$$\left(\frac{\partial \ln \phi_2}{\partial x_2}\right)_{P,T} = -\frac{x_1 \rho \Delta H}{1 + x_1 x_2 \rho \Delta H} \tag{15}$$

whose limit can be calculated and identified as thermodynamic factor Γ_{12}^{∞}:

$$\Gamma_{12}^{\infty} \equiv \lim_{x_2 \to 0}\left(\frac{\partial \ln \phi_2}{\partial x_2}\right)_{P,T} = -\lim_{x_2 \to 0} \rho \Delta H \tag{16}$$

The correlation length at infinite dilution, $\lim_{x_2 \to 0} \xi$, necessary in Eq. (10) is then obtained from Eqs. (14) and (16):

$$\lim_{x_2 \to 0} \xi = \left[\frac{\rho_1}{4\pi b}\left(1 - \frac{1}{2}\Gamma_{12}^{\infty}\right)\right]^{1/2} \tag{17}$$

The resulting expression for the singular contribution of tracer diffusivities arises after substitution of Eq. (17) into Eq. (10):

$$D_{12}^{\ s} = \frac{k_B T}{6\pi \eta_1 \sigma_{12}}\left[\frac{1}{1 + \theta\left(1 - \frac{1}{2}\Gamma_{12}^{\infty}\right)^{1/2}}\right] \tag{18}$$

where $\theta = \sigma_{12}^{-1}\sqrt{\rho_1 / 4\pi b}$ is a dimensionless quantity. In this work, the best result is obtained when θ is taken as constant.

2.3 Final D_{12} model

Taking into account Eq. (3), the complete expression for tracer diffusion coefficients arises by summing the contributions given by Eqs. (5) and (18):

$$D_{12} = D_{12}^{b} + D_{12}^{s} = A\left(\frac{T}{\eta_1}\right)^{\alpha} \frac{1}{\left(M_2 V_{bp,2}\right)^{\beta}} + \frac{k_B T}{6\pi \eta_1 \sigma_{12}}\left[\frac{1}{1 + \theta\left(1 - \frac{1}{2}\Gamma_{12}^{\infty}\right)^{1/2}}\right] \tag{19}$$

This model contains four universal parameters: α and β are firstly fitted to background data (as explained in section 2.1), and A and θ are then optimized using the whole database. At this stage, it is only necessary to compute Γ_{12}^{∞}, which is the next and last step of our derivation.

2.4 Thermodynamic factor (Γ_{12}^{∞})

The thermodynamic factor at infinite dilution, Γ_{12}^{∞}, can be calculated using an equation of state (EoS) and its definition (see Eq. (16)). In this work, the well known Peng-Robinson [36] EoS is adopted, since it furnishes an analytical and explicit expression for Γ_{12}^{∞}, that is also able to provide accurate results for D_{12}. The set of equations are compiled in Table 1.

The binary interaction parameter (k_{12}) embodied in Γ_{12}^{∞} (see Eq. (27) in Table 1) may be obtained from phase equilibrium data, but the published values are scarce. Fortunately, the diffusivities are not very sensitive to k_{12}, and the following weak dependence of k_{12} upon the acentric factor of the solute, ω_2, is able to achieve good results:

$$k_{12} = 0.065 + 0.129\omega_2 \tag{20}$$

3. Database and properties of pure substances

The new model is validated with an extensive database of experimental tracer diffusivities in SC-CO_2 comprising 149 systems and 4469 data points. The detailed description of the systems is provided in Table S.1 (Supplementary data): number of data points, reduced ranges of temperature, pressure and solvent density, and data sources. Data available exclusively in graphical form is not included in the calculations.

In Table S.2 (Supplementary data) the properties of all molecules involved in the calculations are listed, namely, name, molecular formula, CAS number, molecular weight, critical constants, acentric factor, and molar volume at normal boiling point. The densities of SC-CO_2 (solvent) are calculated by the correlation of Pitzer and Schreiber [37] whenever they are not provided in the original papers. The correlation of Altunin and Sakhabetdinov [38] is used to compute absent SC-CO_2 viscosities, and Tyn-Calus equation [31, 39] is employed for the estimation of solute molar volumes at normal boiling point. The unknown critical constants are estimated by Joback [31, 40-41], Somayajulu [42], Klincewicz [31, 43], Ambrose [31, 44-45], Wen–Qiang [46], and Constantinou–Gani [47] methods. Nonexistent acentric factors are obtained by Lee-Kesler method [48].

Table 1. Calculation of the thermodynamic factor (Γ_{12}^{∞}) necessary in the proposed D_{12} model (Eq. (19)). The analytical expressions were derived using the Peng-Robinson equation of state.

Equation	No.
$\Gamma_{12}^{\infty} = \left[\frac{1}{Z_1 - B_1} - \frac{B_2(Z_1 - 1)}{B_1^2}\right]B_x + \left(\frac{B_2}{B_1} - \frac{1}{Z_1 - B_1}\right)Z_x + \frac{A_1 F_{12} E_x}{2\sqrt{2}B_1} + \frac{A_1 E_1 F_x}{2\sqrt{2}B_1} + \frac{F_{12} E_1}{2\sqrt{2}B_1^2}(B_1 A_x - A_1 B_x)$	(21)
$m_{\mathrm{i}}(T) = \left[1 + (0.37464 + 1.54226\omega_i - 0.26992\omega_i^2)\left(1 - \sqrt{T_{\mathrm{r,i}}}\right)\right]^2$, **(i = 1,2)**	(22)
$A_{\mathrm{i}} = 0.45724 m_{\mathrm{i}}(T) P_{\mathrm{r,i}} / T_{\mathrm{r,i}}^2$, **(i = 1,2)**	(23)
$B_{\mathrm{i}} = 0.0778 P_{\mathrm{r,i}} / T_{\mathrm{r,i}}$, **(i = 1,2)**	(24)
$f(Z_1) = Z_1^3 - (1 - B_1)Z_1^2 + (A_1 - 2B_1 - 3B_1^2)Z_1 - (A_1 B_1 - B_1^2 - B_1^3) = 0$	(25)
$E_1 = \ln\left[\frac{Z_1 + (\sqrt{2} + 1)B_1}{Z_1 - (\sqrt{2} - 1)B_1}\right]$	(26)
$A_{12} = (1 - k_{12})\sqrt{A_1 A_2}$ (k_{12} is estimated by Eq.(20))	(27)
$F_{12} = \frac{B_2}{B_1} - \frac{2A_{12}}{A_1}$	(28)
$A_{\mathrm{x}} = 2(A_{12} - A_1)$	(29)
$B_{\mathrm{x}} = B_2 - B_1$	(30)
$Z_x = -\frac{B_x(Z_1^2 - 6B_1 Z_1 - 2Z_1 - A_1 + 2B_1 + 3B_1^2) + A_x(Z_1 - B_1)}{3Z_1^2 - 2(1 - B_1)Z_1 + A_1 - 3B_1^2 - 2B_1}$	(31)
$E_{\mathrm{x}} = \frac{Z_x + (\sqrt{2} + 1)B_x}{Z_1 + (\sqrt{2} + 1)B_1} - \frac{Z_x - (\sqrt{2} - 1)B_x}{Z_1 - (\sqrt{2} - 1)B_1}$	(32)
$F_x = -\frac{B_2 B_x}{B_1^2} - \frac{2(A_2 - A_{12})}{A_1} + \frac{2A_{12}A_x}{A_1^2}$	(33)

4. Results and discussion

In this section, the proposed model is analyzed and validated using common performance indicators like the average absolute relative deviation (AARD) and the average relative deviation (ARD):

$$\text{AARD}\,(\%) = \frac{100}{\text{NDP}} \sum_{i=1}^{\text{NDP}} \left| \frac{D_{12}^{\text{calc}} - D_{12}^{\text{exp}}}{D_{12}^{\text{exp}}} \right|_i \tag{34}$$

$$\text{ARD}\,(\%) = \frac{100}{\text{NDP}} \sum_{i=1}^{\text{NDP}} \left(\frac{D_{12}^{\text{calc}} - D_{12}^{\text{exp}}}{D_{12}^{\text{exp}}} \right)_i \tag{35}$$

The superscripts ‘exp’ and ‘calc’ denote experimental and calculated tracer diffusivities, and NDP is the number of data points. The AARD is also taken as objective function for the optimization of the model parameters; the ARD is adopted to check if the model provides biased results since its expected value should vanish.

As mentioned in section 2.1, the parameters α and β are firstly fitted exclusively to background diffusivity data (the equations implied in calculations are Eqs. (5) and (34)). Then, α and β are fixed, and A and θ are obtained from the entire database by minimizing Eq. (34) with Eq. (19). The numerical method utilized is the Nelder-Mead algorithm. Following this methodology, the universal values found for α, β, A and θ are compiled in Table 2.

Table 3 shows the detailed results obtained with the new model – Eq. (19) – and with six predictive hydrodynamic expressions from the literature (see Supplementary data): Wilke-Chang (Eq. (S.1)), Scheibel (Eq. (S.2)), Lusis-Ratcliff (Eq. (S.3)), Lai-Tan (Eq. (S.4)), Tyn-Calus (Eq. (S.6)) and Reddy-Doraiswamy (Eq. (S.7)). These comparative equations do not demand system-specific parameters, but only take account of the regular or background behavior of mixtures. In addition to the individual errors for each system, global results are also compiled in Table 4.

Table 2. Universal parameters of the D_{12} model proposed in this work, when variables are expressed in cgs system.

New model	α	β	A	θ
Eq. (19)	0.8140	0.2530	$3.247\text{x}10^{-7}$	8.570

Table 3. Average absolute relative deviations (AARD) achieved with the new model and other predictive expressions adopted for comparison.

ID	Solute	Data Sources	NDP	New model	Wilke-Chang	Scheibel	Lusis-Ratcliff	Lai-Tan	Tyn-Calus	Reddy-Doraiswamy
				Eq. (19)	Eq. (S.1)	Eq. (S.2)	Eq. (S.3)	Eq. (S.4)	Eq. (S.6)	Eq. (S.7)
1	Acetone	[49-53]	214	3.65	5.64	20.60	12.90	30.96	5.23	38.55
2	Acridine	[54]	6	3.94	4.93	10.72	20.98	6.75	12.06	72.93
3	Allylbenzene	[55]	15	5.30	5.36	11.96	17.71	13.65	8.42	62.71
4	Anisole	[56]	15	6.87	7.33	20.82	22.66	12.72	11.77	64.09
5	Anthracene	[57]	22	8.96	10.38	1.72	9.98	19.22	2.86	57.43
6	Arachidonic acid (AA)	[32]	75	2.78	9.70	7.12	25.84	1.36	16.13	92.80
7	AA ethyl ester	[58]	48	5.63	15.17	0.94	19.77	8.19	10.26	84.76
8	Behenic acid ethyl ester	[59]	17	7.80	21.34	6.43	14.66	8.44	5.03	78.86
9	Benzene	[49, 60-67]	249	8.45	8.76	13.36	11.14	29.60	8.86	40.30
10	Benzoic acid	[54, 68-70]	35	6.40	10.18	22.93	25.05	13.72	14.17	67.59
11	Benzyl acetate	[71]	15	8.78	7.79	20.20	27.69	5.23	17.75	78.14
12	Benzylacetone	[72]	15	11.31	6.19	18.07	27.48	4.10	17.90	80.40
13	Biphenyl	[70, 73]	83	7.04	7.90	7.23	13.91	21.25	7.78	61.05
14	2-Bromoanisole	[55]	15	4.90	16.52	30.64	35.12	2.79	23.81	83.97
15	Bromobenzene	[74-75]	21	6.71	6.32	17.84	18.87	15.82	8.36	58.02
16	2-Butanone	[50, 75-76]	40	2.64	5.13	10.49	7.91	27.64	5.14	38.79
17	*n*-Butylbenzene	[77]	15	2.52	6.29	5.62	13.93	14.19	5.39	61.07
18	*sec*-Butylbenzene	[78]	15	4.31	5.26	7.66	16.02	12.64	7.41	64.03
19	*tert*-Butylbenzene	[79]	15	3.81	7.92	3.51	10.83	16.01	3.34	56.49
20	Butyric acid ethyl ester	[80-81]	16	4.02	4.31	7.13	11.80	22.28	2.96	53.47
21	Caffeine	[23, 82-83]	25	8.59	19.34	32.43	42.21	7.19	31.71	100.59
22	Capric acid ethyl ester	[80-81]	16	5.41	13.46	2.46	11.25	15.88	3.77	64.43

Table 3. (continued)

ID	Solute	Data Sources	NDP	New model	Wilke-Chang	Scheibel	Lusis-Ratcliff	Lai-Tan	Tyn-Calus	Reddy-Doraiswamy
				Eq. (19)	Eq. (S.1)	Eq. (S.2)	Eq. (S.3)	Eq. (S.4)	Eq. (S.6)	Eq. (S.7)
23	Caprylic acid ethyl ester	[80-81]	16	4.44	10.23	1.73	12.15	16.96	4.14	62.85
24	β-Carotene	[84-86]	90	4.44	14.88	5.82	33.25	14.41	20.36	112.10
25	L-Carvone	[87-88]	27	5.78	3.66	12.01	21.08	8.51	12.00	71.52
26	Chlorobenzene	[74-75]	21	2.98	5.80	18.41	18.45	16.66	7.43	56.16
27	Chrysene	[49]	4	10.02	16.16	5.59	6.63	14.41	2.80	56.60
28	Citral	[89]	15	4.61	8.63	3.45	13.20	19.14	5.29	63.44
29	Cobalt(III) acetylacetonate	[90]	38	1.35	11.53	25.24	40.06	7.03	29.97	104.07
30	Copper(II) trifluoroacetylacetonate	[91]	12	8.53	37.09	53.26	62.37	13.23	49.65	125.98
31	Dibenzo-24-crown-8	[92]	28	3.26	12.73	2.71	22.77	6.83	13.08	89.14
32	15-Crown-5	[92]	29	7.99	7.85	11.20	21.59	15.69	12.64	74.02
33	Cycloheptanone	[93]	8	11.54	24.01	40.45	39.72	10.28	26.38	83.17
34	Cyclononanone	[93]	8	9.35	17.62	31.85	36.52	8.50	25.13	86.08
35	Cyclopentanone	[93]	8	10.57	20.31	37.55	33.53	16.66	19.56	70.71
36	Dibenzyl ether	[71]	15	9.65	5.32	17.22	30.14	2.17	20.72	88.51
37	1,2-Dichlorobenzene	[79]	15	2.01	6.89	19.05	22.17	12.08	11.69	65.12
38	1,3-Dichlorobenzene	[88]	4	5.65	11.52	25.33	28.09	7.23	16.96	72.45
39	*p*-Dichlorobenzene	[70]	13	3.60	10.61	24.31	27.05	12.36	16.00	71.04
40	Diethyl ether	[75-76, 94]	17	5.39	10.54	23.28	21.37	29.99	10.96	57.44
41	1,2-Diethylbenzene	[74]	15	3.14	6.19	6.09	14.44	13.70	6.01	62.00
42	1,4-Diethylbenzene	[74]	15	3.68	5.65	6.97	15.36	13.09	6.72	63.10
43	Diisopropyl ether	[94]	15	9.03	7.14	9.42	12.53	32.81	6.46	52.65
44	2,3-Dimethylaniline	[95]	15	18.97	16.04	29.92	35.59	1.90	24.54	86.16
45	2,6-Dimethylaniline	[95]	15	14.26	11.47	24.80	30.25	5.11	19.64	78.84
46	1,1′-Dimethylferrocene	[96]	68	3.66	12.16	25.53	31.02	11.68	20.35	79.91

Table 3. (continued)

ID	Solute	Data Sources	NDP	New model	Wilke-Chang	Scheibel	Lusis-Ratcliff	Lai-Tan	Tyn-Calus	Reddy-Doraiswamy
				Eq. (19)	Eq. (S.1)	Eq. (S.2)	Eq. (S.3)	Eq. (S.4)	Eq. (S.6)	Eq. (S.7)
47	2,6-Dimethylnaphthalene	[97-98]	6	3.78	7.15	8.88	17.98	12.83	9.26	67.76
48	2,7-Dimethylnaphthalene	[97-98]	6	4.43	6.91	5.64	13.01	14.77	6.00	60.69
49	2,4-Dimethylphenol	[56]	15	10.88	9.42	22.58	27.40	7.21	16.90	74.26
50	Diolein	[99]	9	8.36	23.69	5.27	22.33	1.87	9.91	95.83
51	1,3-Divinylbenzene	[55]	15	2.77	3.74	10.19	16.70	13.66	7.74	62.36
52	Docosahexaenoic acid (DHA)	[100]	63	5.29	7.28	8.29	30.05	4.79	19.86	100.02
53	DHA ethyl ester	[58-59]	65	6.70	16.73	2.00	18.88	7.81	9.26	84.14
54	DHA methyl ester	[59]	17	5.77	16.76	2.47	17.74	7.29	8.37	81.78
55	Eicosapentaenoic acid (EPA)	[100]	55	3.08	7.79	7.30	27.28	2.02	17.55	94.51
56	EPA ethyl ester	[58]	48	5.90	14.98	1.02	19.58	8.50	10.14	84.21
57	EPA methyl ester	[59]	17	5.34	17.37	3.34	16.49	8.16	7.27	79.62
58	Ethanol	[68]	24	4.16	11.29	32.94	19.52	29.83	5.39	39.86
59	Ethyl acetate	[23, 76]	16	8.53	17.59	30.81	29.24	26.40	18.48	68.26
60	Ethylbenzene	[62]	15	2.97	7.44	4.76	7.97	21.78	3.41	46.77
61	Ethyl benzoate	[72]	15	8.17	3.88	13.39	22.01	8.21	12.77	72.14
62	2-Ethyltoluene	[101]	15	2.77	8.95	4.63	9.76	18.32	4.63	53.63
63	3-Ethyltoluene	[101]	15	2.97	11.68	5.07	7.07	19.63	5.28	50.98
64	4-Ethyltoluene	[101]	15	2.26	7.46	4.86	11.41	16.79	4.10	56.37
65	Eugenol	[72]	15	15.58	17.29	31.11	39.20	5.50	28.35	94.09
66	Ferrocene	[96, 102]	107	4.36	17.43	32.55	33.28	11.90	21.04	76.62
67	2-Fluoroanisole	[55]	15	12.26	18.48	33.51	35.01	4.84	22.85	79.91
68	Fluorobenzene	[74]	15	5.73	11.04	26.57	23.76	15.90	11.16	59.41
69	3-Fluorophenol	[88]	4	13.11	13.15	27.33	29.44	6.79	17.99	73.37
70	Geraniol	[88]	4	14.40	3.34	15.70	27.33	4.37	18.04	83.12

Table 3. (continued)

ID	Solute	Data Sources	NDP	New model	Wilke-Chang	Scheibel	Lusis-Ratcliff	Lai-Tan	Tyn-Calus	Reddy-Doraiswamy
				Eq. (19)	Eq. (S.1)	Eq. (S.2)	Eq. (S.3)	Eq. (S.4)	Eq. (S.6)	Eq. (S.7)
71	Hexachlorobenzene	[103]	14	14.52	10.99	12.63	20.34	16.18	13.01	71.35
72	1-Hexadecene	[104]	11	9.56	16.17	10.73	18.73	13.62	11.89	76.80
73	1,1,1,5,5,5-Hexafluoroacetylacetone	[91]	15	6.01	18.95	33.14	39.26	4.34	27.98	91.59
74	Iodobenzene	[74-75]	20	5.98	9.02	22.52	25.22	9.49	14.34	68.58
75	Isobutylbenzene	[78]	15	3.36	4.51	7.83	15.64	13.35	6.83	62.67
76	D-Limonene	[89]	15	4.81	9.32	4.20	10.54	22.45	4.27	57.32
77	Linalool	[61]	15	4.80	7.24	4.13	13.86	19.33	5.63	63.29
78	Linoleic acid	[32]	71	3.23	9.63	7.28	25.29	2.56	15.88	90.40
79	Linoleic acid methyl ester	[105-106]	21	1.88	15.74	3.30	16.35	2.72	7.44	77.97
80	α-Linolenic acid	[100]	56	2.26	14.25	4.65	18.39	6.23	9.32	81.08
81	γ-Linolenic acid	[107]	142	2.80	7.79	8.37	26.40	2.99	16.90	92.13
82	γ-Linolenic acid ethyl ester	[107]	41	6.74	6.92	19.79	37.84	10.97	27.88	105.41
83	γ-Linolenic acid methyl ester	[105, 107]	52	8.75	13.41	4.68	19.17	15.10	10.20	82.00
84	L-Menthone	[87]	23	3.71	5.18	6.71	15.93	12.06	7.36	65.04
85	Methanol	[68]	10	3.72	16.79	46.84	23.92	35.33	7.10	33.18
86	2-Methylanisole	[95]	15	9.59	9.67	23.02	26.90	8.23	16.19	72.34
87	4-Methylanisole	[95]	15	17.47	17.52	31.83	35.98	2.74	24.50	84.67
88	3-Methylbutylbenzene	[78]	15	3.53	5.75	6.66	16.37	11.36	7.77	66.13
89	1-Methylnaphthalene	[104]	11	15.45	20.35	32.73	41.75	6.26	30.86	98.69
90	Monoolein	[99]	11	2.02	8.71	7.31	29.20	1.34	18.91	99.51
91	Myristic acid ethyl ester	[80-81]	16	6.14	15.97	3.60	13.35	11.84	4.92	71.66
92	Myristoleic acid	[108]	42	5.62	5.68	14.76	32.51	5.61	22.90	98.00
93	Myristoleic acid methyl ester	[108-109]	81	11.42	10.43	12.73	28.83	21.02	19.53	93.69

Table 3. (continued)

ID	Solute	Data Sources	NDP	New model	Wilke-Chang	Scheibel	Lusis-Ratcliff	Lai-Tan	Tyn-Calus	Reddy-Doraiswamy
				Eq. (19)	Eq. (S.1)	Eq. (S.2)	Eq. (S.3)	Eq. (S.4)	Eq. (S.6)	Eq. (S.7)
94	Naphthalene	[49, 83, 97, 102, 110]	114	9.68	10.84	10.78	13.40	23.69	10.19	53.54
95	1-Naphthol	[57]	11	13.26	5.77	5.67	9.17	26.32	0.39	48.49
96	2-Naphthol	[57]	16	18.59	7.84	5.02	7.67	32.29	2.46	45.23
97	2-Nitroanisole	[79]	15	9.61	11.47	24.69	31.20	3.27	20.75	81.49
98	Nitrobenzene	[56, 75]	23	5.47	8.19	21.46	24.02	10.85	13.21	66.82
99	3-Nitrotoluene	[95]	15	2.71	4.00	11.30	17.91	12.31	8.67	64.10
100	Oleic acid	[99]	19	3.97	10.03	7.86	26.11	1.15	16.61	91.81
101	Oleic acid ethyl ester	[99]	5	4.43	5.72	16.67	38.56	8.80	27.68	113.18
102	Oleic acid methyl ester	[99, 105, 111]	21	3.56	7.29	17.35	39.80	8.95	29.00	114.27
103	Palladium(II) acetylacetonate	[90]	125	3.42	21.93	36.33	44.15	4.14	32.80	100.26
104	Palmitic acid ethyl ester	[112]	17	4.31	15.14	1.75	16.97	8.66	8.02	78.79
105	2-Pentanone	[50]	23	2.21	4.45	13.04	12.64	25.29	4.27	47.94
106	3-Pentanone	[50, 93]	46	4.89	8.28	5.03	5.82	27.52	5.83	40.41
107	*n*-Pentylbenzene	[77]	31	2.87	8.38	4.21	13.44	14.17	5.24	62.41
108	Phenanthrene	[49, 54, 103]	25	13.59	15.48	8.71	7.79	23.27	8.170	48.50
109	Phenol	[23, 52, 68, 85-86]	109	6.24	21.20	39.93	33.07	15.59	17.97	66.34
110	Phenylacetic acid	[113]	16	3.34	4.25	16.60	22.72	14.03	12.95	69.79
111	Phenylacetylene	[74]	15	8.54	7.80	21.03	22.91	12.92	12.00	64.46
112	Phenylbutazone	[114]	78	5.19	8.18	7.66	25.06	6.47	15.80	89.10
113	1-Phenyldodecane	[77]	15	11.22	6.96	7.99	27.70	5.15	18.09	94.23
114	1-Phenylethanol	[115]	15	11.70	10.32	23.57	28.54	6.65	17.97	75.96

Table 3. (continued)

ID	Solute	Data Sources	NDP	New model	Wilke-Chang	Scheibel	Lusis-Ratcliff	Lai-Tan	Tyn-Calus	Reddy-Doraiswamy
				Eq. (19)	Eq. (S.1)	Eq. (S.2)	Eq. (S.3)	Eq. (S.4)	Eq. (S.6)	Eq. (S.7)
115	2-Phenylethanol	[115]	15	12.85	12.10	25.60	30.39	5.50	19.59	78.14
116	2-Phenylethyl acetate	[71]	15	13.49	8.63	21.45	32.02	1.88	22.22	87.91
117	1-Phenylhexane	[77]	15	3.65	7.53	5.06	16.20	9.85	7.80	68.62
118	Phenylmethanol	[115]	15	12.11	13.91	28.26	30.10	7.95	18.50	73.87
119	1-Phenyloctane	[77]	15	3.18	8.65	3.91	16.88	7.84	8.49	72.00
120	3-Phenylpropyl acetate	[71]	15	12.65	7.12	18.93	31.18	2.20	21.63	89.00
121	α-Pinene	[116]	15	5.88	7.00	4.68	12.54	21.26	4.66	59.39
122	β-Pinene	[116]	15	8.47	11.72	4.09	7.30	25.50	4.07	51.21
123	2-Phenyl-1-propanol	[115]	15	13.06	9.72	22.66	30.05	3.89	19.88	81.11
124	3-Phenyl-1-propanol	[115]	15	10.36	6.21	18.65	26.32	6.11	16.54	76.57
125	1-Propanol	[68]	17	7.02	15.43	33.81	26.25	26.22	11.60	56.46
126	2-Propanol	[68]	18	3.15	9.57	26.96	19.89	29.22	6.96	48.70
127	*i*-Propylbenzene	[49, 62, 76, 117]	36	3.67	8.75	4.40	8.16	20.69	3.87	49.89
128	*n*-Propylbenzene	[60, 62, 76]	60	6.18	11.89	13.39	17.52	19.99	12.48	62.63
129	Pyrene	[49, 57]	21	6.18	9.75	3.86	13.38	13.82	6.51	64.89
130	Squalene	[118]	5	6.63	13.56	3.78	20.60	5.78	11.21	85.24
131	Stearic acid ethyl ester	[59]	17	7.72	24.40	10.18	9.95	12.01	1.101	71.39
132	Styrene	[119]	15	6.84	5.38	17.70	20.35	14.10	9.91	62.10
133	Tetrahydrofuran	[94]	15	5.68	15.96	34.15	27.07	31.18	12.43	58.17
134	Thenoyltrifluoroacetone	[91]	15	15.17	30.20	45.60	53.55	10.02	41.38	112.83
135	α-Tocopherol	[84-86]	82	15.14	31.55	16.48	4.98	11.95	5.63	65.05
136	Toluene	[23, 62, 66]	35	3.37	5.32	11.33	11.85	25.09	5.02	48.08
137	Triarachidonin	[120]	27	6.88	17.49	8.39	34.89	16.12	20.63	116.86
138	Trierucin	[120]	101	5.10	13.57	14.68	48.33	23.17	31.19	140.57

Table 3. (continued)

ID	Solute	Data Sources	NDP	New model	Wilke-Chang	Scheibel	Lusis-Ratcliff	Lai-Tan	Tyn-Calus	Reddy-Doraiswamy
				Eq. (19)	Eq. (S.1)	Eq. (S.2)	Eq. (S.3)	Eq. (S.4)	Eq. (S.6)	Eq. (S.7)
139	Trifluoroacetylacetone	[91]	15	4.54	3.74	15.88	19.21	16.91	9.06	61.49
140	1,3,5-Trimethylbenzene	[49, 60, 75, 119]	34	5.47	6.27	11.68	17.99	14.38	9.16	63.79
141	Trinervonin	[120]	38	4.69	16.62	12.12	45.38	23.26	27.91	136.63
142	Triolein	[69, 120]	14	12.34	29.49	9.31	23.02	3.61	11.34	100.25
143	Ubiquinone CoQ10	[86, 121]	80	4.22	13.90	8.60	37.98	17.50	23.98	120.86
144	Vanillin	[113]	15	7.25	12.64	26.02	32.26	7.43	21.65	82.53
145	Vitamin K_1	[92, 109]	17	13.44	27.24	11.90	9.52	8.88	4.02	72.52
146	Vitamin K_3	[86, 106, 109]	22	6.45	9.59	6.78	12.86	17.84	7.18	61.01
147	*m*-Xylene	[104]	12	12.04	17.73	30.75	35.11	16.35	23.95	83.81
148	5-*tert*-Butyl-*m*-xylene	[74]	31	2.60	8.49	3.61	14.06	12.86	5.78	64.71
149	*p*-Xylene	[75-76]	7	4.71	6.55	5.30	8.40	22.47	4.12	47.65

Table 4. Calculated deviations for the proposed model and for the equations adopted for comparison.

Deviation*	New Model	Wilke-Chang	Scheibel	Lusis-Ratcliff	Lai-Tan	Tyn-Calus	Reddy-Doraiswamy
	Eq. (19)	Eq. (S.1)	Eq. (S.2)	Eq. (S.3)	Eq. (S.4)	Eq. (S.6)	Eq. (S.7)
AARD (%)	6.20	11.62	14.76	23.07	14.72	14.12	75.17
$AARD_{max}$ (%)	18.97	37.09	53.26	62.37	35.33	49.65	140.57
$AARD_{min}$ (%)	1.35	3.34	0.94	4.98	1.15	0.39	33.18
Δ(AARD) (%)	17.62	33.75	52.32	57.39	34.18	49.27	107.39
ARD (%)	-0.69	-1.75	12.81	22.87	-10.95	12.16	75.17
$AARD_{polar}$ (%)	6.19	12.36	16.17	25.69	12.85	15.75	81.00
$AARD_{non\text{-}polar}$ (%)	6.22	10.16	11.93	17.74	18.54	10.82	63.32

*AARD = global AARD, $AARD_{max}$ = maximum AARD, $AARD_{min}$ = minimum AARD, $\Delta(AARD) = AARD_{max} - AARD_{min}$, ARD = global ARD, $AARD_{polar}$ = AARD for polar solutes, and $AARD_{non\text{-}polar}$ = AARD for non-polar solutes.

The new model achieves global AARD of only 6.20%, maximum deviation of 18.97% (CO_2/2,3-dimethylaniline) and minimum deviation of 1.35% (CO_2/cobalt(III)acetylacetonate) (see Tables 3 and 4). Considering that the experimental uncertainty is usually around 6% [22], the agreement between predicted and measured values is very good. On the contrary, the overall AARDs of the remaining equations range from 11.62% (Wilke-Chang) to 75.17% (Reddy-Doraiswamy). Furthermore, the amplitude of the AARD values achieved by the new model is only 17.62%, against spreads of 33.75%, 52.32%, 57.39%, 34.18%, 49.27% and 107.39% offered by the selected hydrodynamic equations. In terms of relative deviations, the new model and the Wilke-Chang expression provide the smaller values (-0.69% and -1.75%), while the others exhibit biased behaviors in view of the fact the computed ARDs are very different from zero (12.81%, 22.87%, -10.95%, 12.16% and 75.17%).

The failure of these Stokes-Einstein-based equations is especially noticeable in regions of low CO_2 density (viscosity), where compressibility is large and clustering is enhanced, which justifies the significant deviations usually found in SCFs [22, 24-26, 94]. This is evident from the nonlinear plots and nonzero intercepts observed in $T/\eta_1 - D_{12}$ coordinates, as Fig. 1 shows. Our model solves these limitations since takes such effects into account by including the singular contribution into the diffusivity (Eq. (19)). In a different work, Liu and Ruckenstein [29] also considered singular and regular terms in SC-CO_2 diffusivities, but some weaknesses may be raised: the database utilized by them is quite small (30 systems/598 points against 149 systems/4469 points of this work); data is essentially located in the vicinity of the critical point; the model parameters of their two contributions were simultaneously optimized and thus the background parcel may be not able to represent accurately the regular diffusion behavior of the systems.

Another relevant feature analyzed in detail is the influence of solute polarity upon D_{12} model performance. Accordingly, the database is divided into polar and non-polar solutes, and the corresponding average deviations are computed. It is clear from Table 4 that the proposed model behaves equally well in both cases (AARDs = 6.19% and 6.22%, respectively) while the remaining equations achieve very distinct errors: Wilke-Chang, 12.36% and 10.16%; Scheibel,

16.17% and 11.93%, Lusis-Ratcliff, 25.69% and 17.74%, Lai-Tan, 12.85% and 18.54%, Tyn-Calus, 15.75% and 10.82%, and Reddy-Doraiswamy, 81.00% and 63.32%.

With respect to the accuracy of the diffusivity equations as function of pressure and temperature, Fig. 2 highlights once again the good results accomplished by the new model in comparison to the hydrodynamic expressions from literature. The AARDs calculated for four regions of the $T_r - P_r$ plane, with boundary values T_r = 1.1 and P_r = 3.0, demonstrate that the new model provides the lowest errors in all sectors (3.98% – 9.63%) while the others range from 9.77% – 12.09% (lowest variation) to 64.77% – 93.83% (highest variation).

In the whole, the calculated results emphasize that the proposed model predicts very consistent and reliable tracer diffusivities, taking into account the small AARD, ARD and Δ(AARD) found for the large database compiled for its validation (149 systems and 4469 data points), as well as the similar errors found for polar and non-polar solutes, and over all $T_r - P_r$ plane.

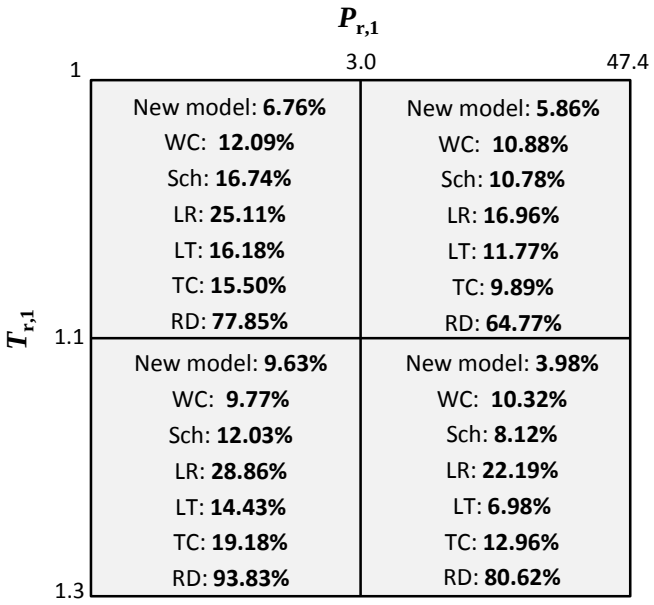

Fig. 2. Calculated deviations for this work, Wilke-Chang (WC), Scheibel (Sch), Lusis-Ratcliff (LR), Lai-Tan (LT), Tyn-Calus (TC) and Reddy-Doraiswamy (RD) for different reduced pressure (P_r) and temperature (T_r) regions.

In Fig. 3 the calculated diffusivities and relative deviations are plotted against the experimental data for: the new model, the Wilke-Chang equation (best comparative expression), and the Lai-Tan equation (specific for SC-CO_2). Such graphs reinforce the accurate estimations accomplished by the proposed model as the unbiased plots along diagonal (in the case of $D_{12}^{\text{exp}} - D_{12}^{\text{calc}}$) and around zero (in the case of $D_{12}^{\text{exp}} - \text{ARD}$) point out. Fig. 3d detaches the relevant scattering associated to the Wilke-Chang model, notwithstanding the small ARD obtained (-1.63%). Figs. 3e and 3f highlight that the Lai-Tan model systematically underestimates the tracer diffusivities at high values, which is equivalent to say at increasing temperatures and/or decreasing pressures. According to the relative deviations listed in Table 4, it is possible to conclude that the Scheibel, Lusis-Ratcliff, Tyn-Calus and mainly Reddy-Doraiswamy equations overpredict D_{12}.

To better illustrate the agreement between the new model and experimental data, several isotherms are graphed in Fig. 4; the Wilke-Chang and Lai-Tan diffusivities are also plotted for comparison. Four systems are selected: CO_2/cobalt(III)acetylacetonate, CO_2/1,2-dichlorobenzene, CO_2/4-ethyltoluene, and CO_2/α-linoleic acid. From this figure it is possible to observe that the proposed model generally follows data accurately, while Wilke-Chang and Lai-Tan predictions are systematically deviating from experimental trends, which is consistent with the numerical results listed in Tables 3 and 4. It is worth noting that our model is trustworthy even near the critical point (smaller pressures at the lowest temperatures in Figs. 4a and 4d).

5. Conclusions

In this work a new model to predict tracer diffusion coefficients in supercritical carbon dioxide is proposed and validated. It comprehends a background contribution to describe the diffusive phenomenon far from the critical point, and a singular contribution to interpret the asymptotic behavior in its vicinity. The validation of the model is accomplished against several predictive hydrodynamic expressions from literature, using a large database of 149 solutes in carbon dioxide (4469 data points totally). The average error obtained is only 6.20%, while the

comparison expressions (Wilke-Chang, Scheibel, Lusis-Ratcliff, Lai-Tan, Tyn-Calus and Reddy-Doraiswamy) achieve errors between 11.62% and 75.17%. Furthermore, our model

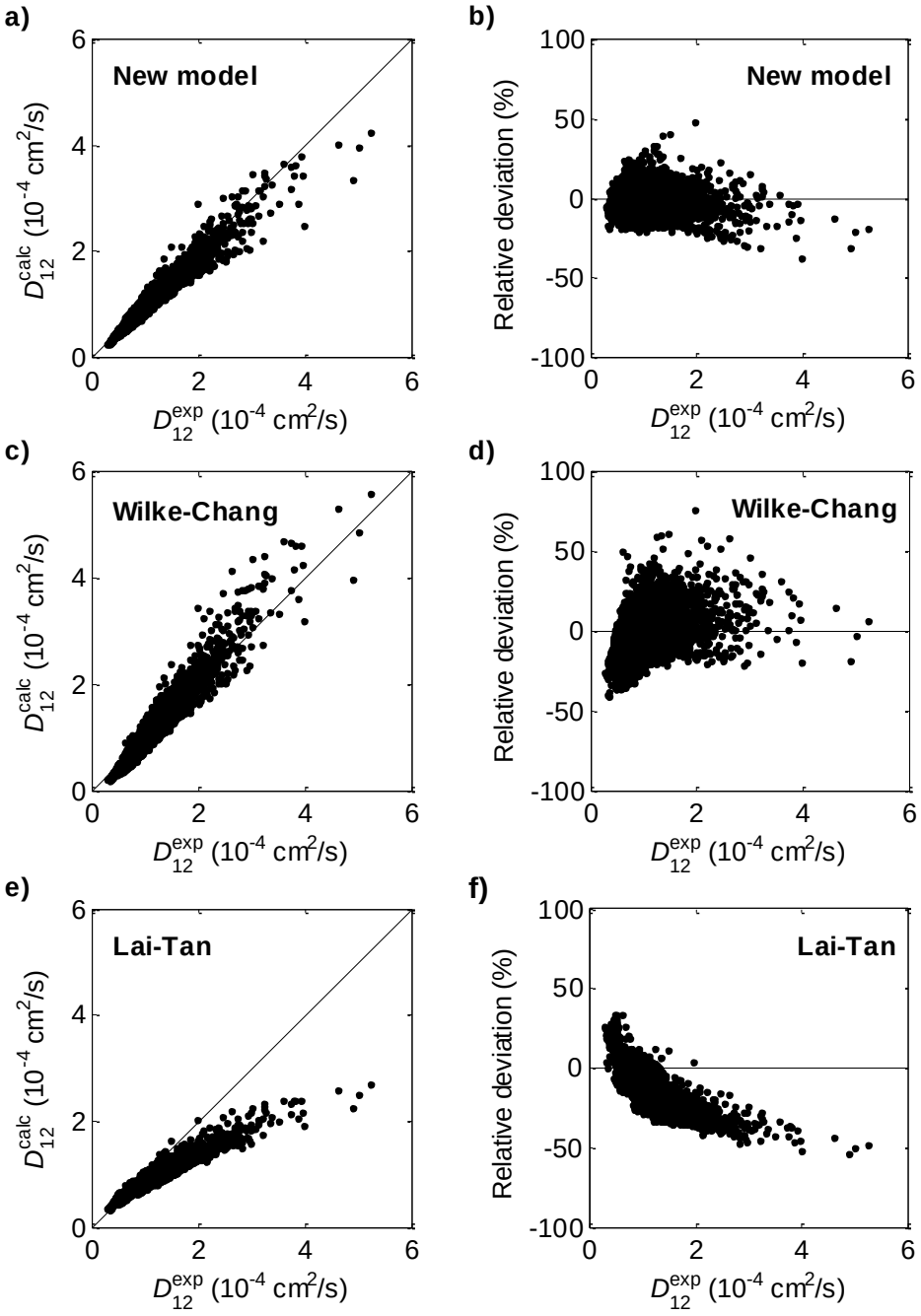

Fig. 3. Calculated tracer diffusivities (left) and relative deviations (right) *versus* experimental data for the new model (Eq. (19)), Wilke-Chang equation (Eq. (S.1)), and Lai-Tan equation (Eq. (S.4)).

provides unbiased results, evidenced by the average relative deviation close to zero (ARD = -0.69%) and by $D_{12}^{\text{exp}} - D_{12}^{\text{calc}}$ plots well distributed along diagonal. It performs equally well for polar and non-polar solutes, and in the whole pressure-temperature plane. Globally, the new model exhibits fine predictive capability for all kinds of solutes at any conditions, even near the critical point.

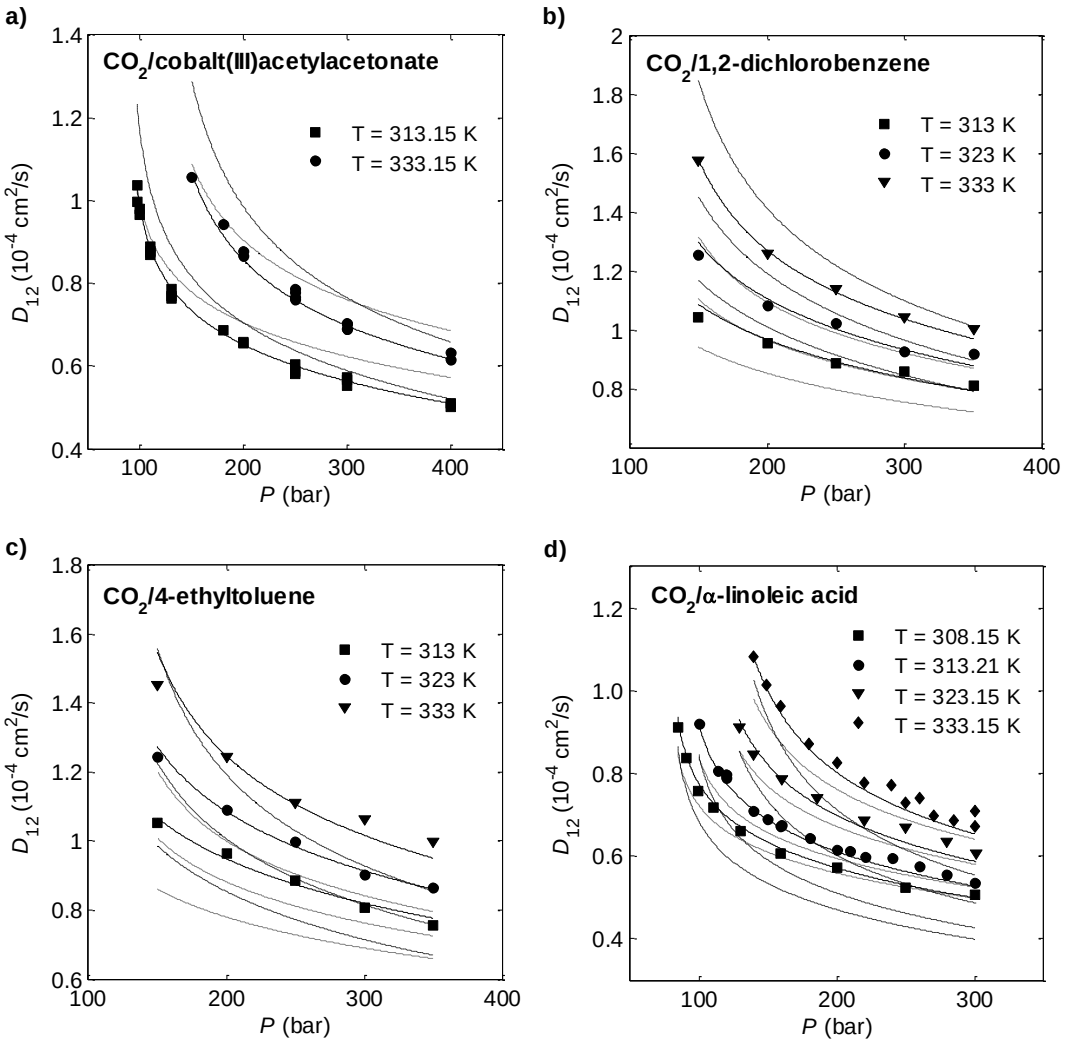

Fig. 4. Experimental and calculated tracer diffusion coefficients at constant temperatures for CO_2/cobalt(III)acetylacetonate, CO_2/1,2-dichlorobenzene, CO_2/4-ethyltoluene, and CO_2/α-linoleic acid systems. Modeling: (–) New model (Eq. (19)), (--) Wilke-Chang (Eq. (S.1)), and (···) Lai-Tan (Eq. (S.4)). Data from [79, 90, 100-101].

Appendix A. Supplementary data

Supplementary data associated with this article can be found, in the online version, at http://dx.doi.org/10.1016/j.supflu.2014.03.011.

The DOCX file contains (i) the integration of Ferrel expression (from Eq. (6) to Eq. (7)), (ii) the database compiled for the validation of the new model, and all properties and data necessary in the calculations, and (iii) the expressions of Wilke-Chang, Scheibel, Lusis-Ratcliff, Lai-Tan, Tyn-Calus and Reddy-Doraiswamy, adopted for comparison. Specific nomenclature and references are also included to assist readers.

The XLSX file contains a spreadsheet where readers insert the properties of the solute (see Table S.2 for the systems studied) and the operating condition (temperature, pressure, and corresponding CO_2 viscosity), and D_{12} value is automatically returned.

Nomenclature

A	Universal constant in Eq. (19) (Table 2)
AARD	Average absolute relative deviation, Eq. (34)
ARD	Average relative deviation, Eq. (35)
b	Quantity with dimension length^{-5}
D_{12}	Tracer diffusion coefficient of solute (2) through solvent (1)
F	Integrated velocity correlation function
G	Number density correlation function
H	Total correlation function integral
J_d	Diffusional flux
k_B	= 1.38065x10^{-16} erg K^{-1}, Boltzmann's constant
k_{12}	Binary interaction parameter
M	Molecular weight
NDP	Number of data points
P	Pressure

r	Average interparticle distance
SC-CO_2	Supercritical carbon dioxide
SCF	Supercritical fluid
T	Absolute temperature
V_{bp}	Molar volume at normal boiling point
V_c	Critical molar volume
x_2	Molar fraction of the solute

Greek letters

α	Universal constant in Eq. (19) (Table 2)
$\tilde{\alpha}$	Onsager kinetic coefficient
β	Universal constant in Eq. (19) (Table 2)
Γ_{12}^{∞}	Thermodynamic factor at infinite dilution
Δ(AARD)	$AARD_{max}$ - $AARD_{min}$
δ_{ij}	Kronecker delta
η	Solution viscosity
η_1	Solvent (SC-CO_2) viscosity
θ	Universal constant in Eq. (19) (Table 2)
μ	Chemical potential
ξ	Correlation length
ρ	Number density
σ_{12}	Binary diameter
σ_i	Diameter of component i
ϕ_2	Fugacity coefficient of solute
ω	Acentric factor

Subscripts

1	Solvent (SC-CO_2)
2	Solute
12	Binary
c	Critical property
LJ	Lennard-Jones
max	Maximum value
min	Minimum value
r	Reduced property (calculated with critical constant)

Superscripts

b	Background or regular contribution for $\tilde{\alpha}$ and
calc	Calculated value
exp	Experimental value
i, j	Component i or j
s	Singular contribution for $\tilde{\alpha}$ and

References

[1] G. Brunner, Applications of Supercritical Fluids, in: J.M. Prausnitz, M.F. Doherty, M.A. Segalman (Eds.) Annual Review of Chemical and Biomolecular Engineering, Vol 1, 2010, pp. 321-342.

[2] M.M.R. de Melo, R.M.A. Domingues, A.J.D. Silvestre, C.M. Silva, Extraction and purification of triterpenoids using supercritical fluids: from lab to exploitation, Mini-Reviews in Organic Chemistry, 11 (2014) 3362-381.

[3] M.M.R. de Melo, A.J.D. Silvestre, C.M. Silva, Supercritical fluid extraction of vegetable matrices: applications, trends and future perspective of a convincing new technology, The Journal of Supercritical Fluids, 92 (2014) 115-176.

[4] E.L.G. Oliveira, A.J.D. Silvestre, C.M. Silva, Review of kinetic models for supercritical fluid extraction, Chemical Engineering Research & Design, 89 (2011) 1104-1117.

[5] P.C. Wankat, Rate-Controlled Separations, Blackie Academic and Professional, Glasgow, UK, 1994.

[6] R. Taylor, R. Krishna, Multicomponent Mass Transfer, John Wiley & Sons, Inc, New York, 1993.

[7] A. Vignes, Diffusion in binary solutions - Variation of diffusion coefficient with composition, Industrial & Engineering Chemistry Fundamentals, 5 (1966) 189-199.

[8] L.S. Darken, Diffusion, mobility and their interrelation through free energy in binary metallic systems, Transactions of the American Institute of Mining and Metallurgical Engineers, 175 (1948) 184-201.

[9] C.M. Silva, H.Q. Liu, Modeling of Transport Properties of Hard Sphere Fluids and its Applications, in: A. Mulero (Ed.) Theory and Simulation of Hard Sphere Fluids and Related Systems, Lecture Notes in Physics 753, Springer, 2008, pp. 383-492.

[10] S.H. Chen, A rough-hard-sphere theory for diffusion in supercritical carbon dioxide, Chemical Engineering Science, 38 (1983) 655-660.

[11] C. Erkey, H. Gadalla, A. Akgerman, Application of rough hard sphere theory to diffusion in supercritical fluids, The Journal of Supercritical Fluids, 3 (1990) 180-185.

[12] H. Liu, C.M. Silva, E.A. Macedo, New equations for tracer diffusion coefficients of solutes in supercritical and liquid solvents based on the Lennard-Jones fluid model, Industrial & Engineering Chemistry Research, 36 (1997) 246-252.

[13] A.L. Magalhães, S.o.P. Cardoso, B.R. Figueiredo, F.A. Da Silva, C.M. Silva, Revisiting the Liu−Silva−Macedo Model for Tracer Diffusion Coefficients of Supercritical, Liquid, and Gaseous Systems, Industrial & Engineering Chemistry Research, 49 (2010) 7697-7700.

[14] H. Liu, C.M. Silva, E.A. Macedo, Generalised free-volume theory for transport properties and new trends about the relationship between free volume and equations of state, Fluid Phase Equilibria, 202 (2002) 89-107.

[15] A.L. Magalhães, F.A. Da Silva, C.M. Silva, Free-volume model for the diffusion coefficients of solutes at infinite dilution in supercritical CO2 and liquid H2O, The Journal of Supercritical Fluids, 74 (2013) 89-104.

[16] S.A. Rice, P. Gray, The Statistical Mechanics of Simple Liquids, Interscience Publisher, New York, 1965.

[17] A.L. Magalhães, F.A. Da Silva, C.M. Silva, New models for tracer diffusion coefficients of hard sphere and real systems: Application to gases, liquids and supercritical fluids, The Journal of Supercritical Fluids, 55 (2011) 898-923.

[18] H. Liu, E. Ruckenstein, A predictive equation for the tracer diffusion of various solutes in gases, supercritical fluids, and liquids, Industrial & Engineering Chemistry Research, 36 (1997) 5488-5500.

[19] A.L. Magalhães, P.F. Lito, F.A. Da Silva, C.M. Silva, Simple and accurate correlations for diffusion coefficients of solutes in liquids and supercritical fluids over wide ranges of temperature and density, The Journal of Supercritical Fluids, 76 (2013) 94-114.

[20] J.J. Suárez, I. Medina, J.L. Bueno, Diffusion coefficients in supercritical fluids: available data and graphical correlations, Fluid Phase Equilibria, 153 (1998) 167-212.

[21] C.R. Wilke, P. Chang, Correlation of diffusion coefficients in dilute solutions, AIChE Journal, 1 (1955) 264-270.

[22] K.K. Liong, P.A. Wells, N.R. Foster, Diffusion in supercritical fluids, The Journal of Supercritical Fluids, 4 (1991) 91-108.

[23] C.C. Lai, C.S. Tan, Measurement of molecular diffusion coefficients in supercritical carbon dioxide using a coated capillary column, Industrial & Engineering Chemistry Research, 34 (1995) 674-680.

[24] A.L. Magalhães, R.V. Vaz, R.M.G. Gonçalves, F.A. Da Silva, C.M. Silva, Accurate hydrodynamic models for the prediction of tracer diffusivities in supercritical carbon dioxide, The Journal of Supercritical Fluids, 83 (2013) 15-27.

[25] R.V. Vaz, A.L. Magalhães, C.M. Silva, Improved hydrodynamic equations for the accurate prediction of diffusivities in supercritical carbon dioxide, Fluid Phase Equilibria, 360 (2013) 401-415.

[26] R.V. Vaz, A.L. Magalhães, C.M. Silva, Improved Stokes–Einstein based models for diffusivities in supercritical CO_2, Journal of the Taiwan Institute of Chemical Engineers, http://dx.doi.org/10.1016/j.jtice.2013.12.005 (2013).

[27] A.L. Magalhães, F.A. Da Silva, C.M. Silva, New tracer diffusion correlation for real systems over wide ranges of temperature and density, Chemical Engineering Journal, 166 (2011) 49-72.

[28] A.L. Magalhães, F.A. Da Silva, C.M. Silva, Tracer diffusion coefficients of polar systems, Chemical Engineering Science, 73 (2012) 151-168.

[29] H.Q. Liu, E. Ruckenstein, Predicting the diffusion coefficients in supercritical fluids, Industrial & Engineering Chemistry Research, 36 (1997) 888-895.

[30] M.A. Anisimov, S.B. Kiselev, Transport properties of critical dilute solutions, International Journal of Thermophysics, 13 (1992) 873-893.

[31] R.C. Reid, J.M. Prausnitz, B.E. Poling, The Properties of Gases and Liquids, 5th ed., McGraw-Hill Professional, New York, 2001.

[32] T. Funazukuri, C.Y. Kong, T. Kikuchi, S. Kagei, Measurements of binary diffusion coefficient and partition ratio at infinite dilution for linoleic acid and arachidonic acid in supercritical carbon dioxide, Journal of Chemical & Engineering Data, 48 (2003) 684-688.

[33] R.A. Ferrell, Decoupled-mode dynamical scaling theory of the binary-liquid phase transition, Physical Review Letters, 24 (1970) 1169-1172.

[34] J.G. Kirkwood, F.P. Buff, The statistical mechanical theory of solutions. I, Journal of Chemical Physics, 19 (1951) 774-777.

[35] E.L. Cussler, Cluster diffusion in liquids, AIChE Journal, 26 (1980) 43-51.

[36] D. Peng, D.B. Robinson, New 2-constant equation of state, Industrial & Engineering Chemistry Fundamentals, 15 (1976) 59-64.

[37] K.S. Pitzer, D.R. Schreiber, Improving equation-of-state accuracy in the critical region; equations for carbon dioxide and neopentane as examples, Fluid Phase Equilibria, 41 (1988) 1-17.

[38] V.V. Altunin, M.A. Sakhabetdinov, Viscosity of liquid and gaseous carbon dioxide at temperatures 220-1300 K and pressure up to 1200 bar, Teploenergetika, 8 (1972) 85-89.

[39] M.T. Tyn, W.F. Calus, Estimating liquid molal volume, Processing, 21 (1975) 16-17.

[40] K.G. Joback, A unified approach to physical property estimation using multivariate statistical techniques, in: Department of Chemical Engineering, Massachusetts Institute of Technology, Cambridge, MA, 1984.

[41] K.G. Joback, R.C. Reid, Estimation of pure-component properties from group-contributions, Chemical Engineering Communications, 57 (1987) 233 - 243.

[42] G.R. Somayajulu, Estimation procedures for critical constants, Journal of Chemical & Engineering Data, 34 (1989) 106-120.

[43] K.M. Klincewicz, R.C. Reid, Estimation of critical properties with group contribution methods, AIChE Journal, 30 (1984) 137-142.

[44] D. Ambrose, Correlation and Estimation of Vapour-Liquid Critical Properties. II: Critical Pressure and Critical Volume, in: NPL Technical Report. Chem. 92, National Physical Laboratory, Teddington, UK, 1979.

[45] D. Ambrose, Correlation and Estimation of Vapour-liquid Critical Properties: I, Critical Temperatures of Organic Compounds, in: NPL Technical Report. Chem. 92, National Physical Laboratory, Madison, WI, 1978.

[46] X. Wen, Y. Qiang, A new group contribution method for estimating critical properties of organic compounds, Industrial & Engineering Chemistry Research, 40 (2001) 6245-6250.

[47] L. Constantinou, R. Gani, New group contribution method for estimating properties of pure compounds, AIChE Journal, 40 (1994) 1697-1710.

[48] B.I. Lee, M.G. Kesler, A generalized thermodynamic correlation based on three-parameter corresponding states, AIChE Journal, 21 (1975) 510-527.

[49] P.R. Sassiat, P. Mourier, M.H. Caude, R.H. Rosset, Measurement of diffusion coefficients in supercritical carbon dioxide and correlation with the equation of Wilke and Chang, Analytical Chemistry, 59 (1987) 1164-1170.

[50] T. Funazukuri, C.Y. Kong, S. Kagei, Infinite dilution binary diffusion coefficients of 2-propanone, 2-butanone, 2-pentanone, and 3-pentanone in CO_2 by the Taylor dispersion technique from 308.15 to 328.15 K in the pressure range from 8 to 35 MPa, International Journal of Thermophysics, 21 (2000) 1279-1290.

[51] T. Funazukuri, C.Y. Kong, S. Kagei, Binary diffusion coefficients of acetone in carbon dioxide at 308.2 and 313.2 K in the pressure range from 7.9 to 40 MPa, International Journal of Thermophysics, 21 (2000) 651-669.

[52] C.Y. Kong, T. Funazukuri, S. Kagei, Chromatographic impulse response technique with curve fitting to measure binary diffusion coefficients and retention factors using polymer-coated capillary columns, Journal of Chromatography A, 1035 (2004) 177-193.

[53] H. Nishiumi, M. Fujita, K. Agou, Diffusion of acetone in supercritical carbon dioxide, Fluid Phase Equilibria, 117 (1996) 356-363.

[54] V.M. Shenai, B.L. Hamilton, M.A. Matthews, Diffusion in Liquid and Supercritical Fluid Mixtures, in: Supercritical Fluid Engineering Science, 1993, pp. 92-103.

[55] O. Suárez-Iglesias, I. Medina, C. Pizarro, J.L. Bueno, Diffusion coefficients of 2-fluoroanisole, 2-bromoanisole, allylbenzene and 1,3-divinylbenzene at infinite dilution in supercritical carbon dioxide, Fluid Phase Equilibria, 260 (2007) 279-286.

[56] L.M. González, J.L. Bueno, I. Medina, Determination of binary diffusion coefficients of anisole, 2,4-dimethylphenol, and nitrobenzene in supercritical carbon dioxide, Industrial & Engineering Chemistry Research, 40 (2001) 3711-3716.

[57] K. Abaroudi, Limpieza de Matrices Sólidas Porosas de Interés Medioambiental con Fluidos Supercríticos, in: Departamento de Ingeniería Química, Universidad Politécnica de Catalunã, 2001.

[58] Y.S. Han, Y.W. Yang, P.D. Wu, Binary diffusion coefficients of arachidonic acid ethyl ester, *cis*-5,8,11,14,17-eicosapentaenoic acid ethyl ester, and *cis*-4,7,10,13,16,19-docosahexanenoic acid ethyl ester in supercritical carbon dioxide, Journal of Chemical & Engineering Data, 52 (2007) 555-559.

[59] K.K. Liong, P.A. Wells, N.R. Foster, Diffusion coefficients of long-chain esters in supercritical carbon dioxide, Industrial & Engineering Chemistry Research, 30 (1991) 1329-1335.

[60] I. Swaid, G.M. Schneider, Determination of binary diffusion coefficients of benzene and some alkylbenzenes in supercritical CO_2 between 308 and 328 K in the pressure range 80 to 160

bar with supercritical fluid chromatography (SFC), Berichte Der Bunsen-Gesellschaft-Physical Chemistry Chemical Physics, 83 (1979) 969-974.

[61] C.A. Filho, C.M. Silva, M.B. Quadri, E.A. Macedo, Infinite dilution diffusion coefficients of linalool and benzene in supercritical carbon dioxide, Journal of Chemical & Engineering Data, 47 (2002) 1351-1354.

[62] J.J. Suárez, J.L. Bueno, I. Medina, Determination of binary diffusion coefficients of benzene and derivatives in supercritical carbon dioxide, Chemical Engineering Science, 48 (1993) 2419-2427.

[63] J.L. Bueno, J.J. Suárez, J. Dizy, I. Medina, Infinite dilution diffusion coefficients:benzene derivatives as solutes in supercritical carbon dioxide, Journal of Chemical & Engineering Data, 38 (1993) 344-349.

[64] T. Funazukuri, N. Nishimoto, Tracer diffusion coefficients of benzene in dense CO_2 at 313.2 K and 8.5-30 MPa, Fluid Phase Equilibria, 125 (1996) 235-243.

[65] T. Funazukuri, C.Y. Kong, S. Kagei, Infinite dilution binary diffusion coefficients of benzene in carbon dioxide by the Taylor dispersion technique at temperatures from 308.15 to 328.15 K and pressures from 6 to 30 MPa, International Journal of Thermophysics, 22 (2001) 1643-1660.

[66] J.M.H.L. Sengers, U.K. Deiters, U. Klask, P. Swidersky, G.M. Schneider, Application of the Taylor dispersion method in supercritical fluids, International Journal of Thermophysics, 14 (1993) 893-922.

[67] K. Ago, H. Nishiumi, Mutual diffusion coefficients of benzene in supercritical carbon dioxide, Journal of Chemical Engineering of Japan, 32 (1999) 563-568.

[68] C.Y. Kong, T. Funazukuri, S. Kagei, Binary diffusion coefficients and retention factors for polar compounds in supercritical carbon dioxide by chromatographic impulse response method, The Journal of Supercritical Fluids, 37 (2006) 359-366.

[69] O.J. Catchpole, M.B. King, Measurement and correlation of binary diffusion coefficients in near critical fluids, Industrial & Engineering Chemistry Research, 33 (1994) 1828-1837.

[70] H. Fu, L.A.F. Coelho, M.A. Matthews, Diffusion coefficients of model contaminants in dense CO_2, The Journal of Supercritical Fluids, 18 (2000) 141-155.

[71] O. Suárez-Iglesias, I. Medina, C. Pizarro, J.L. Bueno, Diffusion of benzyl acetate, 2-phenylethyl acetate, 3-phenylpropyl acetate, and dibenzyl ether in mixtures of carbon dioxide and ethanol, Industrial & Engineering Chemistry Research, 46 (2007) 3810-3819.

[72] O. Suárez-Iglesias, I. Medina, C. Pizarro, J.L. Bueno, Limiting diffusion coefficients of ethyl benzoate, benzylacetone, and eugenol in carbon dioxide at supercritical conditions, Journal of Chemical & Engineering Data, 53 (2008) 779-784.

[73] H. Weingärtner, U. Klask, G.M. Schneider, Solute diffusion in supercritical solvents - diffusion coefficients D_{12}^{∞} and diffusion-viscosity relationship for the aromatic model solute biphenyl in carbon dioxide, Zeitschrift Für Physikalische Chemie-International Journal of Research in Physical Chemistry & Chemical Physics, 219 (2005) 1261-1271.

[74] L.M. González, O. Suárez-Iglesias, J.L. Bueno, C. Pizarro, I. Medina, Application of the corresponding states principle to the diffusion in CO_2, AIChE Journal, 53 (2007) 3054-3061.

[75] J.J. Suarez, I. Medina, J.L. Bueno, Diffusion coefficients in supercritical fluids: available data and graphical correlations, Fluid Phase Equilibria, 153 (1998) 167-212.

[76] T. Funazukuri, Measurements of binary diffusion coefficients of 20 organic compounds in CO_2 at 313.2 K and 16.0 MPa, Journal of Chemical Engineering of Japan, 29 (1996) 191-192.

[77] C. Pizarro, O. Suárez-Iglesias, I. Medina, J.L. Bueno, Diffusion coefficients of *n*-butylbenzene, *n*-pentylbenzene, 1-phenylhexane, 1-phenyloctane, and 1-phenyldodecane in supercritical carbon dioxide, Industrial & Engineering Chemistry Research, 47 (2008) 6783-6789.

[78] C. Pizarro, O. Suárez-Iglesias, I. Medina, J.L. Bueno, Diffusion coefficients of isobutylbenzene, *sec*-butylbenzene, and 3-methylbutylbenzene in supercritical carbon dioxide, Journal of Chemical & Engineering Data, 58 (2013) 2001-2007.

[79] K.M. González, J.L. Bueno, I. Medina, Measurement of diffusion coefficients for 2-nitroanisole, 1,2-dichlorobenzene and *tert*-butylbenzene in carbon dioxide containing modifiers, The Journal of Supercritical Fluids, 24 (2002) 219-229.

[80] P.A. Wells, Diffusion in Supercritical Fluids, in, The University of New South Wales, Kensington, Australia, 1991.

[81] K.K. Liong, P.A. Wells, N.R. Foster, Diffusion of fatty acid esters in supercritical carbon dioxide, Industrial & Engineering Chemistry Research, 31 (1992) 390-399.

[82] G. Knaff, E.U. Schlünder, Diffusion coefficients of naphthalene and caffeine in supercritical carbon dioxide, Chemical Engineering and Processing, 21 (1987) 101-105.

[83] H.H. Lauer, D. McManigill, R.D. Board, Mobile-phase transport-properties of liquefied gases in near-critical and supercritical fluid chromatography, Analytical Chemistry, 55 (1983) 1370-1375.

[84] T. Funazukuri, C.Y. Kong, S. Kagei, Binary diffusion coefficients, partition ratios and partial molar volumes at infinite dilution for b-carotene and a-tocopherol in supercritical carbon dioxide, The Journal of Supercritical Fluids, 27 (2003) 85-96.

[85] T. Funazukuri, C.Y. Kong, N. Murooka, S. Kagei, Measurements of binary diffusion coefficients and partition ratios for acetone, phenol, a-tocopherol, and b-carotene in supercritical carbon dioxide with a poly(ethylene glycol)-coated capillary column, Industrial & Engineering Chemistry Research, 39 (2000) 4462-4469.

[86] T. Funazukuri, C.Y. Kong, S. Kagei, Measurements of binary diffusion coefficients for some low volatile compounds in supercritical carbon dioxide by input-output response

technique with two diffusion columns connected in series, Fluid Phase Equilibria, 194 (2002) 1169-1178.

[87] X.Y. Dong, B.G. Su, H.B. Xing, Y.W. Yang, Q.L. Ren, Diffusion coefficients of L-menthone and L-carvone in mixtures of carbon dioxide and ethanol, The Journal of Supercritical Fluids, 55 (2010) 86-95.

[88] X.Y. Dong, B.G. Su, H.B. Xing, Z.B. Bao, Y.W. Yang, Q.L. Ren, Cosolvent effects on the diffusions of 1,3-dichlorobenzene, L-carvone, geraniol and 3-fluorophenol in supercritical carbon dioxide, The Journal of Supercritical Fluids, 58 (2011) 216-225.

[89] C.A. Filho, C.M. Silva, M.B. Quadri, E.A. Macedo, Tracer diffusion coefficients of citral and D-limonene in supercritical carbon dioxide, Fluid Phase Equilibria, 204 (2003) 65-73.

[90] C.Y. Kong, Y.Y. Gu, M. Nakamura, T. Funazukuri, S. Kagei, Diffusion coefficients of metal acetylacetonates in supercritical carbon dioxide, Fluid Phase Equilibria, 297 (2010) 162-167.

[91] Y.N. Yang, M.A. Matthews, Diffusion of chelating agents in supercritical CO_2 and a predictive approach for diffusion coefficients, Journal of Chemical & Engineering Data, 46 (2001) 588-595.

[92] C.Y. Kong, N. Takahashi, T. Funazukuri, S. Kagei, Measurements of binary diffusion coefficients and retention factors for dibenzo-24-crown-8 and 15-crown-5 in supercritical carbon dioxide by chromatographic impulse response technique, Fluid Phase Equilibria, 257 (2007) 223-227.

[93] N. Dahmen, A. Dulberg, G.M. Schneider, Determination of binary diffusion coefficients in supercritical carbon dioxide with supercritical fluid chromatography (SFC), Berichte Der Bunsen-Gesellschaft-Physical Chemistry Chemical Physics, 94 (1990) 384-386.

[94] C.M. Silva, E.A. Macedo, Diffusion coefficients of ethers in supercritical carbon dioxide, Industrial & Engineering Chemistry Research, 37 (1998) 1490-1498.

[95] C. Pizarro, O. Suarez-Iglesias, I. Medina, J.L. Bueno, Binary diffusion coefficients for 2,3-dimethylaniline, 2,6-dimethylaniline, 2-methylanisole, 4-methylanisole and 3-nitrotoluene in supercritical carbon dioxide, The Journal of Supercritical Fluids, 48 (2009) 1-8.

[96] C.Y. Kong, M. Nakamura, K. Sone, T. Funazukuri, S. Kagei, Measurements of binary diffusion coefficients for ferrocene and 1,1'-dimethylferrocene in supercritical carbon dioxide, Journal of Chemical & Engineering Data, 55 (2010) 3095-3100.

[97] H. Higashi, Y. Iwai, Y. Nakamura, S. Yamamoto, Y. Arai, Correlation of diffusion coefficients for naphthalene and dimethylnaphthalene isomers in supercritical carbon dioxide, Fluid Phase Equilibria, 166 (1999) 101-110.

[98] H. Higashi, Y. Iwai, Y. Takahashi, H. Uchida, Y. Arai, Diffusion coefficients of naphthalene and dimethylnaphthalene in supercritical carbon dioxide, Fluid Phase Equilibria, 144 (1998) 269-278.

[99] T. Funazukuri, C.Y. Kong, S. Kagei, Effects of molecular weight and degree of unsaturation on binary diffusion coefficients for lipids in supercritical carbon dioxide, Fluid Phase Equilibria, 219 (2004) 67-73.

[100] T. Funazukuri, C.Y. Kong, S. Kagei, Binary diffusion coefficient, partition ratio, and partial molar volume for docosahexaenoic acid, eicosapentaenoic acid and a-linolenic acid at infinite dilution in supercritical carbon dioxide, Fluid Phase Equilibria, 206 (2003) 163-178.

[101] C. Pizarro, O. Suárez-Iglesias, I. Medina, J.L. Bueno, Binary diffusion coefficients of 2-ethyltoluene, 3-ethyltoluene, and 4-ethyltoluene in supercritical carbon dioxide, Journal of Chemical & Engineering Data, 54 (2009) 1467-1471.

[102] C.Y. Kong, K. Sone, T. Sako, T. Funazukuri, S. Kagei, Solubility determination of organometallic complexes in supercritical carbon dioxide by chromatographic impulse response method, Fluid Phase Equilibria, 302 (2011) 347-353.

[103] A. Akgerman, C. Erkey, M. Orejuela, Limiting diffusion coefficients of heavy molecular weight organic contaminants in supercritical carbon dioxide, Industrial & Engineering Chemistry Research, 35 (1996) 911-917.

[104] R.H. Lin, L.L. Tavlarides, Diffusion coefficients of diesel fuel and surrogate compounds in supercritical carbon dioxide, The Journal of Supercritical Fluids, 52 (2010) 47-55.

[105] T. Funazukuri, S. Hachisu, N. Wakao, Measurements of binary diffusion coefficients of C_{16}-C_{24} unsaturated fatty acid methyl esters in supercritical carbon dioxide, Industrial & Engineering Chemistry Research, 30 (1991) 1323-1329.

[106] T. Funazukuri, Y. Ishiwata, Diffusion coefficients of linoleic acid methyl ester, vitamin K_3 and indole in mixtures of carbon dioxide and *n*-hexane at 313.2 K, and 16.0 MPa and 25.0 MPa, Fluid Phase Equilibria, 164 (1999) 117-129.

[107] C.Y. Kong, N.R.W. Withanage, T. Funazukuri, S. Kagei, Binary diffusion coefficients and retention factors for g-linolenic acid and its methyl and ethyl esters in supercritical carbon dioxide, The Journal of Supercritical Fluids, 37 (2006) 63-71.

[108] C.Y. Kong, M. Mori, T. Funazukuri, S. Kagei, Measurements of binary diffusion coefficients, retention factors and partial molar volumes for myristoleic acid and its methyl ester in supercritical carbon dioxide, Analytical Sciences, 22 (2006) 1431-1436.

[109] T. Funazukuri, Y. Ishiwata, N. Wakao, Predictive correlation for binary diffusion coefficients in dense carbon dioxide, AIChE Journal, 38 (1992) 1761-1768.

[110] D.M. Lamb, S.T. Adamy, K.W. Woo, J. Jonas, Transport and relaxation of naphthalene in supercritical fluids, Journal of Physical Chemistry, 93 (1989) 5002-5005.

[111] T. Funazukuri, S. Hachisu, N. Wakao, Measurement of diffusion coefficients of C_{18} unsaturated fatty acid methyl esters, naphthalene, and benzene in supercritical carbon dioxide by a tracer response technique, Analytical Chemistry, 61 (1989) 118-122.

[112] P.G. Debenedetti, R.C. Reid, Diffusion and mass transfer in supercritical fluids, AIChE Journal, 32 (1986) 2034-2046.

[113] T. Wells, N.R. Foster, R.P. Chaplin, Diffusion of phenylacetic acid and vanillin in supercritical carbon dioxide, Industrial & Engineering Chemistry Research, 31 (1992) 927-934.

[114] C.Y. Kong, K. Watanabe, T. Funazukuri, Diffusion coefficients of phenylbutazone in supercritical CO2 and in ethanol, Journal of Chromatography A, 1279 (2013) 92-97.

[115] C. Pizarro, O. Suárez-Iglesias, I. Medina, J.L. Bueno, Molecular diffusion coefficients of phenylmethanol, 1-phenylethanol, 2-phenylethanol, 2-phenyl-1-propanol, and 3-phenyl-1-propanol in supercritical carbon dioxide, The Journal of Supercritical Fluids, 43 (2008) 469-476.

[116] C.M. Silva, C.A. Filho, M.B. Quadri, E.A. Macedo, Binary diffusion coefficients of a-pinene and b-pinene in supercritical carbon dioxide, Journal of Supercritical Fluids, 32 (2004) 167-175.

[117] J.J. Suárez, J.L. Bueno, I. Medina, J. Dizy, Applications of supercritical chromatography - Determination of molecular diffusivity, Afinidad, 49 (1992) 101-113.

[118] N. Dahmen, A. Kordikowski, G.M. Schneider, Determination of binary diffusion coefficients of organic compounds in supercritical carbon dioxide by supercritical fluid chromatography, Journal of Chromatography A, 505 (1990) 169-178.

[119] L.M. González, O. Suárez-Iglesias, J.L. Bueno, C. Pizarro, I. Medina, Limiting binary diffusivities of aniline, styrene, and mesitylene in supercritical carbon dioxide, Journal of Chemical & Engineering Data, 52 (2007) 1286-1290.

[120] C.Y. Kong, N.R.W. Withanage, T. Funazukuri, S. Kagei, Binary diffusion coefficients and retention factors for long-chain triglycerides in supercritical carbon dioxide by the chromatographic impulse response method, Journal of Chemical & Engineering Data, 50 (2005) 1635-1640.

[121] T. Funazukuri, C.Y. Kong, S. Kagei, Infinite-dilution binary diffusion coefficient, partition ratio, and partial molar volume for ubiquinone CoQ10 in supercritical carbon dioxide, Industrial & Engineering Chemistry Research, 41 (2002) 2812-2818.

4 Molecular simulations of tracer diffusion coefficients

Computational tools have been used for the last decades in solving the most diverse problems in a wide range of areas. Whenever applicable, they are preferred over experimental measurements, since lab work is usually more expensive, time consuming, and sometimes impossible or dangerous. Moreover, they give us the opportunity to study microscopic properties impossible to acess by experiments, such as materials and fluids microstructure, and their connection to macroscopic properties.

Molecular Dynamics (MD) is one of this methods which has been sucessfully employed for a long time and it has been object of considerable progresses. The idea underlyind this method is simple: a system is simulated by a set of particles with a preassigned law of interaction, after which the Newton's equations of motion for the particles are numerically integrated. The result is a trajectory that specifies how the positions and velocities of the particles in the system vary with time. Analyzing them, it is possible to extract a wide spectrum of physical information about the system.

The first simulations [1, 2] were very simple due to computational limitations at the time, but currently it is possible to simulate systems with an impressive degree of complexity and detail [3-7], making use of dedicated code available in the literature or general purpose simulation software packages. These last ones are versatile programs and libraries, suitable for all kinds of simulations based on pair potential functions. Generaly they offer a choice between

some popular force fields (FF), which refer to the form and parameters of mathematical functions used to describe the potential energy of a system of particles. FF functions and parameter sets are derived from both experimental work and high level quantum mechanical calculations to correctly describe the compounds under study.

This powerfull tool was apllied in this PhD thesis to complement the phenomenological and experimental study of transport properties, specifically to simulate supercritical mixtures and extract infinite dilution diffusivities in supercritical carbon dioxide (SC-CO_2). Classical MD simulations allow us to disclose the influence of solute chemical groups, substituents, alkyl chain size, and molecular symmetry upon D_{12} values. Accordingly, propanone, butanone, 2-pentanone and 3-pentanone in SC-CO_2 were simulated for distinct state conditions (temperature and pressure or density) – Paper V. The computed diffusivities were validated by comparison with experimental data. The effect of solvent and solute properties upon D_{12} values was also evaluated. Additionally, the local structure of ketone/SC-CO_2 systems was investigated by computing radial distribution functions and coordination numbers, with the objective to interpret their diffusive behavior.

References

[1] B.J. Alder, D.M. Gass, T.E. Wainwright, Studies in molecular dynamics. VIII. The transport coefficients for a hard-sphere fluid, The Journal of Chemical Physics, 53 (1970) 3813-3826.

[2] D. Levesque, L. Verlet, Computer "experiments" on classical fluids. III. Time-dependent self-correlation functions, Physical Review A, 2 (1970) 2514-2528.

[3] P. Biggin, P. Bond, Molecular Dynamics Simulations of Membrane Proteins, in: A. Kukol (Ed.) Molecular Modeling of Proteins, Humana Press, 2008, pp. 147-160.

[4] S.R. Badu, R. Melnik, M. Paliy, S. Prabhakar, A. Sebetci, B.A. Shapiro, Modeling of RNA nanotubes using molecular dynamics simulation, European Biophysics Journal, 43 (2014) 555-564.

[5] M. Greiner, E. Elts, J. Schneider, K. Reuter, H. Briesen, Dissolution study of active pharmaceutical ingredients using molecular dynamics simulations with classical force fields, Journal of Crystal Growth, 405 (2014) 122-130.

[6] K.D. Vargheese, A. Tandia, J.C. Mauro, Molecular dynamics simulations of ion-exchanged glass, Journal of Non-Crystalline Solids, 403 (2014) 107-112.

[7] S. Bhoi, T. Banerjee, K. Mohanty, Molecular dynamic simulation of spontaneous combustion and pyrolysis of brown coal using ReaxFF, Fuel, 136 (2014) 326-333.

Paper V

Adapted from

Molecular dynamics simulation of diffusion coefficients and structural properties of ketones in supercritical CO_2 at infinite dilution

Journal of Supercritical Fluids (submitted)

Abstract

Molecular dynamics (MD) simulations were employed to determine tracer diffusion coefficients (D_{12}) of propanone, butanone, 2-pentanone and 3-pentanone in supercritical CO_2, which are in quite good agreement with experimental data available in the literature. It was confirmed that D_{12} is enhanced by pressure decrease, temperature increase, and solute size reduction. The radial distribution functions and coordination numbers derived from the simulations were further employed to understand how molecular structure specificities affect D_{12}. The simulations proved that the molecular structuring of the solvent around the solute is similar for all ketones, and that the decrease of the coordination numbers on going from propanone to the pentanones is due to the growth of the molecular chain. The good agreement between calculated and measured data validates the MD simulations as a cheap alternative to predict D_{12} values of ketones in supercritical CO_2.

1. Introduction

The well-known characteristics of supercritical fluids (SCF), especially carbon dioxide, make them advantageous over many conventional solvents. Their large compressibility and thermal expansion coefficients originate substantial changes in density by pressure, *P*, and temperature, *T*, variation, which affects relevant properties like viscosity, solvent capacity, and diffusivity, with large impact upon the kinetics and equilibrium of supercritical processes. These features justify the interesting gas-liquid intermediate properties of SCFs, which can be beneficially exploited and manipulated to maximize solubilities, reaction yields, extraction rates, etc. This ability to fine tune solvent properties through the manipulation of pressure and/or temperature, and/or by the addition of small quantities of polar cosolvents, makes SCFs very attractive to research and industry [1-3]. The application areas include extraction, impregnation and cleaning, multistage countercurrent separation, particle formation, coating, and reactive systems like hydrogenation and biomass gasification [1]. They embody mass transfer, phase-transition and/or reaction operations, where transport properties gain special attention for

modeling and interpreting such rate-controlled processes [4-6]. Therefore, infinite dilution or tracer diffusion coefficients, D_{12}, have been investigated for decades through experimental measurement [7-11], phenomenological modeling [9, 12-20], and molecular dynamics (MD) simulations [14, 21, 22]. For measuring diffusion coefficients of solutes in supercritical carbon dioxide (SC-CO_2), the most adopted techniques are the geometric and chromatographic methods [9, 11, 23] despite the inherent technical difficulties and equipment costs associated to the last one [23].

Experiments are fundamental for accessing reliable diffusivity values, but the existence of accurate models is necessary to support process design and simulation over wide ranges of operating conditions and systems composition. In the particular case of unknown solutes, predictive models [19, 20, 24-27] are obviously required.

With respect to computer simulations, they are very useful for investigating dynamic, structural and thermodynamic properties, allowing researchers to complement other existing studies and get valuable information not directly obtained by experiment [22, 28-30], as for instance, radial distribution functions, coordination numbers, and energetic data.

During the last decades, the MD simulation techniques opened avenues in the prediction of thermo-physical properties, under equilibrium and non-equilibrium conditions, of a wide variety of systems [22, 29-32]. The information acquired from microscopic computations is vital for the development of reliable and robust macroscopic models, which means the MD and phenomenological modeling may complement each other.

In recent years, some authors have successfully used MD for D_{12} calculation of organic molecules in SC-CO_2 [22, 29, 33, 34], taking advantage of the accurate potential functions available in the literature. More than replacing or incrementing D_{12} measurements, MD is also very desired to unveil and interpret experimental trends observed. One may cite, for instance, the influence of solute chemical groups, substituents, alkyl chain size, molecular symmetry, and isomerism upon D_{12} values.

In this work, MD simulations were performed to calculate the diffusivities of a group of ketones (propanone, butanone, 2-pentanone and 3-pentanone) in SC-CO_2, over pressure and temperatures ranges consistent with supercritical extraction conditions. The simulations were

compared with experimental data to validate the computed results. The influence of pressure, temperature and structural formula of the solutes upon D_{12} was investigated, as well as their effect on the local structure of CO_2 around such solutes.

2. Potential functions

The accuracy of properties computed by MD strongly depends on the accuracy of the intermolecular potentials involved [30]. In this study, the semi-empirical classical potential called Elementary Physical Model (EPM2) [35] was used for carbon dioxide. It is an atomistic model that mimics CO_2 geometry and quadrupole momentum, and was developed to reproduce its critical point and vapor-liquid coexistence curve. However, it has been verified to correctly simulate densities, radial distribution functions, coordination numbers, isothermal compressibility, isochoric heat capacity, diffusivity, and other quantities [36, 37] of pure CO_2 and its mixtures, even in the supercritical region [22, 29, 33, 34]. In conjugation with adequate potentials for the solute, EPM2 has been successfully employed to compute tracer diffusion coefficients in SC-CO_2 [22, 29].

EPM2 model uses partially charged Lennard-Jones (LJ) beads for modeling the carbon atom and the two oxygen counterparts [37]. This LJ contribution, combined with the Coulomb potential function, represents the non-bonded interactions between pairs of particles according to:

$$V_{\text{non-bonded}} = 4\varepsilon_{ij}\left[\left(\frac{\sigma_{ij}}{r_{ij}}\right)^{12} - \left(\frac{\sigma_{ij}}{r_{ij}}\right)^{6}\right] + \frac{q_i q_j}{4\pi\varepsilon_{\mathrm{r}} r_{ij}} \qquad (1)$$

Here, $V_{\text{non-bonded}}$ is the intermolecular potential, ε_{ij} is the well depth in the potential energy between particles i and j, σ_{ij} is the distance for which the potential is zero, r_{ij} is the interparticle distance, q_i and q_j are the partial charges for particles i and j, and ε_{r} is the relative permittivity. The potential parameters and partial charges of CO_2 atoms are listed in Table 1.

The non-bonded parameters for pairs of different particles are calculated *via* combining rules, in this case geometric averages for both σ_{ij} and ε_{ij}:

$$\sigma_{ij} = \left(\sigma_{ii}\sigma_{jj}\right)^{1/2}$$
$$\varepsilon_{ij} = \left(\varepsilon_{ii}\varepsilon_{jj}\right)^{1/2} \quad (2)$$

The LJ potential function expresses the van der Waals energy, which describes the repulsive and attractive interactions between two uncharged molecules or atoms that create temporarily an induced dipole moment occurring by the motion of electrons [30, 34]. The Coulomb potential function represents particle interactions due to their permanent dipole moments that attract and repel one another [30, 34].

The complete potential energy function is obtained with the addition of intramolecular potentials describing bond stretching and bending energy contributions. In this case, the EPM2 model considers rigid carbon-oxygen bonds of 1.149 Å, but flexible bond angle harmonic potential of $1/2\,k_\theta\left(\theta-\theta_0\right)^2$ [35]. The bond bending force constant, k_θ, the equilibrium bond angle, θ_0, and bond length, l_0, are also compiled in Table 1.

For the simulation of ketone molecules, the OPLS-AA (Optimized Potentials for Liquid Simulation – All Atoms) model [38-42] was adopted since it is an appropriate force field that has already been validated for this type of simple compounds. The potential parameters for the constituting atoms in the ketones considered in this work are also compiled in Table 2.

Table 1. Potential parameters of EPM2 model for CO_2.

	σ_{ii} (Å)	ε_{ii} (K)	q_{ii} (e)	l_0 (Å)	θ_0 (º)	k_θ (kJ/mol/rad^2)
C_{CO_2}	2.757	28.129	0.6512	1.149	180	1236
O_{CO_2}	3.033	80.507	-0.3256			

3. Molecular Dynamics simulation of D_{12}

The GROMACS [43] software package version 4.5.4 was used to perform the MD simulations. All simulations were conducted in the canonical ensemble (NVT), *i.e.* for constant number of molecules, *N*, temperature, *T*, and system volume, *V*, and using cubic boxes and standard periodic boundary conditions. The number of CO_2 molecules was 4000, while the number of ketone molecules varied in order to keep a low and nearly constant concentration of each solute: 25 for propanone, 20 for butanone and 17 for each of the pentanones, giving rise to concentrations of 0.82, 0.81 and 0.82 wt.%, (equivalently, 0.62, 0.50 and 0.42 mol%), respectively (Table 3 and discussion in section 4.2). Both CO_2 and ketones were placed randomly inside the cubic cells, whose volume was previously fixed in order to match the desired system density. The values of temperature and pressure are shown in Table 4, together with the SC-CO_2 densities taken from NIST Chemistry WebBook [44]. Since the ketones concentrations are very small, approaching infinite dilution, the CO_2 densities were taken as those of the system. In each simulation, the cell temperature was kept constant using the Nosé-Hoover [45, 46] temperature coupling algorithm to enable correct canonical ensemble computations.

Table 2. OPLS-AA potential parameters for the ketones [38-42].

	σ_{ii} (Å)	ε_{ii} (K)	q_{ii} (e)
C_{CH_3}	3.500	33.214	-0.180
C_{CH_2}	3.500	33.214	-0.120
H_{CH_x} (α-carbon)	2.420	75.487	0.060
H_{CH_x} (other C)	2.500	15.097	0.060
$C_{C=O}$	3.750	52.841	0.470
$O_{C=O}$	2.960	105.682	-0.470

Each simulation was carried out using constraint LINCS algorithm, in order to keep the correct bond lengths. After some preliminary tests (cf. section 4.2), the van der Waals interactions were modeled using a cut-off distance of 1.4 nm, and the long-range electrostatic interactions were taken into account by means of the particle-mesh Ewald (PME) [47] summation. For the short-range non-bonded interactions, a neighbor list of 1.4 nm was maintained and updated every 10 simulation time steps.

After creating the starting random configurations, energy minimizations of the entire ketone/SC-CO_2 systems were performed using steepest descendent algorithm to relax the systems. After some preliminary tests (cf. section 4.2), the simulations performed considered the NVT ensemble and were carried out with leap-frog algorithm [48] for integrating Newton's equations of motion, with an integration time step of 1 fs and initial velocities generated according to Maxwell distribution. The systems were firstly equilibrated by performing 3×10^6 time steps runs, followed by trajectories of 3×10^6 time steps to calculate diffusivities (production phase).

The diffusion coefficients were computed using the long time limit of the mean square displacement (MSD) by the Einstein relationship [30]:

$$D_{12} = \lim_{t\to\infty} \frac{\left\langle \left[r(t) - r(t_0) \right]^2 \right\rangle}{6t} \tag{3}$$

where t is the elapsed time from the time origin t_0, and r is the position of a particle for each component. The average was carried out over all time origins, and over all tracer molecules. The diffusivity corresponds to the slope of linear MSD *versus* t plot.

Table 3. Number of molecules (*N*) and concentrations (*c*) of ketones used in the MD simulations.

	propanone	butanone	2-pentanone	3-pentanone
N	25	20	17	17
c (%, wt.)	0.82	0.81	0.82	0.82
c (%, mol)	0.62	0.50	0.42	0.42

4. Results and discussion

4.1 Experimental and correlated D_{12} values

To validate the MD diffusivities of ketones in SC-CO_2, they were compared with experimental data taken from literature [10, 49-55]. Despite the large number of existent points (214 for propanone, 40 for butanone, 23 for 2-pentanone, and 46 for 3-pentanone), for some (P,T) conditions there is no data reported. In these cases, the D_{12} values were estimated using the empirical equation tested by Magalhães et al. [17], which relates D_{12}/T with solvent density, ρ_1:

$$D_{12}/T = a\ln(\rho_1) + b \quad (4)$$

This expression was chosen due to its simplicity, small number of parameters involved (2 *per* system), and low deviations achieved: 3.63% for the entire database (8219 data points and 539 binary systems) and, particularly, 3.70% for propanone/CO_2, 1.59% for butanone/CO_2, 1.67% for 2-pentanone/CO_2, and 1.88% for 3-pentanone/CO_2 systems [17].

In the case of propanone/CO_2 system at 323.15 K, the correlated diffusivities exhibited a systematic deviation from experimental data, therefore parameters a and b were refitted to this set of data in order to achieve better results. Concerning 2-pentanone/CO_2 pair, the available data was confined to 308.15, 313.15 and 314.5 K. Nonetheless, Eq. (4) was also used due to its excellent prediction ability, since Magalhães et al. proved that with only two experimental D_{12} values it is possible to obtain parameters for the estimation of reliable diffusivities far away from the conditions of the data used to fit them [17].

In summary, experimental (when existent) and estimated data were used indistinguishably hereafter for comparison with the D_{12} values obtained by MD.

4.2 Cut-off distance, number of solute molecules, integration time step, length of simulations

The MD simulations were performed according to the details provided in section 3. However, some important parameters of the simulation were previously studied in order to find

the best values to achieve accurate results without loss of computational efficiency. For that, a set of complete simulations – 3 ns equilibration followed by 3 ns production phases – varying independently the number of solute molecules and the cut-off distance were carried out and analyzed. Moreover, some tests for the integration time step length, Δt, and total duration of simulation (specifically production phase, used to compute diffusivities) were also accomplished.

***N* of solute.** In tracer diffusivities, only one molecule of solute is theoretically involved. However, for statistical accuracy, a small quantity of solute is actually considered in the simulations (note that the same happens in experimental measurements). The adequate number of ketone molecules should be large enough to minimize uncertainties, but still small to obey infinite dilution restriction. N = 10, 20, 25 and 30 solute molecules were considered in the simulation of propanone/CO_2 system (molar concentrations of 0.25-0.75%) at different conditions, namely for the smaller and larger densities. The 2-pentanone/CO_2 system was also simulated to cover the widest range of molecular sizes of ketones. In the case of propanone in SC-CO_2 at high density (using a fixed 1.2 nm cut-off distance) the results were: for N = 10 the MSD function showed an unsatisfactory linear portion for D_{12} calculation; for N = 20 the diffusivity deviation was 12.1%; for N = 25 a relative deviation of 6.9% was achieved; and for N = 30 the obtained error was 6.3%, suggesting that diffusivity values are already converged for N > 25.

Cut-off distance. The effect of cut-off was evaluated by testing distances of 1.2, 1.4 and 1.6 nm in the computation of D_{12} of propanone and 2-pentanone for the lowest and highest densities. An additional test was made for the self-diffusion of SC-CO_2. Very similar errors were found for 1.4 and 1.6 nm (< 1% on average), but for 1.2 nm the deviations were 3-4% higher than those for 1.4 cut-off simulations. Therefore, 1.4 nm allowed a good compromise between computational efficiency and accuracy.

Integration time step and length of simulation. The maximum time step used for the integration of equations of motion in MD simulations is limited by the smallest oscillation period that can be found in the simulated system. With a small time step, only a small portion of the conformational space is explored, while a large Δt may originate instabilities in the

algorithm due to high energies caused by atoms overlapping. The value of 1 fs is at least one order of magnitude lower than the shortest period of motion (C-H bond stretching frequency of around 10 fs), thus being frequently recommended for this kind of simulations. Due to the imposition of constraint bond lengths with LINCS algorithm ("freezing" bond lengths usually allows to double the time step, which halves the number of calculations required), 2 fs time step simulations were also tested. Since the D_{12} values obtained with Δt = 2 fs were not so precise nor exact, the time step was kept at 1 fs. Besides that, longer production phases were executed to check if simulations were long enough to yield accurate diffusion coefficients. When using the correct time step of 1 fs, doubling the production phase from 3 to 6 ns did not improve results (*i.e.*, diffusivities were similar), just lengthened the linear portion of MSD function used to extract D_{12}. For that reason, the remaining simulations were performed with 3 ns long production phases.

4.3 Diffusivities from molecular dynamics simulations

Table 4 presents temperature and pressure of each simulation, the corresponding CO_2 density obtained from NIST Chemistry WebBook [44], tracer diffusivities calculated for propanone, butanone, 2-pentanone and 3-pentanone, and the absolute relative deviations between them and experimental data (displayed ahead in parenthesis).

The deviations achieved between calculated and experimental diffusivities were generally small, specially taking into account the common errors associated with experimental measurements and the uncertainties of simulated diffusivities. The errors ranged from 0.28% (for 3-pentanone at 164.2 bar and 323.15 K) to 16.17% (for butanone at 164.2 bar and 313.15 K). One may emphasize that some simulations were repeated; for instance three independent runs starting from distinct initial structures (which are already random) were performed in an attempt to understand the larger deviation found for 3-pentanone at 164.2 bar and 323.15 K, but the results remained unaltered.

The quality of the diffusivities originated from the MD simulations may also be evaluated by plotting calculated values against the experimental ones. The comparison can be seen in Fig. 1 and shows a quite low scattering from linearity of the data points. From these observations,

the MD diffusivities may be considered validated due to the good and unbiased distribution of data points along diagonal, and average error of only 5.60%.

The diffusion coefficients depend upon temperature and pressure (or temperature and density). Fig. 2 illustrates such dependencies for propanone in SC-CO_2, though similar trends were observed for the other systems. This plot shows that diffusivity decreases with increasing pressure (or density) at constant temperature, which is consistent with free-volume theories since, at higher densities, the free volume available for diffusion is lower with a concomitant penalization of D_{12} [14, 56]. However, this influence is less important at higher pressures and varies significantly with temperature. On the other hand, at constant pressure, D_{12} increases with *T*. Once again, taking into account free-volume theories, in particular their hybrid models, at higher temperature the molecules possess sufficient energy to escape from the force field of their neighbors and jump between adjacent holes [14, 56]. The pronounced temperature dependency is also potentiated by the augmentation in free volume due to solvent density reduction with increasing *T* [57, 58], *i.e*. both requirements for diffusion to occur are improved.

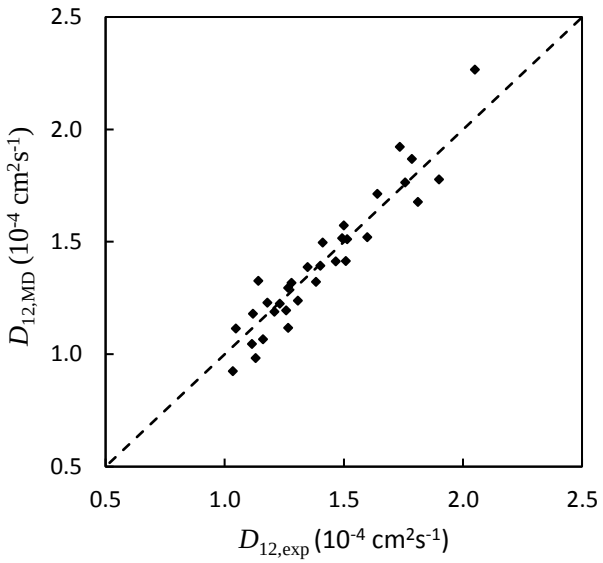

Fig. 1. Experimental *versus* computed (MD) tracer diffusivities of ketones in SC-CO_2.

Table 4. State conditions and simulated diffusivities (10^{-4} cm^2 s^{-1}) of ketones in SC-CO_2.

Variable	State condition							
P (bar)	133.3	164.2	246.0	292.5	133.3	164.2	246.0	292.5
T (K)	313.15	313.15	313.15	313.15	323.15	323.15	323.15	323.15
ρ_1 (g cm^{-3})	0.7502	0.8005	0.8767	0.9057	0.6493	0.7303	0.8308	0.8656
Solute	Tracer diffusivities *							
propanone	1.677 (7.38%)	1.572 (4.72%)	1.387 (2.80%)	1.224 (0.60%)	2.266 (10.49%)	1.868 (4.59%)	1.515 (1.40%)	1.394 (0.54%)
butanone	1.520 (4.96%)	1.326 (16.17%)	1.188 (1.70%)	0.982 (13.08%)	1.777 (6.43%)	1.712 (4.34%)	1.322 (4.42%)	1.295 (2.23%)
2-pentanone	1.496 (6.00%)	1.317 (2.84%)	1.179 (5.36%)	1.113 (6.24%)	1.922 (10.79%)	1.415 (6.22%)	1.194 (5.17%)	1.229 (4.21%)
3-pentanone	1.412 (3.70%)	1.237 (5.34%)	1.045 (6.27%)	0.924 (10.70%)	1.763 (0.32%)	1.510 (0.28%)	1.117 (11.84%)	1.066 (8.22%)

* Absolute relative deviations between MD and experimental diffusivities are displayed in parenthesis.

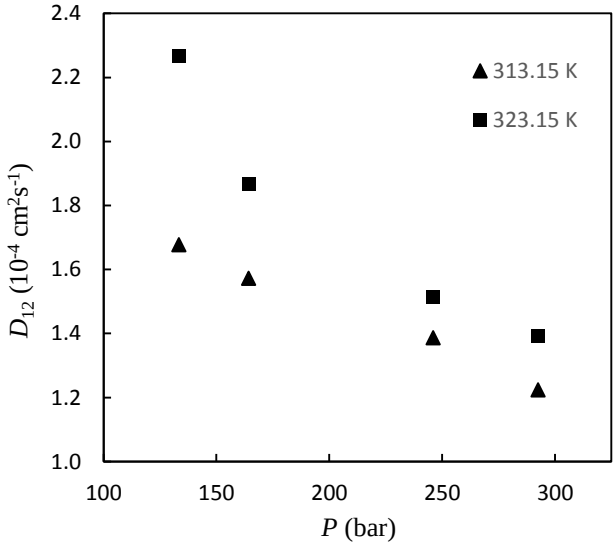

Fig. 2. Molecular dynamics results for propanone in SC-CO_2 at 133.3, 164.2, 246.0 and 292.5 bar, for 313.15 and 323.15 K.

In Fig. 3, the D_{12} values of the different ketones are plotted for four pressures at 323.15 K, just for illustration. For each condition, propanone presents the higher diffusivities, followed by butanone and then pentanones. Since we are dealing with solutes having the same functional group, *i.e.*, the ketone group, the distinctive factor in the solutes considered in this work is the number of carbon atoms in each of the alkyl chains. Accordingly, D_{12} decreases with molecular size: propanone (C3), butanone (C4) and pentanones (C5), respectively. This fact is predicted by several theories of transport, either embodying an inverse dependence of D_{12} upon the solute molecular weight, or its Lennard-Jones diameter, or its molar volume (normally evaluated at normal boiling point), as it is frequently expressed by hydrodynamic equations [9, 19, 59]. This is expected since a larger or bulkier solute will tend to diffuse at a lower rate under comparable conditions [9, 57].

Concerning the two pentanones, despite their carbon chain presents the same size, the position of the carbonyl group makes them diffuse differently, as MD predicts. Taking into account the similarity between 2-pentanone and 3-pentanone, and the experimental errors involved in the D_{12} measurement, such small difference is not captured by the diffusivity values available in the literature.

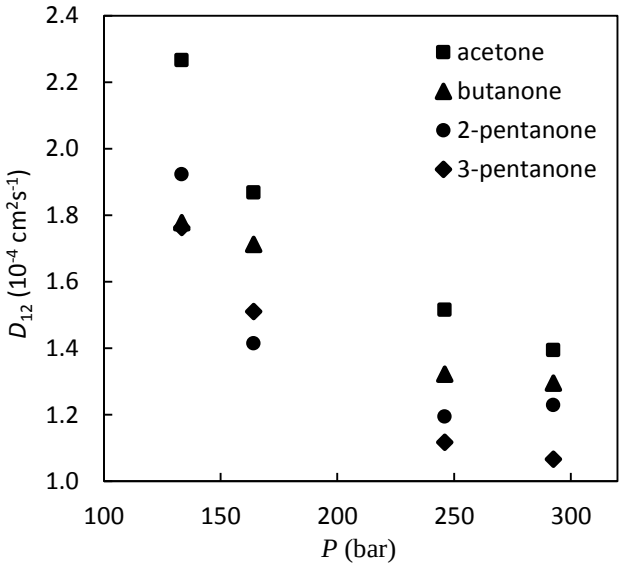

Fig. 3. Molecular dynamics results for propanone, butanone, 2-pentanone and 3-pentanone in SC-CO_2 at 164.2, 246.0 and 292.5 bar, and 323.15 K.

Structural analysis. The results obtained in this work for tracer diffusivities of ketones in SC-CO_2 were further investigated and related to structural properties of the same systems. Based on the computed trajectories to determine D_{12}, the radial distribution functions or pair correlation functions, $g(r)$, and the corresponding coordination numbers, $n(r)$, were also calculated.

The radial distribution function is computed between a central particle A and the surrounding particles B, giving a measure of the probability of finding particles B at a distance r from A. Averaging over all particles A, the $g(r)$ gives us a correction to the average local density (by the presence of particles B) around particles A. To understand how CO_2 molecules distribute around ketone molecules, the central particles chosen were $C_{C=O}$, $O_{C=O}$, C_{CH_2} (whenever applicable), and C_{CH_3}. C atoms from CH_2 and CH_3 groups were also distinguished for asymmetric ketones; for example 2-pentanone has a CH_2 connected to C=O group which is different from the CH_2 connected to CH_3 group. Pair correlation functions were computed between each one of these atoms and C or O from CO_2, depending on the central particle (O or

C from ketones, respectively). For simplicity, only the central atom will be identified henceforth, taking into consideration that the surrounding particles represent CO_2 in all cases.

In Fig. 4, radial distribution functions for propanone are represented at 313.15 K and 164.2 bar (corresponding to 0.8005 g.cm^{-3}, an intermediate density among the simulated conditions), without loss of generality. Each one of the central atoms is identified and, as it can be seen, the resulting $g(r)$ for $O_{C=O}$ presents a first peak at short distances (first solvation shell at ~0.31 nm) followed by a smaller one at larger distances (second solvation shell at ~0.64 nm); the $g(r)$ for C_{CH_3} possesses also two reduced peaks which are close together (with maxima at 0.37 and 0.53 nm); and the $g(r)$ for $C_{C=O}$ shows only a single defined peak with maximum at 0.45 nm, which is much broader than the previous ones. Also in Fig. 4, the same functions are represented for a higher temperature (dashed line: P = 164.2 bar, T = 323.15 K, and ρ_1 = 0.7303 g.cm^{-3}) in order to evaluate the temperature effect on structural properties. Despite this variable greatly affects diffusion, it weakly influences $g(r)$, as already noticed by Wang et al. [22] for alkylbenzenes in SC-CO_2 at 313, 323 and 333 K; the peak maxima are slightly higher with increasing temperature but the shape of the curves is kept unchanged.

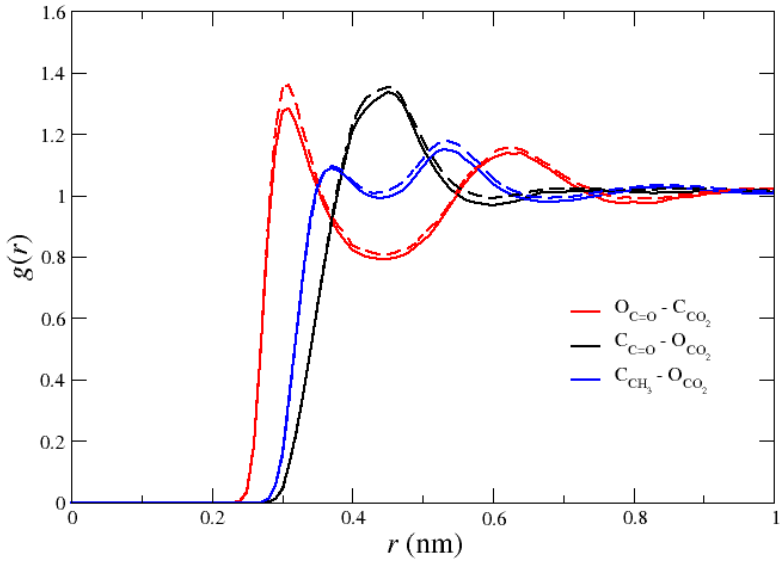

Fig. 4. Radial distribution functions for propanone in SC-CO_2 at 164.2 bar, and 313.15 K (full line) and 323.15 K (dashed line).

The effect of pressure (and thus density) on structural properties was evaluated using $C_{C=O}$ of propanone as example (see Fig. 5). The $g(r)$ for the three pressures (133.3, 164.2 and 246.0 bar) at constant temperature (313.15 K) are included, and the differences observed were quite small, as occurred above with temperature. Nonetheless, the effect upon $g(r)$ followed an opposite direction, with maximum peak height slightly falling with pressure (or density) increase. The shape of the curves is, however, unaltered, and the maximum and minimum locations are the same.

The radial distribution functions concerning the interaction between CO_2 and atoms in the ketone functional group of the four compounds considered in this work at 313.15 K and 164.2 bar are represented in Fig. 6.

Analyzing the curves for interactions $C_{C=O} - O_{CO_2}$ (Fig 6a) one may observe that propanone presents both well defined peak and minimum well at *r* values of approximately 0.45 nm, butanone has an additional CH_2 which results in a less pronounced peak, the even longer 2-pentanone has a decrease in the peak intensity, and the $g(r)$ for 3-pentanone presents also a decrease in the intensity of the peak and a closer second peak. Generally speaking, the increasing molecular size tends to transform a sharp and well defined $g(r)$ into more diffuse and broader functions, which once again agrees with the observations of Wang el al. [22] for alkylbenzenes with rising carbon chain size. Notice that the decrease of the intensity of the first peak in the $g(r)$ is accompanied by a tiny shift (up to 0.02 nm) of the peak maxima to smaller values of *r* (cf. inset in Fig. 6), which suggests that less carbon dioxide molecules are interacting with the ketone group but that on average they are closer.

The $g(r)$ for the interaction $O_{C=O} - O_{CO_2}$ (see Fig. 6b) shows two very well defined peaks in the case of the four ketones considered in this work, with the first of the peaks appearing at *r* values of approximately 0.31 nm and the second at 0.62 – 0.64 nm. These results show clearly the formation of two shells of carbon dioxide surrounding the ketone's oxygen atom. Furthermore, the curves in the two panels of Fig. 6 suggest a preferential interaction of the carbon dioxide through its carbon atom with the ketone's oxygen atom and that the peak in Fig. 6a is a consequence of such interaction.

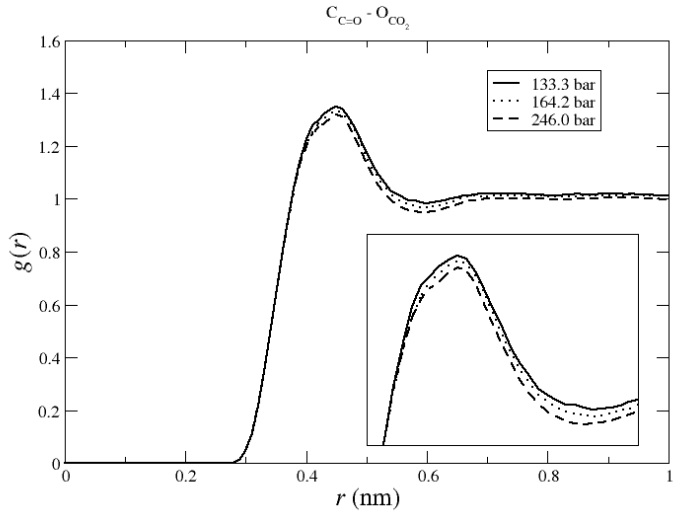

Fig. 5. Radial distribution functions for the pair $C_{C=O} - O_{CO_2}$ of propanone in SC-CO_2 at 313.15 K for 133.3, 164.2 and 246.0 bar. The inset is a magnification of the peak maxima.

Based on all $g(r)$ functions and on the *r* values corresponding to their first maxima (see Fig. 7), some conclusions may be drawn. First of all, the distance for which C_{CH_3} presents a maximum is similar between ketones (0.36 – 0.38 nm). By adding the approximate distance of simple C–C bonds (~0.14 nm) one gets a range of 0.50 – 0.52 nm, which matches the distance found for the maxima of C_{CH_2} (bonded with C_{CH_3}) for butanone and 3-pentanone. Then, the O_{CO_2} is mainly interacting with the terminal carbon atoms, and the results observed for C_{CH_2} connected to them are merely a reflex of the former. Similarly, the $O_{C=O}$ always presents an intense peak at around 0.31 nm (not represented for clarity), while the maxima for $C_{C=O}$ occur at a bigger distance (0.45 nm) for all ketones. Taking into account that, for C_{CH_2} connected to the C=O group, the distances for the peak maxima are 0.52, 0.54 and 0.50 nm for butanone, 2-pentanone and 3-pentanone, respectively, it suggests that the interactions observed between CO_2 and $C_{C=O}$ are actually a consequence of the interaction that CO_2 establishes with $O_{C=O}$ (otherwise, distances between such C_{CH_2} and CO_2 would be smaller). In the whole, CO_2 interacts similarly with all ketones considered, and that interactions are of the type $O_{CO_2} - C_{CH_3}$ and $C_{CO_2} - O_{C=O}$.

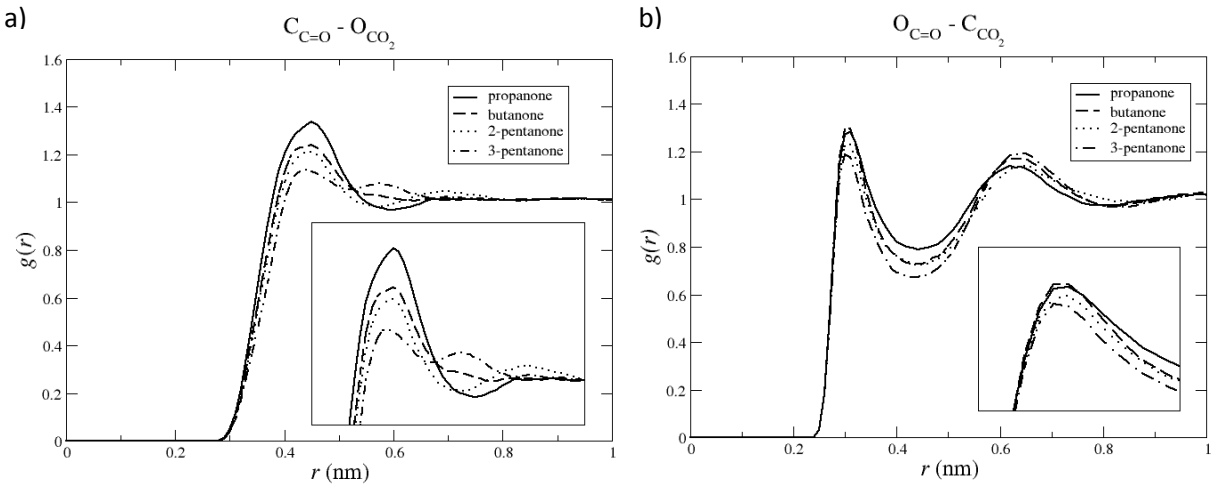

Fig. 6. Radial distribution functions for the interactions $C_{C=O} - O_{CO_2}$ (a) and $O_{C=O} - O_{CO_2}$ (b) of the different ketones in SC-CO_2, at 313.15 K and 164.2 bar. The insets are magnifications of the peaks.

Concerning coordination numbers, they provide the number of nearest neighbors relative to the central atom, usually counted up to the first minimum of $g(r)$ according to

$$n(r) = 4\pi\rho \int_0^{r_{min}} g(r) r^2 dr \qquad (5)$$

where r is the radial position from the central particle, and r_{min} is the position of the first minimum of $g(r)$. This quantity is, therefore, a measure of the size of the first solvation shell around the central particle.

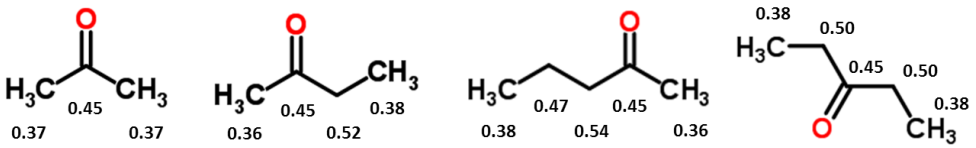

Fig. 7. Maximum peak height distances for radial distribution functions of the pairs C_{ketone} - O_{CO_2}. The values are represented near the corresponding central atom (C_{CH_3}, C_{CH_2} and $C_{C=O}$) in each molecular structure.

The coordination numbers were computed for the radial distribution functions identified above. However, the $n(r)$ results for C atoms from CH_2 and CH_3 groups are not presented due their similarity between ketones. For example, at 313.15 K and 164.2 bar, the first (near carbonyl) C_{CH_3} of propanone, butanone and 2-pentanone have $n(r)$ of 2.50, 2.58 and 2.52 for the first coordination shell, respectively. Given that, our attention is focused on C and O from C=O group of each ketone. As already mentioned, for $C_{C=O}$ we studied its interaction with O_{CO_2}, and for $O_{C=O}$ the interest is on C_{CO_2} (but both represent the neighborhood of CO_2 molecules).

Afterwards, the coordination numbers of C and O from C=O of the different ketones for an intermediate density (to set an example) are shown in Table 5. From propanone to butanone, $n(r)$ of $C_{C=O}$ decreases from 5.14 to 4.78 due to the existence of an additional methyl group that reduces the number of CO_2 molecules existent inside a similar coordination shell (same radius/distance) around the central atom. Moving now to 2-pentanone, a reduction in $n(r)$ is also perceived (from 4.78 to 4.23) and may be caused similarly by the existence of another ethyl group. Finally, from 2-pentanone to 3-pentanone, there is a large decrease of the $n(r)$ of CO_2 around $C_{C=O}$ (4.63 to 3.30), which is justified by the existence of bulkier groups in both sides of the central atom, reducing the presence of CO_2 in their coordination shell. In the case of $O_{C=O}$, the coordination number follows a similar trend, *i.e*. it reduces with increasing molecular size: diminish in the order propanone, butanone, 2-pentanone and 3-pentanone (2.89, 2.76, 2.70 and 2.52, respectively). In general, the reduction in coordination numbers is due to the elongation of the molecular chain, which is the dominant effect explaining the differences in tracer diffusivities, *i.e.* larger molecules diffuse slower.

Table 5. Coordination numbers of CO_2 around C and O from carbonyl group of each ketone, at 313.15 K and 164.2 bar.

Central atom	Propanone	Butanone	2-pentanone	3-pentanone
$C_{C=O}$	5.14	4.78	4.23	3.30
$O_{C=O}$	2.89	2.76	2.70	2.52

5. Conclusions

In this essay, MD simulations were performed to compute tracer diffusion coefficients of ketones (propanone, butanone, 2-pentanone and 3-pentanone) in SC-CO_2. The obtained diffusivities were validated by comparison with experimental data, being found an average deviation of 5.60%. Such good agreement proves the reliability of MD to predict D_{12} of ketones in SC-CO_2.

The influence of solute properties and operating conditions upon D_{12} values was assessed: the tracer diffusivity is enhanced by decreasing CO_2 pressure (or density) and/or augmenting temperature, while it decays according to the molecular size of the solute. These trends are corroborated by the most important transport theories, like free-volume approaches.

The local structures of ketone/SC-CO_2 systems were further investigated by computing radial distribution functions and coordination numbers around each group composing solute molecules. From the computed $g(r)$ functions, the number of peaks (corresponding to consecutive coordination shells) and their shape change according to the central atom considered (C from CH_2, CH_3 or C=O groups, and O from C=O). The shape of the functions was also analyzed according to CO_2 pressure (or density) and temperature, but a small influence was perceived upon $g(r)$. In contrast, when comparing results for propanone, butanone, 2-pentanone and 3-pentanone, the sharp and well defined $g(r)$ observed for the smaller ketone become more diffuse and broader as molecular size increases. It was found that the molecular structuring of the solvent around the solute is similar, and that the decrease of the coordination numbers on going from propanone to the pentanones is due to the molecular chain growing. Then, the calculated diffusivities of the solutes are not influenced by molecular structure specificities, but affected by the size and volume of the diffusing molecule.

In the whole, MD offers a useful and simple tool to investigate molecular behavior of simple molecules in SC-CO_2, enabling accurate D_{12} predictions and providing useful information to understand the local interactions at molecular level that rule the dynamics of the system.

Nomenclature

a	Parameter of Eq. (4)
b	Parameter of Eq. (4)
c	Mass concentration
D_{11}	Self-diffusion coefficient
D_{12}	Tracer diffusion coefficient of solute (2) through solvent (1)
EPM2	Elementary Physical Model
$g(r)$	Radial distribution function or pair correlation function
k_θ	Bond bending force constant
l_0	Equilibrium bond length
LJ	Lennard-Jones
MD	Molecular dynamics
MSD	Mean square displacement
N	Number of molecules
NVT	Canonical ensemble
$n(r)$	Coordination number
OPLS-AA	Optimized Potentials for Liquid Simulation – All Atoms
P	Pressure
PME	Particle-mesh Ewald
q	Charge parameter
r	Particle distance; position of the particle
$r_{\min}$	Position of the first minimum of $g(r)$
SC-CO_2	Supercritical carbon dioxide
SCF	Supercritical fluids
t	Time
T	Absolute temperature
t_0	Time origin or initial time

V	Volume
$V_{\text{non-bonded}}$	Intermolecular potential
wt	Weight

Greek letters

Δt	Integration time step
ε	Energy parameter
ε_0	Permittivity of free space
θ_0	Equilibrium bond angle
ρ	Number density
σ	Size parameter

Subscripts

1	Solvent (SC-CO_2)
2	Solute
12	Binary

Superscripts

exp	Experimental value
MD	Value from molecular dynamics simulation

References

[1] G. Brunner, Applications of Supercritical Fluids, in: J.M. Prausnitz, M.F. Dohert, M.A. Segalman (Eds.) Annual Review of Chemical and Biomolecular Engineering, Vol. 1, 2010, pp. 321-342.

[2] M.M.R. de Melo, A.J.D. Silvestre, C.M. Silva, Supercritical fluid extraction of vegetable matrices: applications, trends and future perspectives of a convincing green technology, The Journal of Supercritical Fluids, 92 (2014) 115-176.

[3] M.M.R. de Melo, R.M.A. Domingues, A.J.D. Silvestre, C.M. Silva, Extraction and purification of triterpenoids using supercritical fluids: from lab to exploitation, Mini-Reviews in Organic Chemistry, 11 (2014) 362-381.

[4] E.L.G. Oliveira, A.J.D. Silvestre, C.M. Silva, Review of kinetic models for supercritical fluid extraction, Chemical Engineering Research and Design, 89 (2011) 1104-1117.

[5] P.C. Wankat, Rate-Controlled Separations, Blackie Academic and Professional, Glasgow, UK, 1994.

[6] R. Taylor, R. Krishna, Multicomponent Mass Transfer, John Wiley & Sons, Inc, New York, 1993.

[7] C.Y. Kong, T. Siratori, G. Wang, T. Sako, T. Funazukuri, Binary diffusion coefficients of platinum(II) acetylacetonate in supercritical carbon dioxide, Journal of Chemical and Engineering Data, 58 (2013) 2919-2924.

[8] C.A. Filho, C.M. Silva, M.B. Quadri, E.A. Macedo, Infinite dilution diffusion coefficients of linalool and benzene in supercritical carbon dioxide, Journal of Chemical & Engineering Data, 47 (2002) 1351-1354.

[9] K.K. Liong, P.A. Wells, N.R. Foster, Diffusion in supercritical fluids, The Journal of Supercritical Fluids, 4 (1991) 91-108.

[10] C.Y. Kong, T. Funazukuri, S. Kagei, Chromatographic impulse response technique with curve fitting to measure binary diffusion coefficients and retention factors using polymer-coated capillary columns, Journal of Chromatography A, 1035 (2004) 177-193.

[11] T. Funazukuri, C.Y. Kong, S. Kagei, Binary diffusion coefficients in supercritical fluids: Recent progress in measurements and correlations for binary diffusion coefficients, The Journal of Supercritical Fluids, 38 (2006) 201-210.

[12] J. Millat, J.H. Dymond, C.A. Nieto de Castro, Transport Properties of Fluids – Their Correlation Prediction and Estimation, Cambridge University Press, London, 1996.

[13] H. Liu, C.M. Silva, E.A. Macedo, New equations for tracer diffusion coefficients of solutes in supercritical and liquid solvents based on the Lennard-Jones fluid model, Industrial and Engineering Chemistry Research, 36 (1997) 246-252.

[14] C.M. Silva, H. Liu, Modelling of Transport Properties of Hard Sphere Fluids and Related Systems, and its Applications, in: Á. Mulero (Ed.) Theory and Simulation of Hard-Sphere Fluids and Related Systems, Springer Berlin Heidelberg, 2008, pp. 383-492.

[15] A.L. Magalhães, S.P. Cardoso, B.R. Figueiredo, F.A. Da Silva, C.M. Silva, Revisiting the Liu-Silva-Macedo model for tracer diffusion coefficients of supercritical, liquid, and gaseous systems, Industrial and Engineering Chemistry Research, 49 (2010) 7697-7700.

[16] A.L. Magalhães, F.A. Da Silva, C.M. Silva, New models for tracer diffusion coefficients of hard sphere and real systems: Application to gases, liquids and supercritical fluids, The Journal of Supercritical Fluids, 55 (2011) 898-923.

[17] A.L. Magalhães, P.F. Lito, F.A. Da Silva, C.M. Silva, Simple and accurate correlations for diffusion coefficients of solutes in liquids and supercritical fluids over wide ranges of temperature and density, The Journal of Supercritical Fluids, 76 (2013) 94-114.

[18] P.F. Lito, A.L. Magalhães, J.R.B. Gomes, C.M. Silva, Universal model for accurate calculation of tracer diffusion coefficients in gas, liquid and supercritical systems, Journal of Chromatography A, 1290 (2013) 1-26.

[19] R.V. Vaz, A.L. Magalhães, C.M. Silva, Improved hydrodynamic equations for the accurate prediction of diffusivities in supercritical carbon dioxide, Fluid Phase Equilibria, 360 (2013) 401-415.

[20] R.V. Vaz, A.L. Magalhães, C.M. Silva, Prediction of binary diffusion coefficients in supercritical CO_2 with improved behavior near the critical point, The Journal of Supercritical Fluids, 91 (2014) 24-36.

[21] Y. Iwai, H. Higashi, H. Uchida, Y. Arai, Molecular dynamics simulation of diffusion coefficients of naphthalene and 2-naphthol in supercritical carbon dioxide, Fluid Phase Equilibria, 127 (1997) 251-261.

[22] J. Wang, H. Zhong, H. Feng, W. Qiu, L. Chen, Molecular dynamics simulation of diffusion coefficients and structural properties of some alkylbenzenes in supercritical carbon dioxide at infinite dilution, The Journal of Chemical Physics, 140 (2014) 104501.

[23] T. Funazukuri, C.Y. Kong, S. Kagei, Impulse response techniques to measure binary diffusion coefficients under supercritical conditions, Journal of Chromatography A, 1037 (2004) 411-429.

[24] R.V. Vaz, A.L. Magalhães, C.M. Silva, Improved Stokes–Einstein based models for diffusivities in supercritical CO_2, Journal of the Taiwan Institute of Chemical Engineers, 45 (2014) 1280-1284.

[25] A.L. Magalhães, R.V. Vaz, R.M.G. Gonçalves, F.A. Da Silva, C.M. Silva, Accurate hydrodynamic models for the prediction of tracer diffusivities in supercritical carbon dioxide, The Journal of Supercritical Fluids, 83 (2013) 15-27.

[26] C.H. He, Y.S. Yu, W.K. Su, Tracer diffusion coefficients of solutes in supercritical solvents, Fluid Phase Equilibria, 142 (1998) 281-286.

[27] O.J. Catchpole, M.B. King, Measurement and correlation of binary diffusion coefficients in near critical fluids, Industrial and Engineering Chemistry Research, 33 (1994) 1828-1837.

[28] W. Xu, J. Yang, Y. Hu, Microscopic Structure and Interaction Analysis for Supercritical Carbon Dioxide-Ethanol Mixtures: A Monte Carlo Simulation Study, The Journal of Physical Chemistry B, 113 (2009) 4781-4789.

[29] H. Feng, W. Gao, Z. Sun, B. Lei, G. Li, L. Chen, Molecular dynamics simulation of diffusion and structure of some *n*-alkanes in near critical and supercritical carbon dioxide at infinite dilution, The Journal of Physical Chemistry B, 117 (2013) 12525-12534.

[30] A. Leach, Molecular Modelling: Principles and Applications, 2nd ed., Prentice Hall, 2001.

[31] M. Fermeglia, S. Pricl, Equation-of-state parameters for pure polymers by molecular dynamics simulations, AIChE Journal, 45 (1999) 2619-2627.

[32] M.L.S. Batista, J.A.P. Coutinho, J.R.B. Gomes, Prediction of ionic liquids properties through molecular dynamics simulations, Current Physical Chemistry, 4 (2014) 151-172.

[33] H. Higashi, K. Tamura, Calculation of diffusion coefficient for supercritical carbon dioxide and carbon dioxide+naphthalene system by molecular dynamics simulation using EPM2 model, Molecular Simulation, 36 (2010) 772-777.

[34] J.H. Yoo, A. Breitholz, Y. Iwai, K.P. Yoo, Diffusion coefficients of supercritical carbon dioxide and its mixtures using molecular dynamic simulations, Korean Journal of Chemical Engineering, 29 (2012) 935-940.

[35] J.G. Harris, K.H. Yung, Carbon dioxide's liquid-vapor coexistence curve and critical properties as predicted by a simple molecular model, The Journal of Physical Chemistry, 99 (1995) 12021-12024.

[36] P. Parris, Molecular Simulation Studies in the Supercritical Region, in: Department of Chemical Engineering, University College London, London, WC1E 7JE, 2010.

[37] J. Vorholz, V.I. Harismiadis, B. Rumpf, A.Z. Panagiotopoulos, G. Maurer, Vapor+liquid equilibrium of water, carbon dioxide, and the binary system, water+carbon dioxide, from molecular simulation, Fluid Phase Equilibria, 170 (2000) 203-234.

[38] W.L. Jorgensen, D.S. Maxwell, J. Tirado-Rives, Development and testing of the OPLS all-atom force field on conformational energetics and properties of organic liquids, Journal of the American Chemical Society, 118 (1996) 11225-11236.

[39] N.A. McDonald, W.L. Jorgensen, Development of an all-atom force field for heterocycles. Properties of liquid pyrrole, furan, diazoles, and oxazoles, The Journal of Physical Chemistry B, 102 (1998) 8049-8059.

[40] R.C. Rizzo, W.L. Jorgensen, OPLS all-atom model for amines: Resolution of the amine hydration problem, Journal of the American Chemical Society, 121 (1999) 4827-4836.

[41] E.K. Watkins, W.L. Jorgensen, Perfluoroalkanes: Conformational analysis and liquid-state properties from ab initio and Monte Carlo calculations, Journal of Physical Chemistry A, 105 (2001) 4118-4125.

[42] G.A. Kaminski, R.A. Friesner, J. Tirado-Rives, W.L. Jorgensen, Evaluation and reparametrization of the OPLS-AA force field for proteins via comparison with accurate quantum chemical calculations on peptides, The Journal of Physical Chemistry B, 105 (2001) 6474-6487.

[43] B. Hess, C. Kutzner, D. van der Spoel, E. Lindahl, GROMACS 4: Algorithms for Highly Efficient, Load-Balanced, and Scalable Molecular Simulation, Journal of Chemical Theory and Computation, 4 (2008) 435-447.

[44] E.W. Lemmon, M.O. McLinden, D.G. Friend, Thermophysical Properties of Fluid Systems, in: P.J. Linstrom, W.G. Mallard (Eds.) NIST Chemistry WebBook, National Institute of Standards and Technology, Gaithersburg MD, 2011.

[45] W.G. Hoover, Canonical dynamics: Equilibrium phase-space distributions, Physical Review A, 31 (1985) 1695-1697.

[46] S. Nosé, A molecular dynamics method for simulations in the canonical ensemble, Molecular Physics, 52 (1984) 255-268.

[47] U. Essmann, L. Perera, M.L. Berkowitz, T. Darden, H. Lee, L.G. Pedersen, A smooth particle mesh Ewald method, The Journal of Chemical Physics, 103 (1995) 8577-8593.

[48] R.W. Hockney, S.P. Goel, J.W. Eastwood, Quiet high-resolution computer models of a plasma, Journal of Computational Physics, 14 (1974) 148-158.

[49] P.R. Sassiat, P. Mourier, M.H. Caude, R.H. Rosset, Measurement of diffusion coefficients in supercritical carbon dioxide and correlation with the equation of Wilke and Change, Analytical Chemistry, 59 (1987) 1164-1170.

[50] T. Funazukuri, C.Y. Kong, S. Kagei, Infinite-dilution binary diffusion coefficients of 2-propanone, 2-butanone, 2-pentanone, and 3-pentanone in CO_2 by the Taylor dispersion technique from 308.15 to 328.15 K in the pressure range from 8 to 35 MPa, International Journal of Thermophysics, 21 (2000) 1279-1290.

[51] T. Funazukuri, C.Y. Kong, S. Kagei, Binary diffusion coefficients of acetone in carbon dioxide at 308.2 and 313.2 K in the pressure range from 7.9 to 40 MPa, International Journal of Thermophysics, 21 (2000) 651-669.

[52] H. Nishiumi, M. Fujita, K. Agou, Diffusion of acetone in supercritical carbon dioxide, Fluid Phase Equilibria, 117 (1996) 356-363.

[53] J.J. Suárez, I. Medina, J.L. Bueno, Diffusion coefficients in supercritical fluids: Available data and graphical correlations, Fluid Phase Equilibria, 153 (1998) 167-212.

[54] T. Funazukuri, Measurements of binary diffusion coefficients of 20 organic compounds in CO2 at 313.2K and 16.0 MPa, Journal of Chemical Engineering of Japan, 29 (1996) 191-192.

[55] N. Dahmen, A. Dülberg, G.M. Schneider, Determination of Binary Diffusion Coefficients in Supercritical Carbon Dioxide with Supercritical Fluid Chromatography (SFC), Berichte der Bunsengesellschaft für physikalische Chemie, 94 (1990) 384-386.

[56] H. Liu, C.M. Silva, E.A. Macedo, Generalised free-volume theory for transport properties and new trends about the relationship between free volume and equations of state, Fluid Phase Equilibria, 202 (2002) 89-107.

[57] C.M. Silva, C.A. Filho, M.B. Quadri, E.A. Macedo, Binary diffusion coefficients of α-pinene and β-pinene in supercritical carbon dioxide, The Journal of Supercritical Fluids, 32 (2004) 167-175.

[58] C.A. Filho, C.M. Silva, M.B. Quadri, E.A. Macedo, Tracer diffusion coefficients of citral and D-limonene in supercritical carbon dioxide, Fluid Phase Equilibria, 204 (2003) 65-73.

[59] R.C. Reid, J.M. Prausnitz, B.E. Poling, The Properties of Gases and Liquids, 5th ed., McGraw-Hill Professional, New York, 2001.

5 Experimental setup and procedure

Transport and thermodynamic properties are fundamental in the design and/or simulation of processes involving supercritical fluids (SCFs). Nevertheless, the last ones are frequently studied in the literature while diffusivities are recognizably needed but still commonly unavailable. Particularly, tracer diffusion coefficients, D_{12}, are required in rate-controlled processes, not only to systems at infinite dilution, but also for subsequent prediction of the necessary coefficients for the concentrations found in real solutions [1, 2]. Diffusivity values in the range of current applications of interest may be obtained experimentally, calculated *via* computer simulations or estimated by phenomenological models. Despite the importance and utility of the last two methods to complement and somewhat replace experimental data, measurements are always needed. It is the reliable method to obtain trustworthy values, which are in turn the basis to devise and/or validate models and even computer simulations.

Diffusion coefficients in SCFs are experimentally assessed by several techniques, which generally consist of adapted methodologies originally developed for gases, dense gases, and liquids: photo-correlation spectroscopy, geometric method, and chromatographic techniques [3]. The latest is the most popular one due to execution facility [3], and it has been highly applied in the last decades in the measurement of diffusivities in supercritical systems.

The chromatographic method was also used in this work to measure tracer diffusion coefficients. For that, a new experimental set-up was designed, assembled and tested, in order

to carry out experiments to obtain diffusion coefficients in liquid and supercritical fluids, using pure solvents or mixtures. This chapter initiates with a description of the theoretical background of this technique, where the principles of the method are presented, together with the main equations describing the involved phenomena and procedure to determine D_{12}. Subsequently, the experimental apparatus is described in detail, along with the calibrations accomplished to obtain all the necessary information for the successful implementation of the method in order to determine trustful diffusivity values. Finally, the experimental procedure adopted is presented.

5.1 Theoretical background

The original chromatographic method is rigorously called chromatographic peak broadening technique (CPB), and is commonly known as Tayler dispersion method. It owes its name to the fundamental work of Taylor [4-6], later developed and formalized by Aris [7], describing the dispersion of a solute in a laminar steady-state flow of a solvent through a circular tube. Giddings and Seager [8] firstly employed this method to measure diffusion coefficients in gaseous mixtures at low pressures, being subsequently extended to dense gases, liquid and supercritical systems.

This method is a transient response technique, generally offering advantages over methods conducted under steady-state conditions, because the D_{12} measurement requires the injection of small quantities and shorter run times. Thus, the Taylor dispersion method is quite accurate [9], and less time-consuming [3, 9] than steady state methods.

In this transient method, a delta or delta-like function of solute pulse is injected into a flowing solvent, and the response is measured at a point downstream (see Fig. 1). The injected peak will broaden due to the combined action of convection parallel to the axis and molecular diffusion in the radial direction (in this application the axial dispersion is always negligible, which is ensured by a large longitudinal Peclet number, $\mathrm{Pe}_x = u_0 L / D_{12}$, where u_0 is the average linear velocity of the solute, and L is the length of the tube). Thus, the broadening of the injected peak is a measure of the mutual diffusion coefficient, and its value is obtained from the difference in the variances between the two points. If diffusion is insignificant, only convection

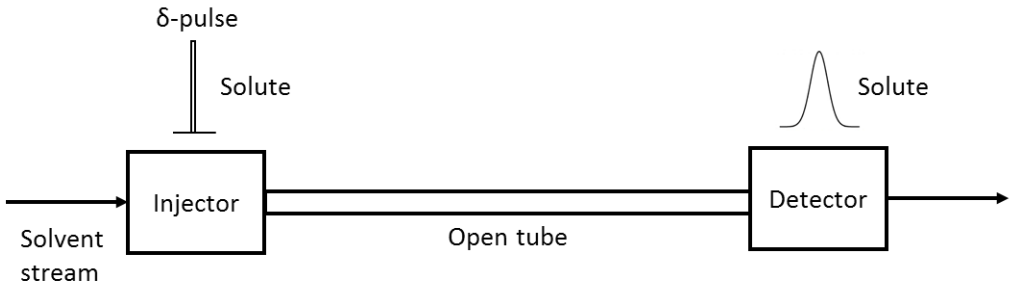

Fig. 1 Schematic diagram of the chromatographic method.

parallel to the axis is present and the delta-like injected pulse will transform into a widely dispersed peak. On the other hand, if the solute possesses an enormous diffusivity, it will sample all different stream lines in a short period of time, and the parabolic profile will not be developed since molecules move with the average speed; the detector will consequently show an intact sharp pulse at the outlet. Situations in between these two will lead to different diffusion coefficients that are quantified through the analysis of the peak variance.

The mathematical description of the solute concentration profile in the column is obtained from the mass balance combined with Fick's first law:

$$D_{12}\left(\frac{\partial^2 c}{\partial r^2}+\frac{1}{r}\frac{\partial c}{\partial r}\right)=\frac{\partial c}{\partial t}+2u_0\left(1-\frac{r^2}{R^2}\right)\frac{\partial c}{\partial z} \tag{1}$$

where c is the concentration of the solute, R is the inner radius of the dispersion tube, t is the time, and r and z are the radial and axial distances, respectively. The axial diffusion term was ignored due to the enormous time for convection in comparison with time for diffusion (large Pe_x, as already mentioned).

The initial and boundary conditions to solve Eq. (1) are given by:

$$c=\frac{m}{\pi R^2}\delta(z), \quad \text{at} \quad t=0 \tag{2}$$

$$\frac{\partial c}{\partial r}=0, \quad \text{at} \quad r=0 \quad \text{and} \quad r=R \tag{3}$$

$$c=0, \quad \text{at} \quad z=\infty \tag{4}$$

where m is the total mass of the solute injected. If we define the average concentration in the cross section of the tube as

$$C(z,t) = \frac{2}{R^2}\int_0^R c(r,z,t)\, r\, dr \tag{5}$$

and apply it to calculate the solute distribution along the tube on Eq. (1), the asymptotic behavior of the last is described by the axial dispersion model, as shown by Taylor [4] and Aris [7]:

$$\frac{\partial C_{app}}{\partial t} + u_0 \frac{\partial C_{app}}{\partial z} = D\frac{\partial^2 C_{app}}{\partial z^2} \tag{6}$$

Here, C_{app} is the approximate average concentration of the solute, and D is a dispersion coefficient that combines the effects of the parabolic axial profile and radial molecular diffusion, according to:

$$D = D_{12} + \frac{R^2 {u_0}^2}{48 D_{12}} \tag{7}$$

Thus, the first two terms in Eq. (6) represent a plug flow in unsteady state, and the right hand side term corresponds to a diffusive mechanism. The relation patent in Eq. (7) predicts that increasing velocity and/or column diameter the dispersion growths, while a larger molecular diffusion has a negative effect provided that $R^2 {u_0}^2 / (48 D_{12}) >> D_{12}$.

The solution of Eq. (6) is known [10]:

$$C_{app}(z,t) = \frac{m}{\pi R^2}\frac{1}{2\sqrt{\pi D t}}\exp\left[-\frac{(z-u_0 t)^2}{4Dt}\right] \tag{8}$$

The concentration profile inside the diffusion column given by Eq. (8) represents the Gaussian peak that is expected at $z = L$, and can be directly or indirectly used to calculate D_{12} by several approaches. Nevertheless, their validity depends on the fulfillment of some restrictions.

First of all, to ensure that the concentration profile resulting from the dispersion of the injected pulse is Gaussian, Levenspiel and Smith [11] shown that the following condition must apply:

$$\frac{D}{u_0 L} < 0.01 \tag{9}$$

Furthermore, the validity of the above mentioned equations is rigorously restricted to straight tubes. In practice, long tubes must be coiled to fit the oven or bath in which they are

placed to maintain the desired temperature. Consequently, centrifugal forces may cause a secondary flow in the cross section of the tube, which may be neglected for high values of the curvature ratio. To ensure that, some quantities must be taken into consideration, namely the dimensionless Reynolds and Schmidt numbers, $\mathrm{Re} = 2\rho_1 u_0 R/\eta_1$ and $\mathrm{Sc} = \eta_1/(\rho_1 D_{12})$, respectively, where ρ_1 and η_1 are the density and viscosity of the solvent, correspondingly, and a curvature ratio, $\lambda = R_c/R$, where R_c is the tube coil radius. It has been shown that these variables are not independent at all conditions, and thus the restriction to satisfy is

$$\mathrm{De}\sqrt{\mathrm{Sc}} < 10 \tag{10}$$

where $\mathrm{De} = \mathrm{Re}/\sqrt{\lambda}$ is the Dean number which expresses the relation between centrifugal and inertial forces. This criterion proposed by Moulijn [12] and Alizadeh et al. [13] guarantees negligible secondary flow effects, although Funazukury and co-workers [10, 14] are more conservative and frequently recommend $\mathrm{De}\sqrt{\mathrm{Sc}} < 8$ to ensure D_{12} errors inferior to 1%.

Besides that, van der Lann [15] defined that one may neglet temperature/pressure perturbations in small tubing portions outside the oven/bath (for instance, connection between the diffusion column and the detector) when

$$\frac{u_0 L}{D} > 1000 \tag{11}$$

Taking into consideration the overhead information that diffusion depends (inversely) on the broadening of the peak, the variance of the response curve, σ^2, may then be used to obtain diffusivities:

$$\sigma^2 = \frac{2DL}{u_0} = \frac{2D_{12}L}{u_0} + \frac{R^2 u_0 L}{24 D_{12}} = LH \tag{12}$$

where H is the well-known theoretical plate height. After rearrangement, one gets

$$D_{12} = \frac{u_0}{4}\left(H \pm \sqrt{H^2 - \frac{R^2}{3}}\right) \tag{13}$$

which exhibits two solutions. The one with physical meaning depends on the value of the velocity that minimizes H, $u_{0,\mathrm{opt}} = \sqrt{48}(D_{12}/R)$: if the solvent linear velocity is greater than this value $(u_0 > u_{0,\mathrm{opt}})$, the negative root should be taken, and vice-versa [3, 8]. Since liquid and

supercritical systems generally have small optimal velocities, it is easy to exceed them and D_{12} is obtained using the negative root. The experimental theoretical plate height can be obtained by the following expression:

$$H = \frac{{u_0}^2 W_{0.607}^2}{L} \tag{14}$$

where $W_{0.607}$ is the peak half-width measured at 60.7% of total peak height, in time units.

Alternatively, the diffusion coefficient may be simply determined by fitting the theoretical concentration curve to the experimental data by minimizing the root mean square error, ε:

$$\varepsilon = \left\{ \frac{\int_{t_1}^{t_2} \left[C_{\exp}(t) - C_{\text{app}}(L,t) \right]^2 dt}{\int_{t_1}^{t_2} \left[C_{\exp}(t) \right]^2 dt} \right\}^{1/2} \tag{15}$$

where $C_{\exp}(t)$ is the solute concentration measured at the end of the diffusion column, and t_1 and t_2 are the times corresponding to 10% peak high of the response curve ($t_1 < t_2$). Generally, an acceptable fit is achieved when ε <0.03, and a good fit considered for ε <0.01 [16].

The CPB method then allows the determination of diffusion coefficients at infinite dilution (the injected quantities are very small) in pure/mixed solvents. Only liquid tracer species may be analyzed, while adaptations to this method have been developed in order to extend the measurements to solid solutes or highly viscous liquids – chromatographic impulse response (CIR) method with film coated columns is usually used for that purpose, as may be consulted in the literature [10, 14]. Notwithstanding, the CPB method offers a precision around 5 % (absolute value) when properly employed, based on simple chromatographic principles and setup.

5.2 Experimental setup

The experimental apparatus installed in this work to measure tracer diffusion coefficients is schematically represented in Fig. 2. The essential components are a syringe pump to deliver the solvent, an oven to keep temperature constant, an open tubular capillary column (diffusion column), an injector to load the solute at column inlet, a detector at column exit to measure and register the response signal, and a back pressure regulator to maintain the desired pressure. Besides these main elements, there is also a CO_2 cylinder to feed the entire unit, a thermostatic

bath connected to the CO_2 pump to keep a constant volumetric flow rate (*i.e.* avoid temperature fluctuations that would lead to density changes), an additional syringe pump to feed liquid solvents or cosolvents (pure or mixtures, respectively), a pre-heating (and pre-mixing, if applicable) column prior to the diffusion column, a selector immediately after the injector to choose the diffusion column to be used (not represented in the scheme for clarity), a computer connected to the detector with a signal acquisition system, and a flow meter to access/confirm the fluid velocity.

The extra syringe pump provides a huge flexibility to this setup, allowing the use of other solvents (liquids, for example) for which the diffusivities are desired, or to combine both to produce mixtures (for example, CO_2 with a cosolvent). Besides, the existence of a selector allows the alternative use of distinct diffusion columns with the objective to study the effect of the length of the diffusion column (this allows the quantification of dispersion effects caused by dead volumes – injection and detection areas, connecting tube portions – that affect D_{12} values) or to use coated capillary columns with different polarities to apply CIR method.

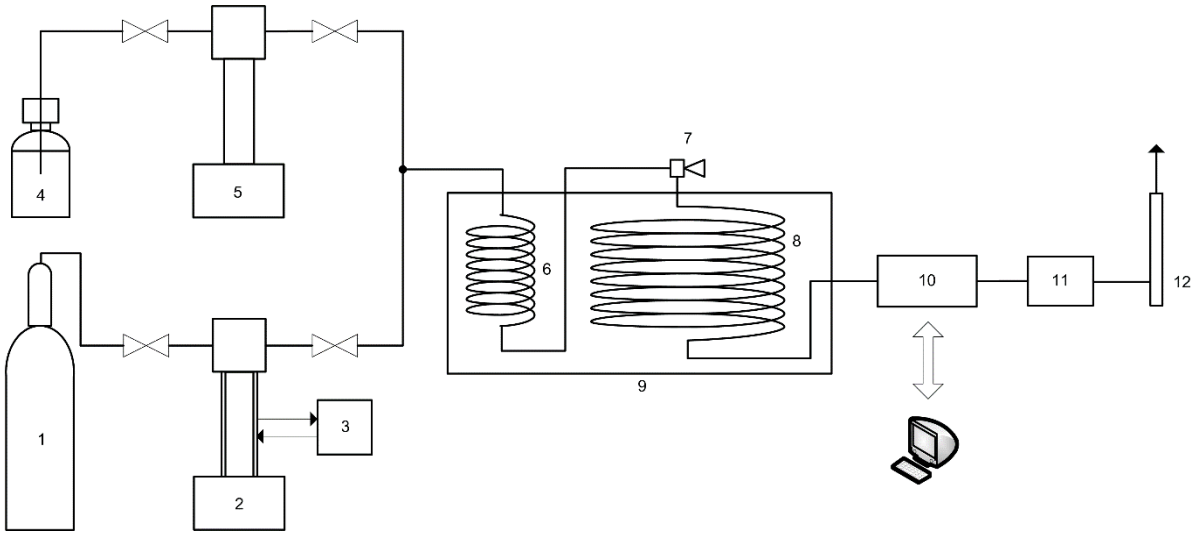

Fig. 2 Schematic layout of the experimental apparatus to measure tracer diffusion coefficients: 1) CO_2 cylinder, 2) jacketed syringe pump, 3) thermostatic bath, 4) liquid solvent/cosolvent vessel, 5) syringe pump, 6) pre-heating/pre-mixing column, 7) injector, 8) diffusion column, 9) oven, 10) UV-vis detector, 11) BPR, and 12) soap bubble flow meter.

Some pictures of our apparatus may be found in Fig. 3, followed by a detailed description of its components:

i) thermostatic bath (F12, Julabo) to control temperature (±0.1K) of CO_2 inside solvent pump and assure a constant volumetric flow rate along experiments;

ii) two syringe pumps (260D and 100DM, Teledyne ISCO) with 266.05 mL and 102.93 mL (respectively) coupled with a controller unit to impose the volumetric flow rate (±1.0 μL.min^{-1} and ±0.01 μL.min^{-1}, respectively);

iii) panel with four high pressure valves (15-11AF2, High Pressure Equipment Company – HiP) to manually control the solvent/cosolvent admission and exit to/from the syringe pumps;

iv) oven (LSIS-B2V/IC 22, Venticell, MMM Group) to set the temperature (±1K) of the solvent inside diffusion columns constant;

v) pre-heating (and pre-mixing column, when applicable) column (stainless steel tubing, 1/16″ O.D. × .03″ I.D) with around 10 m long, placed inside the oven before the diffusion column to heat (and homogenize, if applicable) the mobile phase before injection;

vi) injector – 4 port, 2 position, high pressure valve – with internal 0.1 μL loop (C74H-1674-.1, Valco Instruments Co Inc) to load the pulse of the solute to be analyzed;

vii) manual selector – both ends selected, 4 column, high pressure valve (CSR4UW, Valco Instruments Co Inc) – to choose the diffusion column;

viii) diffusion column (PEEK tubing, 1/16″ O.D. × .020″ I.D.) with a length of 10.243 m and coiled with a diameter of ca. 30 cm;

ix) UV-vis detector (UV Detector 2500, Knauer) with an analytical flow cell (A4061, Knauer) to measure the signal at column outlet;

x) automatic back pressure regulator (BPR) (BP-2080 Plus, Jasco) with temperature controller, to establish the upstream pressure of the system;

xi) soap bubble flow meter with 50.0 mL at system end to measure/confirm the flow rate of the solvent stream.

Some additional considerations will now be made about a few setup details.

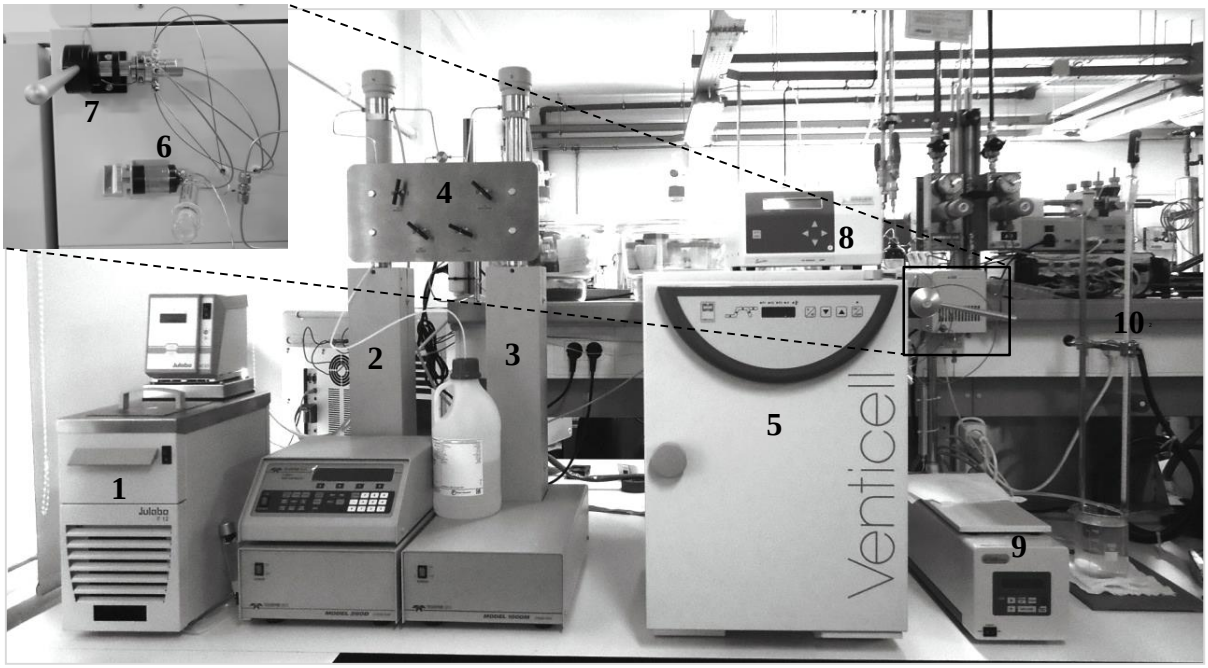

Fig. 3 Experimental setup conceived in this work to measure tracer diffusion coefficients (inset – zoom of the identified area): 1) thermostatic bath, 2) jacketed syringe pump, 3) syringe pump, 4) panel valve, 5) oven with pre-heating/pre-mixing and diffusion columns inside, 6) injector, 7) column selector, 8) detector, 9) BPR, and 10) soap bubble flow meter.

Usually, when applying Taylor dispersion method, stainless steel tubing is used as diffusion column. However, it is known that solute adsorption onto the inner wall of such columns frequently occur. This unexpected adsorption causes elution profiles with pronounced tailings, and then the diffusion coefficients cannot be measured accurately from those peaks. Even when ignoring the portion of the response curves under 10% of peak height, as it is adopted in the fitting method, or considering just the points at 60.7% of peak height, like in the variance methodology, the asymmetry of the curves generates erroneous D_{12} values. In an attempt to solve this problem, inactivated stainless steel tubing is often employed, for example using cadmium on its internal surface to minimize the interaction between the solute and the inner walls of the column.

In this work, PEEK (polyetheretherketone) tubing was acquired for its features: chemically inert and resistant material, supporting continuously high temperatures (100ºC) and high pressures (up to 483 bar), but flexible and offering very smooth internal surface, with the additional advantage of being easily cut to the desired length.

The characteristics of this column allowed also a meticulous determination of its parameters, regardless of the nominal values provided by the supplier. They were subsequently used in the measurement of D_{12} values (using the equations presented in the previous section), with the objective to ensure the required accuracy of the determinations.

The exact length of the column, important for the correct knowledge of $u_0 = L/t$, was measured prior to coiling. Then, using the retention time of the solutes, the true velocity is computed individually for each determination. These values were compared with velocities provided by the flow meter.

Another extremely important parameter is the radius or diameter of the column because a small error in this variable greatly influences the resulting diffusivity. The precision of the value furnished by the manufacture (IDEX) was not satisfactory for our application, and thus additional calibrations were executed. A mean internal diameter of 0.522 cm was found by weight difference between a full and empty portion of PEEK tubing with known length (two values were used for statistical accuracy), using a liquid with known density at fixed temperature (distilled gas-free water). Moreover, SEM (scanning electron microscope) images of the tube cross section confirmed this value.

All connections interfering in the results (injection and detection zones) were made with PEEK tubing equal to the diffusion column in order to avoid additional dispersion effects.

Table 1 presents a compilation of the geometric parameters of our diffusion column. The measurements were accomplished by recording the system response – time and absorbance, for a fixed wavelength – in a spreadsheet using a LabVIEW® program written specifically for this setup. Data were further and systematically analyzed in Matlab 2009b® on the basis of the CPB mathematical principles described in previous section.

Table 1. Diffusion column parameters.

L (cm)	R (cm)	R_c (cm)
1024.3	0.261	15.0

5.3 Experimental procedure for D_{12} measurement

In this work, experimental measurements of tracer diffusion coefficients in supercritical CO_2 were performed using the apparatus described in section 5.2. The solvent is admitted from the CO_2 cylinder at room temperature to the 266.05 mL syringe pump, and is fed to the system until reaching the BPR (pre-heating column, diffusion column, detector and BPR, sequentially). The desired pressure is fixed here, and the system is allowed to pressurize until the set-point value is attained. Then, the temperature, pressure and volumetric flow rate are maintained for 2-3 h to reach steady-state operation prior to the experimental measurements. The solute is then injected into the solvent stream, and the absorbance at column outlet is monitored by the UV-vis detector at a specified wavelength. At least ten pulses of solute were injected into the column *per* run, spaced by a sufficient interval of time to avoid peaks overlapping (7 minutes were usually enough).

Nomenclature

c	Concentration of the solute
C	Average cross section concentration of the solute
C_{app}	Approximate average concentration of the solute
C_{exp}	Concentration of the solute measured at column exit
CIR	Chromatographic impulse response
CPB	Chromatographic peak broadening
D	Dispersion coefficient
D_{12}	Tracer diffusion coefficient of solute 2 through solvent 1
De	Dean number, $\mathrm{De} = \mathrm{Re}/\sqrt{\lambda}$
H	Theoretical plate height

I.D.	Internal diameter of the tube
L	Length of the tube
m	Injected mass of the solute
O.D.	Outer diameter of the tube
Pe_x	Longitudinal Peclet number, $\mathrm{Pe}_x = u_0 L/D_{12}$
r	Radial coordinate
R	Inner radius of the tube
R_c	Coil radius of the tube
Re	Reynolds number, $\mathrm{Re} = 2\rho_1 u_0 R/\eta_1$
Sc	Schmidt number, $\mathrm{Sc} = \eta_1/(\rho_1 D_{12})$
SCF	Supercritical fluid
t	Time
t_1, t_2	Time at 10% peak high of the response curve ($t_1 < t_2$)
u_0	Average linear velocity of the solute
$u_{0,\mathrm{opt}}$	Optimum velocity that minimizes $H, u_{0,\mathrm{opt}} = \sqrt{48}(D_{12}/R)$
$W_{0.607}$	Peak half-width measured at 60.7% of total peak height
z	Axial coordinate

Greek letters

ε	Root mean square error
η_1	Solvent viscosity
λ	Curvature ratio, $\lambda = R_c/R$
ρ_1	Solvent density
σ^2	Variance of the response curve

References

[1] R. Taylor, R. Krishna, Multicomponent Mass Transfer, John Wiley & Sons, Inc, New York, 1993.

[2] M. Pertler, E. Blass, G.W. Stevens, Fickian diffusion in binary mixtures that form two liquid phases, AIChE Journal, 42 (1996) 910-920.

[3] K.K. Liong, P.A. Wells, N.R. Foster, Diffusion in supercritical fluids, The Journal of Supercritical Fluids, 4 (1991) 91-108.

[4] G. Taylor, Dispersion of soluble matter in solvent flowing slowly through a tube, Proceedings of the Royal Society of London. Series A. Mathematical and Physical Sciences, 219 (1953) 186-203.

[5] G. Taylor, The dispersion of matter in turbulent flow through a pipe, Proceedings of the Royal Society of London. Series A. Mathematical and Physical Sciences, 223 (1954) 446-468.

[6] G. Taylor, Conditions under which dispersion of a solute in a stream of solvent can be used to measure molecular diffusion, Proceedings of the Royal Society of London. Series A. Mathematical and Physical Sciences, 225 (1954) 473-477.

[7] R. Aris, On the dispersion of a solute in a fluid flowing through a tube, Proceedings of the Royal Society of London. Series A. Mathematical and Physical Sciences, 235 (1956) 67-77.

[8] J.C. Giddings, S.L. Seager, Rapid tetermination of gaseous diffusion coefficients by means of gas chromatography Apparatus, The Journal of Chemical Physics, 33 (1960) 1579-1580.

[9] W.A. Wakeham, A. Nagashima, J.V. Sengers, Measurement of the Transport Properties of Fluids, Blackwell Scientific Publications, 1991.

[10] T. Funazukuri, C.Y. Kong, S. Kagei, Impulse response techniques to measure binary diffusion coefficients under supercritical conditions, Journal of Chromatography A, 1037 (2004) 411-429.

[11] O. Levenspiel, W.K. Smith, Notes on the diffusion-type model for the longitudinal mixing of fluids in flow, Chemical Engineering Science, 6 (1957) 227-235.

[12] J.A. Moulijn, R. Spijker, J.F.M. Kolk, Axial dispersion of gases flowing through coiled columns, Journal of Chromatography A, 142 (1977) 155-166.

[13] A. Alizadeh, C.A. Nieto de Castro, W.A. Wakeham, The theory of the Taylor dispersion technique for liquid diffusivity measurements, International Journal of Thermophysics, 1 (1980) 243-284.

[14] T. Funazukuri, C.Y. Kong, S. Kagei, Binary diffusion coefficients in supercritical fluids: Recent progress in measurements and correlations for binary diffusion coefficients, The Journal of Supercritical Fluids, 38 (2006) 201-210.

[15] E.T. van der Laan, Notes on the Diffusion Type Model for Longitudinal Mixing in Flow, Chemical Engineering Science, 7 (1958) 187-191.

[16] T. Funazukuri, C.Y. Kong, S. Kagei, Infinite-dilution binary diffusion coefficients of 2-propanone, 2-butanone, 2-pentanone, and 3-pentanone in CO_2 by the Taylor dispersion technique from 308.15 to 328.15 K in the pressure range from 8 to 35 MPa, International Journal of Thermophysics, 21 (2000) 1279-1290.

6 Measurement of tracer diffusivities of α-pinene in supercritical CO_2

Given the increasing interest on supercritical technologies like extraction of bioactive compounds from natural matrices (mainly using supercritical carbon dioxide, SC-CO_2), the experimental measurement of tracer diffusivities of such molecules is highly desired.

α-pinene (CAS number 80-56-8) is a bicyclic monoterpenic hydrocarbon with molecular formula $C_{10}H_{16}$. Terpenes are a class of naturally occurring compounds mainly in plants as constituents of essential oils, consisting of isoprene multiples in a cyclic or acyclic, saturated or unsaturated structure. The essential oil of rosemary, eucalypt oil, orange peel oil, and oils of many species of coniferous trees, especially pine, are rich in α-pinene. It is a powerful solvent and possesses interesting properties for application in the pharmaceutical and cosmetic industries such as production of menthol and resins, and camphor manufacture.

In this work, the D_{12} measurement of α-pinene in SC-CO_2 was carried out at 313.15, 323.15 and 333.15 K, and pressures from 175 to 275 bar using the chromatographic peak broadening (CPB) technique. Despite the existence of some experimental data in the range 120-200 bar [1], more data are needed because the supercritical extractions of biomass are frequently performed at higher densities [2-4]. In the following, the list of chemicals and experimental conditions of the determinations are firstly presented. Several expressions from the literature were selected to compute the tracer diffusivities. After, the experimental results are presented and discussed,

namely, the dependency of D_{12} upon temperature, pressure, solvent density, and hydrodynamic behavior, and the modeling results achieved.

6.1 Chemicals

The experimental measurements were carried out with the apparatus described in Chapter 5 using α-pinene (Sigma Aldrich, purity 98% w/w) as solute and carbon dioxide (Praxair, purity 99.999% v/v) as solvent.

6.2 Experimental conditions for D_{12} measurement

The determination of tracer diffusivities of α-pinene in SC-CO_2 were carried out at three temperatures (T = 313.15, 323.15 and 333.15 K), and five pressures for each temperature (P = 175, 200, 225, 250 and 275 bar). Table 1 compiles the state conditions for all runs. The density of carbon dioxide, ρ_1, was calculated by the correlation of Pitzer and Schreiber [5], and the CO_2 viscosity, η_1, was estimated using the equation proposed by Altunin and Sakhabetdinov [6].

6.3 Expressions for D_{12} modeling

In this work, eight predictive equations from literature were selected to estimate the α-pinene tracer diffusivities, namely, six Stokes-Einstein expressions, the free-volume model of He-Yu-Su [7], and the Catchpole-King correlation [8]. These models are briefly presented in the following.

Wilke-Chang equation [9]. In this equation, ϕ is a dimensionless association factor of the solvent, M_1 is the solvent molecular weight (g/mol), and $V_{bp,2}$ is solute molar volume at its normal boiling point (cm^3/mol). The solvent viscosity is in cP.

$$D_{12} = 7.4\times10^{-8}\frac{T\sqrt{\phi M_1}}{\eta_1 V_{bp,2}^{0.6}} \quad (1)$$

Scheibel equation [10]. Here the units are those of the Wilke-Chang correlation, and $V_{bp,1}$ is the solvent molar volume at its normal boiling point (cm^3/mol).

$$D_{12} = \frac{8.2\times10^{-8}T}{\eta_1 V_{bp,2}^{1/3}}\left[1+\left(\frac{3V_{bp,1}}{V_{bp,2}}\right)^{2/3}\right] \quad (2)$$

Lusis-Ratcliff equation [11]. Here the units are those of equations (1) and (2).

$$D_{12} = \frac{8.52\times10^{-8}T}{\eta_1 V_{bp,1}^{1/3}}\left[1.40\left(\frac{V_{bp,1}}{V_{bp,2}}\right)^{1/3} + \left(\frac{V_{bp,1}}{V_{bp,2}}\right)\right] \quad (3)$$

Lai-Tan equation [12]. This equation has been proposed for supercritical carbon dioxide systems. The unique variable not yet introduced is the critical volume of the solute, $V_{c,2}$, in cm^3/mol. The remaining units are the same as above.

$$D_{12} = 2.50\times10^{-7}\frac{T\sqrt{M_1}}{(10\times\eta_1)^{0.688}V_{c,2}^{1/3}} \quad (4)$$

Tyn-Calus equation [13]. In this equation $\mathbf{P_i}$ identifies the parachor of component i, which is related with the liquid surface tension and may be estimated by additive group contributions. For most organic solvents, an approximation is used in the calculation. The precise and approximate correlations, in the same units of the Wilke-Chang correlation, are given by, respectively:

$$D_{12} = 8.93\times10^{-8}\left(\frac{V_{bp,2}}{V_{bp,1}^2}\right)^{1/6}\left(\frac{\mathbf{P_1}}{\mathbf{P_2}}\right)\frac{T}{\eta_1} \quad (5)$$

$$D_{12} = 8.93\times10^{-8}\frac{V_{bp,1}^{0.267}}{V_{bp,2}^{0.433}}\frac{T}{\eta_1} \quad (6)$$

Reddy-Doraiswamy equation [14]. This expression has the same units of the previous hydrodynamic models.

$$D_{12} = \beta \times \frac{T\sqrt{M_1}}{\eta_1 \left(V_{\mathrm{bp},1}\, V_{\mathrm{bp},2}\right)^{1/3}}$$
$$V_{\mathrm{bp},1}/V_{\mathrm{bp},2} \le 1.5 \;\Rightarrow\; \beta = 10\times 10^{-8} \qquad (7)$$
$$V_{\mathrm{bp},1}/V_{\mathrm{bp},2} > 1.5 \;\Rightarrow\; \beta = 8.5\times 10^{-8}$$

He-Yu-Su equation [7]**.** This free-volume model is specific for supercritical systems. Besides the variables (and respective units) already introduced, M_2 is the solute molecular weight (g/mol), V_1 is the solvent molar volume (cm^3/mol), $\rho_{\mathrm{r},1}$ is the reduced density of the solvent, and $T_{\mathrm{c},1}$ and $P_{\mathrm{c},1}$ are their critical temperature (K) and pressure (bar), respectively.

$$D_{12} = A'\times 10^{-7}\left(V_1^{k} - B'\right)T/\sqrt{M_2}$$
$$A' = 0.29263 + 1.6736\exp\left(-0.75832\sqrt{M_1 V_{\mathrm{c},1}}/P_{\mathrm{c},1}\right), \quad \rho_{\mathrm{r},1} \ge 0.21$$
$$B' = 0.077 T_{\mathrm{c},1}, \quad \rho_{\mathrm{r},1} \ge 0.21 \qquad (8)$$
$$\rho_{\mathrm{r},1} \ge 1.2 \;\Rightarrow\; k = 1$$
$$\rho_{\mathrm{r},1} < 1.2 \;\Rightarrow\; k = 1 + \left(\rho_{\mathrm{r},1} - 1.2\right)/\sqrt{M_1}$$

Catchpole-King equation [8]. This correlation was devised for near-critical fluids. *F* and *X* are correction factors, and $D_{\mathrm{c},1}$ is the solvent self-diffusion coefficient at the critical point. It may be estimated from a modified Fuller-Schettler-Giddings [15] empirical correlation, where $\rho_{\mathrm{c},1}$ is the critical density of the solvent (kg/m^3), and the diffusion volumes $\sum_{\mathrm{v},1}$ are calculated according to Reid el al. [16].

$$D_{12} = 5.152 D_{\mathrm{c},1} T_{\mathrm{r},1}\left(\rho_{\mathrm{r},1}^{-2/3} - 0.4510\right)F/X$$
$$X = \left[1 + \left(V_{\mathrm{c},2}/V_{\mathrm{c},1}\right)^{1/3}\right]^2 \Big/ \sqrt{1 + M_1/M_2}$$
$$F = 1.0 \pm 0.1, \quad 2 < X \quad \text{for class 1 type systems}^{*} \qquad (9)$$
$$F = 0.664 X^{0.17} \pm 0.1, \quad 2 < X < 10 \quad \text{for class 2 type systems}^{*}$$

$$D_{c,1} = \frac{4.300\times10^{-7} M_1^{1/2} T_c^{0.75}}{\left(\sum_{v,1}\right)^{2/3} \rho_{c,1}}$$

*The two types of systems were originally defined as: class 1 – all aliphatics except ketones and (for ethylene) naphthalene in carbon dioxide and ethylene; class 2 – all aromatics, ketones, and carbon tetrachloride in carbon dioxide; all aromatics, (for $CClF_3$) 2-propanone, (for SF_6) carbon tetrachloride in propane, hexane, dimethylbutane, SF_6, and $CClF_3$.

Table 1. Experimental conditions and measured tracer diffusion coefficients of *α*-pinene in supercritical carbon dioxide.

T (K)	P (bar)	ρ_1 (g.cm^{-3}) [a]	η_1 (g.cm^{-1}.s^{-1}) [b]	D_{12} (10^{-4} cm^2.s^{-1})
313.15	175	0.8147	7.467	0.9161
	200	0.8406	7.961	0.8730
	225	0.8620	8.400	0.8346
	250	0.8803	8.799	0.8083
	275	0.8963	9.170	0.7919
323.15	175	0.7503	6.411	1.1005
	200	0.7851	6.966	1.0163
	225	0.8124	7.441	0.9686
	250	0.8350	7.863	0.9222
	275	0.8543	8.249	0.8873
333.15	175	0.6775	5.441	1.2343
	200	0.7245	6.061	1.1217
	225	0.7595	6.575	1.0483
	250	0.7873	7.022	1.0029
	275	0.8105	7.425	0.9863

[a] Calculated by the correlation of Pitzer and Schreiber [5]; [b] Estimated with the equation of Altunin and Sakhabetdinov [6].

6.4 Experimental results

The tracer diffusivities of α-pinene were determined by analyzing the experimental response curves obtained at the end of the diffusion column using the UV-vis detector. The wavelength used to acquire signal was previously evaluated, in order to obtain a large absorbance intensity and negligible experimental noise. To select the adequate wavelength for α-pinene in SC-CO_2, the system was allowed to equilibrate and several pulses were loaded and studied at different wavelengths. They were first coarsely scanned from 190 to 400 nm to locate the region where signal intensity was large, and then more finely inspected in that region. Since the maximum absorbance intensity does not necessarily yield the better results, the wavelength was chosen with the objective to originate Gaussian peaks that match calculated response curves. After these tests, all subsequent experiments were conducted at 235 nm.

Fig. 1 shows a typical CPB response obtained in this work. The measured curve did not evidence tailing and was fine fitted by the calculated one, which was observed in all range of experimental conditions. Thus, D_{12} values were computed using the variance method (see Chapter 5) that produced similar results than the curve fitting method. All responses presented an asymmetric factor, S_{10} (defined as the ratio between the peak half-widths at 10% peak height) close to one (S_{10} < 1.14).

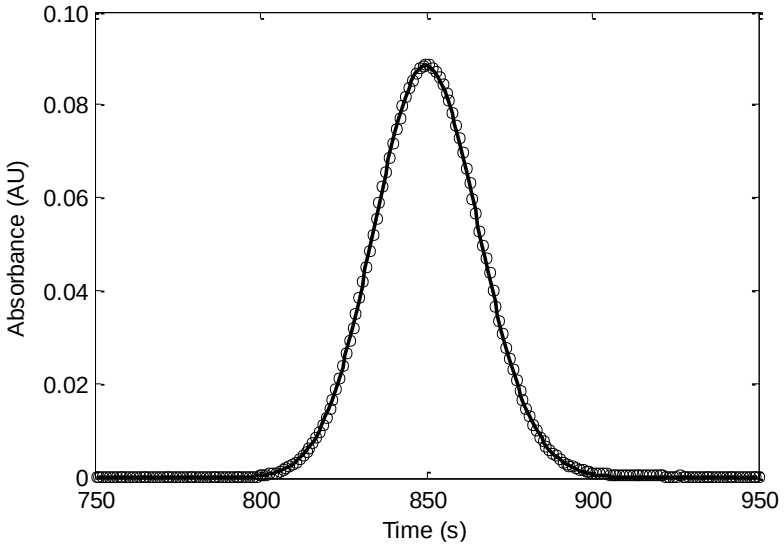

Fig. 1. Experimental (○) and calculated (−) response curves for α-pinene at 235 nm in SC-CO_2 at 333.15 K and 275 bar.

To guarantee the applicability of the CPB method, small linear velocities were employed in the experiments (1.11–1.20 cm.s^{-1}) and laminar flow was always obtained. The Reynolds numbers ranged from 57 to 89, and longitudinal Peclet numbers were in the order 10^7 ensuring negligible axial dispersion in the column. The pressure drop was also insignificant by comparing pressure values measured at the CO_2 pump with those delivered by the BPR. The effect of secondary flow due to column coiling was taken into consideration by computing the Dean number and ensuring $\mathrm{De}\sqrt{\mathrm{Sc}} < 9.5$ (close to 8 in most cases). The other criteria were fulfilled with $D/u_0 L < 0.0002$ and $u_0 L/D > 5100$. For each condition, final D_{12} values were then obtained by averaging over all peaks suitable for analyzis, and are presented in Table 1.

6.4.1 Influence of pressure at constant temperature

In Fig. 2 the effect of pressure on α-pinene diffusivity at constant temperature is shown. As expected, a decrease was observed as pressure rises for each isotherm, which is in line with free-volume theories. In fact, as density increases, the available free volume for diffusion decreases thus reducing D_{12}. Moreover, at lower free volumes, the energy barrier that molecules must overcome to escape from the force field of their neighbors and jump to an adjacent hole is higher, which penalizes diffusion [17, 18]. The pressure effect was more pronounced at lower values due to the alterations of the solvent properties, namely CO_2 density and viscosity, that change significantly with pressure closer to the critical point.

6.4.2 Influence of temperature at constant pressure

The effect of temperature on tracer diffusivities of α-pinene for isobaric conditions is illustrated in Fig. 3. The observed trends showed a high dependence of D_{12} upon temperature, being greatly enhanced by the associated increase of the system energy (the diffusion barrier patent in many transport theories is easily overcame). The temperature raising is also linked to solvent density reduction, and consequently the available free volume is greater, which also favors diffusion. Hence, both requirements of hybrid free-volume theories of diffusion are improved with increasing *T*: the solute possesses sufficient energy to move between adjacent holes, whose size is increasingly higher due to free volume augmentation [17, 18].

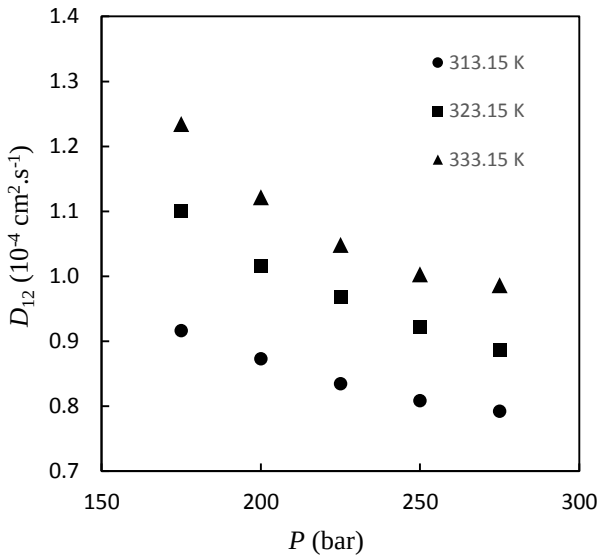

Fig. 2. Tracer diffusion coefficients of α-pinene in SC-CO_2 as function of pressure at constant temperature.

6.4.3 Influence of density at constant temperature

The effect of solvent density on diffusion was further investigated by plotting Fig. 4. Accordingly, a great density influence was patent, which may be explained by the erratic path taken by the solute between solvent molecules when density increases. The consequent diffusivity reduction is associated to the larger number of collisions undergone by the solute as the molecular diameter becomes more significant in comparison to the average intermolecular distance. Once again, free-volume theories explain this behavior by the free volume reduction at higher densities and also activation energy increment.

An almost linear behavior was observed in this work, in opposition to data from Silva et al. [1]. Particularly at higher temperatures their experimental values are superior to those extrapolated using the linear fitting at high densities (see Fig. 4). Nevertheless, these two sets of diffusivities (from this work and Silva et al.) complemented each other and extended the density range of data. This comparison also confirmed the reliability of our measurements to validate the experimental setup and procedure.

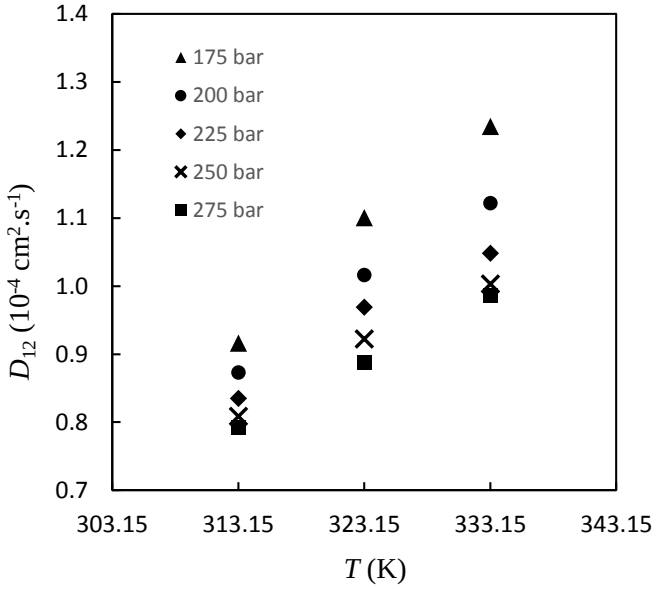

Fig. 3. Tracer diffusion coefficients of α-pinene in SC-CO_2 as function of temperature at constant pressure.

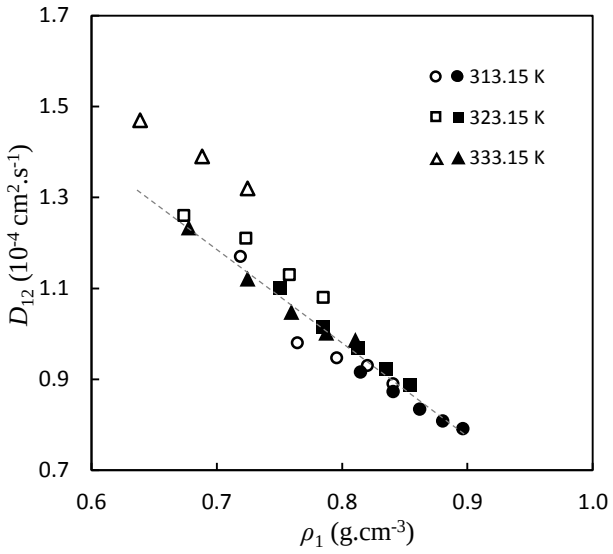

Fig. 4. Tracer diffusion coefficients of α-pinene in SC-CO_2 as function of solvent density. Filled symbols: this work; unfilled symbols: data from Silva et al. [1].

6.4.4 Influence of Stokes-Einstein type

The hydrodynamic behavior of the measured values was also evaluated by representing the α-pinene diffusivities using Stokes-Einstein coordinates: D_{12} *versus* T/η_1 (see Fig. 5). The trend was quite linear over the T/η_1 range but a nonzero intercept exists. This deviation was already reported in the literature for other solutes [19-23].

6.4.5 Modeling diffusion data

The data measured in this work was restricted to the high density region of SC-CO_2, far for the critical point, where hydrodynamic behavior applies. Accordingly, pure Stokes-Einstein based relationships were used in the modeling of the experimental results. Moreover, some models proposed in this work were also tested, one from each adopted approach: modified Wilke-Chang (Model 1: Eq (1) from Paper II), modified Wilke-Chang using critical volumes (Model 2: Eq. (2) from Paper III), and critical enhancement (Eq. (19) from Paper IV). Additionally, the free-volume model of He-Yu-Su and the correlation of Catchpole-King were

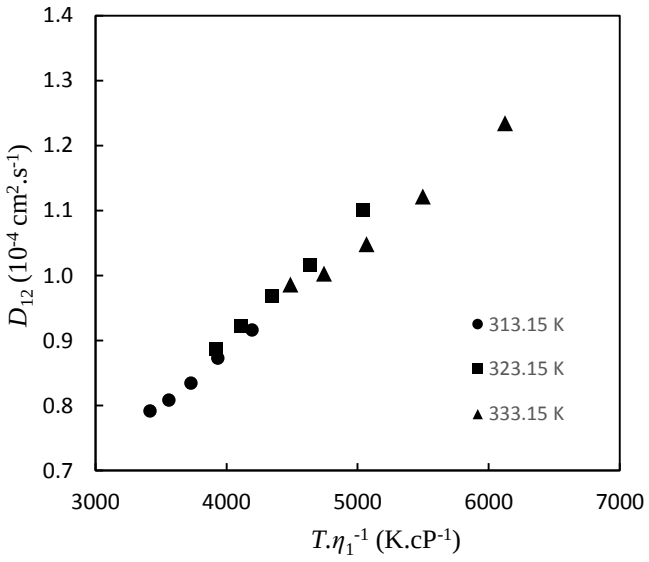

Fig. 5. Tracer diffusion coefficients of α-pinene in SC-CO_2 represented in Stokes-Einstein fashion.

also tested due to their predictive nature. The solute and solvent parameters necessary in all calculations are provided in Table 2. Data was taken from Reid et al. [16] for carbon dioxide and from Yaws [24] for *α*-pinene, except molar volumes at normal boiling point which were estimated by Tyn-Calus expression [25]. In the case of our models, V_{bp} values were further corrected according to $V_{bp} = 1.459\left(V_{bp}^{TC}\right)^{0.894}$, where 'TC' means 'calculated by Tyn-Calus expression'.

Table 3 contains the absolute average relative deviations (AARD) achieved by all predictive models. It may be observed that quite good results were provided by the majority of them (deviations between 2.48% and 13.31%), except Lusis-Ratcliff and Reddy-Doraiswamy hydrodynamic equations (35.89% and 63.37% of error, respectively), and Catchpole-King correlation (53.78% of error). The best results for the calculation of *α*-pinene diffusivities in SC-CO_2 are those achieved by our Models 1, 2 and 3. These accuracies were expected in advance since they are based on the Wilke-Chang expression, which already provides reliable results (AARD = 5.34%). Nonetheless, the simple modifications introduced into Model 1 and Model 2 decrease the error by half. In comparison, Model 3 offers no gain to estimate *α*-pinene diffusivities since the measured data are located far from CO_2 critical point.

Table 2. Properties of pure substances: molecular weight (M), critical constants (T_c, P_c, V_c), acentric factor (ω), and molar volume at normal boiling point (V_{bp}).

Substance	M (g/mol)	T_c (K)	P_c (bar)	V_c (cm^3/mol)	ω	V_{bp} [c] (cm^3/mol)
carbon dioxide [a]	44.01	304.10	73.80	93.90	0.3040	33.28
α-pinene [b]	136.24	632.00	27.60	504.00	0.2860	193.64

[a] Taken from Reid et al. [16]; [b] Taken from Yaws [24]; [c] Estimated by Tyn-Calus expression [25].

Table 3. Modeling results obtained for the experimental diffusivities of α-pinene in SC-CO_2.

Model	Equation	AARD (%)
Wilke-Chang	Eq. (1)	5.34
Scheibel	Eq. (2)	6.72
Lusis-Ratcliff	Eq. (3)	35.89
Lai-Tan	Eq. (4)	13.31
Tyn-Calus	Eq. (6)	6.69
Reddy-Doraiswamy	Eq. (7)	63.37
He-Yu-Su	Eq. (8)	4.20
Catchpole-King	Eq. (9)	53.78
Model 1	Eq. (1) from Paper II	2.48
Model 2	Eq. (2) from Paper III	2.50
Model 3	Eq. (19) from Paper IV	3.56

Nomenclature

AARD	Absolute average relative deviation
BPR	Back pressure regulator
CPB	Chromatographic peak broadening
D	Dispersion coefficient
D_{12}	Tracer diffusion coefficient of solute 2 through solvent 1
$D_{c,1}$	Solvent self-diffusion coefficient at the critical point
De	Dean number, $\mathrm{De} = \mathrm{Re}/\sqrt{\lambda}$
L	Length of the column
LR	Lusis-Ratcliff equation
LT	Lai-Tan equation
M	Molecular weight

P	Pressure
P_c	Critical pressure
$\mathbf{P_i}$	Parachor of component *i*
RD	Reddy-Doraiswamy equation
Sc	Schmidt number, $Sc = \eta_1 / \rho_1 D_{12}$
Sch	Scheibel equation
S_{10}	Asymmetric factor (ratio between peak half-widths at 0.1 peak height)
SC-CO_2	Supercritical carbon dioxide
T	Absolute temperature
T_c	Critical temperature
TC	Tyn-Calus equation
u_0	Average linear velocity of the solute
V_1	Solvent molar volume
V_{bp}	Molar volume at normal boiling point
V_c	Critical molar volume
WC	Wilke-Chang equation

Greek letters

ϕ	Dimensionless association factor in the Wilke-Chang equation
η_1	Solvent (SC-CO_2) viscosity
ρ_1	Solvent density
ω	Acentric factor

Subscripts

1	Solvent (SC-CO_2)
2	Solute
c	Critical property
r	Reduced property

Superscripts

TC Estimated by the group contribution method of Tyn-Calus

References

[1] C.M. Silva, C.A. Filho, M.B. Quadri, E.A. Macedo, Binary diffusion coefficients of α-pinene and β-pinene in supercritical carbon dioxide, The Journal of Supercritical Fluids, 32 (2004) 167-175.

[2] M.M.R. de Melo, A.J.D. Silvestre, C.M. Silva, Supercritical fluid extraction of vegetable matrices: Applications, trends and future perspectives of a convincing green technology, The Journal of Supercritical Fluids, 92 (2014) 115-176.

[3] M.M.R. de Melo, H.M.A. Barbosa, C.P. Passos, C.M. Silva, Supercritical fluid extraction of spent coffee grounds: Measurement of extraction curves, oil characterization and economic analysis, The Journal of Supercritical Fluids, 86 (2014) 150-159.

[4] M.M.R. Melo, R.M.A. Domingues, A.J.D. Silvestre, C.M. Silva, Extraction and purification of triterpenoids using supercritical fluids: from lab to exploitation, Mini-Reviews in Organic Chemistry, 11 (2014) 362-381.

[5] K.S. Pitzer, D.R. Schreiber, Improving equation-of-state accuracy in the critical region; equations for carbon dioxide and neopentane as examples, Fluid Phase Equilibria, 41 (1988) 1-17.

[6] V.V. Altunin, M.A. Sakhabetdinov, Viscosity of liquid and gaseous carbon dioxide at temperatures 220–1300 K and pressure up to 1200 bar, Teploenergetika, 8 (1972) 85-89.

[7] C.H. He, Y.S. Yu, W.K. Su, Tracer diffusion coefficients of solutes in supercritical solvents, Fluid Phase Equilibria, 142 (1998) 281-286.

[8] O.J. Catchpole, M.B. King, Measurement and correlation of binary diffusion coefficients in near critical fluids, Industrial and Engineering Chemistry Research, 33 (1994) 1828-1837.

[9] C.R. Wilke, P. Chang, Correlation of diffusion coefficients in dilute solutions, AIChE Journal, 1 (1955) 264-270.

[10] E.G. Scheibel, Liquid diffusivities. Viscosity of gases, Industrial & Engineering Chemistry, 46 (1954) 2007-2008.

[11] M.A. Lusis, C.A. Ratcliff, Diffusion in binary liquid mixtures at infinite dilution, The Canadian Journal of Chemical Engineering, 46 (1968) 385-387.

[12] C.C. Lai, C.S. Tan, Measurement of molecular diffusion coefficients in supercritical carbon dioxide using a coated capillary column, Industrial and Engineering Chemistry Research, 34 (1995) 674-680.

[13] M.T. Tyn, W.F. Calus, Diffusion coefficients in dilute binary liquid mixtures, Journal of Chemical & Engineering Data, 20 (1975) 106-109.

[14] K.A. Reddy, L.K. Doraiswamy, Estimating liquid diffusivity, Industrial & Engineering Chemistry Fundamentals, 6 (1967) 77-79.

[15] E.N. Fuller, P.D. Schettler, J.C. Giddings, New method for prediction of binary gas-phase diffusion coefficients, Industrial & Engineering Chemistry, 58 (1966) 18-27.

[16] R.C. Reid, J.M. Prausnitz, B.E. Poling, The Properties of Gases and Liquids, 5th ed., McGraw-Hill Professional, New York, 2001.

[17] C.M. Silva, H. Liu, Modelling of Transport Properties of Hard Sphere Fluids and Related Systems, and its Applications, in: Á. Mulero (Ed.) Theory and Simulation of Hard-Sphere Fluids and Related Systems, Springer Berlin Heidelberg, 2008, pp. 383-492.

[18] H. Liu, C.M. Silva, E.A. Macedo, Generalised free-volume theory for transport properties and new trends about the relationship between free volume and equations of state, Fluid Phase Equilibria, 202 (2002) 89-107.

[19] C.M. Silva, E.A. Macedo, Diffusion coefficients of ethers in supercritical carbon dioxide, Industrial & Engineering Chemistry Research, 37 (1998) 1490-1498.

[20] R. Feist, G.M. Schneider, Determination of binary diffusion coefficients of benzene, phenol, naphthalene and caffeine in supercritical CO_2 between 308 and 933 K in the pressure range 90 to 160 bar with supercritical fluid chromatography (SFC), Separation Science and Technology, 17 (1982) 261-270.

[21] R.V. Vaz, A.L. Magalhães, C.M. Silva, Improved hydrodynamic equations for the accurate prediction of diffusivities in supercritical carbon dioxide, Fluid Phase Equilibria, 360 (2013) 401-415.

[22] R.V. Vaz, A.L. Magalhães, C.M. Silva, Improved Stokes–Einstein based models for diffusivities in supercritical CO_2, Journal of the Taiwan Institute of Chemical Engineers, 45 (2014) 1280-1284.

[23] R.V. Vaz, A.L. Magalhães, C.M. Silva, Prediction of binary diffusion coefficients in supercritical CO_2 with improved behavior near the critical point, The Journal of Supercritical Fluids, 91 (2014) 24-36.

[24] C.L. Yaws, Chemical Properties Handbook: Physical, Thermodynamic, Environmental, Transport, Safety, and Health Related Properties for Organic and Inorganic Chemicals, McGraw-Hill Professional, New York, 1998.

[25] M.T. Tyn, W.F. Calus, Estimating liquid molal volume, Processing, 21 (1975) 16-17.

7 General conclusions and future work

7.1 Conclusions

In this work, diffusion coefficients were studied from three distinct perspectives: phenomenological modeling, molecular dynamics simulation, and experimental measurement.

The first approach consisted on the development of several models for the estimation of diffusivities of a great variety of systems and experimental conditions of interest.

Initially, self-diffusion coefficients were focused due to their importance to estimate Fick´s binary diffusivities, and to capture the essential relationships involved in the diffusive phenomenon. Entropy based scaling laws were selected for this purpose, which presumes the existence of a universal relationship between reduced self-diffusion coefficient and residual entropy, i.e. between dynamic and structural properties. For that, a large database embodying 1727 points of model (hard-sphere, hard-sphere chain, Lennard-Jones) and real fluids (polar, non-polar, symmetrical and asymmetrical, light and heavy molecules) was compiled. The attributed universal character of the existent scaling laws of Rosenfeld, Dzugutov and Bretonnet was refuted since it was shown that they fail over the entire range of density (ρ) and temperature (T), even for atomic and simple fluids for which they have been originally proposed. This study also revealed a dependence of the self-diffusivity upon the chain size of the molecule and not only on ρ and T (through residual entropy). Then, a new statistical model based on an artificial neural network was proposed, being able to accurately estimate the self-diffusivity of all fluids studied (AARD = 9.13%) as function of the residual entropy and a chain size parameter.

Furthermore, a simple and reliable analytical expression was proposed for spherical particles (hard-sphere and Lennard-Jones), capable of predicting their self-diffusivities as function of residual entropy with an average error of only 4.61% for 657 points.

Binary diffusion coefficients at infinite dilution were then studied, particularly in supercritical carbon dioxide given its importance under the context of green technologies and biorefinery. Our aim was the development of simple models to predict tracer diffusivities of those systems without the need of any previous information about them. Hydrodynamic equations were especially focused, given their simplicity and predictive nature. Accordingly, the original expressions, which were initially developed for liquids, were modified in order to enhance their performance in supercritical systems.

Firstly, three Stokes-Einstein models were improved by introducing two universal parameters and refitting a third one, keeping the dependence between D_{12} and T/η_1 and V_{bp}. When tested against a large database of 150 systems and 4484 data points of very distinct molecules, our modified expressions achieve average errors between 8.26% and 8.51%, while the seminal models give rise to larger deviations (11.70% to 23.16%).

Later, a very similar approach was adopted, but the functional dependences on V_{bp}, patent in the original Stokes-Einstein based models, were replaced by analogous relationships on the solute critical volume, V_c. Hence, four improved models were proposed, based on the original equations of Wilke-Chang, Scheibel, Lusis-Ratcliff, and Tyn-Calus. They provide equivalent and reliable results (AARD between 7.86% and 8.56%) to those obtained before with V_{bp}.

Since Stokes-Einstein based expressions only take into consideration the system behavior far from the critical point, another model was devised to interpret and include the critical enhancement of D_{12} near that point. It comprehends a background contribution to describe the regular behavior of the fluid, and a singular term to represent the near-critical phenomenon that increments D_{12}. Once again, the new model was tested and compared with hydrodynamic expressions from the literature, using a large database of 149 solutes in carbon dioxide (4469 data points totally). The average deviation obtained was only 6.20%, while the Wilke-Chang, Scheibel, Lusis-Ratcliff, Lai-Tan, Tyn-Calus and Reddy-Doraiswamy models achieved 11.62–

75.17% of error. The new equation performs equally well for polar and non-polar solutes, and in the whole pressure-temperature plane.

Globally, all developed models for supercritical systems exhibit fine predictive capability for all kinds of solutes at any conditions. However, near the critical point the expression from Paper IV is recommended given its accuracy in this region. They present unbiased results, relative deviations close to zero, and small standard deviations, which reinforces their superior performance in comparison with expressions from literature.

Concerning microscopic modeling, molecular dynamics simulations were performed to calculate tracer diffusivities of ketones (propanone, butanone, 2-pentanone and 3-pentanone) in SC-CO_2. It was shown that, after testing the most important parameters embodied in the simulations (i.e., cut-off, number of solute molecules, integration time step and length of the simulation), it is possible to produce results in quite good agreement with experimental data (AARD = 5.60%, which is compatible with experimental uncertainty). From computer simulations, the common dependencies of D_{12} were confirmed, namely its enhancement after pressure decrease, temperature increase, and solute size reduction. The radial distribution functions and coordination numbers were further calculated to understand how molecular structure specificities affect D_{12}. The influence of the same variables (temperature, pressure and solute size) on radial distribution function was also assessed. The simulations proved that the molecular structuring of the solvent around the solute is similar for all ketones, and that the decrease of the coordination numbers on going from propanone to the pentanones was due to the growth of the molecular chain. Therefore, the tracer diffusivities of the ketone series are essentially dependent on the solute size, while their structural properties are not so important as the functional group is the same.

Tracer diffusion coefficients were also experimentally measured in this work using the chromatographic peak broadening technique. For that an experimental setup was designed, assembled and tested to measure diffusivities in liquids and supercritical fluids, using pure solvents or mixtures. The geometric parameters of the diffusion column were rigorously

determined with additional calibrations to allow the appropriate implementation of the method and determination of trustful D_{12} values. Afterwards, α-pinene tracer diffusion coefficients were measured at 313.15, 323.15 and 333.15 K and 175, 200, 225, 250 and 275 bar, which are the conditions more commonly found in the supercritical extractions of this kind of biobased compounds. The expected dependences of D_{12} on temperature, pressure and solvent density were confirmed, as well as the hydrodynamic behavior of the data points. Their modeling was accomplished with several predictive expressions, namely three models developed in this thesis (one from each approach for SC-CO_2 – Papers II, III and IV), several hydrodynamic equations, a free-volume model and the Catchpole-King correlation. With some exceptions, a good agreement was achieved between experimental and calculated data, particularly using our models (for which the average deviations ranged between 2.48 and 3.56%).

Globally, three distinct approaches were employed to study diffusion coefficients. Each one exhibits its specificities and utility, but in the whole they complement each other to provide useful information to understand and interpret the diffusive phenomena.

7.2 Suggestion for future work

In terms of modeling, it is now necessary to develop reliable models for the pure prediction of diffusivities over wide ranges of temperature and pressure, in order to cover gas, liquid and supercritical regions. Up till now, various accurate correlations have been proposed by our research group at University of Aveiro, but a universal predictive model is extremely desired. Under the scope of this thesis, multivariate statistical models are being devised, with very promising results.

With respect to D_{12} measurement, improved chromatographic methods are necessary for the determination of tracer diffusivities of solids and even highly viscous liquids. For instance, the measurement of good eucalyptol diffusivities was impossible in this work, due to viscosity limitations. Therefore, the chromatographic impulse response technique proposed by

Funazukuri and coworkers should be implemented, which implies experimental and theoretical adaptations.

Finally, computer simulations should be performed for distinct solutes in order to test the influence of their functional groups and structural formulas upon D_{12}. This is necessary to gain confidence to extend the method to unknown systems (*i.e.*, not yet studied in the lab) and to molecules for which the potential parameters are not (all) available. In this case, *ab initio* calculations can be carried out.